must be massless, since a mass term for the gauge fields, $m_A^2 A_\mu^a A^{a\mu}$, would not be gauge invariant due to the inhomogeneous term in eqn (3.5).

In addition to eqn (3.9) there is one other invariant term involving the gauge fields of mass dimension four or less which could be added to the standard Lagrangian density. In terms of the dual field strength tensor,

$$\tilde{F}^a_{\mu\nu} = \frac{1}{2}\epsilon_{\mu\nu}{}^{\sigma\tau} F^a_{\sigma\tau} \quad \text{normalized such that} \quad \tilde{\tilde{F}} = F\,, \tag{3.11}$$

the so-called θ-term is given by

$$\begin{aligned}\mathcal{L}_\theta &= \theta \frac{g_s^2 T_F}{16\pi^2} F^a_{\mu\nu} \tilde{F}^{a\mu\nu} \\ &= \theta \frac{g_s^2 T_F}{16\pi^2} \frac{\partial}{\partial x^\mu} \left[2\epsilon^{\mu\nu\sigma\tau} \left(A^a_\nu \partial_\sigma A^a_\tau + \frac{2}{3} g_s f_{abc} A^a_\nu A^b_\sigma A^c_\tau \right) \right] .\end{aligned} \tag{3.12}$$

The parameter θ appearing above has nothing to do with the parameters θ_a in eqn (3.2). As the second form makes clear, $\mathcal{L}_\theta$ can be expressed as the total divergence of a gauge dependent current. As such it contributes only a surface term to the action which naïvely may be neglected. Unfortunately, life is not so simple and the surface integral is related to a topological invariant, called the Pontryagin index.[1] The non-trivial topological structure of the vacuum in QCD is such that in practice the θ-term does give a non-perturbative contribution. This represents a serious problem since the θ-term violates both the discrete symmetries parity (P) and time reversal (T), which are known to be respected by QCD to high accuracy, along with charge conjugation (C) invariance (Cheng, 1988). Since T-violation is equivalent to CP-violation, one would expect a contribution to the CP-violating electric dipole moment of the neutron

$$\text{e.d.m.} = \bar{\theta} \times 10^{-(15-16)}\, e{\cdot}\text{cm}\,, \tag{3.13}$$

where $\bar{\theta}$ is the sum of θ and the electroweak, CP-violating phase in the quark mass matrix. Given the measured value, e.d.m. $\leq 10^{-25}\, e{\cdot}$cm (PDG, 2000), this requires $\bar{\theta} \leq 10^{-10}$; far smaller than the CP-violation observed in weak interactions. This is the 'strong CP problem' for which several putative solutions are available in the literature, most prominent of which is the axion. However, we adopt a pragmatic approach and simply set $\theta = 0$; in any case the θ-term does not give rise to any perturbative physics.

The classical QCD Lagrangian density $\mathcal{L}_{\text{class}} = \mathcal{L}_{\text{quark}} + \mathcal{L}_{\text{gauge}}$, described so far, is constructed to be invariant under local gauge transformations. However, this requirement leads to difficulties in formulating the quantum theory. The crux of the problem is the large degeneracy between sets of gluon field configurations which are all equivalent under gauge transformations. The treatment of this

[1] Loosely speaking, the number of twists in the mapping of the 3-sphere, at infinity, into the SU(3) gauge space.

problem requires the apparatus of gauge fixing and ghost fields. Here we provide a heuristic discussion of the solution using the Feynman path integral method; more complete details can be found in any modern quantum field theory text book, such as the one by Peskin and Schroeder (1995).

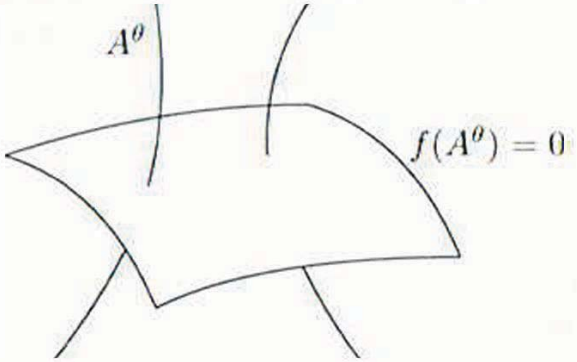

FIG. 3.1. A schematic diagram of gauge field space showing the 'fibres' of gauge equivalent field configurations, A^θ, and the surface defined by the gauge fixing condition, $f(A^\theta) = 0$

In the Feynman path integral approach, quantities of interest are evaluated as averages over all configurations of the quark and gluon fields weighted by the exponential of the action for the fields. This is similar to the use of the partition function in statistical mechanics. It is the naïve functional integral over all the gluon fields, including the gauge equivalent copies, which causes a divergence. This divergence is completely unrelated to those discussed later in the context of renormalization. The basic resolution, due to Faddeev and Popov (1967), is to split the functional integral into an integral over unique elements representing the sets of gauge equivalent field configurations and a common integral over the space of gauge transformations. The latter integral represents a constant (infinite) factor which can be safely dropped. The gauge degeneracy is broken by imposing a gauge fixing condition of the form $f(A^\theta) = 0$. Here A^θ is the transform of the gauge field A under the action of $U(\theta)$, eqn (3.5), and $f(A)$ is a function such that for a given A a solution exists for only one value of the gauge parameters θ. In a non-abelian theory this may be true only if we exclude topologically non-trivial gauge field configurations, which in any case give only very small contributions to the action and do not affect perturbation theory (Gribov, 1978). The situation is illustrated in Fig. 3.1. By inserting the identity in a suitable form, c.f. $1 = \int \mathrm{d}x |\mathrm{d}f/\mathrm{d}x| \delta(f(x))$, and not showing source terms, the fundamental partition function can be symbolically written as

$$Z = \int \mathcal{D}\bar{\psi}\mathcal{D}\psi\mathcal{D}A \exp\left(\frac{\mathrm{i}}{\hbar}\int \mathrm{d}^4x \mathcal{L}_{\mathrm{class}}(\bar{\psi},\psi,A)\right) \times \int \mathcal{D}\theta \det\left|\frac{\delta f(A^\theta)}{\delta\theta}\right| \delta\left(f(A^\theta)\right)$$
$$\rightarrow \int \mathcal{D}\bar{\psi}\mathcal{D}\psi\mathcal{D}A\mathcal{D}\eta^\dagger\mathcal{D}\eta \exp\left(\frac{\mathrm{i}}{\hbar}\int \mathrm{d}^4x \left\{\mathcal{L}_{\mathrm{class}} - \frac{1}{2\xi}f(A)^2 + \eta^\dagger \frac{\delta f(A^\theta)}{\delta\theta}\eta\right\}\right) .$$

(3.14)

Source terms are not shown. In the second line the divergent θ integral has been discarded as the remaining terms are actually θ-independent. Formally, this means that we have redefined the integration measure. The δ-function has been implemented in the action as the quadratic term. The parameter ξ is arbitrary, contributing only to the overall normalization, and as such it cannot enter into any physical quantity, like S-matrix elements, though it may appear in intermediate expressions. As is made clear below, particular choices, such as $\xi = 1$, are often preferred due to the relative simplicity of the resulting gluon propagator. The determinant of the Jacobian matrix is incorporated into the action as an integral over the octet of ghost fields, η^a. These are unphysical, complex valued, Lorentz scalars which obey Fermi–Dirac statistics, that is, they are represented by Grassmann variables, and transform under the adjoint representation of the gauge group. Ghost fields only appear internally in loop diagrams, their physical rôle is discussed in a less abstract fashion in Section 3.3.3.1. The result of these manipulations is the addition of gauge fixing and ghost terms to the Lagrangian density.

The gauge divergence in the path integral which is associated with the gauge degeneracy of the gluon fields manifests itself perturbatively in the lack of a gluon propagator. The addition of a gauge fixing term allows this propagator to be defined. To see how this works consider the popular choice of covariant gauge: $\partial_\mu A^{a\mu} = 0$. As indicated above, this requires two new terms to be added to the classical Lagrangian.

$$\mathcal{L}_{\text{fix+ghost}} = -\frac{1}{2\xi}(\partial_\mu A^{a\mu})(\partial_\nu A^{a\nu}) + \partial_\mu \eta^{a\dagger}\left(\partial^\mu \delta^{ab} + g_s f_{abc} A^{c\mu}\right)\eta^b \tag{3.15}$$

Observe that the bracketed term in the ghost Lagrangian is the appropriate generalization of the covariant derivative for the adjoint representation: $T^a(A)_{bc} = -\mathrm{i}\, f_{abc}$. It provides a kinetic term for the ghost fields and in this covariant gauge a ghost–gluon coupling. Propagators are derived from the quadratic, free particle, terms in the action; for the A^a_μ field these are

$$\begin{aligned} &2S_{\text{gauge}} \\ &= -\mathrm{i}\int \mathrm{d}^4x \left\{(\partial_\mu A^a_\nu - \partial_\nu A^a_\mu)(\partial^\mu A^{a\nu} - \partial^\nu A^{a\mu}) + \frac{1}{\xi}\partial_\mu A^{a\mu}\partial_\nu A^{a\nu} + \mathcal{O}(A^3)\right\} \\ &= +\mathrm{i}\int \mathrm{d}^4x\, A^a_\mu(x)\left[\eta^{\mu\nu}\partial^2 - \left(1 - \frac{1}{\xi}\right)\partial^\mu\partial^\nu\right]\delta_{ab}A^b_\nu(x) \\ &= -\mathrm{i}\int \mathrm{d}^4p\, \tilde{A}^a_\mu(p)\left[\eta^{\mu\nu}p^2 - \left(1 - \frac{1}{\xi}\right)p^\mu p^\nu\right]\delta_{ab}\tilde{A}^b_\nu(p)\,. \end{aligned} \tag{3.16}$$

In the second line, integration by parts is used whilst in the third a Fourier transform, $\partial_\mu \mapsto -\mathrm{i}\, p_\mu$, is used to go to momentum space. The gluon propagator, $\prod(p)^{\mu\nu ab}$, is given by the inverse of the bracketed term.

$$\eta^{\mu\nu}\delta^{ab} = \prod(p)^{\mu}{}_{\sigma}{}^{a}{}_{c} \cdot \mathrm{i}\left[\eta^{\sigma\nu}p^2 - \left(1 - \frac{1}{\xi}\right)p^{\sigma}p^{\nu}\right]\delta^{cb}$$

$$\Longrightarrow \quad \prod(p)^{\mu\nu ab} = \frac{\mathrm{i}}{p^2 + \mathrm{i}\,\epsilon}\left[-\eta^{\mu\nu} + (1-\xi)\frac{p^{\mu}p^{\nu}}{p^2}\right]\delta^{ab} \tag{3.17}$$

It is easy to see that this inverse would not exist in the absence of the gauge fixing term, that is, in the limit $\xi \to \infty$. Since then the momentum-vector p^{μ} would be an eigenvector of the inverse propagator with eigenvalue zero, this results in a matrix with at least one vanishing eigenvalue which cannot be inverted. The $i\epsilon$ term enforces causality. It can be traced to adding a term $+\mathrm{i}\,\epsilon A^{a}_{\mu}A^{a\mu}$ to the action to ensure that the action integral is convergent.

Another popular choice is the axial or physical gauge defined by $n \cdot A^{a} = 0$ where n is a fixed Lorentz four-vector. Sometimes, the additional restriction $n^2 = 1$ or $n^2 = 0$ is applied. The required gauge fixing term is

$$\mathcal{L}_{\mathrm{fix}} = -\frac{1}{2\xi}(n \cdot A^{a})(n \cdot A^{a})\,. \tag{3.18}$$

Since in this axial gauge the corresponding ghost term only contains the kinetic piece and does not couple ghosts to any other fields, the ghosts may be trivially integrated out and need not be considered further. The corresponding, momentum space, gluon propagator is given by

$$\prod(p)^{\mu\nu ab} = \frac{\mathrm{i}}{p^2 + \mathrm{i}\,\epsilon}\left[-\eta^{\mu\nu} + \frac{n^{\mu}p^{\nu} + p^{\mu}n^{\nu}}{n \cdot p} - (n^2 + \xi p^2)\frac{p^{\mu}p^{\nu}}{(n \cdot p)^2}\right]\delta^{ab}\,. \tag{3.19}$$

Now, in any gauge the gluon propagator can be decomposed into a weighted sum of direct products of polarization vectors $\epsilon(p)^{\mu}$ for the off mass-shell gluon:

$$\prod(p)^{\mu\nu} = \frac{\mathrm{i}}{p^2 + \mathrm{i}\,\epsilon}\sum_{T,L,S} C_i \cdot \epsilon(p)^{\mu}_{i}\epsilon^{*}(p)^{\nu}_{i}\,, \tag{3.20}$$

where, in general, the sum includes contributions from two transverse (T), one longitudinal (L) and one scalar component (S). Significantly, for an axial gauge in the on mass-shell limit, $p^2 = 0$, only the physical, transverse polarizations propagate ($C_L = C_S = 0$). This proves to be very useful in situations where physical arguments are to be used. The price to be paid is the relative complexity of the propagator, in particular the presence of the spurious singularities in $(n \cdot p)^{-1}$ which require a careful treatment in terms of principal values (Leibbrandt, 1987). In practice, it proves popular to use the Feynman gauge for higher order calculations and the axial gauges to gain physical insight.

Finally, we give the complete QCD Lagrangian density, in the covariant gauge:

$$\mathcal{L}_{\mathrm{QCD}} = \bar{q}_j(x)[\mathrm{i}\,\partial\!\!\!/ - m]q_j(x)$$
$$-\frac{1}{2}\left[(\partial_{\mu}A^{a}_{\nu} - \partial_{\nu}A^{a}_{\mu})(\partial^{\mu}A^{a\nu} - \partial^{\nu}A^{a\mu}) + \frac{1}{\xi}(\partial^{\mu}A^{a}_{\mu})(\partial^{\nu}A^{a}_{\nu})\right]$$

$$+(\partial^\mu \eta^{a\dagger})(\partial_\mu \eta^a) - g_s T^a_{jk} \bar{q}_j(x) \not{A}^a q_k(x) + g_s f_{abc} (\partial_\mu \eta^{a\dagger}) \eta^b A^{c\mu}$$
$$+g_s f_{abc} (\partial_\mu A^a_\nu) A^{b\mu} A^{c\nu} - \frac{g_s^2}{4} f_{abc} f_{adc} A^{b\mu} A^{c\nu} A^d_\mu A^e_\nu \qquad (3.21)$$

This has been separated into the quadratic parts and the remaining 'perturbations' which are proportional to either g_s or g_s^2. The first three terms give rise to the quark, gluon and ghost propagators, the fourth and fifth the quark–gluon and ghost–gluon vertices, whilst the sixth and seventh terms give rise to triple- and quartic-gluon vertices. The corresponding Feynman rules are detailed in Appendix B, together with those for the axial gauge.

3.2 The QCD description of basic reactions

In the following section, we attempt to give an overview of three basic aspects of hadron production in collider experiments. These are: a summary of the actual properties of the events that are seen in lepton–lepton, lepton–hadron and hadron–hadron collisions; an outline of these events' formal description using QCD; and an insight into the physical pictures which guide people's thinking.

In general, the use of QCD to describe a reaction means the use of perturbative QCD (pQCD). This restriction is purely practical and merely reflects our present inability to calculate more than a few non-perturbative properties within QCD. The applicability of perturbation theory relies on the strong coupling being small. A very important property of QCD is that the size of the strong coupling varies with the size of the characteristic momentum transfer in a process. The coupling runs in such a way that it is small for large momentum transfers, $Q \gg \Lambda_{\rm QCD}$, and large for small momentum transfers. To leading order one has

$$\alpha_s(Q^2) \equiv \frac{g_s^2(Q^2)}{4\pi} = \frac{1}{\beta_0 \ln(Q^2/\Lambda^2_{\rm QCD})} \,. \qquad (3.22)$$

Here $\Lambda_{\rm QCD}$ is an energy scale at which non-perturbative effects become important. Experimentally, it is found to be $\mathcal{O}(200)$ MeV, that is, the mass scale of hadronic physics as given by the pion mass or equivalently the inverse of a typical hadron size R_0. The coefficient $\beta_0 > 0$ in eqn (3.22) is defined in Section 3.4.5. The appearance of the scale $\Lambda_{\rm QCD}$ and the running of the coupling is a subtle aspect of renormalizable theories, such as QCD, which we shall discuss later. As a consequence, the major part of this book is dedicated, necessarily, to discussing hard processes that involve a large momentum transfer. This may arise naturally, as for example in the production of a heavy particle, or may be engineered, by, for example, only considering jets with large transverse energies. Of course, we do need to discuss non-perturbative aspects of QCD, in particular hadronization. Here, when detailed descriptions are needed, we must mainly rely on models rather than theoretically secure QCD predictions. Fortunately, the effects of hadronization on pQCD predictions appear to be modest.

Restricting our attention to large momentum transfer processes, $Q^2 \gg \Lambda_{\rm QCD}$ with $\Lambda_{\rm QCD} \sim R_0^{-1}$, implies, by virtue of the uncertainty principle, that we see

nature on a small, sub-nuclear scale. At these scales hadrons appear to be composed of the (anti)quarks and gluons which appear in the QCD Lagrangian. Furthermore, they are only weakly self-interacting thanks to the running strong coupling. This allows the individual, target hadrons to be characterized by parton density functions (p.d.f.s) describing the distributions of partons as a function of the fraction of their parent hadron's momentum that they carry. In the parton model, cross sections for hard processes are calculated in terms of the tree-level scattering or annihilation of individual (anti)quarks and gluons convoluted with the appropriate p.d.f.s. What gives this statement its power is the fact that the p.d.f.s are independent of the hard subprocess. In essence what we have is that the cross section can be factorized into a process dependent, short-distance, hard subprocess, involving partons, and a process independent, long-distance part, the p.d.f.s, describing the hadrons involved.

Now, many of the hard subprocesses of interest are electroweak in nature so that QCD really only enters via the higher order corrections. Two important features of this QCD improved parton model are the dependence of the p.d.f.s on the hard scale of the interaction and the appearance of multiparton final states. It is the QCD improved parton model that provides the framework for most of what follows.

As we have just said, calculations in pQCD are carried out in terms of the quark and gluon degrees of freedom appearing in the QCD Lagrangian rather than the colourless hadrons observed in experiments. The confinement transition from the almost free partons to the bound state hadrons is still not well understood but must be addressed before making comparisons with experiment. Fortunately, given the necessary restriction to hard processes, it is believed that non-perturbative effects, which involve small momentum transfers, $Q \leq \Lambda_{\rm QCD}$, do not spoil parton level predictions. This can be seen in two complementary ways. First, the disparity in momentum transfers argues that the perturbative features of an event can not be modified significantly by hadronization without introducing a new, perturbative scale. Second, the uncertainty principle can be used to relate the four-momentum of a virtual particle, Q^μ, to the space time distance it travels, Q^μ/Q^2; see Ex. (3-2). Thus, perturbative physics takes place on short-distance scales, whilst non-perturbative effects are long range in nature and can only have limited effect on the widely separated hard partons.

Two basic approaches are available to calculate hadronic event properties within pQCD. One approach is fixed-order perturbation theory, the other one is based on a summation of leading logarithms.

To describe a given type of event using fixed order perturbation theory, its dominant features are identified, typically collimated sprays of hadrons known as jets, and these are associated with well separated primary partons. In the absence of flavour tagging these may be either quarks or gluons. In this way the event is matched to a scattering amplitude containing the primary partons as external states. This amplitude is described by a sequence of ever more complex Feynman diagrams which may be grouped into sets according to how

many gauge couplings, $g_s = \sqrt{4\pi\alpha_s}$, they contain. The simplest set of (tree) diagrams contribute to the cross section, which is proportional to the amplitude squared, at $\mathcal{O}(\alpha_s^n)$ where the power n is characteristic of the process. In gluon–gluon scattering, for example, one has $n = 2$, whilst for three-jet production in e^+e^- annihilation it is $n = 1$. This is the *leading order* (LO) approximation. The next simplest set of (one-loop) diagrams contribute at $\mathcal{O}(\alpha_s^{n+1})$; this is the *next-to-leading order* (NLO) approximation, etc. Given a sufficiently small coupling, this perturbation series should converge to the correct answer as more terms are added. In practice, the series is expected to be only asymptotically convergent so that beyond a certain order the numerical evaluation of the series begins to diverge from the true answer.

A complication arises in this approach because tree-level diagrams diverge whenever external partons become soft or collinear and related divergences arise in virtual (loop) diagrams. This is in addition to the ultraviolet divergences treated by renormalization. Fortunately, in sufficiently inclusive measurements, such as the total hadronic cross section, it is guaranteed that the two sets of divergences cancel. Unfortunately, in more exclusive quantities, which involve restricted regions of the external partons' available phase space, the cancellation is less complete and large logarithmic terms remain, generically of the form $L = \ln(Q^2/Q_0^2)$. Since $\alpha_s(Q^2)L$ is of order unity for $Q^2 \gg Q_0^2$, see eqn (3.22), this can spoil the convergence of finite order perturbation theory.

In the second approach, the original perturbation series is rearranged in terms of powers of $\alpha_s L$.

$$\mathrm{d}\sigma = \sum_n a_n(\alpha_s L)^n + \alpha_s(Q^2)\sum_n b_n(\alpha_s L)^n + \cdots \tag{3.23}$$

The first, infinite set of terms represent the *leading logarithm approximation* (LLA), then comes the genuinely α_s-suppressed next-to-LLA (NLLA) and so on. Since the enhanced regions of phase space involve near collinear or soft gluon emission, it is favourable for the primary partons to dress themselves with a shower of near collinear or soft partons. These are the parton precursors of hadronic jets. An important feature of such multiparton matrix elements is that in the enhanced regions of phase space they factorize into products of relatively simple expressions allowing significant simplifications in the treatment of leading logarithms. In some cases, it is actually possible to sum analytically the LLA- and NLLA-series to all orders in α_s.

The emerging picture of an event follows a sequence of decreasing scales. A genuinely hard subprocess produces a number of primary partons which then undergo semi-hard gluon radiation resulting in showers of soft partons which ultimately hadronize. The main features of an event are determined during its perturbative stages, thereby allowing tests of (p)QCD. In the following subsections we describe the basic phenomenology of the three main types of particle collision and how QCD applies to them.

3.2.1 *Electron–positron annihilation*

Electron–positron annihilation to hadrons provides the simplest colliding beam processes that can be described using pQCD. The simplicity follows from both the well-defined energies of the initial state particles and the fact that the leptons interact via a weakly coupled, colour singlet, virtual photon. This allows a clean separation of the initial and final state particles. The combined momentum of the incoming leptons provides a large scale justifying the use of pQCD. In the parton model the basic interaction is an electroweak process, $e^+e^- \to \gamma^*/Z \to q\bar{q}$; this has essentially the same cross section as the well established process $e^+e^- \to \mu^+\mu^-$. It is usually adequate to consider single photon exchange due to the small value of the electromagnetic coupling $\alpha_{em} = e^2/(4\pi) \approx 1/137$. The structure of the hadronic final state depends only on the centre-of-momentum (C.o.M.) energy, $\sqrt{s}$, of the collision and if polarized the polarizations of the incoming leptons. The C.o.M. system is often also referred to as 'centre-of-mass' system, since in the system where the momenta balance, the centre-of-mass of the interacting particles is at rest. Dealing with relativistic particles, however, the name 'centre-of-momentum' is more to the point.

At low C.o.M. energies, $0 \leq \sqrt{s} \leq 5\,\text{GeV}$, the most interesting quantity is the total hadronic cross section. This shows a lot of structure characterized by 'steps' at quark thresholds together with strong resonances, associated with $q\bar{q}$ bound states that possess the same quantum numbers as the exchanged photon. In essence the off mass-shell photon behaves as a $J^{PC} = 1^{--}$ vector meson: ρ, ω, ϕ, J/ψ, $\Upsilon(1S)$, etc. The hadronic final state is characterised by low multiplicities and only modest structure. It can be described adequately by a mix of isotropic phase space and resonance decays.

As the C.o.M. energy increases, the final state hadrons show a tendency to align along an axis and a back-to-back two-jet structure begins to appear. This is followed, at around $\sqrt{s} = 30\,\text{GeV}$, by the emergence of three-jet features in a fraction, $\mathcal{O}(10\%)$, of the events. By identifying these jets with primary partons it is possible to test the nature of QCD's basic constituents and their couplings. For example, three-jet events are believed to be a manifestation of vector gluon emission in the process $e^+e^- \to q\bar{q}g$. An example of a three-jet event is shown in Fig. 6.1. The rate of this three-jet production gives a measure of the strong coupling, α_s, whilst the angular distribution of the jets reflects the spin-1 nature of the gluon. At even higher energies, small fractions of well separated four, five and more jet events appear, allowing tests of the triple and quartic gluon couplings. Note that these jets are required to be well separated to avoid the collinear and soft enhancements that would invalidate fixed order perturbation theory, thereby complicating any comparisons to theory. A more precise definition of a jet is given in Section 6.2.

On dimensional grounds the total cross section must take the form

$$\sigma(s) = \frac{1}{s} f\left(\frac{m_i^2}{s}\right) , \tag{3.24}$$

where the $\{m_i\}$ represent the relevant masses, such as quark or hadron masses. The function $f(x_i)$ tends to a non-zero constant as $x_i \to 0$. Since the quark and hadron masses are mostly small, their effect becomes negligible as s increases and the cross section falls as s^{-1}, as prescribed by the photon propagator. This remains true until around $\sqrt{s} = 40\,\text{GeV}$ when deviations begin to be seen: this is the tail of the Z resonance which becomes dominant at $\sqrt{s} = 91\,\text{GeV}$. Apart from the large enhancement in the total cross section, the main effect of Z exchange is to modify the flavour mix of produced quarks and to introduce asymmetries into the polar angle distributions of the primary quarks, compared to pure photon exchange. Above $\sqrt{s} = 91\,\text{GeV}$, photon and Z exchange remain of comparable importance, but the total hadronic cross section continues to fall and becomes of less relative importance as other production channels, such as $e^+e^- \to W^+W^-$, open up.

An example of a less inclusive quantity in e^+e^- annihilation is the cross section for the production of a specific type of hadron in the final state. Suppose this hadron, h, has momentum p^μ, then the differential cross section can be written in the form of a convolution

$$\mathrm{d}\sigma^{e^+e^- \to hX}(p,s) = \sum_a \int_0^1 \frac{\mathrm{d}z}{z} \mathrm{d}\hat{\sigma}^{e^+e^- \to aX}\left(\frac{p}{z}, s\right) D_a^h(z)\,. \qquad (3.25)$$

The first term, $\mathrm{d}\hat{\sigma}$, is the hard cross section for the production of a parton a such that it carries momentum p^μ/z. The second term is a fragmentation function, $D_a^h(z)dz$, which gives the probability that the parton a produces the hadron h carrying a fraction z of the primary parton's momentum. This fragmentation function is the final state analogue of the previously mentioned p.d.f.s, to be discussed more fully in Section 3.2.2. The product of these two terms is summed over all the possible contributing partons and integrated over the momentum fractions. The factorization is between a perturbatively calculable, short-distance cross section and a non-perturbative fragmentation function. It is important to realize that $\hat{\sigma}$ does not depend on the identity of the hadron h, which would be a long-distance effect, but only on the parton a and the colliding beams. Conversely, D_a^h does not depend on the short-distance, hard subprocesses; in this sense it is universal and can be applied to any subprocess that produces the outgoing parton a.

At the lowest order the relevant hard subprocess is $e^+e^- \to q\bar{q}$, so that in eqn (3.25) the sum is over quarks with $2m_q < \sqrt{s}$. This gives the parton model prediction for which, as indicated, the fragmentation function depends only on the momentum fraction z. The inclusion of QCD corrections complicates matters, though the basic factorized form remains the same. In particular, renormalization requires the introduction of an arbitrary renormalization scale, μ_R, whilst the factorization procedure introduces a second, arbitrary factorization scale, μ_F. This acts as a cut-off on the virtuality of intermediate particles, equivalent to a cut-off on the (inverse) distance it travels. The exact origin of the scales μ_R and

μ_F will become clear in Sections 3.4 and 3.6. The QCD improved parton model prediction is

$$\mathrm{d}\sigma^{\mathrm{e^+e^-}\to\mathrm{h}X}(p,s) = \sum_a \int_0^1 \frac{\mathrm{d}z}{z} \mathrm{d}\hat{C}^{\mathrm{e^+e^-}\to aX}\left(\frac{p}{z}, s; \mu_R, \mu_F\right) D_a^{\mathrm{h}}(z; \mu_R, \mu_F), \quad (3.26)$$

where the parton sum now includes contributions from gluons. Here the coefficient function $\hat{C}$ is derived from the partonic cross section for the subprocess, $\mathrm{e^+e^-} \to aX$. Thanks to its short-distance nature $\hat{C}$ is calculable using pQCD and is devoid of any divergences. On the other hand, D_a^{h} is not calculable with today's technology and therefore must be determined from experiment. That said, the dependence on the scale μ_F, which is introduced in order to separate short- and long-distance effects, is calculable. Recall that both μ_R and μ_F are arbitrary as are aspects of the renormalization and factorization schemes. However, the physical cross section, on the left-hand side of eqn (3.26), is independent of the particular scales and schemes used, provided that the same choices are used consistently in both $\hat{C}$ and D_a^{h}. Whilst not necessary, it is common practice to only consider the case that $\mu_R = \mu_F (= \sqrt{s})$.

A simplification in the above description of electron–positron annihilation is the assumption that the colliding leptons are mono-energetic. This is not true. In a process known as bremsstrahlung they decelerate into the collision by emitting photons which reduces the effective C.o.M. energy. This *initial state photon radiation* (ISR) may be treated using structure functions (perhaps more properly called electron density functions) (Kleiss *et al.*, 1989). The idea is that the incident electron is really surrounded by a cloud of photons and further $\mathrm{e^+e^-}$ pairs. What the structure function, $f_{\mathrm{e/e}}(x, \mu^2)$, gives is the probability density for finding an electron in this cloud of particles carrying a fraction x of the parent electron's momentum when it is probed at a scale μ. The electron–positron collision is then between these constituents. Summing up all the contributions gives

$$\mathrm{d}\sigma_{\mathrm{ISR}}(s) = \int_0^1 \mathrm{d}x_1 \int_0^1 \mathrm{d}x_2\, f_{\mathrm{e/e}}(x_1, s) f_{\mathrm{e/e}}(x_2, s)\, \mathrm{d}\hat{\sigma}(\hat{s} = x_1 x_2 s)\,. \quad (3.27)$$

On the assumption of massless electrons, the C.o.M. energy squared in the hard subprocess is given by $\hat{s} \equiv (x_1 p_{\mathrm{e^-}} + x_2 p_{\mathrm{e^+}})^2 = x_1 x_2 s$. It is possible to calculate this structure function in QED perturbation theory. An approximate form is

$$f_{\mathrm{e/e}}(x, \mu^2) = \beta(1-x)^{\beta-1} \quad \text{with} \quad \beta(\mu^2) = \frac{2\alpha_{\mathrm{em}}}{\pi}\left[\ln\left(\frac{\mu^2}{m_{\mathrm{e}}^2}\right) - 1\right]. \quad (3.28)$$

In practice, one has $0 < \beta \ll 1$ so that $f_{\mathrm{e/e}}(x, \mu^2)$ acquires an integrable singularity for $x \to 1$, which favours soft photon emission. Whilst the singularity can be treated analytically, its treatment in a numerical implementation takes some care. (Computers don't handle singularities very well ...)

The effect of initial state photon emission on a total cross section is strongly influenced by the C.o.M. energy dependence of the hard subprocess cross section. There is a trade-off between the two terms in eqn (3.27). If s is tuned to lie on a resonance then any ISR will reduce the effective C.o.M. energy, $\hat{s} = x_1 x_2 s$, and $d\tilde{\sigma}(\hat{s})$ will be significantly reduced compared to $d\hat{\sigma}(s)$. In this case, the effect of ISR is modest, only distorting the resonance's line shape. However, if s is tuned to lie above a resonance then any ISR which reduces s to $\hat{s} \approx m_R^2$ is favoured by the increase in cross section. For an illustration see Fig. 6.3. Such 'radiative returns' can have a major impact on the line shape and lead to individual events being thrown to the left or right according to the energy imbalances in the post bremsstrahlung leptons actually entering the hard subprocess.

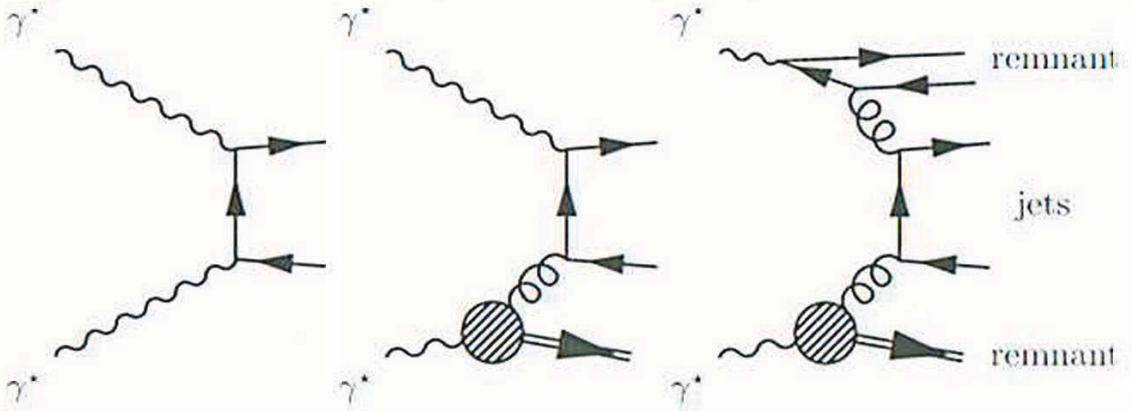

FIG. 3.2. Left, direct $\gamma\gamma$ interaction with QED photon–quark couplings. Centre, singly resolved $\gamma\gamma$ interaction with the lower photon behaving as a collection of partons characterized by its own p.d.f. Right, doubly resolved $\gamma\gamma$ interaction; in the upper photon the partons can be traced to a pointlike component originating from a perturbative $\gamma^* \to q\bar{q}$ vertex, whilst in the lower photon the 'remaining' hadron-like partons have a non-perturbative origin.

Not all the photons emitted as bremsstrahlung escape without interacting. A rich variety of processes resulting in resonance pairs, jet events etc. can occur due to photon–photon interactions (Aurenche *et al.*, 1996). Indeed, the total cross section for $e^+e^- \to e^+e^-$ + hadrons grows as $\ln^2(s/m_e^2)$. A source of this complexity is that photons, as sketched in Fig. 3.2, are not as simple as might be naïvely thought. The reader is warned that the notations used to describe photons have become rather confused in the literature. Here we follow Chyla (2001). We are familiar with the idea of a direct photon which has pointlike couplings and can lead to hadron production via the hard subprocess $\gamma^*\gamma^* \to q\bar{q}$. In addition, there are resolved photons that behave as dense clouds of (anti)quarks and gluons. Such a photon behaves like a hadron and is characterized by parton density functions. A pointlike component of these partons can be traced back to an initial QED vertex $\gamma^* \to q\bar{q}$ and the subsequent radiation of gluons which in turn may split into gluon-pairs or further $q\bar{q}$-pairs (Witten, 1977).

A hadron-like component accounts for the remaining partons which have their origins in non-perturbative physics, perhaps associated with the (negative virtuality) photon fluctuating into a vector meson. This opens up the possibility of effective lepton–hadron, known as singly resolved, and hadron–hadron, known as doubly resolved, collisions. These are discussed in detail below. All these types of $\gamma\gamma$-events are characterized by low C.o.M. energies and sizeable longitudinal momentum imbalances. Often these events constitute a hadronic background to the events of real interest in an experiment.

We also mention one further complication. At very high energies it is necessary to use beams with very small transverse sizes in order to increase the luminosity and compensate for the falling cross section. This gives very high charge density particle bunches whose intense electromagnetic fields can induce radiation in one another as they approach each other, the so-called beamstrahlung. The details of this depend on the specifics of the beam profile, but can be treated in a similar vein to bremsstrahlung (Palmer, 1990).

3.2.2 *Lepton–hadron scattering*

Lepton–hadron scattering is a traditional method of probing the structure of hadrons. Since hadrons are now known to be composite particles with partonic, (anti)quark and gluon, constituents, such collisions are more complex to describe than lepton–lepton collisions. In essence, we view the observed scattering, $\ell\,\mathrm{h} \to \ell' X$, as a manifestation of the hard subprocess $\ell\mathrm{q} \to \ell'\mathrm{q}'$. The advantage of lepton probes is that they undergo experimentally and theoretically clean, pointlike interactions which are describable in terms of the exchange of a single, virtual, gauge boson. Multiple boson exchange, whilst possible, is suppressed by additional factors of the electroweak couplings, α_{em}^2 or G_{F}^2. A basic classification of the events is based on the nature of the boson exchanged by the initial lepton and quark. In neutral current events, characterized by $\ell = \ell'$, a photon or Z is exchanged. Whilst in charged current events, characterized by $\ell = \mathrm{e},\ \mu,\ \tau$ and $\ell' = \nu_{\mathrm{e}},\ \nu_\mu,\ \nu_\tau$ or vice-versa, a $\mathrm{W}^\pm$ is exchanged. For charged leptons the exchanged particle is predominantly a photon. Weak boson, Z or $\mathrm{W}^\pm$, exchange is observed, however, at low $Q^2 \ll M_{\mathrm{W}}^2$ their contributions are many orders of magnitude lower, $\mathcal{O}(G_{\mathrm{F}}^2/\alpha_{\mathrm{em}}^2)$. If a neutrino beam is used, only weak interactions can occur, making them a useful probe to disentangle the contributions from quarks and antiquarks.

Figure 2.1 illustrates the basic process underlying lepton–hadron scattering as viewed from the target hadron's rest frame. This frame coincides with the laboratory frame for fixed target experiments. To date, only the HERA machine at DESY provides (asymmetric) colliding beams of electrons/positrons and protons. Once the square of the C.o.M. energy, $s = (\ell + p)^2$, is fixed, the most important quantity for describing the scattering is the momentum transfer $q^\mu = \ell^\mu - \ell'^\mu$ and the Lorentz invariant $Q^2 \equiv -q^2 > 0$. The significance of Q^2 is that it characterizes the wavelength, or resolving power, of the probe. Also of interest is ν, the energy transferred to the target hadron. For a charged lepton neutral current

event these can be determined experimentally by measuring the energy and angular deflection θ of the scattered lepton. Neglecting the relatively small lepton masses one finds

$$\begin{aligned} Q^2 &\equiv -(\ell - \ell')^2 & \nu &\equiv (\ell - \ell') \cdot p / M_{\rm h} \\ &= +4E_\ell E_{\ell'} \sin^2(\theta/2) & &= (E_\ell - E_{\ell'})|_{\rm rest} \ . \end{aligned} \tag{3.29}$$

In addition, experiments may also measure details of the hadronic final state, X. This can provide complementary, or indeed when $\ell' = \nu$ the only determination of Q^2 and ν. The invariant mass, W, of the hadronic final state is given by

$$\begin{aligned} W^2 &= (p+q)^2 \\ &= M_{\rm h}^2 + 2M_{\rm h}\nu - Q^2 \ . \end{aligned} \tag{3.30}$$

$$\text{If} \quad W^2 = M_{\rm h}^2 \quad \Longrightarrow \quad Q^2 = 2M_{\rm h}\nu \ .$$

In the special case of elastic scattering, when the target hadron remains intact in the final state, eqn (3.30) implies that Q^2 and ν are not independent.

The formal description of lepton–hadron scattering is facilitated greatly by the 'factorized' nature of the interaction. Details of the calculations can be found in the following sections. In terms of the leptonic and hadronic currents the matrix element is given by

$$\mathcal{M}(\ell {\rm h} \to \ell' X) = \langle \ell' | J_\mu | \ell \rangle g_{\ell V} \frac{-\eta^{\mu\nu}}{q^2 - M_V^2} g_{{\rm h}V} \langle X | J_\nu | {\rm h} \rangle \tag{3.31}$$

where the electroweak couplings have been factored out: $g_{fV}^2 = \kappa_V^2 (v_{fV}^2 + a_{fV}^2)$, see Appendix B. In (high-Q^2) neutral current events the matrix element should include both γ and Z exchange contributions. Equation (3.31) suggests writing the inclusive lepton–hadron scattering cross section in terms of two tensors $L_{\mu\nu}$ and $H^{\mu\nu}$ as

$$\begin{aligned} {\rm d}\sigma^{\ell {\rm h}} &= \frac{1}{4\ell \cdot p} \frac{(g_{\ell V} g_{{\rm h}V})^2}{(Q^2 + M_V^2)^2} L_{\mu\nu} H^{\mu\nu} (4\pi) \frac{{\rm d}^3 \ell'}{2E_{\ell'}(2\pi)^3} \qquad \text{with} \\ L_{\mu\nu} &= \frac{1}{2} \langle \ell | J_\mu^\dagger | \ell' \rangle \langle \ell' | J_\nu | \ell \rangle \qquad \text{and} \\ H^{\mu\nu} &= \frac{1}{2 \cdot 4\pi} \sum_X \langle {\rm h} | J^{\dagger\mu} | X \rangle \langle X | J^\nu | {\rm h} \rangle (2\pi)^4 \delta^{(4)}(p_X - k - p) \ . \end{aligned} \tag{3.32}$$

The hadronic tensor is summed over all the allowed final states and by convention includes a factor $(4\pi)^{-1}$ and an overall four-momentum conserving δ-function. Also, the definition of both tensors includes an average over spins on the assumption that the incoming particles are unpolarized. As mentioned earlier, the simplicity of leptons means that the tensor $L_{\mu\nu}$ is calculated readily to be

$$L_{\mu\nu} = 2\left[\ell_\mu \ell'_\nu + \ell'_\mu \ell_\nu - (Q^2/2)\eta_{\mu\nu} + {\rm i} C_{\ell V} \epsilon_{\mu\nu}{}^{\sigma\tau} \ell_\sigma \ell'_\tau\right] + 2D_{\ell V} m_\ell^2 \eta_{\mu\nu} \ . \tag{3.33}$$

The last two terms are associated with parity violation. The coefficient $C_{\ell V} = 2a_{\ell V} v_{\ell V}/(v_{\ell V}^2 + a_{\ell V}^2)$ depends on the type of vector boson emitted by the incoming

lepton. For a photon it is $C_{\ell\gamma} = 0$, for a W boson one has $C_{\ell W^+} = +1$ (ν_ℓ or ℓ^+ beam) and $C_{\ell W^-} = -1$ ($\bar{\nu}_\ell$ or ℓ^- beam), respectively. The last term, with coefficient $D_{\ell V} = (v_{\ell V}^2 - a_{\ell V}^2)/(v_{\ell V}^2 + a_{\ell V}^2)$, is suppressed by a relative factor m_ℓ^2/Q^2 and is almost always neglected. It is not straightforward to calculate the hadronic tensor. However, since it must be constructed from the only available four-vectors, p^μ and q^μ, and the two isotropic tensors, $\eta^{\mu\nu}$ and $\epsilon^{\mu\nu\sigma\tau}$, it is possible to write down its general form as

$$H^{\mu\nu} = -F_1\eta^{\mu\nu} + \left[F_2 p^\mu p^\nu + \mathrm{i}\,F_3\epsilon^{\mu\nu}{}_{\sigma\tau}p^\sigma q^\tau + (F_4 + \mathrm{i}\,F_5)p^\mu q^\nu + (F_4 - \mathrm{i}\,F_5)q^\mu p^\nu + F_6 q^\mu q^\nu\right](p\cdot q)^{-1}\,. \tag{3.34}$$

Here, the hadron specific structure functions, F_i, are dimensionless (thanks to the factor of $(p\cdot q)^{-1}$), Lorentz scalars. It is also common to see eqn (3.34) defined in terms of the equivalent structure functions $W_1 = F_1$ and $W_{2-6} = (M_\mathrm{h}^2/p\cdot q)F_{2-6}$. We do not do this as it only adds unnecessarily to the notational burden. If the spin of the colliding particles is specified, then extra terms, containing S_ℓ^μ and S_h^μ, would be possible in eqn (3.34). Terms involving further four-momenta would arise also if measurements are made on the hadronic final state.

Quantum mechanics and symmetries impose important constraints on the F_i (Treiman *et al.*, 1972). As defined in eqn (3.34) they are all real. The time reversal invariance of QCD implies that $F_5 = 0$. As we shall learn in Section 3.3.1, electromagnetic gauge invariance implies the following current conservation constraints

$$q_\mu \cdot H^{\mu\nu} = 0 \quad \text{and} \quad H^{\mu\nu}\cdot q_\nu = 0\,. \tag{3.35}$$

A similar, approximate constraint applies to the weak currents. By imposing eqn (3.35), see Ex. (3-3), the form of the hadronic tensor is restricted further to

$$H^{\mu\nu} = F_1\left(-\eta^{\mu\nu} + \frac{q^\mu q^\nu}{q^2}\right) + \frac{F_2}{p\cdot q}\left(p^\mu - \frac{p\cdot q}{q^2}q^\mu\right)\left(p^\nu - \frac{p\cdot q}{q^2}q^\nu\right) + \mathrm{i}\frac{F_3}{p\cdot q}\epsilon^{\mu\nu\sigma\tau}p_\sigma q_\tau\,. \tag{3.36}$$

If we do not impose eqn (3.35) then we must add residual F_4' and F_6' structure functions, *à la* eqn (3.34), to eqn (3.36) but these would be suppressed as $(m_\ell m_\mathrm{q}/Q^2)^2$, c.f. eqn (3.33), and will not subsequently trouble us (Jaffe and Llewellyn-Smith, 1973). Combining eqn (3.36) with eqn (3.33), which satisfies also the equivalent of eqn (3.35), gives

$$L_{\mu\nu}\cdot H^{\mu\nu} = F_1 2Q^2 + \frac{F_2}{p\cdot q}\left[4(p\cdot\ell)(p\cdot\ell') - M_\mathrm{h}^2Q^2\right] - C_{\ell V}\frac{F_3}{p\cdot q}p\cdot(\ell+\ell')Q^2\,, \tag{3.37}$$

where we used $\epsilon_{\mu\nu\sigma\tau}\epsilon^{\mu\nu}{}_{\sigma'\tau'} = -2[\eta_{\sigma\sigma'}\eta_{\tau\tau'} - \eta_{\sigma\tau'}\eta_{\sigma'\tau}]$. Applying this result in eqn (3.32) gives the general expression for unpolarized, inclusive lepton–hadron scattering; see also Ex. (3-4):

$$\frac{\mathrm{d}^2\sigma^{\ell\mathrm{h}}}{\mathrm{d}E'\mathrm{d}\cos\theta} = 8\pi\frac{\alpha_{\ell V}\alpha_{\mathrm{h}V}}{(Q^2 + M_V^2)^2}\frac{E'^2}{M_\mathrm{h}}$$

$$\times \left\{ \left[2F_1 - C_{\ell V} F_3 \frac{E+E'}{E-E'} \right] \sin^2(\theta/2) + F_2 \frac{M_\mathrm{h}}{E-E'} \cos^2(\theta/2) \right\}$$

$$\frac{\mathrm{d}^2\sigma^{\ell\mathrm{h}}}{\mathrm{d}x\mathrm{d}Q^2} = \frac{4\pi}{x} \frac{\alpha_{\ell V}\alpha_{\mathrm{h}V}}{(Q^2+M_V^2)^2}$$

$$\times \left\{ xy^2 F_1 + \left(1 - y - \frac{(xyM_\mathrm{h})^2}{Q^2} \right) F_2 - C_{\ell V} x \left(y - \frac{y^2}{2} \right) F_3 \right\}$$

$$= \frac{y}{Q^2} \times \frac{\mathrm{d}^2\sigma^{\ell\mathrm{h}}}{\mathrm{d}x\mathrm{d}y} \,. \tag{3.38}$$

Here, we have defined $\alpha_{fV} = g_{fV}^2/(4\pi)$. The first form uses the energy and angle of the scattered lepton in the target rest frame. The second and third form use the Lorentz invariant variables Q^2, defined in eqn (3.29), and x and y defined by

$$\left. \begin{aligned} x &= \frac{Q^2}{2M_\mathrm{h}\nu} \\ y &= \frac{q\cdot p}{\ell\cdot p} = \left.\frac{E-E'}{E}\right|_{\mathrm{rest}} \end{aligned} \right\} \quad \Longrightarrow \quad s = \frac{Q^2}{xy} + M_\mathrm{h}^2 \,. \tag{3.39}$$

In this framework all information on the possible scatterings resides in the structure functions F_{1-3}. These, in turn, may be only functions of dimensionless ratios of Q^2, $p\cdot q$ and 'M^2', where 'M' represents any mass (or inverse length) characteristic of the hadron.

At low C.o.M. energy and low Q^2, $\lesssim 0.01\,(\mathrm{GeV})^2$, elastic, electromagnetic scattering is dominant (Taylor, 1975). Since $Q^2 = 2M_\mathrm{h}\nu$ for an elastic scattering the structure functions $F_{1,2}$ have to be functions of $Q^2/$'M^2' or be constant; $F_3 = 0$ for purely electromagnetic processes. Furthermore, the long wavelength of the exchanged photon means that the target hadron is seen as a coherent whole, so that 'M' must be a macroscopic property of the hadron. In this low-virtuality limit the form of the hadronic current is actually known to be

$$J^\mu = \frac{1}{2M_\mathrm{h}} \bar{u}(p') \left[(p+p')^\mu \mathcal{F}_1(Q^2, \text{`}M\text{'}) + \mathrm{i}\,(\mu_\mathrm{h} - 1) q_\nu \sigma^{\nu\mu} \mathcal{F}_2(Q^2, \text{`}M\text{'}) \right] u(p) \,. \tag{3.40}$$

Here μ_h is the magnetic moment of the hadron measured in units of the nuclear magneton, $eh/(2M_\mathrm{p})$, and $\mathcal{F}_1$ and $\mathcal{F}_2$ correspond directly to the electric and magnetic form factors of the hadron. For the proton and the neutron $\mu_\mathrm{p} = +2.793$ and $\mu_\mathrm{n} = -2.913$ respectively. These form factors can be related to the Fourier transform of the hadron's electric charge distribution. Using eqn (3.40) in eqn (3.32) gives the Rosenbluth formula, which takes the form of eqn (3.38) with F_1 and F_2 given in terms of $\mathcal{F}_1$ and $\mathcal{F}_2$. Empirically, the two form factors are both described well by the dipole formula which corresponds to a spherically symmetric, exponentially falling charge distribution. One has

$$\rho(\boldsymbol{r}) = \frac{\mathrm{e}^{-|\boldsymbol{r}|/\sigma}}{8\pi\sigma^3} \quad \Longleftrightarrow \quad \mathcal{F}_i(\boldsymbol{q}) = \frac{1}{(1+\sigma^2|\boldsymbol{q}|^2)^2} \,. \tag{3.41}$$

The parameter σ is related to the hadron's mean charge radius squared according to $\langle r_{\rm ch}^2 \rangle = 12\sigma^2$. That the structure functions vanish for $Q^2 \to \infty$ reflects the lack of high frequency Fourier components in a smooth charge distribution.

At slightly higher C.o.M. energies, quasi-elastic scatterings become important. Here, the target hadron is excited and breaks up into a low multiplicity system of hadrons, for example, $\gamma^* \mathrm{p} \to \Delta^+ \to \mathrm{n}\pi^+$. Again this process can be described by eqn (3.38) with form factors similar to those in eqn (3.41).

At larger C.o.M. energies, high Q^2 processes become kinematically possible, allowing the internal structure of the target hadron to be probed. In this regime, the fast falling (quasi-)elastic cross sections vanish and the majority of collisions become inelastic — the target hadron being broken up. This is *deep inelastic scattering* (DIS). Since the invariant mass of the hadronic final state, W, is not determined, Q^2 and $\nu = p\cdot q/M_{\rm h}$ are independent variables. Again eqn (3.38) applies, but the form of the structure functions F_{1-3} undergo a qualitative change. Rather than vanish as $Q^2 \to \infty$ they remain finite and become practically a function of the single variable $x = Q^2/(2M_{\rm h}\nu) \in (0,1)$ (MIT-SLAC Collab., 1972).

$$F_{1,2,3}(q^2, p\cdot q, `M') \xrightarrow{Q^2\to\infty} F_{1,2,3}(x) \neq 0 \tag{3.42}$$

This Bjorken scaling (Bjorken, 1969) demonstrates that the exchanged vector boson now scatters off pointlike objects that have no mass scale 'M' associated with them. Furthermore, the effective constraint $Q^2 = x \times 2M_{\rm h}\nu = 2xp\cdot q$ is reminiscent of elastic scattering, c.f. eqn (3.30). It is interpreted as being due to the lepton scattering elastically off a charged, constituent (anti)quark which carries a fraction x of its parent hadron's momentum.

In the parton model (Bjorken and Paschos, 1969; Feynman, 1972) the hadron is viewed as a collection of independent, that is, essentially non-interacting or free, (anti)quarks and gluons each carrying a fraction of the parent hadron's longitudinal momentum; any transverse momentum is taken to be small by comparison. The hadron is now described by giving the probability density distributions for the momentum fractions of its parton constituents

$$f(x)\mathrm{d}x = \mathcal{P}\big(x' \in [x, x+\mathrm{d}x]\big) \quad f = q,\ \bar{q} \text{ or } g\,. \tag{3.43}$$

The $f(x)$ are known as *parton density functions* (p.d.f.) or also, somewhat confusingly, as 'structure functions'. Here, and in the following, we shall reserve the name structure function for physically observable quantities. These functions are similar to the fragmentation functions, which we met in Section 3.2.1, but in a reverse sense. The hadron cross section is then formed as a sum of pointlike (anti)quark cross sections weighted by their p.d.f.s, in direct analogy to eqn (3.25). Again, in this factorized form the long-distance p.d.f.s are universal, that is, independent of the particular hard subprocess. As the exchanged vector bosons only couple to (anti)quarks, the presence of gluons in the hadron is felt only indirectly in DIS experiments.

Depending on the nature of the exchanged particle the structure functions F_{1-3} measure different combinations of the p.d.f.s.

$$\begin{aligned}
2xF_1 &= F_2 \\
F_2^{\gamma} &= x\sum_{D,U}\left[\frac{1}{9}(D+\overline{D})+\frac{4}{9}(U+\overline{U})\right] \qquad xF_3^{\gamma} = 0 \\
F_2^{\mathrm{W}^+} &= 2x\sum_{D,U}[D+\overline{U}] \qquad xF_3^{\mathrm{W}^+} = 2x\sum_{D,U}[D-\overline{U}] \\
F_2^{\mathrm{W}^-} &= 2x\sum_{D,U}[U+\overline{D}] \qquad xF_3^{\mathrm{W}^-} = 2x\sum_{D,U}[U-\overline{D}]
\end{aligned} \tag{3.44}$$

Here, D represents any down-type quark (d, s, b) and U represents any up-type quark (u, c, t). Whilst these formal sums include the heavy quarks (c, b, t) their practical contribution is negligible if the probing boson is unable to resolve them. In the transverse plane, which is unaffected by Lorentz boosts along the beam axis, the size of the heavy quark is given by $\sim 1/M_{\mathrm{Q}}$, whilst the exchanged boson sees scales $\geq 1/Q$. Therefore, if $M_{\mathrm{Q}} > Q$, the quark can be dropped from the summation. The coefficients in eqn (3.44) reflect the normalized electric and weak charges of the (anti)quarks.

The constituent quark model (Close, 1979) together with the conservation of flavour imposes a number of constraints on the p.d.f.s. For example, for a proton we have

$$\begin{aligned}
&\int_0^1 \mathrm{d}x\big[u(x)-\bar{u}(x)\big] = 2 \qquad \int_0^1 \mathrm{d}x\big[s(x)-\bar{s}(x)\big] = 0 \\
&\int_0^1 \mathrm{d}x\big[d(x)-\bar{d}(x)\big] = 1 \qquad\qquad etc.
\end{aligned} \tag{3.45}$$

These equations state that the proton contains two units of up-ness, one unit of down-ness and no net strangeness. There is no such constraint on the gluons, $\int_0^1 \mathrm{d}x\, g(x)$, as the number of bosons is not conserved. It is usual to see the quark p.d.f.s separated into two components (Kuti and Weisskopf, 1971; Landshoff and Polkinghorne, 1971): the valence quarks which carry all of the proton's quantum numbers and the sea quarks and antiquarks which make up the remainder and carry no net charges. For example,

$$\begin{aligned}
u(x) &= u_{\mathrm{v}}(x) + u_{\mathrm{s}}(x) \qquad \int_0^1 \mathrm{d}x\, u_{\mathrm{v}}(x) = 2 \\
\bar{u}(x) &= \bar{u}_{\mathrm{s}}(x) \qquad \int_0^1 \mathrm{d}x\big[u_{\mathrm{s}}(x)-\bar{u}_{\mathrm{s}}(x)\big] = 0\,.
\end{aligned} \tag{3.46}$$

The sea quarks are commonly assumed to be produced in $\mathrm{g} \to \mathrm{q}\bar{\mathrm{q}}$ splittings. This suggests the idea that the sea quarks are symmetric in the sense that $u_{\mathrm{s}} = \bar{u}_{\mathrm{s}} = d_{\mathrm{s}} = \bar{d}_{\mathrm{s}} = s_{\mathrm{s}} = \bar{s}_{\mathrm{s}} = \cdots$. Whilst this makes many formulae simpler, it is known empirically not to be exactly true, though a theoretical understanding of how this comes about remains elusive.

The parton model interpretation of deep inelastic lepton–hadron scattering is only approximate and QCD corrections should be taken into account. In the QCD improved parton model the DIS cross section again can be written in a factorized form, but one which can now be proved formally to hold (Collins and Soper, 1987), with the structure functions given by

$$F_i^{(Vh)}(x,Q^2) = \sum_{f=q,\bar{q},g} \int_x^1 \frac{dz}{z} f_h\left(\frac{x}{z},\mu_F,\mu_R\right) \hat{F}_i^{(Vf)}\left(Q^2,z,\mu_F,\mu_R\right) . \quad (3.47)$$

Here $\hat{F}_i^{(Vf)}$ is a projection of the cross section for the partonic scattering $Vf \to f'$ appropriate to the ith structure function. Again, it has been necessary to introduce a factorization scale, μ_F, and scheme, plus a renormalization scale, μ_R, and scheme. The (projected) parton cross sections, $\hat{F}_i^{(Vf)}$, contain only short-distance physics and are calculable in perturbation theory. They do not depend on the hadron h. By contrast, the p.d.f.s, f_h, know nothing of the hard subprocess and depend on the incoming hadron; they are not calculable using only perturbation theory. The proof of eqn (3.47) also justifies the assumption of incoherent scattering and provides a formal definition of the p.d.f.s. This definition shows that in a frame in which the target hadron has infinite momentum the p.d.f.s reduce to the matrix elements, $\langle h|\hat{N}_f(x)|h\rangle$, where $\hat{N}_f(x)$ is the number density operator for partons of type f with given momentum fraction.

Formally, eqn (3.47) only represents the first term in an operator product expansion for $F_i^{(Vh)}(x,Q^2)$ (Altarelli, 1982). This means that it is only exact for $Q^2 \to \infty$. The expansion is organized in terms of the operators' twist (= mass dimension − spin). Thus, at finite values of Q^2 there are higher twist corrections which are suppressed as

$$\frac{[\ln(Q^2/Q_0^2)]^{m<n}}{Q^n} , \quad (3.48)$$

where $n = 4$ for DIS. In general, these non-perturbative corrections are neglected, though there are situations where their effects should be taken into account.

In eqn (3.47) the factorization and renormalization scales are arbitrary. In practice, it is common to set all scales equal, $\mu^2 \equiv Q^2 = \mu_R^2 = \mu_F^2$. This simplifies the coefficient function, giving, for example, $\hat{F}_i^{(Vf)}(\mu^2,z;\mu,\mu) \propto \delta(1-z)$ in the so-called DIS factorization scheme, which allows combinations of the $f_h(x,\mu^2 = Q^2)$ to be determined directly in an experiment. Whilst the f_h involve long-distance physics, the scale μ may still be sufficiently large that $\alpha_s(\mu^2)$ is small enough to allow the dependence on the scale to be calculable at least down to some low scale $\mu_0 \gtrsim \Lambda_{QCD}$. This results in the p.d.f.s developing small, but measurable, logarithmic dependences on μ^2. Such scaling violations are described well by the coupled, integro-differential DGLAP equations (Altarelli and Parisi,

1977; Gribov and Lipatov, 1972; Dokshitzer, 1977).[2] At leading order these are given by

$$\begin{aligned}
\mu^2\frac{\partial q}{\partial\mu^2}(x,\mu^2) &= \int_x^1\frac{\mathrm{d}z}{z}\frac{\alpha_s}{2\pi}\left[P_{\mathrm{qq}}^{(0)}(z)q\left(\frac{x}{z},\mu^2\right)+P_{\mathrm{qg}}^{(0)}(z)g\left(\frac{x}{z},\mu^2\right)\right]\\
\mu^2\frac{\partial \bar{q}}{\partial\mu^2}(x,\mu^2) &= \int_x^1\frac{\mathrm{d}z}{z}\frac{\alpha_s}{2\pi}\left[P_{\mathrm{qq}}^{(0)}(z)\bar{q}\left(\frac{x}{z},\mu^2\right)+P_{\mathrm{qg}}^{(0)}(z)g\left(\frac{x}{z},\mu^2\right)\right] \qquad (3.49)\\
\mu^2\frac{\partial g}{\partial\mu^2}(x,\mu^2) &= \int_x^1\frac{\mathrm{d}z}{z}\frac{\alpha_s}{2\pi}\left[P_{\mathrm{gg}}^{(0)}(z)g\left(\frac{x}{z},\mu^2\right)+\sum_{f=q,\bar{q}}P_{\mathrm{gq}}^{(0)}(z)f\left(\frac{x}{z},\mu^2\right)\right].
\end{aligned}$$

The kernel functions, $P_{ab}(z,\alpha_s(\mu^2))$, are known as Altarelli–Parisi splitting functions and are associated with the branchings $b\to aX$. They can be expanded as a power series in α_s. The leading order expressions are

$$\begin{aligned}
P_{\mathrm{qq}}^{(0)}(z) &= C_F\left(\frac{1+z^2}{1-z}\right)_+\\
P_{\mathrm{qg}}^{(0)}(z) &= T_F[z^2+(1-z)^2]\\
P_{\mathrm{gg}}^{(0)}(z) &= 2C_A\left(\frac{z}{(1-z)_+}+\frac{(1-z)}{z}+z(1-z)\right)+\frac{(11C_A-4n_fT_F)}{6}\delta(1-z)\\
P_{\mathrm{gq}}^{(0)}(z) &= C_F\frac{[1+(1-z)^2]}{z}. \qquad (3.50)
\end{aligned}$$

Away from $z=1$ these are ordinary functions, but at $z=1$ the diagonal splitting functions, $P_{aa}^{(0)}$, must be regarded as distribution functions. Details are elaborated in Section 3.6.3, where also the meaning of the plus-prescription is explained. Since the virtualities involved in this initial state evolution are negative these are the space-like splitting functions. Equations very much like eqn (3.49) control the $\mu_F(=Q)$ behaviour of the fragmentation functions (Owens, 1978). The structure and interpretation of these sets of equations are essentially the same and to $\mathcal{O}(\alpha_s)$ so are the splitting functions. However, beyond this leading order the space-like and time-like splitting functions differ. The full NLO splitting functions for time-like evolution can be found in Appendix E.

The equations in eqn (3.49) have an appealing physical interpretation. We picture the (anti)quarks which make up the hadron as surrounded by clouds of virtual particles, constantly being emitted and absorbed. These virtual particles may in turn emit and absorb further virtual particles. Thus, as the Q^2 of the probing vector boson increases, the content of the hadron appears to change as it is seen on smaller distance scales. It is this evolution which is described by eqn (3.49). The terms $(\alpha_s/2\pi)P_{ab}^{(0)}(z)\mathrm{d}z$ are interpreted as the probability

[2] These equations have quite a history and the name reflects the main contributors to their elucidation: Dokshitzer, Gribov, Lipatov, Altarelli and Parisi. In the past, the name was often shortened to Altarelli–Parisi equations.

densities that in the branching $b \to aX$ parton a will carry a fraction in the range $[z, z + \mathrm{d}z]$ of its parent, b's, momentum, and any other products, X, a fraction $1 - z$. Strictly, the branching probability densities are given by the distribution functions $\delta(1-z)\delta_{ab} + (\alpha_s/2\pi)P^{(0)}_{ab}(z)$ which are regular functions away from $z = 1$. Thus, for example, the probability that a high virtuality gluon, carrying momentum fraction x, came from a low virtuality gluon, with a larger momentum fraction y, is given by

$$\int_0^1 \mathrm{d}z \int_0^1 \mathrm{d}y \frac{\alpha_s}{2\pi} P^{(0)}_{gg}(z) g(y) \delta(x - yz) = \int_x^1 \frac{\mathrm{d}z}{z} \frac{\alpha_s}{2\pi} P^{(0)}_{gg}(z) g\left(\frac{x}{z}\right) . \qquad (3.51)$$

All the terms in eqn (3.49) have a similar interpretation. Figure 3.3 shows schematically this interpretation.

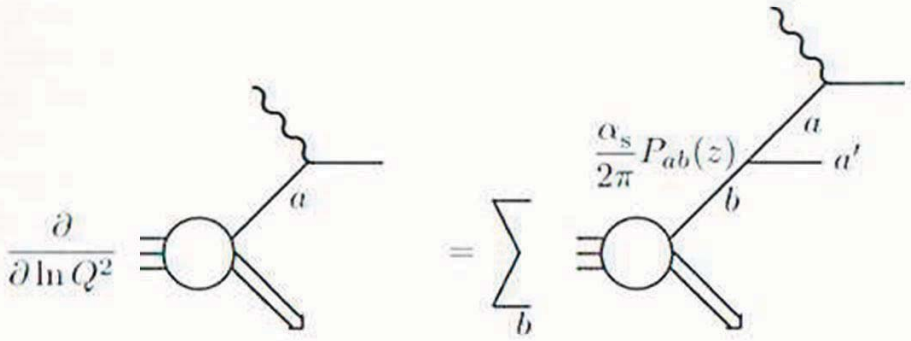

FIG. 3.3. A schematic interpretation of the space-like DGLAP equations whereby the scale dependence follows from the presence of partons within other higher momentum partons

Given the above interpretation of eqn (3.49) it is straightforward to anticipate how the p.d.f.s will change with Q^2. At low Q^2, one might expect that there are few partons in a hadron and that subsequently their p.d.f.s are skewed to high momentum fractions. This picture is not too far from saying, for example, that a proton consists only of two u-quarks and one d-quark, each with momentum fractions smeared around the value $x = 1/3$. As the Q^2 increases, the typical parton momentum fractions decrease as momentum is shared via parton branchings. Thus, we anticipate a growth in the small-x component of the p.d.f.s. Furthermore, we expect many of these small-x partons to be gluons, which have a high probability to undergo $\mathrm{g} \to \mathrm{gg}$ branchings, and sea quarks such as $\bar{\mathrm{u}}$ and $\bar{\mathrm{s}}$ which arise in $\mathrm{g} \to \mathrm{q\bar{q}}$ branchings. As the p.d.f.s shift towards small x and the sea grows we must respect the sum rules for the quark flavours, eqn (3.45), and the conservation of momentum,

$$1 = \int_0^1 \mathrm{d}x\, x \left[g(x) + \sum_{f=q,\bar{q}} f(x) \right] . \qquad (3.52)$$

It is the application of this sum rule which provides compelling evidence for the existence of gluons, carrying over 50% of the momentum, in a proton (Llewellyn-Smith, 1972).

Equation (3.49) allows us to calculate how the p.d.f.s change between the scales μ_0 and μ. However, since the $f(x, \mu_0)$ ($f = q, \bar{q}, g$) only involve a non-perturbative scale, we can not use pQCD to calculate them. In principle, non-perturbative techniques, such as lattice calculations, may allow them to be calculated. However, at the present time only a few moments of their distributions have been obtained and we must rely on experiment (Capitani *et al.*, 2002). Their determination relies on an interplay between the use of eqn (3.49) and the measurement of structure functions giving various combinations of p.d.f.s at different Q^2 scales. In essence, one tries to 'guess' a set of $f(x, \mu_0)$, evolve them to higher scales using eqn (3.49), and then optimize the fit to the measured combinations at the higher scales. Details of the procedure and results are discussed in Section 7.5. The overall consistency of this procedure gives evidence for the validity of the evolution equations and thereby pQCD. Many sets of p.d.f.s are available, for example the package PDFLIB (Plothow-Besch, 1993) contains a a compendium.

As mentioned above, the formal proof of the parton model can be achieved using the apparatus of field theory. However, we can gain insight into its motivation by considering the space–time structure of the collision. The hadron is pictured as a collection of partons sitting within clouds of further partons that are being emitted and absorbed constantly by one another . The virtualities involved must be low, $k^2 \lesssim M_{\rm h}^2$, if the hadron is to remain intact. Indeed, high momentum transfers are suppressed as $[\alpha_{\rm s}(Q^2)M_{\rm h}^2/k^2]^n$, where $n = 2$ for mesons and $n = 3$ for baryons. This, in turn, implies that the partons have lifetimes $\sim 1/M_{\rm h}$, whilst the incoming exchanged boson interacts for a mere $1/Q$. Thus, to the incoming boson the partons appear almost frozen having been formed well in advance of the near instantaneous collision. The struck parton has essentially no time to communicate with the other partons and therefore behaves as if it were free. This also implies that the hard scattering knows nothing of the target hadron beyond the probability that it contains the struck parton.

Returning to the struck parton, it is impulsively kicked out of the hadron and leaves behind its cloud of partons. These remaining partons have been 'shaken free' and as they have nothing to be re-absorbed by, they continue to fly forwards on near collinear trajectories. This initial state radiation continues to shower and hadronize, resulting in a target region jet. The struck parton behaves much like a quark produced in an e^+e^- collision and fragments to produce a current region jet. Between the colour charge on the scattered quark and the anticolour left behind on the hadron remnant is a colour field which converts into low energy hadrons lying between the two jets. Actually, since these intermediate hadrons are produced in a statistical Poisson-like process, it is possible that no hadrons form between the two jets, although the probability for such a gap is expected to be exponentially suppressed as the distance between the jets increases. A typical

neutral current DIS event is shown in Fig. 7.2 and a typical charged current event is shown in Fig. 7.5.

Jet-like structures start to become apparent in DIS for $Q^2 \gtrsim (4\,\mathrm{GeV})^2$. As the Q^2 (C.o.M. energy) increases multi-jet structures appear, just as in e^+e^- collisions. The LO hard subprocess is $Vq \to q'$, which results in a far forward, target region, beam remnant and a more central, current region, jet. At $\mathcal{O}(\alpha_s)$ the NLO subprocesses are the QCD Compton process, $Vq \to gq'$, for scattering off a(n anti)quark and boson–gluon fusion, $Vg \to q\bar{q}'$, for scattering off a gluon. Both of these processes can give rise to two central jets in addition to the forward jet. The type of vector boson exchanged is strongly dependent on the event's Q^2 and type of lepton involved. For charged leptons at low to intermediate $Q^2 \lesssim (40\,\mathrm{GeV})^2$, the neutral current cross section, mediated by a photon, is very much larger than the charged current cross section, mediated by a $W^\pm$. Measurements are shown in Fig. 7.8. This difference essentially reflects the propagators of the exchanged bosons which lead to different Q^2 behaviour: photons give a $1/Q^4$ fall-off whilst W bosons give a nearly constant cross section for $Q^2 \ll M_W^2$.

$$\frac{\mathrm{d}\sigma_{NC}}{\mathrm{d}Q^2} \propto \alpha_{em}^2 \frac{1}{Q^4} \quad \text{and} \quad \frac{\mathrm{d}\sigma_{CC}}{\mathrm{d}Q^2} \propto \frac{\alpha_{em}^2}{\sin^2\theta_w} \frac{1}{(Q^2 + M_W^2)^2} \approx \frac{2G_F^2}{\pi^2} \,. \tag{3.53}$$

As the Q^2 increases further both cross sections begin to fall faster. This is because kinematics require higher Q^2 events to have higher x values and the p.d.f.s, $f_h(x \sim 1, Q^2)$, vanish as $Q^2 \to \infty$. Also their difference diminishes until they become of equal magnitude for $Q^2 \gtrsim (80\,\mathrm{GeV})^2$. An example of electroweak unification in action! Above $Q^2 = (40\,\mathrm{GeV})^2$ Z exchange starts to visibly contribute to neutral current events. This is manifested by the appearance of the parity violating F_3 structure function through $\gamma - Z$ interference effects, which start to reduce $\sigma_{NC}(\ell^+ h)$ compared to $\sigma_{NC}(\ell^- h)$. In charged current events $\sigma_{CC}(\ell^+ h)$ is always less than $\sigma_{CC}(\ell^- h)$, and vice-versa for antihadrons, with the difference becoming more pronounced as Q^2 increases. This reflects the fact that W^- and W^+ couple to different constituents in the target hadron. Using eqn (3.38) and eqn (3.44) we have:

$$\begin{aligned} \frac{\mathrm{d}^2\sigma_{CC}}{\mathrm{d}x\,\mathrm{d}Q^2}(e^+h) &\propto \left[\bar{u} + \bar{c} + (1-y)^2(d+s)\right] \\ \text{and} \quad \frac{\mathrm{d}^2\sigma_{CC}}{\mathrm{d}x\,\mathrm{d}Q^2}(e^-h) &\propto \left[u + c + (1-y)^2(\bar{d}+\bar{s})\right] \,. \end{aligned} \tag{3.54}$$

For a proton, we expect qualitatively $u(x) = 2d(x) > \bar{q}(x)$, which gives the hierarchy in the cross sections. For neutrino beams only Z exchange can contribute to the neutral current cross section, which is consequently not too dissimilar to the charged current cross section.

Before continuing our discussion we digress slightly in order to introduce a natural variable for describing an outgoing particle. Rapidity, y, and pseudorapidity, η, are defined with respect to an axis, typically the beam or a jet axis assumed to be pointing along the z-direction, by

$$y = \frac{1}{2}\ln\left(\frac{E+p_z}{E-p_z}\right) \quad \stackrel{m\to 0}{\longrightarrow} \quad \eta = \ln[\cot(\theta/2)]\,, \tag{3.55}$$

where θ is the polar angle of the particle and m its mass; see also Ex. (6-2). Rapidity is small for central production, $\theta \sim \pi/2$, and large for far forward/backward production, $\theta \to 0$ or π. In a collision with C.o.M. energy $\sqrt{s}$ the allowed rapidity is restricted kinematically to the range $[-\ln(\sqrt{s}/m), +\ln(\sqrt{s}/m)]$. The usefulness of rapidity stems from its appropriateness in describing the Lorentz invariant phase space of the final state particle:

$$\frac{\mathrm{d}^3\boldsymbol{p}}{2E} = \mathrm{d}p_\perp^2\,\mathrm{d}\phi\mathrm{d}y\,. \tag{3.56}$$

The advantage of this form is the simplicity of the way in which each term transforms under a boost along the beam axis. In particular for a boost of velocity $\beta = v/c$,

$$y \longrightarrow y + \frac{1}{2}\ln\left(\frac{1-\beta}{1+\beta}\right) \tag{3.57}$$

so that $\mathrm{d}y$ is invariant, as are $p_\perp^2$ and ϕ. Also, as we shall learn, soft particle production typically has a flat distribution in rapidity.

In most DIS events the target hadron is 'blown apart', resulting in a trail of soft hadronic activity lying between the colour connected remnant, target region, jet and one or more current region jets. However, at HERA in a large fraction of those inelastic events with small x, and therefore large values of W, the total mass of the outgoing hadronic system, the distribution of hadronic activity is markedly different (Hebecker, 2000). The inverse relation $W^2 = M_{\mathrm{h}}^2 + (1-x)Q^2/x \approx Q^2/x$ is easily derived from eqn (3.30). Whilst central 'jet' activity occurs, it is isolated from the target hadron which is only slightly deflected and appears not to break up. A rapidity gap, typically a region of size $\Delta y \gtrsim 3$ in which no hadrons are found, lies between the 'jet' and the scattered hadron. What is seen in practice is no forward activity in the main detector and, in the absence of specialized, far-forward detectors, a target hadron which can be inferred to have disappeared down the beam pipe. Compared to a regular DIS event, $\gamma^*\mathrm{h} \to X$, this subset of events behave as $\gamma^*\mathrm{h} \to XY$ where Y is the scattered target hadron or possibly a low mass excitation of it. Empirically, both the square of the four-momentum transferred to the forward hadron, $t = (p-p')^2 < 0$, and the mass of the observed hadronic system, $M_X^2 = (q+p-p')^2$, that is excluding the scattered hadron, are characteristically small, with a functional behaviour like

$$\frac{\mathrm{d}\sigma}{\mathrm{d}t} \sim \mathrm{e}^{bt} \quad \text{and} \quad \frac{\mathrm{d}\sigma}{\mathrm{d}M_X} \sim \frac{1}{M_X^2}\,. \tag{3.58}$$

The dependence on $W^2 = (q+p)^2$ and $Q^2 = -(\ell - \ell')^2$ is modest. In particular, the cross section for this type of event stays constant, or even grows, as $s = (\ell + p)^2$ or W^2 increase, in marked contrast to the rapidly falling cross sections of DIS events. These are the so-called diffractive DIS events, characterized by their rapidity gaps and almost constant cross sections. The situation is illustrated in Fig. 3.4.

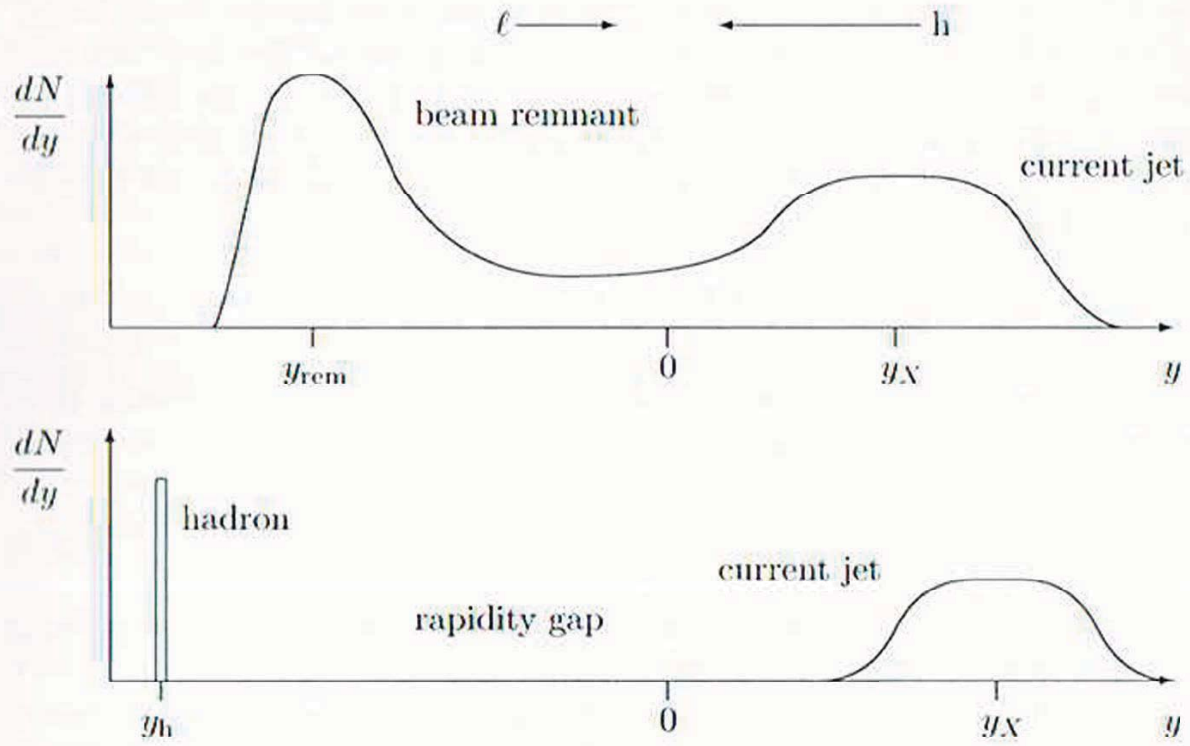

FIG. 3.4. Schematic diagrams of the rapidity distribution for the number of hadrons produced in: top, a regular deep inelastic scattering; bottom, a diffractive deep inelastic scattering

The requirement that the incoming hadron remains intact limits the momentum transfer to $|t| < -t_{\max} \lesssim (1/R_0)^2$, where R_0 is the hadron's size, which is related to the parameter b in eqn (3.58) via $b = R_0^2/6$. A second, lower bound on t is provided by the kinematics of the process, $-t_{\min} \approx M_{\rm h}^2 (M_X^2 + Q^2)^2/W^4$; see Ex. (3-10). Since we require $-t_{\min} < -t_{\max}$, the coherence requirement bounds M_X, in practice $M_X^2 < 0.2\,W^2$. This in turn implies a large separation in rapidity, $\ln(W^2/M_{\rm h}M_X)$, between the scattered hadron and the produced hadronic system. The picture which suggests itself is of the target hadron shedding a near collinear 'object' which is then struck by the virtual photon leading to central jet activity. This object carries a modest fraction, $x_{I\!P}$, of its parent's momentum and no quantum numbers. In particular, it is colour neutral. This ensures a clean separation, in rapidity, of the deflected hadron and the central activity. This object is often identified with the Pomeron, the exchange of which is

believed to dominate the hadron–hadron scattering cross section according to Regge phenomenology: this is discussed in more detail in the next section.

The formal description of these rapidity gap events follows similar lines to that of regular DIS events. The main difference is that the hadronic final state contains a hadron of known quantum numbers and momentum p'. In addition to the usual variables, Q^2, x and y, we introduce the quantities

$$\begin{aligned} t &= (p_{\rm h} - p')^2 \\ x_{I\!P} &= \frac{q\cdot(p-p')}{q\cdot p} \qquad\qquad \approx \frac{M_X^2+Q^2}{W^2+Q^2} \\ \beta &= \frac{Q^2}{2q\cdot(p-p')} = \frac{x}{x_{I\!P}} \approx \frac{Q^2}{Q^2+M_X^2}\,. \end{aligned} \tag{3.59}$$

The approximations hold for low values of $t<0$ and high values of W^2, such as are characteristic of high energy diffraction. A moment's reflection will convince you that, in analogy to the usual phenomenology of DIS, $x_{I\!P}$ should be identified with the momentum fraction of the object, $p^\mu_{I\!P} \equiv p^\mu - p'^\mu \approx x_{I\!P} p^\mu$, and β with the fraction of the object's momentum carried by the struck constituent. Thus x, the constituents momentum fraction with respect to the incoming hadron, is given by $x = x_{I\!P}\beta$. Both $x_{I\!P}$ and β lie in the range $[0,1]$. The four-fold differential, diffractive DIS cross section is given by

$$\frac{{\rm d}^4\sigma_{\rm D}}{{\rm d}x_{I\!P}\,{\rm d}t\,{\rm d}x\,{\rm d}Q^2} = \frac{2\pi\alpha_{\rm em}^2}{xQ^4}\left[1+(1-y)^2\right]F_2^{\rm D(4)}(x_{I\!P},t,x,Q^2)\,. \tag{3.60}$$

Here, for simplicity, we have neglected the small contribution from the longitudinal, diffractive structure function, $F_L^{\rm D(4)} \equiv F_2^{\rm D(4)} - 2xF_1^{\rm D(4)}$. Integrating over t, which is often not observed, gives a three-fold differential distribution, now involving $F_2^{\rm D(3)}$ etc. As with ordinary DIS a factorization theorem has been proved (Collins, 1998),

$$\frac{{\rm d}^2F_2^{\rm D(4)}}{{\rm d}x_{I\!P}\,{\rm d}t}(x_{I\!P},t,x,Q^2) = \sum_{f=q,\bar q,g}\int_{x_{I\!P}}^1 \frac{{\rm d}z}{z}\,\frac{{\rm d}^2f^{\rm D}}{{\rm d}x_{I\!P}\,{\rm d}t}\left(x_{I\!P},t,\frac{x}{z},\mu_F\right)\hat F_2^{(f)}(Q^2,z,\mu_F)\,. \tag{3.61}$$

Here μ_F is the factorization scale (we have suppressed the renormalization scale μ_R) and $\hat F_2^{(f)}(z)$ is the usual DIS structure function describing a photon scattering off a parton f carrying a fraction z of its parent hadron's momentum. The remaining terms are the new diffractive parton density functions (Berera and Soper, 1994), also known as (extended) fracture functions (Trentadue and Veneziano, 1994). The diffractive p.d.f.s satisfy the usual DGLAP evolution equations.

Attempts have been made to go beyond eqn (3.61) using Regge factorization. This assumes that the Pomeron is a real object whose coupling to the parent

hadron is described by a function of $x_{\mathbb{P}}$ and t and whose parton content is then described by functions of β and Q^2. This unproven assumption gives

$$\frac{\mathrm{d}^2 F_2^{\mathrm{D}(4)}}{\mathrm{d}x_{\mathbb{P}}\,\mathrm{d}t}(x_{\mathbb{P}}, t, x, Q^2) = f_{\mathbb{P}/\mathrm{h}}(x_{\mathbb{P}}, t) F_2^{\mathrm{D}(2)}\left(\beta = \frac{x}{x_{\mathbb{P}}}, Q^2\right) , \tag{3.62}$$

where $f_{\mathbb{P}/\mathrm{h}}$ is often referred to as the Pomeron flux factor. Measurements to date suggest that the Pomeron has a high gluon content and that there is a significant probability that a gluon carries nearly all of its momentum. Such a picture has also been promoted in the context of hadron–hadron collisions (Ingelman and Schlein, 1985). Unfortunately, it appears that the same Regge factorized structure functions as measured in DIS will not be applicable, without at least some modification, in the description of hadron–hadron collisions (Collins *et al.*, 1993).

Historically, diffractive events have long been known in hadron–hadron collisions where a well developed phenomenology has arisen. Indeed, this was used to predict that sizeable diffractive cross sections would occur at HERA (Donnachie and Landshoff, 1987). However, the discovery of such events at HERA (ZEUS Collab., 1993; H1 Collab., 1994) still came as surprise to many people and it has led to a resurgence of interest in the nature of diffraction.

Deep inelastic scattering events, whether diffractive in nature or not, are characterized by large values of $Q^2 \gtrsim (3\,\mathrm{GeV})^2$. There also exist events in which an incoming charged lepton emits via bremsstrahlung a quasi-real, $Q^2 \approx 0$, photon which interacts with the incoming hadron: the so-called photo-production events. As mentioned earlier, such photons appear to have a rich structure and variety of behaviours. They may behave as a hadron, giving effectively a hadron–hadron scattering. This in turn could be elastic, here meaning $\gamma^*\mathrm{h} \to V\mathrm{h}$ with V a vector meson, diffractive, soft inelastic or hard inelastic. All these categories are elaborated below. The hard inelastic events are viewed as due to the scattering of (anti)quark or gluon constituents within both the hadron and photon. Thus we require p.d.f.s to describe even the photon. Of course, it is also possible that the photon remains intact and interacts directly with a quark or an antiquark.

3.2.3 *Hadron–hadron scattering*

Hadron–hadron collisions exhibit a rich variety of reactions. These can loosely be divided into two classes. The first class involves soft interactions which have only small momentum transfers so that they are sensitive to long-distance effects and see a hadron as a coherent whole. These have typically large, $\mathcal{O}(10\,\mathrm{mb})$, cross sections which change slowly (logarithmically) with the C.o.M. energy. Examples include the total, elastic and single/double diffractive cross sections discussed in more detail below. The second class involves hard interactions, defined by the presence of a large momentum transfer so that they probe the internal structure of a hadron. These have typically small to tiny cross sections and more pronounced C.o.M. energy dependencies. Examples include high transverse energy jet, heavy quark and high mass lepton pair production. The non-perturbative

nature of the physics involved in the first class of reactions means that a more phenomenological approach is taken when describing them. Since pQCD can be applied directly to the second class of reactions these shall be our main concern.

The above classification of events is a little misleading. For the so-called soft events we intend that the characteristic momentum transfers are small in comparison to the C.o.M. energy $\sqrt{s}$. This leaves open the possibility that at high C.o.M. energies sufficiently large momentum transfers may occur to open up the possibility of applying pQCD. For example, this is under active study for hard diffractive events.

Whilst it is hard to apply QCD to the bulk of hadron–hadron reactions, it is nevertheless helpful to appreciate their basic properties. The general behaviour of the total cross sections is as follows. Initially, the cross section falls from $\mathcal{O}(100\,\text{mb})$ at very low C.o.M. energies to a broad minimum around $\sqrt{s} \sim 20\,\text{GeV}$ before rising slowly. Below $\sqrt{s} \lesssim 3\,\text{GeV}$ resonance structure is apparent. Above the resonance region simple quark counting rules give an indication of the relative cross sections. The rules posit that a total hadron–hadron cross section is proportional to the number of (anti)quarks in the projectile, as determined by the constituent quark model, times the number of (anti)quarks in the target. For $s \to \infty$ one expects, for example, $\sigma_{\text{tot}}(\pi^- \text{p}) \approx \sigma_{\text{tot}}(\text{K}^- \text{p}) \approx 2/3 \times [\sigma_{\text{tot}}(\text{pp}) \approx \sigma_{\text{tot}}(\text{p}\bar{\text{p}})]$. The asymptotic equality of $\sigma_{\text{tot}}(\text{pp})$ and $\sigma_{\text{tot}}(\text{p}\bar{\text{p}})$ is also required by the Pomeranchuk theorem. Figure 3.5 shows these total cross sections as a function of the C.o.M. energy. The total cross section can be parameterized as

$$\sigma_{\text{tot}}(s) = \left[a_0 + a_2 \ln^2\left(\frac{s}{s_0}\right)\right]\left[1 + F(s)\right] \tag{3.63}$$

where $F(s)$, which vanishes as $s \to \infty$, describes the low energy behaviour. This parameterization automatically satisfies the requirement of unitarity as captured in the Froissart bound, $\sigma_{\text{tot}}(s) < (\pi/m_\pi^2)\ln^2(s/s_0)$ for some unknown s_0 (Froissart, 1961; Martin, 1963). We shall largely be concerned with high energy pp and p$\bar{\text{p}}$ collisions as this is where the search for new particles has focused the attention of experimentalists.

In elastic scatterings the hadrons remain intact without excitation of any internal degrees of freedom. They comprise a sizeable component of the total cross section, $\sigma_{\text{el}}(s) \approx 1/6 \times \sigma_{\text{tot}}(s)$. Elastic scatterings are specified by the space-like momentum transfer $t = (p_{\text{in}} - p_{\text{out}})^2 < 0$, which given s is equivalent to the C.o.M. scattering angle, θ^*, via $t = -4p^{*2}\sin^2(\theta^*/2) \approx -s\sin^2(\theta^*/2)$. A number of t-ranges can be identified according to whether electromagnetic or strong forces dominate: the Coulomb region, $|t| < 0.001\,\text{GeV}^2$; the interference region $0.001 < |t| < 0.01\,\text{GeV}^2$; and the diffraction region $0.01 < |t| < 0.15\,\text{GeV}^2$. Only the first region is well understood. The cross section is described by the t-channel exchange of a photon whose coupling to hadrons is described by two form factors, eqn (3.41). A typical behaviour for the differential cross section shows a strong peak below $|t| = 0.01\,\text{GeV}^2$, then a steady fall until reaching a sharp minimum as $|t| \sim 1.4\,\text{GeV}^2$ which is followed by a broad peak at $|t| \sim 2\,\text{GeV}^2$. Above

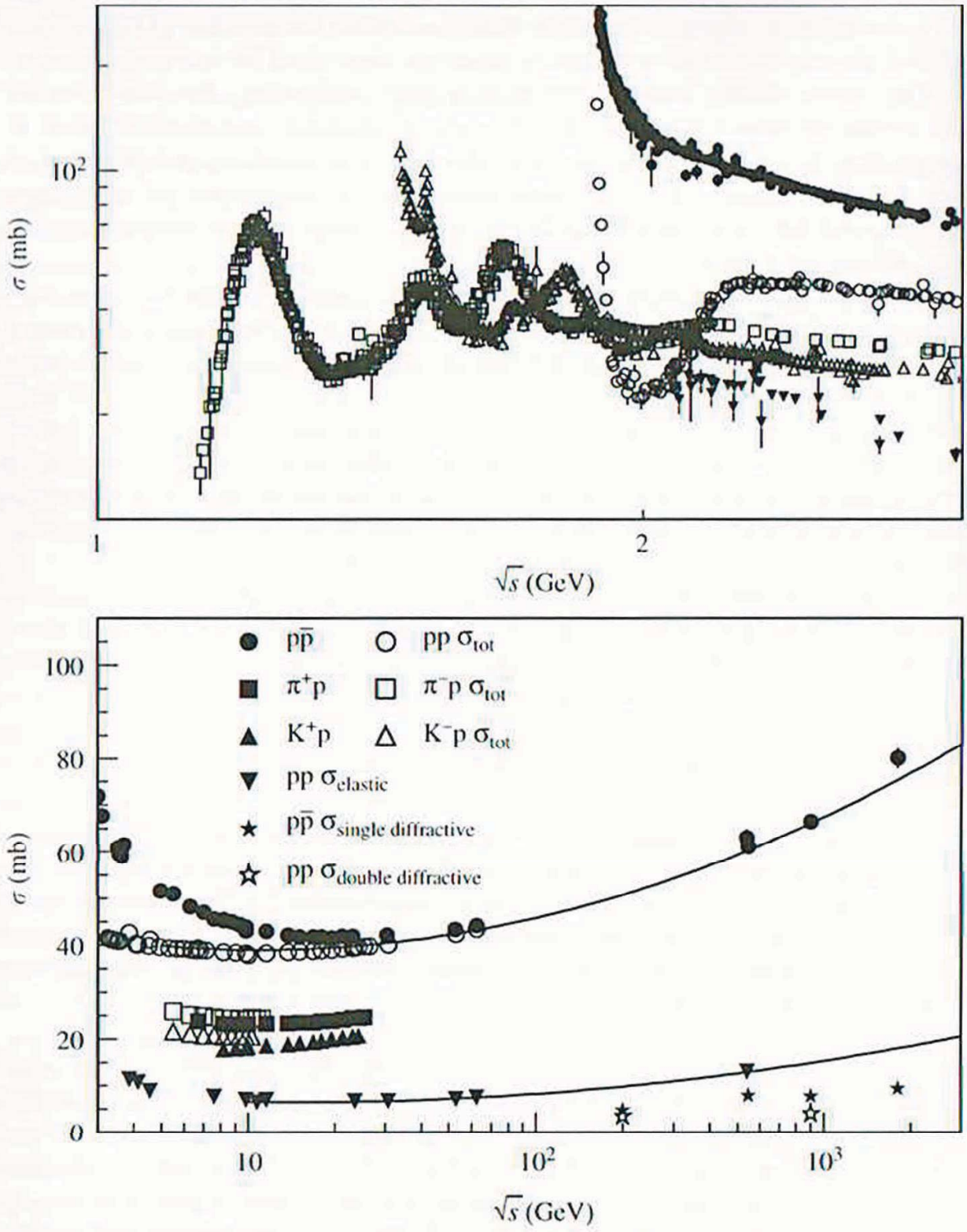

FIG. 3.5. Measured cross sections in hadron–hadron collisions as a function of the C.o.M. energy. Data are taken from the *Review of Particle Properties* (PDG, 2000) and from the Durham reactions database http://durpdg.dur.ac.uk/hepdata/reac.html.

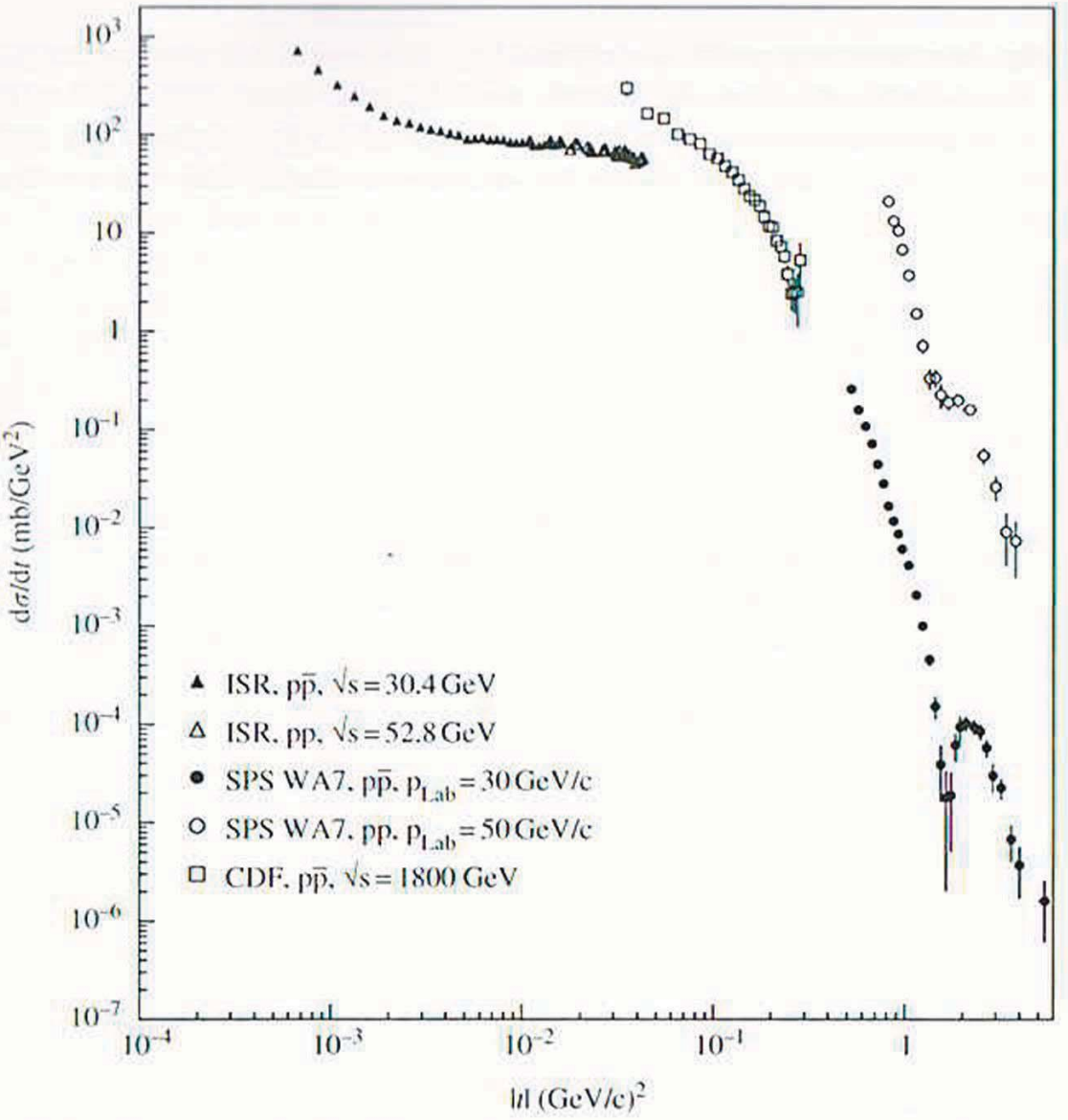

FIG. 3.6. The measured differential cross section in $p\bar{p}$ and pp collisions as a function of the momentum transfer t for various C.o.M. energies. Data are taken from the Durham reactions database http://durpdg.dur.ac.uk/hepdata/reac.html.

$|t| = 2\,\mathrm{GeV}^2$, the hard diffractive region, the differential cross section falls as t^{-n}. The so-called dimensional counting rules (Brodsky and Farrar, 1975) suggest values $n = 6, 8, 10$ for meson–meson, meson–baryon and baryon–baryon scattering, respectively, though more explicit calculations based on gluon exchange between the constituent quarks modify these simple exponents (Landshoff, 1974). Figure 3.6 shows the t-dependence of pp and $p\bar{p}$ scattering. Approximate forms for the differential cross section in the diffractive region are given by

$$\frac{\mathrm{d}\sigma_{\mathrm{el}}}{\mathrm{d}t} \propto \begin{cases} \mathrm{e}^{At+Bt^2} & |t| < 0.4\ \mathrm{GeV}^2 \\ t^{-n} & |t| > 3.0\ \mathrm{GeV}^2\ . \end{cases} \tag{3.64}$$

The 'dip–bump' structure can be described by interference between two exponentials. The t-distribution can be related, via a Fourier–Bessel transformation, to the impact parameter space distribution of the scattering centres in the hadron, $\exp(b_{\rm eff}t) \leftrightarrow \exp(-b_{\rm eff}b^2)$, where b is the impact parameter. Defining an effective slope by

$$\frac{{\rm d}\sigma_{\rm el}}{{\rm d}t}(s,t) = \frac{{\rm d}\sigma_{\rm el}}{{\rm d}t}(s;t_0){\rm e}^{b_{\rm eff}(s;t_0)t} \quad \Longrightarrow \quad b_{\rm eff}(s;t_0) = \frac{\rm d}{{\rm d}t}\left(\ln\left(\frac{{\rm d}\sigma_{el}}{{\rm d}t}\right)\right)\Bigg|_{t=t_0}. \tag{3.65}$$

the measurements show that $b_{\rm eff}$ increases for large s. Thus the hadron shrinks at higher energies.

The very forward peaked nature of the elastic scattering cross section indicates that low momentum transfers are dominant. This essentially straight through behaviour means that specialized low angle detectors, usually in conjunction with low luminosity, are required to measure this large cross section. Interestingly the optical theorem provides a highly non-trivial connection between this forward ($t = 0$) differential cross section and the total cross section; see Ex. (3-11).

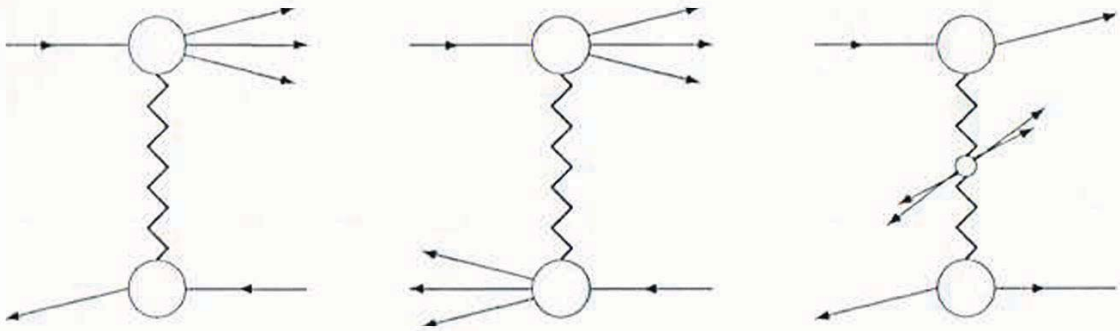

FIG. 3.7. Single diffractive dissociation, double diffractive dissociation and central diffraction. Experimentally these events are characterized by: a forward jet separated by a rapidity gap from an intact, scattered, incoming hadron; or two forward jets separated by a central rapidity gap; or central activity separated by two rapidity gaps from the scattered, incoming hadrons.

The next important class of reactions involve diffractive dissociation processes in which there is some break-up of the scattering hadrons. A possible way to view these events is as the t-channel exchange of a colour singlet object called a Pomeron, see Fig. 3.7. Unlike the case of elastic scattering, in a single/double diffractive dissociation event one/both of the hadrons is left in an excited state which then breaks up into a low multiplicity system of hadrons (jet), for example, $\mathrm{p} \to \Delta^+ \to \mathrm{n}\pi^+$. Typically the mass of the excited hadronic system is distributed as ${\rm d}\sigma \sim {\rm d}M_X/M_X$, whilst the t-dependence of the cross section falls away exponentially with a coefficient which decreases as M_X increases. Experimentally the key signature of these events is the lack of any particle production in between

the scattered/dissociated hadrons. Conventionally, this gap is quoted in units of rapidity. If the final state hadrons have masses M_1 and M_2, then they have a rapidity gap of $\Delta y = \ln(s/M_1 M_2)$. Since the size of the gap is usually $\Delta y \gtrsim 3$, there is a minimum C.o.M. energy $\sqrt{s} \gtrsim 4.5\,\mathrm{GeV}$ required for these events to occur. A related class of events, known as central diffraction events, show two large rapidity gaps separating centrally produced jets from forward/backward going hadrons (UA8 Collab., 1988). These can be interpreted as the interaction of two Pomerons, as shown in Fig. 3.7. They are of particular interest because the jet activity indicates the presence of a hard scale and the possibility to apply pQCD to their description.

At low energies the cross section for all these rapidity gap reactions equals approximately the elastic cross section, with the ratio of single to double diffractive events found to be $\approx 4:1$. As the C.o.M. energy dependence of the cross section for a fixed excited state is flat, the growth of the total dissociation cross section with $\sqrt{s}$ can be attributed to new excitation channels opening up. Experimentally the double diffractive dissociation cross section grows faster than the single diffractive dissociation cross section. This is in accord with the naïve expectation $\sigma_{\mathrm{DD}} \approx \sigma_{\mathrm{SD}}^2/\sigma_{\mathrm{tot}}$. The central diffraction cross section is a few per cent of the total dissociation cross section. At the LHC, a $\sqrt{s} = 14\,\mathrm{TeV}$, pp collider being built at CERN, predictions indicate that $\sigma_{\mathrm{tot}} \approx 105\,\mathrm{mb}$, $\sigma_{\mathrm{el}} \approx 25\,\mathrm{mb}$, $\sigma_{\mathrm{SD}} \approx 15\,\mathrm{mb}$ and $\sigma_{\mathrm{DD}} \approx 10\,\mathrm{mb}$ (Khoze *et al.*, 2000; Block and Halzen, 2001).

The majority of the remainder of the total cross section is made up of what may be termed soft, inelastic collisions, see Fig. 3.8. These can be thought of as peripheral, or glancing, collisions which result in two fast, forward travelling fragments, which carry the quantum numbers of the incident hadrons and typically half of their energy, together with an intervening 'trail' of centrally produced soft particles. These central particles have exponentially damped transverse momenta, $\langle p_T \rangle = 350\,\mathrm{MeV}$, and are uniformly distributed in rapidity, $\mathrm{d}N_{\mathrm{ch}}/\mathrm{d}y \sim 2$. This implies that the multiplicity should grow logarithmically with the C.o.M. energy, $\langle N \rangle = A \ln(s/s_0) + B/\sqrt{s}$. The pion, kaon, and baryon composition is observed to be roughly 85%, 5% and 10% respectively (UA5 Collab., 1987). These soft particles also show short-range order characterized by positive correlations in rapidity. This structure is often interpreted as being due to the production and subsequent decay into stable hadrons of 'universal clusters'. The properties of the soft particles show only a weak dependence on the C.o.M. energy of the colliding hadrons.

The major components of total hadronic cross sections (elastic scattering, single/double diffractive dissociation and soft inelastic collisions) all feature 'small' transverse momentum transfers. This focuses our attention on scattering in the limit $s \to \infty$ whilst t is held relatively small. Here, a successful phenomenology has been developed based upon Regge theory. This pre-QCD theory treats the angular momentum in a scattering amplitude as a complex variable and proceeds to derive consequences from analyticity and crossing symmetries (Collins, 1977). A typical t-channel exchange amplitude for a two-to-two process takes the form

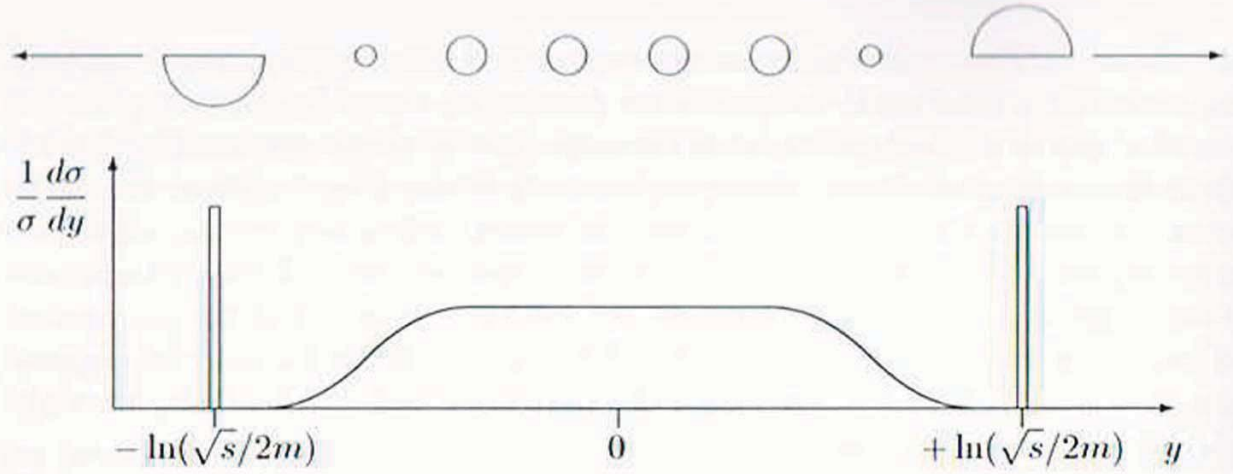

FIG. 3.8. A schematic diagram of a soft, inelastic collision and the associated rapidity distribution

$$\mathcal{M}(s,t) = (\mathrm{i}+\rho)\left(\frac{s}{M_i^2}\right)^{\alpha_i(t)} \mathrm{e}^{b_i t} \quad \text{with} \quad \rho(s,t) \equiv \frac{\mathcal{R}e[\mathcal{M}(s,t)]}{\mathcal{I}m[\mathcal{M}(s,t)]} \approx \rho(s,0)\,. \tag{3.66}$$

The index i in the above equation denotes the flavour quantum numbers exchanged in the interaction. As the practically t-independent ρ is $\mathcal{O}(0.1)$, the amplitudes are mainly imaginary. For the exchange of a particle of spin J the exponent would be $\alpha_i(t) = J$, but in eqn (3.66) this has been 'Reggeized' to include contributions from a whole family of particles lying on a linear Regge trajectory

$$\alpha_i(t) = \alpha_i(0) + \alpha_i' t + \mathcal{O}(t^2)\,. \tag{3.67}$$

The parameters of the trajectories can be found by fitting the spins and masses (s-channel poles) of real mesons and baryons using $J = \alpha_i(M^2)$. The slope is almost universal with $\alpha' \approx 1\,\mathrm{GeV}^{-2}$, whilst the intercept depends on the flavour quantum numbers, i, being exchanged. One finds $\alpha_i(0) \approx 0.5$ for the leading (dominant) contribution from the non-strange vector mesons $\rho, \omega, a_2, f_2, \ldots$. The sub-leading pion trajectory has $\alpha_i(0) \approx 0$. The exponential t-dependence assumed in eqn (3.66) is empirical: it implies $b_{\mathrm{eff}} = 2[b_0 + \alpha' \ln(s/M_i^2)]$ and thus a 'shrinkage' of the t-distribution with increasing C.o.M. energy (Gribov, 1961), c.f. eqn (3.65). More formally it is a measure of the coupling strength between the scattering and exchanged particles. The mass M_i accounts for the dimensions and absorbs any numerical factors.

Using eqn (3.66) one can derive compact expressions for, for example, the total, elastic and singly diffractive cross sections as

$$\sigma_{\mathrm{tot}} = \frac{1}{M_i^2}\left(\frac{s}{M_i^2}\right)^{\alpha_i(0)-1} \tag{3.68}$$

$$\frac{\mathrm{d}\sigma_{\mathrm{el}}}{\mathrm{d}t} = \frac{(1+\rho^2)}{16\pi M_i^4}\left(\frac{s}{M_i^2}\right)^{2(\alpha_i(t)-1)} \mathrm{e}^{2b_{\mathrm{el}}t} \tag{3.69}$$

$$\frac{\mathrm{d}^2\sigma_{\mathrm{D}}}{\mathrm{d}t\,\mathrm{d}M_X^2} \sim \frac{1}{M_i^4}\frac{1}{M_X^2}\left(\frac{s}{M_X^2}\right)^{2(\alpha_{\mathrm{I\!P}}(t)-1)} \mathrm{e}^{2b_{\mathrm{D}}t} \tag{3.70}$$

For simplicity we have included only a single Reggeon exchange and omitted the electromagnetic contributions. Including the interference between the hadronic and, well known, electromagnetic amplitudes allows ρ to be measured experimentally. These formulae provide a very good description of reactions which involve the exchange of flavour. These typically fall as s^{-1}. To apply them to situations where no flavour is exchanged, where cross sections are constant or grow as $s \to \infty$, a new dominant contribution must be included. This is the Pomeron. It has the quantum numbers of the vacuum and the Regge parameters

$$\alpha_{\mathrm{I\!P}}(0) \approx 1.08 \quad \text{and} \quad \alpha'_{\mathrm{I\!P}} \approx 0.25\,. \tag{3.71}$$

These values are derived from successful fits to a remarkably wide range of data (Donnachie and Landshoff 1992; 1994). This trajectory does not correspond to any presently known particles, though it has been conjectured that it is related to the predicted glueballs of QCD. Actually, since $\alpha_{\mathrm{I\!P}}(0) > 1$, the Pomeron is 'supercritical' and, unless eqn (3.68) is modified, will lead to a violation of unitarity in the $s \to \infty$ limit. More apparent is the absurdity $\sigma_{\mathrm{el}}/\sigma_{\mathrm{tot}} \gtrsim (s/M_i^2)^{\alpha_{\mathrm{I\!P}}(0)-1} > 1$ for s sufficiently large. The inclusion of the necessary multiple Pomeron exchanges and unitarization corrections leads to a more complex theory (Khoze *et al.*, 2000).

It is important to remember that Regge theory has not been derived from QCD. One should therefore be wary of regarding it as doing anything more than providing an accurate and economical, phenomenological framework for describing data in the Regge limit. It also acts as a guide in framing the questions addressed in an experiment. That said, pQCD has been applied to the region $s \gg |t| > \Lambda_{\mathrm{QCD}}$, leading to the development of a hard Pomeron with an intercept significantly above one and a small slope. To distinguish it, the usual Pomeron is now often referred to as the soft Pomeron. This hard Pomeron is associated with the summation of leading logarithms of the form $\alpha_{\mathrm{s}} \ln(s/t)$ (Kuraev *et al.*, 1977; Balitsky and Lipatov, 1978). The simplest model for such an object is the t-channel exchange of two gluons (Low, 1975; Nussinov, 1975) (or one 'Reggeized' gluon), which is suggestive of a glueball interpretation. The hard Pomeron also manifests itself in the small-x behaviour of structure functions where it sums leading $[\alpha_{\mathrm{s}} \ln(1/x)]^n$ logarithms. However, a word of caution should be sounded. As the hard Pomeron theory implies a rapid growth in the number of partons then non-perturbative methods will be required ultimately. The search for the predicted hard Pomeron is an active topic of research.

Finally, we turn to the rare, hard events which shall be our main focus of interest. By experimentally requiring an event to contain a large momentum scale we raise the possibility of applying pQCD to its description. Furthermore, the short-distance scales suggest working with the quark and gluon constituents rather than the colliding hadrons themselves. The situation is analogous to DIS and again a factorized formalism can be applied. This is illustrated in Fig. 3.9.

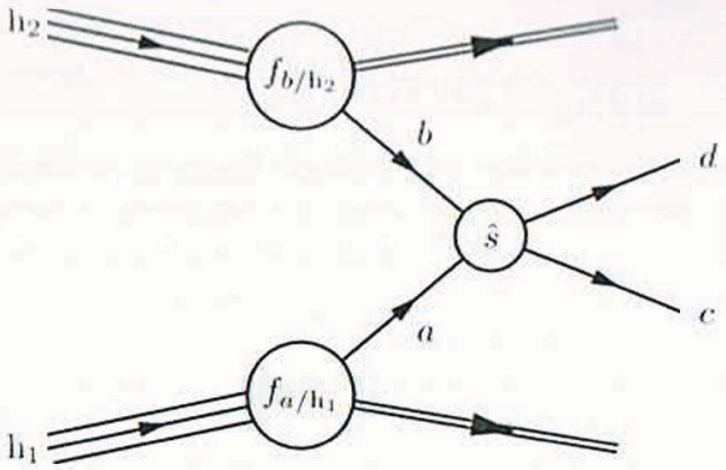

FIG. 3.9. A schematic diagram for the production of final state particles c and d in a hard collision of hadrons h_1 and h_2

The basic cross section formula for the collision of hadrons h_1 and h_2 to produce particles c and d is given by

$$d\sigma(h_1 h_2 \to cd) = \int_0^1 dx_1 dx_2 \sum_{a,b} f_{a/h_1}(x_1, \mu_F^2) f_{b/h_2}(x_2, \mu_F^2) d\hat{\sigma}^{(ab\to cd)}(Q^2, \mu_F^2) \,. \tag{3.72}$$

Here the f_{a/h_1} and f_{b/h_2} are the same p.d.f.s as arose in DIS, where the indices refer to partons $a, b \in \{q, \bar{q}, g\}$ in the interacting hadrons h_1 and h_2. Here there is a technical proviso that we are careful to use the same factorization scheme in the description of both processes. They are evaluated at the factorization scale μ_F, which is typically $\mathcal{O}(Q)$ — a hard scale characteristic of the scattering process. The use of the same p.d.f.s is possible because the presence of an incoming hadron does not cause the target hadron to modify its internal structure. This is the real significance of the factorization theorem and helps to make pQCD a predictive theory. In the matrix element for the hard subprocess the parton momenta are given by $p_a^\mu = x_1 p_{h_1}^\mu$ and $p_b^\mu = x_1 p_{h_2}^\mu$. In general, we do not expect $x_1 = x_2$ so that the hard subprocess will be boosted with $\beta = (x_1 - x_2)/(x_1 + x_2)$ with respect to the $h_1 h_2$ laboratory frame, resulting in the outgoing particles being thrown to one side or the other. The sum is over all partonic subprocesses which contribute to the production of c and d. For example, the production of a pair of heavy quarks receives contributions from $q\bar{q} \to Q\overline{Q}$ and $gg \to Q\overline{Q}$, whilst prompt photon production receives contributions from $qg \to q\gamma$ and $q\bar{q} \to g\gamma$. These two-to-two scatterings give the leading, $\mathcal{O}(\alpha_s^2)$ and $\mathcal{O}(\alpha_s \alpha_{em})$, contributions to the hard subprocess cross section. Beyond the leading order it is necessary to consider two-to-three, etc. processes, which gives rise to a perturbative expansion $\hat{\sigma} = C_{LO}\alpha_s^n + C_{NLO}\alpha_s^{n+1} + C_{NNLO}\alpha_s^{n+2} + \cdots$. A complication arises with the higher order corrections as they contain singularities when two incoming or outgoing partons become collinear. It is the factorization of these singularities, order by order, into the p.d.f.s and fragmentation functions which gives them their calculable μ_F^2 dependencies. This, logarithmically enhanced, near collinear

radiation is manifested as the appearance of initial and final state jets associated with each of the incoming and outgoing partons.

The mix of hard subprocesses which contribute to eqn (3.72) depends non-trivially on the relative sizes of both the cross sections and the p.d.f.s. The latter are influenced by both the type and energy of the colliding beams and any requirements placed on the kinematics of the final state. For example, requiring the outgoing particles to be produced in a given rapidity range, perhaps corresponding to the geometry of a detector element, directly affects the x-ranges being sampled in the integral: see Ex. (3-13). To go further, we consider heavy quark production at the TEVATRON, a $\sqrt{s} = 1.8\,\text{TeV}$ (now 2 TeV) $\mathrm{p\bar{p}}$ collider at FERMILAB. In the case of centrally ($y = 0$) produced bottom quarks one has $x_1 \approx x_2 \sim 2m_\mathrm{b}/\sqrt{s} = 2 \times 5/1800 = 0.0056$, whilst for top quarks it is $x_1 \approx x_2 \sim 2 \times 175/1800 = 0.19$. At small x gluons dominate the p.d.f.s, whilst at large x only valence (anti)quarks are present; this is particularly true at the higher scale appropriate for top production, $Q \sim 2m_\mathrm{Q}$. Thus, bottom quark production is dominated by $\mathrm{gg} \to \mathrm{b\bar{b}}$ scattering, whilst top quark production is dominated by the annihilation process $\mathrm{q\bar{q}} \to \mathrm{t\bar{t}}$. Here, we see that in a high mass 'annihilation process' it pays to have an antihadron in the initial state. In this result the larger cross section for $\mathrm{gg} \to \mathrm{Q\overline{Q}}$ is overwhelmed by the p.d.f. contribution. As a second example we consider di-jet production. In the absence of any flavour determination the outgoing jets may be seeded by either a primary (anti)quark or gluon so that there are many contributing hard subprocesses: $\mathrm{gg} \to \mathrm{gg}$, $\mathrm{gq} \to \mathrm{gq}$, $\mathrm{qq'} \to \mathrm{qq'}$, etc. Loosely speaking, the relative hard subprocess cross sections are in the ratio $C_A^2 : C_A C_F : C_F^2$ etc., reflecting the colour charges of the colliding partons. This allows us to express the integrand in eqn (3.72) in terms of an effective p.d.f. (Combridge and Maxwell, 1984), see Ex. (3-14),

$$f_{\mathrm{h}_1}^{\mathrm{eff}}(x_1) f_{\mathrm{h}_2}^{\mathrm{eff}}(x_2) \mathrm{d}\hat{\sigma}(\mathrm{gg} \to \mathrm{gg}) \quad \text{with} \quad f^{\mathrm{eff}}(x) = g(x) + \frac{C_F}{C_A} \sum_{f=q,\bar{q}} f(x)\,. \qquad (3.73)$$

Here $C_F/C_A = 4/9 \approx 1/2$. Thus at moderate transverse jet energies, equivalent to moderate x values, gg scattering will be dominant.

In addition to a hard subprocess such hadronic scatterings also involve an underlying event arising from the collision of the two beam remnants. In broad outline the underlying event is like a soft, inelastic collision between two hadrons of reduced C.o.M. energy squared $(1 - x_1 x_2)s$. Fortunately, the soft particles produced have limited transverse momentum and so do not unduly obscure the high transverse energy particles produced in the hard subprocess. Observationally there is an increased level of hadronic activity in hard events, even away from any jets, as compared to minimum bias events which are effectively equivalent to normal soft inelastic collisions. This is the so-called pedestal effect. Thus, more refined models build in an interplay between the hard subprocess and the underlying event (Sjöstrand and van Zijl, 1987). One possibility, which becomes more likely with increasing C.o.M. energy, is that a second hard scattering occurs

between the partons in the beam remnants. By treating the two scatters as independent the rate of double scattering can be estimated as $\sigma_{12} = \sigma_1\sigma_2/\sigma_{tot}$. The assumption of independence is plausible provided all the momentum fractions remain small.

In an experiment it is necessary to supply a criterion to decide when to initiate the read-out of the detector. Typically, this trigger condition is based upon known/supposed features of the events which are of interest. This introduces inevitably a bias towards just such events. Therefore, it is also common to collect an 'unbiased' data sample based upon a minimal trigger condition such as the occurrence of a bunch crossing or the presence of an energy deposit somewhere in the detector. Given the relative cross sections for the hadron–hadron scatterings these minimum bias events coincide essentially with the soft, inelastic collision events. Since hadron–hadron colliders are often viewed as discovery machines searching for very rare events, there is a need to use high luminosities. Given large hadron number densities in the colliding bunches it becomes likely that more than one pair of hadrons from the colliding bunches may interact, most likely in soft, inelastic collisions. Thus, even when a hard trigger is satisfied it is quite possible that the detector is seeing an event of interest together with several soft, inelastic events. For example, at nominal luminosity at the planned LHC at CERN, each hard event is, on average, accompanied by $\mathcal{O}(10)$ simultaneous minimum bias events. Fortunately, these extra pile-up events produce mainly low transverse momentum particles, spread throughout longitudinal phase space, whilst the hard event must have high transverse momentum particles, typically restricted kinematically to the central ($y = 0$) region.

3.3 Born level calculations of QCD cross sections

In this section, we shall review the calculational techniques required to evaluate basic tree-level processes. We shall concentrate on the process $e^+e^- \to q\bar{q}$, which is a paradigm for several important processes, together with its lowest, $\mathcal{O}(\alpha_s)$, tree-level, QCD correction, $e^+e^- \to q\bar{q}g$, which we will use in our discussion of the QCD improved parton model. We will also look at the pure QCD process $q\bar{q} \to gg$ which will give us an insight into the nature of gauge invariance. We do assume some previous familiarity with Dirac spinors and working with Feynman diagrams. The interested reader can refresh their memory and find more details in any good text book, such as the one by Aitchison and Hey (1989) or by Peskin and Schroeder (1995).

3.3.1 e^+e^- *annihilation to quarks at* $\mathcal{O}(\alpha_s^0)$

The basic Feynman diagram for $e^+e^- \to q\bar{q}$ is given in Fig. 3.10(a). Strictly speaking, this lowest $\mathcal{O}(\alpha_s^0)$ process is more an electroweak than a QCD interaction. However, it remains of great importance in the description of e^+e^- annihilation to hadrons, and using crossing symmetry, also to deep inelastic scattering, Fig. 3.10(b) and the Drell–Yan process, Fig. 3.10(c). Furthermore, by replacing the lepton pair by a new quark pair ($q \neq q'$), we can learn about di-jet production

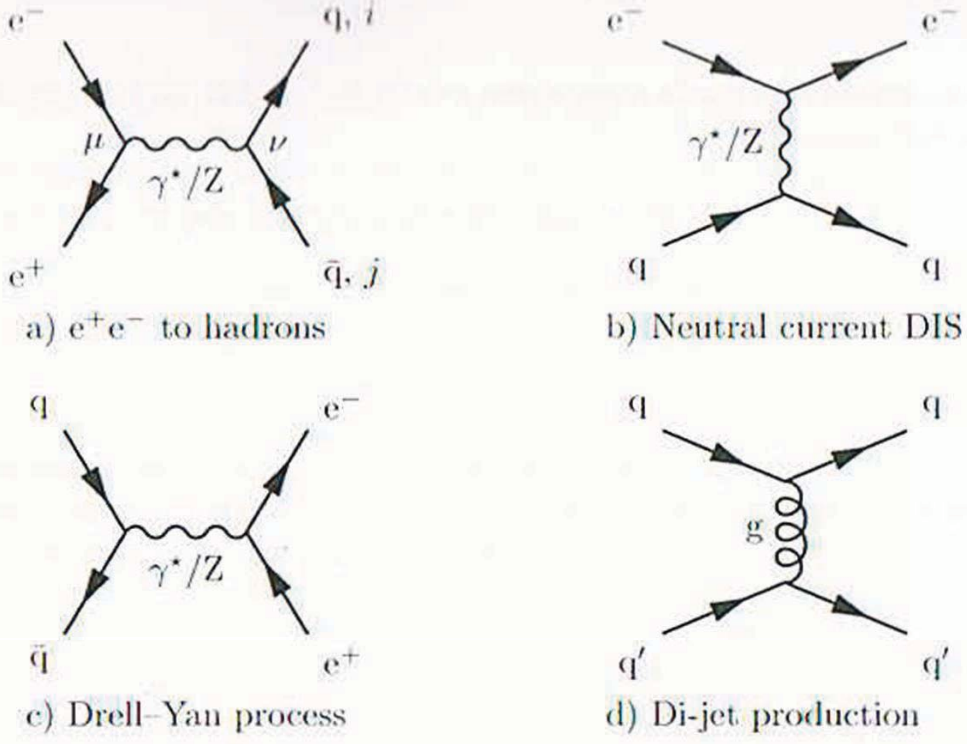

FIG. 3.10. Examples of the basic processes contributing to hard lepton–lepton, lepton–hadron and hadron–hadron scattering. Our convention is such that the Feynman diagrams should be read from incoming states on the left to outgoing states on the right.

in hadron–hadron collisions, Fig. 3.10(d). It should also be noted that since the electroweak couplings are relatively small, $\alpha_{\rm em} \sim 10^{-2}$, diagrams involving single photon exchange should be sufficient for an accurate description of processes (a), (b) and (c). On the other hand, since the strong coupling is relatively large one might wonder about the size of the corrections to the single gluon exchange diagram (d). Asymptotic freedom will have something to say here.

The matrix element for $e^+e^- \to q\bar{q}$ is easily written down using the Feynman rules in Appendix B,

$$\begin{aligned}\mathcal{M} &= \bar{v}(\ell^+) \cdot -\mathrm{i}\, e\gamma_\mu \cdot u(\ell^-) \times \frac{-\mathrm{i}\,\eta^{\mu\nu}}{Q^2} \times \bar{u}(q) \cdot -\mathrm{i}\, e e_q \gamma_\nu \delta_{ij} \cdot v(\bar{q}) \\ &= e\bar{v}(\ell^+)\gamma_\mu u(\ell^-) \times (\mathrm{i}\, Q^{-2}) \times e e_q \delta_{ij} \bar{u}(q)\gamma^\mu v(\bar{q})\ . \end{aligned} \tag{3.74}$$

Here, we use the particle names to also represent their four-momenta and introduce $Q^\mu = (\ell^+ + \ell^-)^\mu$, the four-momentum transfer. For simplicity, only photon exchange is included, which is appropriate for $Q^2 \ll M_Z^2$, and we have chosen to work in the covariant Feynman gauge, $\xi = 1$. The quark colours are specified by the colour indices i and j which run from 1 to N_c. Note that we have explicitly included a colour conserving Kronecker δ-function at the quark–photon vertex which ensures that the $q\bar{q}$-pair forms a colour singlet. The order of the terms carrying spinor indices has been determined by working backwards along each fermion line. Next, we need to evaluate the matrix element squared: $|\mathcal{M}|^2 = \mathcal{M}\mathcal{M}^*$. Now, whilst $\mathcal{M}$ is a complex number it is formed from a product

of matrices, so that it is more convenient to use $\mathcal{M}^\dagger = \mathcal{M}^*$ and rather evaluate $|\mathcal{M}|^2 = \mathcal{M}\mathcal{M}^\dagger$, namely,

$$\begin{aligned}|\mathcal{M}|^2 &= e^2 \cdot \bar{v}(\ell^+)\gamma_\mu u(\ell^-)\left[\bar{v}(\ell^+)\gamma_\nu u(\ell^-)\right]^\dagger \times Q^{-4} \\ &\quad \times (ee_q)^2 \cdot \text{`}\delta_{ij}\delta_{ji}\text{'} \cdot \bar{u}(q)\gamma^\mu v(\bar{q})\left[\bar{u}(q)\gamma^\nu v(\bar{q})\right]^\dagger \\ &= e^2 \cdot \bar{v}(\ell^+)\gamma_\mu u(\ell^-)\bar{u}(\ell^-)\gamma_\nu v(\ell^-) \times Q^{-4} \\ &\quad \times (ee_q)^2 \cdot N_c \cdot \bar{u}(q)\gamma^\mu v(\bar{q})\bar{v}(\bar{q})\gamma^\nu u(q)\ . \end{aligned} \tag{3.75}$$

Here, care has been taken to keep the leptonic and hadronic terms separate and also to sum over the repeated indices. The Hermitian conjugated terms in eqn (3.75) have been dealt with as a special case of the following result.

$$\begin{aligned}[\bar{u}\Gamma_1\Gamma_2\cdots\Gamma_n v]^\dagger &= v^\dagger\Gamma_n^\dagger\cdots\Gamma_2^\dagger\Gamma_1^\dagger\gamma_0^\dagger u \\ &= \bar{v}(\gamma_0\Gamma_n^\dagger\gamma_0)\cdots(\gamma_0\Gamma_2^\dagger\gamma_0)(\gamma_0\Gamma_1^\dagger\gamma_0)u \\ \text{with}\quad \gamma_0\left\{\mathbf{1},\gamma_5,\gamma_\mu,\gamma_\mu\gamma_5,\sigma_{\mu\nu}\right\}^\dagger\gamma_0 &= \left\{+\mathbf{1},-\gamma_5,+\gamma_\mu,+\gamma_\mu\gamma_5,+\sigma_{\mu\nu}\right\}\end{aligned} \tag{3.76}$$

Here Γ_i represents any one of the five basic 4×4 matrices.

At this point we pause to comment on the colour factor in eqn (3.75). Strictly speaking, the quark and antiquark come with colour polarization vectors, so that $\mathcal{M} \propto a^*(\mathrm{q})_i\,\delta_{ij}\,a(\bar{\mathrm{q}})_j$ in eqn (3.74). Then, when we sum $|\mathcal{M}|^2$ over these colour polarizations we must use the result

$$\sum_{\text{col.pols}} a(\mathrm{q})_k a^*(\mathrm{q})_i = \delta_{ki} \qquad \sum_{\text{col.pols}} a(\mathrm{g})_c a^*(\mathrm{g})_a = \delta_{ca}\ , \tag{3.77}$$

appropriate for unpolarized quarks. For completeness we have included the equivalent result for a gluon, where now the indices $\{a,c\} = 1\ldots N_c^2 - 1$. Thus,

$$\begin{aligned}|\mathcal{M}|^2 &\propto \sum a^*(\mathrm{q})_i\,\delta_{ij}\,a(\bar{\mathrm{q}})_j \times \left[a^*(\mathrm{q})_k\,\delta_{kl}\,a(\bar{\mathrm{q}})_l\right]^* \\ &= \sum\left(\sum a(\mathrm{q})_k a^*(\mathrm{q})_i\right)\delta_{ij}\left(\sum a(\bar{\mathrm{q}})_j a^*(\bar{\mathrm{q}})_l\right)\delta_{lk} \\ &= \sum \delta_{ki}\delta_{ij}\delta_{jl}\delta_{lk} = \sum \delta_{ij}\delta_{ji} = N_c\end{aligned} \tag{3.78}$$

Rather reassuringly, the reaction rate is found to be proportional to the number of quark colours, N_c. If a quark or gluon appears in the initial state then the corresponding colours should be averaged, as described in Appendix B. In practice, it is standard not to write out the colour polarization vectors and instead simply keep the same indices on the external particles in both $\mathcal{M}$ and $\mathcal{M}^\dagger$.

A similar result, originally due to van der Waerden, can be used to eliminate the spinor basis states still appearing in eqn (3.75). Denoting the spinor indices by $\{i,j,k,l\} = 1\ldots 4$, the following relations hold

$$u(p)_i\bar{u}(p)_j = \frac{1}{2}\left[(\not{p}+m)(\mathbf{1}+\gamma_5\not{s})\right]_{ij}\Big|_{\boldsymbol{s}\parallel\boldsymbol{p}} \approx \frac{1}{2}\left[(\not{p}+m)(\mathbf{1}\mp\gamma_5)\right]_{ij}$$

$$v(\bar{p})_k \bar{v}(\bar{p})_l = \frac{1}{2}\left[(\not{p} - m)(\mathbf{1} + \gamma_5 \not{s})\right]_{kl} \Big|_{s \| p} \approx \frac{1}{2}\left[(\not{p} + m)(\mathbf{1} \mp \gamma_5)\right]_{kl} \quad (3.79)$$

The spin polarization state is specified by the space-like four-vector s which is orthogonal to p, $s \cdot p = 0$ and which for a pure state is normalized such that $s^2 = -1$. The approximate form is appropriate to the high energy limit, $m \ll E$, when the spin vector is parallel/antiparallel to the particle's direction of travel: the so-called helicity basis. Often the incoming particles in a collision are unpolarized, that is, they are an equal admixture of all possible polarizations. It is therefore conventional to include an average over the incoming particle spins; again see Appendix B. Concentrating on the hadronic part of eqn (3.75), making the spinor indices explicit and assuming no spin sensitive measurements are made on the outgoing quarks this result allows us to write:

$$\begin{aligned}\sum_{\text{spins}} \bar{u}(q)_i \, \gamma^\mu_{ij} \, v(\bar{q})_j \bar{v}(\bar{q})_j \, \gamma^\nu_{kl} \, u(q)_l &= \Big(\sum_{\text{spins}} u(q)_l \bar{u}(q)_i\Big)\gamma^\mu_{ij}\Big(\sum_{\text{spins}} v(\bar{q})_j \bar{v}(\bar{q})_k\Big)\gamma^\nu_{kl} \\ &= (\not{q} + m_q)_{li} \cdot \gamma^\mu_{ij} \cdot (\not{\bar{q}} - m_q)_{jk} \cdot \gamma^\nu_{kl} \\ &= \mathrm{Tr}\left\{(\not{q} + m_q)\gamma^\mu(\not{\bar{q}} - m_q)\gamma^\nu\right\} . \end{aligned} \quad (3.80)$$

In reaching this point we have been careful to make explicit the individual steps involved. Consequently, the derivation seems quite lengthy. However, with practice one can, in principle, go straight from $\mathcal{M}$ to the traces over propagators and vertices appearing in $|\mathcal{M}|^2$. One simply writes down a γ-matrix string from $\mathcal{M}$ followed by a second γ-matrix string from $\mathcal{M}^\dagger$ but with the order of the individual Γ-terms reversed, including minus signs for any γ_5 and $\gamma_\mu\gamma_5$ terms present, see eqn (3.76), and with spin-sums $(\not{p} \pm m)$, as appropriate for the external spinors, inserted between these strings.

To deal with such traces of γ-matrices we adopt the following strategy which is always guaranteed to work. First, expand out the brackets so that you have a sum of terms of the form $\mathrm{Tr}\left\{\gamma^{\mu_1}\gamma^{\mu_2}\cdots\gamma^{\mu_n}\right\}$. Second, set all terms where n is odd equal to zero; here remember that γ_5 is the product of an even number (four) of γ-matrices. Third, for traces of an even number of γ-matrices repeatedly use the following algorithm based on using the Clifford algebra, $\gamma^\mu\gamma^\nu = 2\eta^{\mu\nu} - \gamma^\nu\gamma^\mu$, to permute the first γ-matrix through the rest. We illustrate this for the case $n = 4$, where we need to iterate three times,

$$\begin{aligned}\mathrm{Tr}\left\{\gamma^\mu\gamma^\nu\gamma^\sigma\gamma^\tau\right\} &= \mathrm{Tr}\left\{\left(2\eta^{\mu\nu} - \gamma^\nu\gamma^\mu\right)\gamma^\sigma\gamma^\tau\right\} \\ &= 2\eta^{\mu\nu}\mathrm{Tr}\left\{\gamma^\sigma\gamma^\tau\right\} - \mathrm{Tr}\left\{\gamma^\nu\gamma^\mu\gamma^\sigma\gamma^\tau\right\} \\ &= \cdots \\ &= 2\eta^{\mu\nu}\mathrm{Tr}\left\{\gamma^\sigma\gamma^\tau\right\} - 2\eta^{\mu\sigma}\mathrm{Tr}\left\{\gamma^\nu\gamma^\tau\right\} + 2\eta^{\mu\tau}\mathrm{Tr}\left\{\gamma^\nu\gamma^\sigma\right\} \\ &\quad -\mathrm{Tr}\left\{\gamma^\nu\gamma^\sigma\gamma^\tau\gamma^\mu\right\} \\ \Longrightarrow \quad &= \eta^{\mu\nu}\mathrm{Tr}\left\{\gamma^\sigma\gamma^\tau\right\} - \eta^{\mu\sigma}\mathrm{Tr}\left\{\gamma^\nu\gamma^\tau\right\} + \eta^{\mu\tau}\mathrm{Tr}\left\{\gamma^\nu\gamma^\sigma\right\} . \end{aligned} \quad (3.81)$$

The last line follows because the final trace equals the original one by the cyclicity of traces. The algorithm reduces the number of γ-matrices in a trace by two each

time it is applied. For $n = 2$ it gives $\mathrm{Tr}\{\gamma^\mu\gamma^\nu\} = \eta^{\mu\nu}\mathrm{Tr}\{\mathbf{1}\} = \eta^{\mu\nu}\cdot 4$. Thus the final result becomes

$$\mathrm{Tr}\{\gamma^\mu\gamma^\nu\gamma^\sigma\gamma^\tau\} = 4\left[\eta^{\mu\nu}\eta^{\sigma\tau} - \eta^{\mu\sigma}\eta^{\nu\tau} + \eta^{\mu\tau}\eta^{\nu\sigma}\right] . \tag{3.82}$$

Of course, in practical situations a number of tricks (short cuts) can often be used to speed up evaluations, for example,

$$\begin{aligned} \cdots\gamma_\mu \not{a}\not{a}\gamma_\nu\cdots &= +a^2\times\cdots\gamma_\mu\gamma_\nu\cdots & \cdots\gamma_\mu \not{a}\not{b}\gamma^\mu\cdots &= 4a\cdot b\times\cdots\mathbf{1}\cdots \\ \cdots\gamma_\mu \not{a}\gamma^\mu\cdots &= -2\times\cdots\not{a}\cdots & \cdots\gamma_\mu \not{a}\not{b}\not{c}\gamma^\mu\cdots &= -2\times\cdots\not{c}\not{b}\not{a}\cdots , \end{aligned} \tag{3.83}$$

where the dots are to remind us that the strings of consecutive γ-matrices may be embedded in a larger expression. Unfortunately, familiarity with these tricks only comes with practice. Given these trace results it is now straightforward to evaluate the hadron trace, eqn (3.80), to yield

$$\begin{aligned} \mathrm{Tr}\{(\not{q}+m_\mathrm{q})\gamma^\mu(\not{\bar{q}}-m_\mathrm{q})\gamma^\nu\} &= \mathrm{Tr}\{\not{q}\gamma^\mu\not{\bar{q}}\gamma^\nu\} - m_\mathrm{q}^2\mathrm{Tr}\{\gamma_\mu\gamma_\nu\} \\ &= 4\left[q^\mu\bar{q}^\nu - q\cdot\bar{q}\,\eta^{\mu\nu} + q^\nu\bar{q}^\mu - m_\mathrm{q}^2\eta^{\mu\nu}\right] \\ &= 4\left[q^\mu\bar{q}^\nu + \bar{q}^\mu q^\nu - (Q^2/2)\eta^{\mu\nu}\right] . \end{aligned} \tag{3.84}$$

The leptonic trace, coming from eqn (3.75), can be evaluated in the same way and gives essentially the same result, though with an extra factor 1/4 reflecting the spin average in case of unpolarized beams. If we collect our results so far, we find

$$\begin{aligned} \overline{\sum}|\mathcal{M}|^2 = &\ \frac{1}{4Q^4}e^2\cdot\mathrm{Tr}\{(\not{\ell}^+ - m_\ell)\gamma_\mu(\not{\ell}^- + m_\ell)\gamma_\nu\} \\ &\times(ee_\mathrm{q})^2N_c\cdot\mathrm{Tr}\{(\not{q}+m_\mathrm{q})\gamma^\mu(\not{\bar{q}}-m_\mathrm{q})\gamma^\nu\} \\ = &\ \frac{1}{Q^4}e^2\cdot\left[\ell^+_\mu\ell^-_\nu + \ell^-_\mu\ell^+_\nu - (Q^2/2)\eta_{\mu\nu}\right] \\ &\times(ee_\mathrm{q})^2N_c\cdot 4\left[q^\mu\bar{q}^\nu + \bar{q}^\mu q^\nu - (Q^2/2)\eta^{\mu\nu}\right] \\ \equiv &\ \frac{1}{Q^4}L_{\mu\nu}\cdot H^{\mu\nu} . \end{aligned} \tag{3.85}$$

Here $\overline{\sum}$ is introduced to denote a sum over final state and average over initial state spins and colours. Also, for future reference we have introduced the lepton and hadron tensors $L_{\mu\nu}$ and $H^{\mu\nu}$. The Lorentz contractions are easily carried out to yield

$$\begin{aligned} \overline{\sum}|\mathcal{M}|^2 &= 4\frac{(e^2e_\mathrm{q})^2N_c}{Q^4}\left[2(\ell^+\cdot q)(\ell^-\cdot\bar{q}) + 2(\ell^-\cdot q)(\ell^+\cdot\bar{q}) + (m_\ell^2+m_\mathrm{q}^2)Q^2\right] \\ &= (e^2e_\mathrm{q})^2N_c\frac{1}{2}\left(2-\beta_\mathrm{q}^{*2}+\beta_\mathrm{q}^{*2}\cos^2\theta^*\right) . \end{aligned} \tag{3.86}$$

In the second line the result is written in terms of the C.o.M. variables θ^*, the scattering angle between the incoming lepton and outgoing quark, and β^*, the

velocity of the final state quarks. In this C.o.M. frame, with massless leptons travelling along the z-direction and the scattering in the x-z plane, the four-momenta are given by

$$\ell^{\pm\mu} = \frac{\sqrt{Q^2}}{2}(1,0,0,\pm 1) \tag{3.87}$$

$$\text{and} \qquad \overset{(-)\mu}{q} = \frac{\sqrt{Q^2}}{2}(1,\pm\beta_{\mathrm{q}}^{\star}\sin\theta^{\star},0,\pm\beta_{\mathrm{q}}^{\star}\cos\theta^{\star}) \quad \text{with} \quad \beta_{\mathrm{q}}^{\star} = \sqrt{1-\frac{4m_{\mathrm{q}}^2}{Q^2}}\,.$$

Note that as a Lorentz invariant quantity $|\mathcal{M}|^2$ could only depend on the particles' four-momenta via their invariants, for example, their scalar products, $p_i \cdot p_j$. In a two-to-two scattering, $ab \to cd$, it is common to introduce the Mandelstam variables

$$\begin{aligned} s &= (p_a + p_b)^2 & t &= (p_a - p_c)^2 & u &= (p_a - p_d)^2 \\ &= (p_c + p_d)^2 & &= (p_b - p_d)^2 & &= (p_b - p_c)^2\,. \end{aligned} \tag{3.88}$$

Of these variables only two are independent since they are constrained to satisfy $s + t + u = m_a^2 + m_b^2 + m_c^2 + m_d^2$. Since $s > \max\{m_a^2 + m_b^2, m_c^2 + m_d^2\}$ is always positive, one of t and u, typically both, must be negative. Of course there is some freedom on which particle is labelled c or d. The motivation for a specific choice is to try and ensure that the Mandelstam variables naturally arise in the propagators: s in annihilation processes, for example, $\mathrm{e^+e^-} \to \mathrm{q\bar{q}}$, and t in scattering processes, for example, $\ell\mathrm{q} \to \ell\mathrm{q}$ DIS. One refers to s-, t- or u-channel contributions. In terms of the Mandelstam variables, with $t = (q - \ell^-)^2$, eqn (3.86) can be written

$$\overline{\sum}|\mathcal{M}|^2 = (e^2 e_{\mathrm{q}})^2 N_c \frac{\left[t^2 + u^2 + 2(m_\ell^2 + m_{\mathrm{q}}^2)(2s - m_\ell^2 - m_{\mathrm{q}}^2)\right]}{s^2}\,. \tag{3.89}$$

According to eqn (B.4), to obtain a (differential) cross section we need to include a flux factor for the incoming particles and a (differential) phase space factor for the outgoing particles. In the massless-lepton limit the flux factor, eqn (B.5), is given by $1/(2s)$. The evaluation of two-body, Lorentz invariant phase space, $n = 2$ in eqn (B.6), is relatively straightforward and gives

$$\begin{aligned} \mathrm{d}^2\Phi_2 &= \frac{1}{8\pi}\frac{|\boldsymbol{p}_{\mathrm{out}}^{\star}|}{\sqrt{s}}\mathrm{d}\cos\theta^{\star}\frac{\mathrm{d}\phi}{2\pi} \\ &= \frac{1}{16\pi}\frac{\mathrm{d}t}{|\boldsymbol{p}_{\mathrm{in}}^{\star}|\sqrt{s}}\frac{\mathrm{d}\phi}{2\pi}\,. \end{aligned} \tag{3.90}$$

The first expression for the two-body phase space element is appropriate for a description of the collision in the C.o.M. frame. In the second expression it is

given in terms of the Mandelstam variable t. After integration over the azimuthal angle ϕ and introducing the frequently occuring fine structure constant $\alpha_{\rm em}$,

$$\alpha_{\rm em} = \frac{e^2}{4\pi} \,, \tag{3.91}$$

the final result becomes

$$\begin{aligned} \frac{\mathrm{d}\sigma}{\mathrm{d}\cos\theta^*} &= \frac{\alpha_{\rm em}^2 e_{\rm q}^2 \pi N_c}{2s}\left(2 - \beta_{\rm q}^{*2} + \beta_{\rm q}^{*2}\cos^2\theta^*\right)\beta_{\rm q}^* \\ \frac{\mathrm{d}\sigma}{\mathrm{d}t} &= \frac{\alpha_{\rm em}^2 e_{\rm q}^2 \pi N_c}{s}\frac{\left[t^2 + u^2 - m_{\rm q}^2(2s - m_{\rm q}^2)\right]}{s^2} \,. \end{aligned} \tag{3.92}$$

If both lepton beams had a transverse polarization, then the matrix element eqn (3.86) would acquire a non-trivial ϕ dependence.

Equation (3.92) is easily integrated to give the lowest order expression for the total cross section for $\mathrm{e^+e^-} \to \mathrm{q\bar{q}}$,

$$\sigma_0 = \frac{2\pi\alpha_{\rm em}^2}{s} e_{\rm q}^2 N_c \left(1 - \frac{\beta_{\rm q}^{*2}}{3}\right)\beta_{\rm q}^* \approx \frac{4\pi\alpha_{\rm em}^2}{3s} e_{\rm q}^2 N_c \approx \frac{86.8\,\mathrm{nbGeV}^2}{s} e_{\rm q}^2 N_c \,. \tag{3.93}$$

The approximation holds well above threshold, $\sqrt{s} \gg 2m_{\rm q}$, equivalent to $\beta_{\rm q}^* \to 1$. It should be noted that the fact that the total cross section depends only on s and $m_{\rm q}$ is a result of the quarks (and leptons) having no sub-structure, that is, they are pointlike. Furthermore, the polar angle dependence in eqn (3.86) is a direct consequence of the quarks (and leptons) having spin 1/2. Given (pseudo-)vector boson exchange the lepton and quark spins like to align at the two vertices: a positive (negative) helicity particle with a negative (positive) helicity antiparticle. Thus, we have an initial spin-1 state annihilating into a final spin-1 state aligned at an angle θ^* to the initial state. This θ^* dependence in eqn (3.86) is usefully rewritten as

$$\frac{\mathrm{d}\sigma}{\mathrm{d}\cos\theta^*} \propto (1 + \cos\theta^*)^2 + (1 - \cos\theta^*)^2 + 8\frac{m_{\rm q}^2}{s}\sin^2\theta^* \,. \tag{3.94}$$

The first term corresponds to the contributions with a positive (negative) helicity lepton going to a positive (negative) helicity quark; angular momentum conservation then favours $\theta^* \to 0$ over $\theta^* \to \pi$. Likewise, the second term corresponds to a positive (negative) helicity lepton going to a negative (positive) helicity quark, which is favoured when the quark and lepton are antiparallel. The last term corresponds to a spin zero final state involving a spin-flip, which can only occur for massive quarks. That the first two terms contribute with equal weight is a consequence of QED (and QCD) being parity conserving. The photon couples with equal strength to the left- and right-handed fermions. The weak interaction violates parity conservation and the Z couples differently to left- and right-handed fermions. This changes the balance between the first two terms in

eqn (3.94) and leads to a term linear in $\cos\theta^*$ which induces a forward–backward asymmetry. A similar effect can be obtained by polarizing one or more of the fermions.

To obtain similar results for the processes $\ell^-\mathrm{q} \to \ell^-\mathrm{q}$ and $\mathrm{q\bar{q}} \to \ell^+\ell^-$, shown in Fig. 3.10, one approach is to calculate the matrix element in exactly the same manner as above. An elegant alternative is to take the previous result for $\mathcal{M}(\ell^-\ell^+ \to \mathrm{q\bar{q}})$ and use crossing symmetry. The basic idea is to swap particles between the initial and final states. An example is given by

$$\begin{aligned} &\mathcal{M}^{a\bar{b}\to c\bar{d}}(p_a, p_b, p_c, p_{\bar{d}}) \simeq \mathcal{M}^{a\bar{d}\to b\bar{c}}(p_a, -p_{\bar{d}}, -p_b, p_c) \\ \Longrightarrow \quad &|\mathcal{M}^{a\bar{b}\to c\bar{d}}(s,t,u)|^2 = |\mathcal{M}^{a\bar{d}\to b\bar{c}}(t,u,s)|^2 \,. \end{aligned} \tag{3.95}$$

When fermions are involved the equality of the amplitudes is modulo an unobservable phase. Since the physical regions for the Mandelstam variables in the crossed and uncrossed process do not overlap, the arguments of the second amplitude have to be analytically continued. That this is possible places powerful constraints on the allowed form of the amplitude. The only real, though minor, complication is to remember that the spin and colour averages for the initial state may need to be changed as appropriate. Using these results and neglecting masses we quickly obtain

$$\begin{aligned} &\overline{\sum}|\mathcal{M}(\ell^-\mathrm{q} \to \ell^-\mathrm{q})|^2 = (e^2 e_\mathrm{q})^2 \frac{u^2+s^2}{t^2} \\ \text{and} \quad &\overline{\sum}|\mathcal{M}(\mathrm{q\bar{q}} \to \ell^-\ell^+)|^2 = (e^2 e_\mathrm{q})^2 \frac{1}{N_c} \frac{t^2+u^2}{s^2} \,. \end{aligned} \tag{3.96}$$

Observe that the result for $\mathrm{q\bar{q}} \to \ell^-\ell^+$ is essentially the same as for $\ell^-\ell^+ \to \mathrm{q\bar{q}}$, except for the extra factor $1/N_c^2$ due to the average over the colours of the incoming quarks. In situations where a number of processes are related to one another be crossing symmetries it is common practice to only quote one matrix element (squared) and expect the reader to derive the others using eqn (3.96).

Finally, before finishing our discussion of these processes, we return to a very important property of the lepton and hadron tensors defined by eqn (3.85). Suppose that we introduce a polarization vector for the exchanged (off mass-shell) photon and take $\epsilon(Q)^\mu \propto Q^\mu$, then it is easily verified that

$$Q^\mu L_{\mu\nu} = 0 = L_{\mu\nu} Q^\nu \quad \text{and} \quad Q^\mu H_{\mu\nu} = 0 = H_{\mu\nu} Q^\nu \,, \tag{3.97}$$

which is the embodiment of electromagnetic gauge invariance. As a consequence of this result, had we chosen a gauge in which $\xi \neq 1$, then the extra terms in the numerator of the photon propagator, which are proportional to Q^μ, would have given zero contribution. It was sufficient to use only $-\eta_{\mu\nu}$. This is a trivial example of a more general result which states that the sum of a gauge invariant set of amplitudes cannot depend on the arbitrary gauge parameter ξ. To see why

a sum of amplitudes must vanish when a photon's polarization vector is replaced by its four-momentum consider the Fourier transform of a gauge transformation,

$$A^\mu \mapsto A^\mu + e^{-1}\partial^\mu\theta \quad \Longrightarrow \quad \epsilon(k)^\mu \mapsto \epsilon(k)^\mu + e^{-1}k^\mu\theta\,. \tag{3.98}$$

Since θ is arbitrary, the scalar product $\epsilon^\mu\mathcal{M}_\mu$ is only guaranteed to be gauge invariant if we require $k^\mu\mathcal{M}_\mu = 0$. A similar, though more delicate argument holds in the non-abelian QCD. For more explanations see eqn (3.118) and the discussion in Section 3.3.3.1. Constraints such as this significantly limit the possible tensor structures of amplitudes and provide very useful checks on the intermediate stages of a calculation.

3.3.2 e^+e^- *annihilation to quarks at* $\mathcal{O}(\alpha_s^1)$

We now consider the leading, tree-level QCD correction to the process $e^+e^- \to q\bar{q}$ in which a gluon is radiated from either the quark or the antiquark, $e^+e^- \to q\bar{q}g$. The two Feynman diagrams are shown in Fig. 3.11.

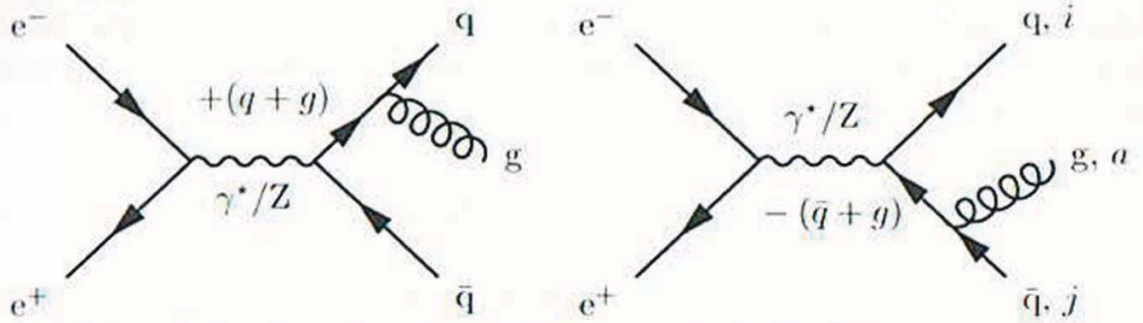

FIG. 3.11. The leading, tree level QCD corrections to $e^+e^- \to q\bar{q}$. The momentum shown at the internal quark flows in the direction of the fermion number, as indicated by the arrow.

Concentrating on the hadronic part of the amplitude, and again assuming only photon exchange, the matrix element is

$$\mathcal{M}_\mu = \mathrm{i}\,ee_q g_s T^a_{ij}\bar{u}(q)\left[\gamma_\sigma\frac{(\not{q}+\not{g}+m_q)}{(q+g)^2-m_q^2}\gamma_\mu + \gamma_\mu\frac{-(\not{\bar{q}}+\not{g})+m_q}{(\bar{q}+g)^2-m_q^2}\gamma_\sigma\right]v(\bar{q})\epsilon^*(g)^\sigma\,. \tag{3.99}$$

The minus sign in the antiquark propagator arises because the momentum is flowing in the opposite direction to the fermion number. Before proceeding to evaluate $|\mathcal{M}|^2$ it is instructive to verify electromagnetic gauge invariance. Using $Q^\mu = q^\mu + \bar{q}^\mu + g^\mu$ and neglecting the constant overall factors we have

$$\begin{aligned}\mathcal{M}_\mu Q^\mu &\propto \bar{u}(q)\left[\not{\epsilon}^*\frac{1}{(\not{q}+\not{g}-m_q)}(\not{q}+\not{g}+\not{\bar{q}}) + (\not{q}+\not{g}+\not{\bar{q}})\frac{1}{(-(\not{\bar{q}}+\not{g})-m_q)}\not{\epsilon}^*\right]v(\bar{q})\\ &= \bar{u}(q)\left[\not{\epsilon}^*\frac{1}{(\not{q}+\not{g}-m_q)}(\not{q}+\not{g}-m_q) - (m_q+\not{g}+\not{\bar{q}})\frac{1}{(\not{\bar{q}}+\not{g}+m_q)}\not{\epsilon}^*\right]v(\bar{q})\end{aligned}$$

$$= \bar{u}(q)\left[\not{\epsilon}^*\mathbf{1} - \mathbf{1}\not{\epsilon}^*\right] = 0\,. \tag{3.100}$$

Here we wrote the propagators as inverses, using $(\not{p} - m)(\not{p} + m) = (p^2 - m^2)\mathbf{1}$, and exploited the Dirac equation

$$\begin{aligned} (\not{q} - m_{\mathrm{q}})u(q) &= 0 \qquad (\not{\bar{q}} + m_{\mathrm{q}})v(\bar{q}) = 0 \\ \bar{u}(q)(\not{q} - m_{\mathrm{q}}) &= 0 \qquad \bar{v}(\bar{q})(\not{\bar{q}} + m_{\mathrm{q}}) = 0\,. \end{aligned} \tag{3.101}$$

Thus, we confirm that our expression for the amplitude is gauge invariant, provided we include the contributions from both diagrams.

At this point, we set the quark masses to zero, as they serve only to complicate our calculations. This is a good approximation for the light quarks. Since we already know the lepton tensor we only need to evaluate the hadron tensor,

$$\sum_{\text{spins}} \mathcal{M}_{\mu\sigma}\mathcal{M}^{\dagger}_{\nu\tau}\epsilon^*(g)^{\sigma}\epsilon(g)^{\tau} = -\sum_{\text{spins}} \mathcal{M}_{\mu\sigma}\mathcal{M}^{\dagger\,\sigma}_{\nu}\,. \tag{3.102}$$

Here, we have expressed $\mathcal{M}_{\mu}$ from eqn (3.99) as $\mathcal{M}_{\mu\sigma}\epsilon(g)^{*\sigma}$ and used

$$\sum_{\text{pol}} \epsilon^*(g)^{\sigma}\epsilon(g)^{\tau} = -\eta^{\sigma\tau} \tag{3.103}$$

for the gluon's polarization tensor. We shall return to a consideration of this expression later. We start by considering the first diagram in Fig. 3.11, in which the gluon is emitted by the quark, which yields

$$\begin{aligned} (2q\cdot g)^2 \sum_{\text{spins}} \mathcal{M}_{\mathrm{q}}\mathcal{M}^{\dagger}_{\mathrm{q}} &\propto -\mathrm{Tr}\left\{\not{\bar{q}}\gamma_{\sigma}(\not{\bar{q}} + \not{g})\gamma_{\mu}\not{q}\gamma_{\nu}(\not{q} + \not{g})\gamma^{\sigma}\right\} \\ &= +2\mathrm{Tr}\left\{\not{\bar{q}}(\not{\bar{q}} + \not{g})\gamma_{\mu}\not{q}\gamma_{\nu}(\not{q} + \not{g})\right\} \\ &= +2\mathrm{Tr}\left\{\not{\bar{q}}\not{g}\gamma_{\mu}\not{\bar{q}}\gamma_{\nu}\not{g}\right\} \\ &= +2\cdot 2(q\cdot g)\cdot 4\left[\bar{q}_{\mu}g_{\nu} + g_{\mu}\bar{q}_{\nu} - (\bar{q}\cdot g)\eta_{\mu\nu}\right]\,. \end{aligned} \tag{3.104}$$

Here, we used some tricks from eqn (3.83) to speed up the evaluation: $\gamma^{\sigma}\not{q}\gamma_{\sigma} = -2\not{q}$, $\not{q}\not{q} = q^2 = 0$ and $\not{g}\not{g} = 2q\cdot g - \not{g}\not{q}$ together with $g^2 = 0$. Note that scalars appearing in an expression which is a product of some γ-matrices have to be multiplied by a 4×4 unit matrix which is usually not written explicitly.

In eqn (3.104) we see that the factor $(q\cdot g)$ partly cancels the singularity from the propagator so that the contribution behaves as $(q\cdot g)^{-1}$ and not $(q\cdot g)^{-2}$ as might have been anticipated naïvely. This cancellation is typical of such calculations. In retrospect, this is not so surprising if we consider the $\mathrm{q}\to\mathrm{qg}$ branching in isolation. This can be achieved by expressing the numerator of the quark propagator, $\not{p}$, as a sum over bispinors, $u(p,s)\bar{u}(p,s)$, c.f. eqn (3.20), and picking out the term $\bar{u}(q)\not{\epsilon}^*(g)u(p)$. This expression has mass dimension one, and since the only relevant quantity carrying mass dimensions is the virtuality of the

propagator, we have that it must be proportional to $\sqrt{2q\cdot g}$. The properties of such branchings will be studied later. They are important when the propagator becomes singular and they start to give the dominant contributions to a matrix element. These propagator singularities can be identified with two physical regions. Looking at the denominator

$$\left[(q+g)^2 - m_{\mathrm{q}}^2\right] = 2q\cdot g = 2E_{\mathrm{q}}E_{\mathrm{g}}(1-\beta_{\mathrm{q}}\cos\theta_{\mathrm{qg}})\,. \tag{3.105}$$

it is clear that this inverse propogator tends to zero for vanishing gluon energy, $E_{\mathrm{g}}\to 0$, known as a soft singularity, and for a massless quark, $\beta_{\mathrm{q}}=1$, when the opening angle vanishes, $\theta_{\mathrm{qg}}\to 0$, known as a collinear or mass singularity.

The evaluation of $\sum_{\mathrm{spins}}\mathcal{M}_{\mathrm{q}}\mathcal{M}_{\mathrm{q}}^{\dagger}$ proceeds in the same manner. The result can be obtained from eqn (3.104) by exchanging q^μ and $\bar{q}^\mu$. The more cumbersome evaluation of the cross-term yields

$$\begin{aligned}(2q\cdot g)(2\bar{q}\cdot g)\sum_{\mathrm{spins}} 2\mathcal{R}e\left\{\mathcal{M}_{\mathrm{q}}\mathcal{M}_{\bar{\mathrm{q}}}^{\dagger}\right\}&\\ \propto\ -16\Big[&(q\cdot\bar{q})\left(Q^2\eta_{\mu\nu}-2Q_\mu q_\nu-2\bar{q}_\mu Q_\nu+2\bar{q}_\mu q_\nu\right)\\ &+2(\bar{q}\cdot Q)q_\mu q_\nu+2(q\cdot Q)\bar{q}_\mu\bar{q}_\nu-Q^2q_\mu\bar{q}_\nu\Big]\,.\end{aligned} \tag{3.106}$$

Combining these results, restoring the constant factor and evaluating the sum over the final state quark colours, which is conveniently done using eqn (A.17), $\mathrm{Tr}\left\{T^aT^a\right\}=C_F\delta_{ii}=C_FN_c$, gives the hadronic tensor

$$\begin{aligned}H_{\mu\nu}=\ &\frac{4(ee_{\mathrm{q}})^2g_s^2C_FN_c}{(q\cdot g)(\bar{q}\cdot g)}\\ &\times\Big\{-Q^2\left(q_\mu q_\nu+\bar{q}_\mu\bar{q}_\nu\right)-\left[(q\cdot Q)^2+(\bar{q}\cdot Q)^2\right]\eta_{\mu\nu}\\ &\quad+(q\cdot Q)\left[q_\mu Q_\nu+Q_\mu q_\nu\right]+(\bar{q}\cdot Q)\left[\bar{q}_\mu Q_\nu+Q_\mu\bar{q}_\nu\right]\\ &\quad+(q\cdot\bar{q})\left[Q_\mu(q-\bar{q})_\nu-(q-\bar{q})_\mu Q_\nu\right]+\left(q\cdot\bar{q}+Q^2/2\right)\left(q_\mu\bar{q}_\nu-\bar{q}_\mu q_\nu\right)\Big\}\,.\end{aligned} \tag{3.107}$$

This can be contracted with the leptonic tensor, eqn (3.85), to yield the following expression for the matrix element squared:

$$L^{\mu\nu}H_{\mu\nu}=8(e^2e_{\mathrm{q}})^2g_s^2C_FN_c\frac{1}{Q^2}\frac{\left[(\ell^-\cdot q)^2+(\ell^-\cdot\bar{q})^2+(\ell^+\cdot q)^2+(\ell^+\cdot\bar{q})^2\right]}{(q\cdot g)(\bar{q}\cdot g)} \tag{3.108}$$

Observe that only the first two terms in eqn (3.107) give non-zero contributions as the others are either proportional to Q^μ and vanish by gauge invariance or are antisymmetric under $\mu\leftrightarrow\nu$.

To obtain the differential cross section eqn (B.4) we need to include the flux factor, which is the same as for $\mathrm{e^+e^-}\to\mathrm{q\bar{q}}$, and the three-body phase space,

$n = 3$ in eqn (B.6). The evaluation of the phase space is best carried out in the C.o.M. frame and yields:

$$\begin{aligned} \mathrm{d}^5\Phi_3\big|_{\mathrm{CoM}} &= \frac{1}{32\pi^3}\mathrm{d}E_1\mathrm{d}E_2\frac{\mathrm{d}\phi_{12}\mathrm{d}\Omega_1}{8\pi^2} \\ \mathrm{d}^2\Phi_3\big|_{\mathrm{CoM}} &= \frac{1}{32\pi^3}\mathrm{d}E_1\mathrm{d}E_2 \\ &= \frac{1}{128\pi^3 Q^2}\mathrm{d}m_{13}^2\mathrm{d}m_{23}^2 \end{aligned} \tag{3.109}$$

Here particles 1 and 2 can be any of the three final state particles; for the problem at hand 1=q, 2=$\bar{\mathrm{q}}$ and 3=g is the natural choice. The second expression follows after integrating over the decay plane's orientation and the third because, for example, $m_{13}^2 = Q^2 + m_2^2 - 2\sqrt{Q^2}E_2^{\mathrm{CoM}}$. Combining these results gives the fully differential cross section

$$\begin{aligned} \mathrm{d}^5\sigma = \frac{\alpha_{\mathrm{em}}^2 e_{\mathrm{q}}^2 N_c}{Q^2}\alpha_{\mathrm{s}}C_F\frac{8}{Q^2}\frac{[(\ell^-\cdot q)^2 + (\ell^-\cdot\bar{q})^2 + (\ell^+\cdot q)^2 + (\ell^+\cdot\bar{q})^2]}{(q\cdot g)(\bar{q}\cdot g)} \\ \times\mathrm{d}E_{\mathrm{q}}\mathrm{d}E_{\bar{\mathrm{q}}}\frac{\mathrm{d}\phi_{\mathrm{q}\bar{\mathrm{q}}}\mathrm{d}\Omega_{\mathrm{q}}}{8\pi^2}\,. \end{aligned} \tag{3.110}$$

Often, in practice, we are not interested in the orientation of the decay plane. That the three particles lie in a plane, in the C.o.M. system, follows trivially from $q + \bar{q} + g = 0$. The integrations over $\phi_{\mathrm{q}\bar{\mathrm{q}}}$, ϕ_{q} and θ_{q} may be done explicitly in eqn (3.110) or done equivalently by replacing $L^{\mu\nu}$ with the orientation-averaged lepton tensor

$$\langle L^{\mu\nu}\rangle = e^2\frac{1}{3}\left(-\eta^{\mu\nu} + \frac{Q^\mu Q^\nu}{Q^2}\right)(Q^2 + 2m_\ell^2)\,. \tag{3.111}$$

Here m_ℓ^2 may be safely ignored. This tensor manifestly satisfies eqn (3.97) and may be thought of as the spin-averaged polarization tensor for the exchanged, off mass-shell, vector boson. Re-evaluating $L_{\mu\nu}H^{\mu\nu}$ then gives for the spin-averaged cross section for massless quarks

$$\begin{aligned} \mathrm{d}^2\sigma &= \sigma_0\frac{\alpha_{\mathrm{s}}}{2\pi}C_F\frac{[(q\cdot Q)^2 + (\bar{q}\cdot Q)^2]}{(q\cdot g)(\bar{q}\cdot g)}\frac{4}{Q^2}\mathrm{d}E_{\mathrm{q}}\mathrm{d}E_{\bar{\mathrm{q}}} \\ \Longrightarrow\quad \frac{\mathrm{d}^2\sigma}{\mathrm{d}x_{\mathrm{q}}\mathrm{d}x_{\bar{\mathrm{q}}}} &= \sigma_0\frac{\alpha_{\mathrm{s}}}{2\pi}C_F\frac{x_{\mathrm{q}}^2 + x_{\bar{\mathrm{q}}}^2}{(1-x_{\bar{\mathrm{q}}})(1-x_{\mathrm{q}})}\,. \end{aligned} \tag{3.112}$$

In the second form we have introduced the variables x_i, equal to the energy fraction of the ith particle in the C.o.M. frame, defined by

$$x_i = 2\frac{p_i\cdot Q}{Q^2} = \frac{E_i^{\mathrm{CoM}}}{E_{\mathrm{beam}}}\,, \tag{3.113}$$

and such that $x_{\mathrm{q}} + x_{\bar{\mathrm{q}}} + x_{\mathrm{g}} = 2$. Projected onto the $x_{\mathrm{q}} - x_{\bar{\mathrm{q}}}$ plane (Fig. 3.12), a Dalitz plot, the allowed phase space lies in the upper-right triangle of the

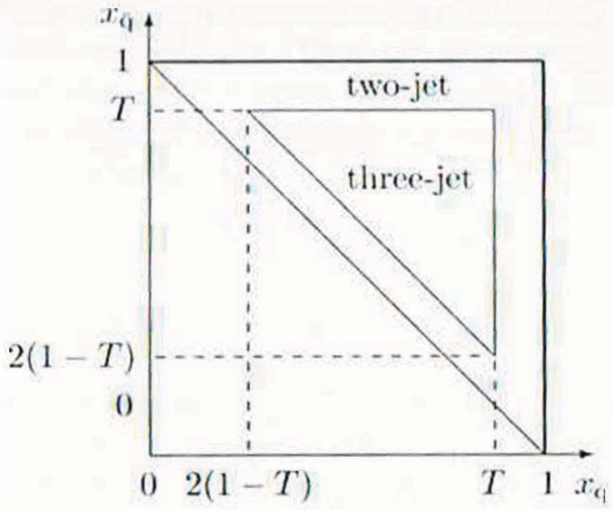

FIG. 3.12. A Dalitz plot showing the allowed region of the $x_q - x_{\bar{q}}$ plane for a $\gamma \to q\bar{q}g$ event with massless partons. The thick lines indicate the collinear singularities, $\theta_{\bar{q}g} \to 0 \Longrightarrow x_q = 1$ and $\theta_{qg} \to 0 \Longrightarrow x_{\bar{q}} = 1$, their intersection marks the position of the soft singularity, $x_g \to 0 \Longrightarrow x_q = 1 = x_{\bar{q}}$. Also shown is the boundary line separating the two- and three-jet regions based on the criterion $\max\{x_q, x_{\bar{q}}, x_g\} < T$.

$x_q = [0,1]$ $x_{\bar{q}} = [0,1]$ square, with lines of constant x_g running parallel to the diagonal edge, where $x_g = 1$. In eqn (3.112) we see very clearly the singularity structure for gluon radiation. If $\theta_{qg} \to 0$ then $2q \cdot g = (1 - x_{\bar{q}})Q^2 \to 0$, that is, $x_{\bar{q}} \to 1$, whilst if $E_g \to 0$ ($x_g \to 0$) then *both* x_q and $x_{\bar{q}} \to 1$.

3.3.3 $q\bar{q} \to gg$ *and the gauge invariant QCD Lagrangian*

We will now consider a pure QCD process, $q\bar{q} \to gg$, at leading order with, for convenience, massless quarks. Our approach will be to try to generalize the well understood theory of abelian QED to describe the non-abelian theory of QCD.

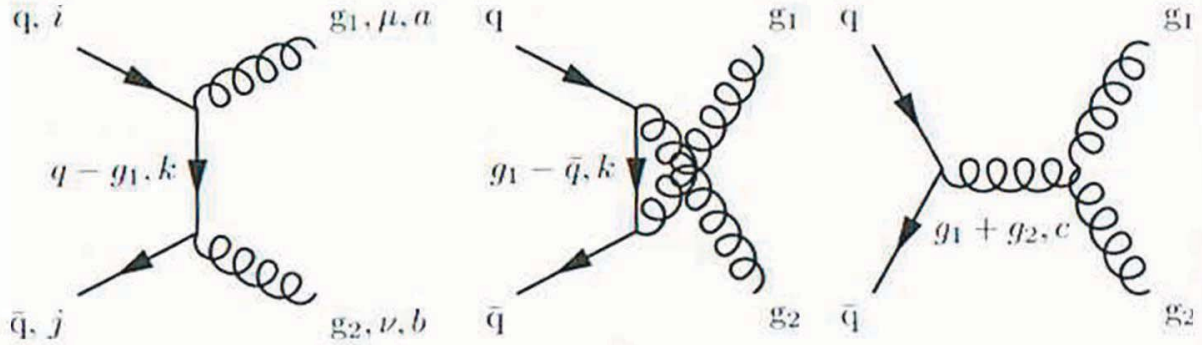

FIG. 3.13. The three leading order Feynman diagrams for $q\bar{q} \to gg$.

By direct analogy to the process $q\bar{q} \to \gamma\gamma$ we are quickly led to the first two Feynman diagrams shown in Fig. 3.13. Their matrix elements are given by

$$\begin{aligned}&(\mathcal{M}_t + \mathcal{M}_u)\big(\epsilon^*(g_1), \epsilon^*(g_2)\big)\\ &= -\mathrm{i}\, g_s^2 \bar{v}(\bar{q}) \left[T^b_{jk} T^a_{ki} \not{\epsilon}^*(g_2) \frac{1}{\not{q} - \not{g}_1} \not{\epsilon}^*(g_1) + T^a_{jk} T^b_{ki} \not{\epsilon}^*(g_1) \frac{1}{\not{g}_1 - \not{\bar{q}}} \not{\epsilon}^*(g_2) \right] u(q) \,.\end{aligned} \tag{3.114}$$

Observe that we have included two non-commuting colour matrices at the quark–gluon vertices. This has significant consequences for gauge invariance. Replacing $\epsilon(g_2)$ by $g_2 = q + \bar{q} - g_1$, c.f. eqn (3.100), we easily find

$$\begin{aligned}(\mathcal{M}_t + \mathcal{M}_u)\big(\epsilon^*(g_1), g_2\big) &= -\mathrm{i}\, g_s^2 (T^b T^a - T^a T^b)_{ji} \bar{v}(\bar{q}) \not{\epsilon}^*(g_1) u(q)\\ &= -g_s^2 f^{abc} T^c_{ji} \bar{v}(\bar{q}) \not{\epsilon}^*(g_1) u(q) \,,\end{aligned} \tag{3.115}$$

so that, unlike the case of abelian QED, gauge invariance appears to be violated! The result is unaffected by including non-zero quark masses. Indeed this would be the case if there were no other diagrams contributing. However, since gluons carry colour charge, we might anticipate the existence of a triple-gluon vertex giving the third diagram in Fig. 3.13. In fact, looking at eqn (3.115), we see that the remainder has the form of a quark–gluon vertex proportional to $-\mathrm{i}\, g_s T^c_{ji}$ times a new factor proportional to $+g_s f^{abc}$, that is, proportional to the appropriate colour matrix for an adjoint representation gluon. That the gluon should be placed in the adjoint representation makes sense from the group theoretical point of view, because when coupled to a particle in the representation R only the adjoint representation, which for SU(3) is an octet, is guaranteed to be contained within the tensor product $R \otimes \overline{R}$. Thus, only octet gluons can directly couple to particles from any other representation.

The properties of this new triple-gluon vertex $+g_s f^{abc} V_{\mu\nu\sigma}(g_1, g_2, g_3)$, with $g_1 + g_2 + g_3 = 0$, are easily established. Looking at eqn (3.115), and bearing in mind the s-channel propagator present in Fig. 3.13, it must have mass dimension one, be a Lorentz tensor and, since gluons are bosons, be totally symmetric under interchange of the labels on any pair of gluons. That is, since f^{abc} is completely antisymmetric in its indices, the same must hold for V. Thus, it must be constructed from terms of the form $\eta_{\mu\nu} g_{1\sigma}$, $\eta_{\mu\nu} g_{2\sigma}$, $\eta_{\mu\nu} g_{3\sigma}$ etc. and be antisymmetric under $\mu \leftrightarrow \nu$ and $g_1 \leftrightarrow g_2$ etc. A little experimentation shows that the only non-trivial possibility is

$$V_{\mu\nu\sigma}(g_1, g_2, g_3) = \big[\eta_{\mu\nu}(g_1 - g_2)_\sigma + \eta_{\nu\sigma}(g_2 - g_3)_\mu + \eta_{\sigma\mu}(g_3 - g_1)_\nu\big] \,, \tag{3.116}$$

as also given by the Feynman rules in Appendix B. Taking over the form of the (Feynman gauge) photon propagator for the gluon we have

$$\mathcal{M}_s\big(\epsilon^*(g_1), \epsilon^*(g_2)\big)$$

$$= \bar{v}(\bar{q}) \cdot -\mathrm{i}\, g_s T^c_{ji} \gamma_\sigma \cdot u(q) \times \frac{-\mathrm{i}\, \eta^{\sigma\tau}}{(g_1+g_2)^2} \times +g_s f^{abc} \tag{3.117}$$
$$\times \left[\eta_{\mu\nu}(g_1-g_2)_\tau + \eta_{\nu\tau}(g_1+2g_2)_\mu - \eta_{\sigma\mu}(2g_1+g_2)_\nu\right] \cdot \epsilon^*(g_1)^\mu \epsilon^*(g_2)^\nu \ ,$$

and again replacing $\epsilon^*(g_2)^\nu$ by g_2^ν in this new contribution gives

$$\mathcal{M}_s\big(\epsilon^*(g_1), g_2\big) = +g_s^2 f^{abc} T^c_{ji} \bar{v}(\bar{q}) \left[\not{\epsilon}^*(g_1) + \not{g}_2 \frac{g_1 \cdot \epsilon^*(g_1)}{2g_1 \cdot g_2} \right] u(q) \ . \tag{3.118}$$

Given the choice of unit numerical coefficient in eqn (3.116) this exactly restores gauge invariance, provided the first gluon is physical, that is, $g_1 \cdot \epsilon(g_1) = 0$.

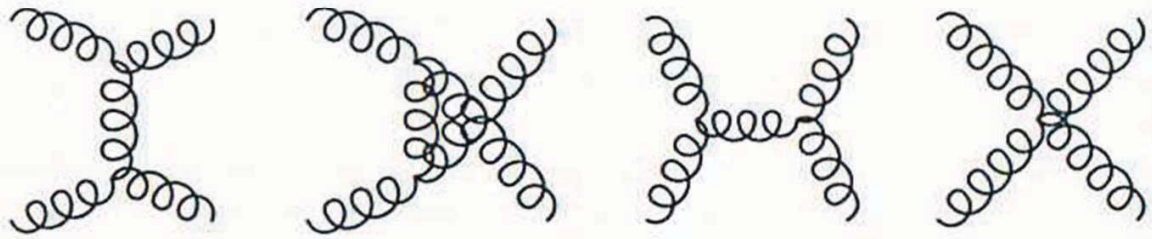

FIG. 3.14. The leading order Feynman diagrams contributing to gluon–gluon scattering

Having been led to introduce a triple-gluon coupling we ought to consider also the process $gg \to gg$, which now can proceed via the first three diagrams in Fig. 3.14. If we test gauge invariance and replace $\epsilon^*(g_4)^\mu$ by g_4^μ, the sum of the first three diagrams in Fig. 3.14 gives the following contribution:

$$\begin{aligned}
&(\mathcal{M}_t + \mathcal{M}_u + \mathcal{M}_s)\big(\epsilon(g_1), \epsilon(g_2), \epsilon^*(g_3), g_4\big) \\
&= -\mathrm{i}\, g_s^2 \big[+ f^{abe} f^{cde} (\epsilon_1 \cdot \epsilon_3^*\, \epsilon_2 \cdot g_4 - \epsilon_1 \cdot g_4\, \epsilon_2 \cdot \epsilon_3^*) \\
&\qquad + f^{ace} f^{dbe} (\epsilon_1 \cdot g_4\, \epsilon_2 \cdot \epsilon_3^* - \epsilon_1 \cdot \epsilon_2\, \epsilon_3^* \cdot g_4) \\
&\qquad + f^{ade} f^{bce} (\epsilon_1 \cdot \epsilon_2\, \epsilon_3^* \cdot g_4 - \epsilon_1 \cdot \epsilon_3^*\, \epsilon_2 \cdot g_4) \big]
\end{aligned} \tag{3.119}$$

Here, we assume on mass-shell ($g_i^2 = 0$), physical ($g_i \cdot \epsilon(g_i) = 0$) external gluons and employ the Jacobi identity, eqn (A.12). Once more, we find problems with gauge invariance for this subset of diagrams which can be remedied by introducing a dimensionless, fully symmetric quartic-gluon vertex. The exact form can be read off directly from eqn (3.119) and can be found in Appendix B. This vertex has exactly the same structure as that derived from the gauge-kinetic term in the Yang–Mills (QCD) Lagrangian. What is more, these triple- and quartic-gluon vertices are sufficient to guarantee the gauge invariance of all QCD processes to all orders — no other gluon self-vertices are needed.

3.3.3.1 *Physical states and ghosts* In eqn (3.118) we demonstrated effectively the gauge invariance of the $q\bar{q} \to gg$ amplitude provided that *both* gluons have

physical polarizations. This raises the issue of how to treat the polarization tensor for the gluon: is the QED form, eqn (3.103), really adequate for QCD? For a vector particle of momentum k^μ its polarization vectors must satisfy

$$\epsilon(k;s)\cdot\epsilon^*(k;s') = -\delta_{ss'} \quad \text{and} \quad k\cdot\epsilon(k) = 0\,. \tag{3.120}$$

The first equation imposes ortho-normality on the basis states whilst the second equation requires that they are orthogonal to the particle's direction of motion. Now, because the gluon (or photon) is massless it only has two physical polarization states whereas the second equation only imposes one constraint on the four components of a polarization vector. Thus, we require an additional constraint, which can be taken to be $n\cdot\epsilon = 0$, where n is any four-vector subject to $n\cdot k \neq 0$. As the physical polarization sum, $T_{\mu\nu}$, can be constructed only from $\eta_{\mu\nu}$, k_μ and n_ν, is required to satisfy $k^\mu T_{\mu\nu} = k^\nu T_{\mu\nu} = n^\mu T_{\mu\nu} = n^\nu T_{\mu\nu} = 0$ and have trace $T^\mu{}_\mu = -2$, it is straightforward to show that it must have the form

$$\sum_{\text{phys}} \epsilon(k)_\mu \epsilon^*(k)_\nu = -\eta_{\mu\nu} + \frac{(k_\mu n_\nu + n_\mu k_\nu)}{n\cdot k} - n^2\frac{k_\mu k_\nu}{(n\cdot k)^2}\,; \tag{3.121}$$

see Ex. (3-15). This is precisely the form of the numerator of the gluon propagator in a physical gauge. There is quite some freedom in the choice of n^μ which we can use to our advantage. In particular, having $n^2 = 0$ simplifies things.

Given the correct polarization tensor, eqn (3.121), you might ask why this expression is not used in QED calculations, since the arguments leading to its construction apply equally well to photons and gluons. The difference lies in the realization of gauge invariance. In QED we have

$$k^\mu \mathcal{M}_{\mu\nu\sigma\ldots} = 0 \tag{3.122}$$

which for a physical photon is independent of the polarization of all other photons. In QCD all other gluons also had to be physical. Thus, the 'extra' terms in eqn (3.121) which subtract out the unphysical longitudinal and scalar polarizations and are proportional to k give vanishing contributions and can be safely dropped. In QED, we can use $-\eta_{\mu\nu}$ for the polarization sum. Likewise we can use $-\eta_{\mu\nu}$ in QCD, provided only a single external gluon is present. If two or more external gluons are present using $-\eta_{\mu\nu}$ will leave unwanted extra contributions. For example, using the full expression for the $q\bar{q} \to gg$ amplitude the additional contribution is given by:

$$\mathcal{M}_{\sigma\tau}\mathcal{M}^\dagger_{\sigma'\tau'}\left\{[-\eta^{\sigma\sigma'}]\times[-\eta^{\tau\tau'}] - \left[-\eta^{\sigma\sigma'} + \frac{(g_1^\sigma n_1^{\sigma'} + n_1^\sigma g_1^{\sigma'})}{n_1\cdot g_1} - n_1^2\frac{g_1^\sigma g_1^{\sigma'}}{(n_1\cdot g_1)^2}\right]\right.$$
$$\left.\times\left[-\eta^{\tau\tau'} + \frac{(g_2^\tau n_2^{\tau'} + n_2^\tau g_2^{\tau'})}{n_2\cdot g_2} - n_2^2\frac{g_2^\tau g_2^{\tau'}}{(n_2\cdot g_2)^2}\right]\right\}$$

$$= \left| \mathrm{i}\, g_s^2 f^{abc} T^c_{ji} \frac{1}{2g_1 \cdot g_2} \bar{v}(\bar{q}) \not{g}_1 u(q) \right|^2 . \tag{3.123}$$

Here, we see that any dependence on the arbitrary four-vectors n_1 and n_2 vanishes, which is in fact required by gauge invariance. The final result also appears to be asymmetric. However, this is illusory: if we replace g_1 by $(q+\bar{q}) - g_2$, then the bracketed term vanishes and we are left with the same expression except that now $\not{g}_2$ appears, and f^{abc} becomes f^{bac}, that is, the result really is 1–2 symmetric.

The obvious way in which to avoid the contribution due to unphysical gluon polarizations, such as in eqn (3.123), is to always use eqn (3.121) for external gluons. However, this is cumbersome and an alternative is available. We retain eqn (3.103) for the polarization sum and add yet another diagram to those in Fig. 3.13 whose contribution is designed to cancel exactly the unwanted contribution. Looking at eqn (3.123) the structure is that of a $\mathrm{q\bar{q}g}$ vertex, followed by a gluon propagator and finally a term proportional to $-g_s f^{abc} g_1^\mu$. This suggests the form of a new $\eta\bar{\eta}\mathrm{g}$ vertex. We choose η to be a Lorentz scalar field, for simplicity, make it complex to give the vertex a 'directionality', so as to distinguish g_1 from g_2, and put it into a colour octet representation to justify the f^{abc} colour factor. Finally, we have this ghost field obey Fermi–Dirac statistics so that closed loops acquire an extra minus sign as do quarks. However, ghosts are scalars and this choice violates the spin-statistics theorem. As a consequence ghosts violate unitarity and give negative cross sections — which cancel precisely the unwanted term eqn (3.123).

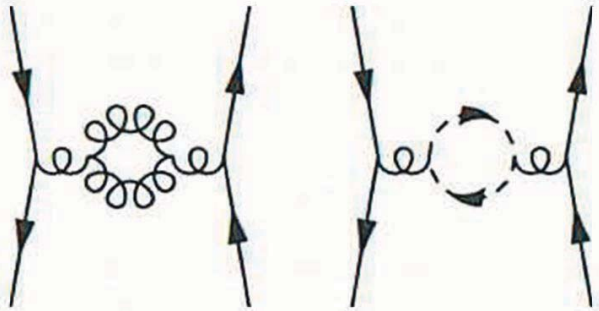

FIG. 3.15. Two of the diagrams contributing to the gluon self-energy

At this point the rôle of the unphysical ghost fields appears to be only to facilitate a trick intended to simplify the calculation of tree-level amplitudes. The situation is more subtle when loop diagrams occur, such as in Fig. 3.15. These diagrams can be viewed as either higher order contributions to the amplitude for $\mathrm{q\bar{q}}$ scattering or, if the diagrams are 'cut' through the loop, as contributions to the amplitude squared, $\mathcal{M}$ (left-hand side) $\times\, \mathcal{M}^\dagger$ (right-hand side), for $\mathrm{q\bar{q}} \to \mathrm{gg}$. This dual interpretation can be made more formal. In the first interpretation there exists a region of the loop momentum integral (see Section 3.4 for an elaboration) in which both internal particles are real, that is, on their positive mass-shells, and generate an imaginary part in the complex amplitude. In the

second interpretation this same integral corresponds to the phase-space integral appearing in the total cross section for the production of a pair of real gluons. (This non-linear relationship between S-matrix elements is in essence the optical theorem.) The significance of this equivalence is that we must restrict the internal gluons in any loop to only physical polarization states or violate unitarity. This can be achieved in two ways. Either, use a physical gauge, so called because only physical polarizations propagate for an on mass-shell gluon. Or use a covariant gauge and whenever a gluon loop occurs add the contribution from a ghost loop, remembering to include the extra minus sign, thereby ensuring the removal of any non-physical contributions.

3.3.4 *The evaluation of colour factors*

The evaluation of the colour factors which occur in the expressions we will encounter for matrix elements can always be found using essentially two results. For any particular sub-amplitude the colour factor consists of an ordered product of T^a and f^{abc} terms. The latter can be eliminated by applying the following identity, derived in Appendix A,

$$f^{abc} = -\frac{\mathrm{i}}{T_F}\mathrm{Tr}\left\{T^aT^bT^c - T^cT^bT^a\right\}, \tag{3.124}$$

to the fundamental representation. After applying eqn (3.124) we are left with a string of T^a matrices. Now all internal indices are already summed over and once the amplitude is squared and colour averaged so are all external indices. Thus, the matrices can be paired as $T^a_{ij}T^a_{kl}\,T^b_{pq}T^b_{rs}\,\cdots$, allowing the completeness relation to be substituted,

$$\sum_a T^a_{ij}T^a_{kl} = T_F\left[\delta_{il}\delta_{jk} - \frac{1}{N_c}\delta_{ij}\delta_{kl}\right]. \tag{3.125}$$

Finally, by carefully contracting the colour δ-functions, a pure number, the colour factor, will remain.

We illustrate this approach using the process $\mathrm{q\bar{q}} \to \mathrm{gg}$. Schematically, the amplitude may be written

$$\begin{aligned}\mathcal{M} &= T^aT^b\mathcal{M}_t + T^bT^a\mathcal{M}_u + \mathrm{i}\,f^{abc}T^c\mathcal{M}_s \\ &= T^aT^b(\mathcal{M}_t + \mathcal{M}_s) + T^bT^a(\mathcal{M}_u - \mathcal{M}_s)\,.\end{aligned} \tag{3.126}$$

The first two terms are associated with the two orderings of the double bremsstrahlung contribution. The third term, which has been eliminated either directly using eqn (A.10) or less directly using eqn (3.124) and eqn (A.7), is associated with splitting of a radiated gluon via the triple-gluon vertex. The T^aT^b and T^bT^a terms in $\mathcal{M}\mathcal{M}^\dagger$, after colour averaging, each give rise to the colour factor

$$\mathrm{Tr}\left\{T^aT^bT^bT^a\right\} = \sum_{ab}\sum_{ijkl} T^a_{ij}T^b_{jk}T^b_{kl}T^a_{li}$$

$$
\begin{aligned}
&= \sum_{ijkl} \sum_{a} T^a_{ij} T^a_{li} \times \sum_{b} T^b_{jk} T^b_{kl} \\
&= \sum_{ijkl} T_F \left(\delta_{ii}\delta_{jl} - \frac{1}{N_c}\delta_{ij}\delta_{li} \right) \times T_F \left(\delta_{jl}\delta_{kk} - \frac{1}{N_c}\delta_{jk}\delta_{kl} \right) \\
&= \sum_{jl} T_F \left(N_c - \frac{1}{N_c} \right) \delta_{jl} \times T_F \left(N_c - \frac{1}{N_c} \right) \delta_{jl} \\
&= N_c C_F^2 \, . \qquad (3.127)
\end{aligned}
$$

After rather more work the cross-term can be evaluated similarly to obtain the colour factor

$$
\mathrm{Tr}\left\{ T^a T^b T^a T^b \right\} = N_c C_F \left(C_F - \frac{C_A}{2} \right) = -N_c C_F \frac{1}{2N_c} \, . \qquad (3.128)
$$

From these two results we can deduce that the colour factor associated with the $|\mathcal{M}_3|^2$ term is given by $N_c C_F C_A$. Thus, we learn that $|\mathcal{M}|^2$ is proportional to the number of quark colours, N_c; the radiation of a gluon off a(n anti)quark is proportional to C_F; whilst radiation off a gluon is proportional to C_A. Also, we see a generic behaviour, the interference between two colour flows, here $T^a T^b$ and $T^b T^a$, is suppressed by a typical factor N_c^{-2} compared to the direct contributions.

Again, in practice, a number of tricks may be applicable in special cases to speed up colour factor calculations. In the case of eqn (3.127) we could use eqn (A.17), $\sum_{aj} T^a_{ij} T^a_{jk} = C_F \delta_{ik}$, to immediately obtain the result. For eqn (3.128) one can substitute $T^a T^b = (T^b T^a + \mathrm{i} f^{abc} T^c)$. The first term has just been evaluated. For the second term one can write

$$
\begin{aligned}
\mathrm{i} f^{abc} \mathrm{Tr}\left\{ T^c T^b T^a \right\} &= \mathrm{i} f^{abc} \mathrm{Tr}\left\{ T^c T^b T^a - T^c T^a T^b \right\}/2 \\
&= T_F f^{abc} f^{abc}/2 \qquad (3.129) \\
&= T_F C_A (N_c^2 - 1)/2 \, ,
\end{aligned}
$$

where we used the antisymmetry of f^{abc}, eqn (3.124), and eqn (A.17). These two terms when combined give the quoted result. However, the approach discussed first is guaranteed to work in all cases and is ideally suited to being done by computer algebra techniques, thereby reducing the risk of error and the tedium.

3.4 Ultraviolet divergences and renormalization

When a Feynman diagram involves a closed loop, the momentum conserving δ-functions at the vertices prove insufficient to specify fully the momentum of the particles in the loop — an integral over a loop momentum remains. For example, in a self-energy diagram an integral of the following form may be encountered:

$$\int \mathrm{d}^4k \frac{1}{[(k+p)^2 - m^2]\,k^2} \sim \int \mathrm{d}\Omega_3 \int \mathrm{d}k k^3 \frac{1}{k^2 \cdot k^2} \sim \int^{\Lambda} \frac{\mathrm{d}k}{k} \sim \ln \Lambda \,. \qquad (3.130)$$

Truncating the integral by an ultraviolet cut-off, Λ, we see that the integral is logarithmically divergent. Renormalization is the treatment of such divergences which are associated with the high frequency — short distance components of the fields. In essence, the procedure first involves using a regulator to artificially render all integrals finite, so that they can be safely manipulated. Second, new terms are introduced into the theory in such a way that all the divergences cancel between the contributions from the bare Lagrangian and the new counterterms when the regulator is removed. Significantly, these additional terms must have exactly the same structure as the original Lagrangian. Finally, the finite matrix elements can be compared to experimentally measured numbers and, after fixing any free parameters, higher order predictions can be made. We will demonstrate this procedure at one-loop. More details can be found in many of the standard field theory texts, such as (Ramond, 1990) or (Peskin and Schroeder, 1995).

Unfortunately, the crude cut-off used to make eqn (3.130) finite is not compatible with either Lorentz or gauge invariance. Technically speaking, the Ward identities are violated. However, it is easy to see that if the k-integral involves fewer dimensions, then the integral again becomes finite but importantly now no longer violates the two symmetries. Dimensional regularization is the preferred choice in pQCD calculations. The method of dimensional regularization and the standard procedures for dealing with (one) loop integrals are described in Appendix C.

3.4.1 *Self-energy and vertex corrections*

Armed with the knowledge of how to use dimensional regularization to calculate one-loop amplitudes, we now sketch the results for the quark and gluon self-energies and quark–gluon and triple-gluon vertices. These are the core corrections to the propagators and couplings in which all the external propagators are 'amputated'. We shall work in a covariant gauge with arbitrary gauge parameter $\xi \neq 1$. This will be followed by a discussion of how renormalization handles the divergences which we isolate.

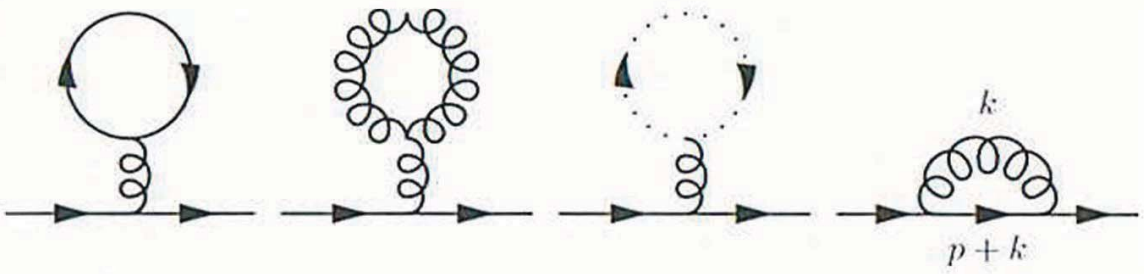

FIG. 3.16. The three tadpole-type diagrams and the quark–gluon loop diagram which contribute to the quark self-energy at leading non-trivial order, $\mathcal{O}(\alpha_s)$

At $\mathcal{O}(\alpha_s)$ four diagrams, shown in Fig. 3.16, appear to contribute to the quark self-energy. However, the three 'tadpole' diagrams give zero contributions. This is seen most easily by considering the diagram's colour factors, $\mathrm{Tr}\{T^a\} = 0$ and $f_{abb} = 0$, for the quark and both the gluon and ghost tadpoles, respectively. This leaves only the fourth diagram, which apart from a group theoretical factor, is the same as in the abelian theory QED. The one-loop integral yields

$$\begin{aligned} -\mathrm{i}\,\Sigma(p) = \int \frac{\mathrm{d}^D k}{(2\pi)^D} \Bigg\{ & -\mathrm{i}\, g_s \mu^\epsilon T^a_{ik} \gamma_\mu \times \mathrm{i}\, \frac{(\not{k} + \not{p} + m)}{[(k+p)^2 - m^2]} \times -\mathrm{i}\, g_s \mu^\epsilon T^a_{kj} \gamma_\nu \\ & \times \frac{\mathrm{i}}{k^2} \left[-\eta^{\mu\nu} + (1-\xi) \frac{k^\mu k^\nu}{k^2} \right] \Bigg\} \qquad (3.131) \\ = -(g_s \mu^\epsilon)^2 C_F \delta_{ij} & \int \frac{\mathrm{d}^D k}{(2\pi)^D} \frac{\gamma_\mu (\not{k} + \not{p} + m) \gamma_\nu}{[(k+p)^2 - m^2] k^2} \left[\eta^{\mu\nu} - (1-\xi) \frac{k^\mu k^\nu}{k^2} \right] . \end{aligned}$$

This expression should be familiar from the discussion in Appendix C and indeed coincides with eqn (C.1) for $\xi = 1$. The full result is

$$\begin{aligned} -\mathrm{i}\,\Sigma(p) = \mathrm{i}\, \frac{\alpha_s}{4\pi} C_F \delta_{ij} \Bigg\{ & \Delta_\epsilon \left[\xi \not{p} - (3+\xi) m \right] \\ & - \not{p} \left[1 + 2 \int_0^1 \mathrm{d}\alpha \left\{ 2\alpha\xi \ln\left(\frac{A(\alpha)}{\mu^2} \right) + (1-\xi) p^2 \frac{\alpha^2 (1-\alpha)}{A(\alpha)} \right\} \right] \\ & + m \left[2 + (3+\xi) \int_0^1 \mathrm{d}\alpha \ln\left(\frac{A(\alpha)}{\mu^2} \right) \right] \Bigg\} , \qquad (3.132) \end{aligned}$$

with $A(\alpha) = \alpha m^2 - \alpha(1-\alpha) p^2$.

The calculation of the gluon self-energy proceeds in a similar manner. At $\mathcal{O}(\alpha_s)$ the relevant Feynman diagrams are shown in Fig. 3.17. Again the four tadpole diagrams do not contribute. The first three diagrams are the same as for the quark propagator and vanish for the same reasons, the fourth diagram is more interesting as its colour factor is non-vanishing. In dimensional regularization it is proportional to a momentum integral which possesses no intrinsic scale,

$$\int \frac{\mathrm{d}^D k}{(2\pi)^D} \frac{1}{k^2} . \qquad (3.133)$$

As a result there is no value of D for which we can evaluate the integral. If $D \geq 2$ then it contains an ultraviolet divergence, whilst if $D \leq 2$ it contains an infrared divergence. In this circumstance we define such an integral to be identically zero (Collins, 1986). To help motivate this choice, if the integral were not zero then it would contribute a mass to the gluon, thereby violating gauge invariance. In fact, we could have also applied this argument to the loop integrals arising from the gluon and ghost tadpoles. The quark loop contribution, for a single quark flavour, is given by

$$-\mathrm{i}\,\Pi(p)^{\mu\nu}_{\mathrm{qq}} = -\,(g_s \mu^\epsilon)^2 \mathrm{Tr}\left\{ T^a T^b \right\} \int \frac{\mathrm{d}^D k}{(2\pi)^D} \frac{\mathrm{Tr}\left\{ \gamma^\mu (\not{k} + \not{p} + m) \gamma^\nu (\not{k} + m) \right\}}{[(k+p)^2 - m^2][k^2 - m^2]}$$

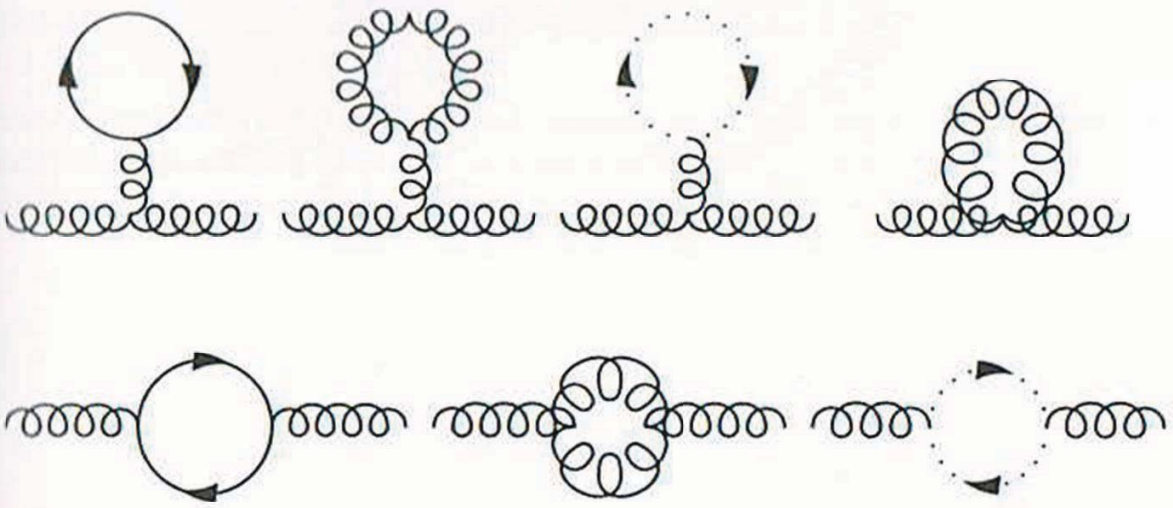

FIG. 3.17. The four tadpole-type diagrams and the quark, gluon and (in a covariant gauge) its associated ghost loop diagrams, which contribute to the gluon self-energy at leading non-trivial order, $\mathcal{O}(\alpha_s)$

$$= -\,\mathrm{i}\,\frac{\alpha_s}{4\pi} T_F \delta^{ab} \frac{4}{3}(p^2\eta^{\mu\nu} - p^\mu p^\nu) \times \left[\Delta_\epsilon - 6\int_0^1 \mathrm{d}\alpha\,\alpha(1-\alpha)\ln\left(\frac{m^2 - \alpha(1-\alpha)p^2}{\mu^2}\right)\right] . \qquad (3.134)$$

The only subtlety in this contribution to the gluon self-energy is the overall minus sign for the closed quark loop, otherwise the evaluation follows the earlier pattern and, if anything, is more straightforward. Modulo the coupling and colour factor the result is the familiar one from QED. In the non-abelian QCD, the new contributions come from the gluon and ghost loops. The gluon loop is given by

$$\begin{aligned}
-\mathrm{i}\,\Pi(p)^{\mu\nu}_{\mathrm{gg}} &= (g_s\mu^\epsilon)^2 f_{acd} f_{bcd} \frac{1}{2}\int \frac{\mathrm{d}^D k}{(2\pi)^D} \\
&\quad \times \left[\eta^\mu{}_\alpha (k+2p)_\beta - \eta_{\alpha\beta}(2k+p)^\mu + \eta_\beta{}^\mu (k-p)_\alpha\right] \\
&\quad \times \frac{1}{(k+p)^2}\left(\eta^{\alpha\gamma} - (1-\xi)\frac{(k+p)^\alpha (k+p)^\gamma}{(k+p)^2}\right) \\
&\quad \times \left[\eta^\nu{}_\delta (k-p)_\gamma - \eta_{\delta\gamma}(2k+p)^\nu + \eta_\gamma{}^\nu (k+2p)_\delta\right] \\
&\quad \times \frac{1}{k^2}\left(\eta^{\beta\delta} - (1-\xi)\frac{k^\beta k^\delta}{k^2}\right) \\
&= \frac{\alpha_s}{4\pi} C_A \delta^{ab} \frac{1}{12}\left\{(19p^2\eta^{\mu\nu} - 22p^\mu p^\nu)\left[\Delta_\epsilon - \ln\left(\frac{-p^2}{\mu^2}\right)\right]\right. \\
&\qquad + \frac{116}{3}p^2\eta^{\mu\nu} - \frac{134}{3}p^\mu p^\nu \\
&\qquad \left. + 6(1-\xi)\left(\left[\Delta_\epsilon - \ln\left(\frac{-p^2}{\mu^2}\right)\right] - 2\right)(p^2\eta^{\mu\nu} - p^\mu p^\nu)\right.
\end{aligned}$$

$$+ 3(1-\xi)^2(p^2\eta^{\mu\nu} - p^\mu p^\nu)\Big\} \,. \tag{3.135}$$

The overall factor of one half is to account for the diagram's symmetry factor. Despite its appearance the calculation is tedious rather than difficult and, given their relative simplicity, we have carried out the Feynman parameter integrals. The ghost contribution is rather less involved and is given by

$$\begin{aligned} -\mathrm{i}\,\Pi(p)^{\mu\nu}_{\eta\eta^\dagger} &= -(g_s\mu^\epsilon)^2 f_{acd}f_{bcd}\int \frac{\mathrm{d}^D k}{(2\pi)^D}\frac{(k+p)^\mu k^\nu}{(k+p)^2k^2} \\ &= \mathrm{i}\,\frac{\alpha_s}{4\pi}C_A\delta^{ab}\frac{1}{12}\Big\{(p^2\eta^{\mu\nu}+2p^\mu p^\nu)\left[\Delta_\epsilon - \ln\left(\frac{-p^2}{\mu^2}\right)\right] \\ &\qquad + \frac{8}{3}p^2\eta^{\mu\nu} + \frac{5}{18}p^\mu p^\nu\Big\} \,. \end{aligned} \tag{3.136}$$

Note that there is an overall minus sign due to the fermionic nature of the ghost fields.

Referring back to the quark loop contribution to the gluon self-energy, given by eqn (3.134), we see that it has a transverse tensor structure, $p_\mu\Pi^{\mu\nu}_{q\bar{q}}(p) = 0 = p_\nu\Pi^{\mu\nu}_{q\bar{q}}(p)$, equivalent to $\Pi^{\mu\nu}_{q\bar{q}} \propto (p^2\eta^{\mu\nu} - p^\mu p^\nu)$. This structure is not shown by either the pure gluon, eqn (3.135), or ghost, eqn (3.136), contributions separately. However, they naturally form a set which when added together gives

$$-\mathrm{i}\,\Pi(p)^{\mu\nu}_{\text{gauge}} \equiv -\mathrm{i}\left(\Pi^{\mu\nu}_{gg} + \Pi^{\mu\nu}_{\eta\eta^\dagger}\right) \tag{3.137}$$

$$= \mathrm{i}\,\frac{\alpha_s}{4\pi}C_A\delta^{ab}\left\{\frac{(13-3\xi)}{6}\left[\Delta_\epsilon - \ln\left(\frac{-p^2}{\mu^2}\right)\right] + \frac{115}{36} + \frac{1}{4}\xi^2\right\} \times (p^2\eta^{\mu\nu} - p^\mu p^\nu) \,.$$

As we shall see, this is an important consequence of gauge invariance. A result all the more surprising since our Lagrangian contains an explicit gauge breaking term and the 'tree-level' propagator is not, in general, transverse.

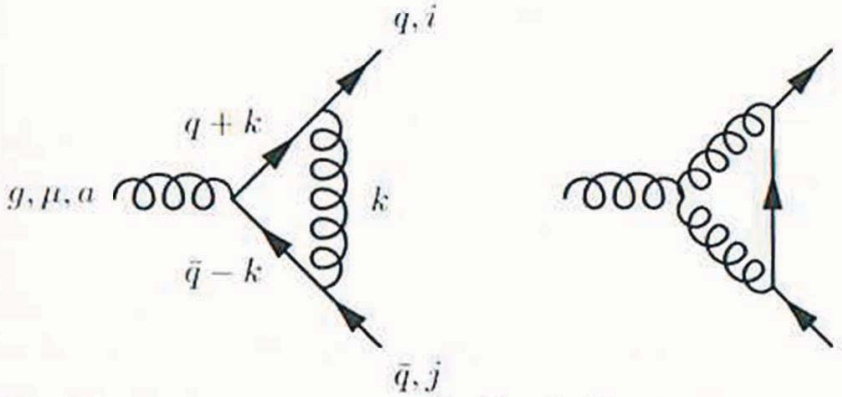

FIG. 3.18. The two diagrams contributing to the quark–gluon vertex at $\mathcal{O}(\alpha_s)$

The calculation of one-loop vertex corrections is more involved and results in rather complicated expressions which we choose not to give in full; details can

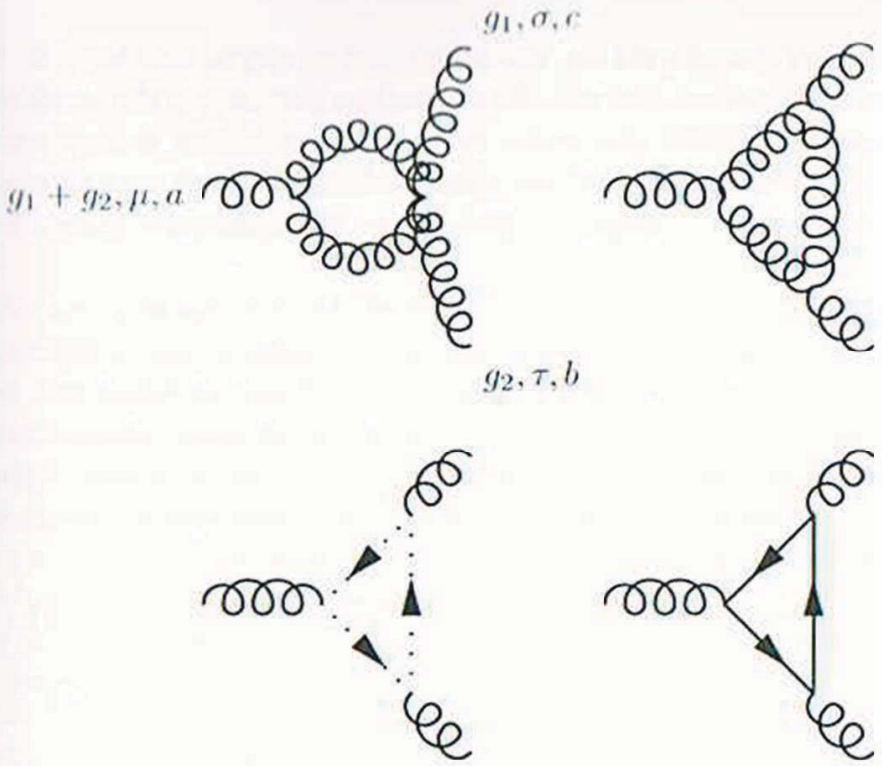

FIG. 3.19. The four basic diagrams contributing to the triple-gluon vertex at $\mathcal{O}(\alpha_s)$. Note that two further permutations of the first diagram exist.

be found in the literature. Instead we only show, the relatively straightforward, divergent parts of the vertex corrections. Figure 3.18 shows the two diagrams which contribute to the quark–gluon vertex at $\mathcal{O}(\alpha_s)$. The first is essentially the same as in QED, whilst the second only arises in a non-abelian theory such as QCD. The result for the ultraviolet divergent part of the vertex correction is

$$\Gamma^a_{ij}(g,q)^\mu = -\mathrm{i}\, g_s \mu^\epsilon T^a_{ji} \gamma^\mu \frac{\alpha_s}{4\pi} \left\{ \left[\xi \left(C_F - \frac{C_A}{2} \right) + \frac{3(1+\xi)}{4} C_A \right] \Delta_\epsilon + \begin{matrix} \text{U.V.} \\ \text{finite} \end{matrix} \right\} . \tag{3.138}$$

The first term comes from the 'QED-like' graph, proportional to $T^b T^a T^b$, whilst the second comes from the non-abelian graph, proportional to $T^b f_{abc} T^c$. Figure 3.19 shows the four basic diagrams which contribute to the triple-gluon vertex at $\mathcal{O}(\alpha_s)$. The result for the ultraviolet divergent part of the vertex is given by

$$\begin{aligned} \Gamma_{abc}(g_1,g_2)^{\mu\sigma\tau} = {} & g_s \mu^\epsilon f_{abc} \left[\eta^{\sigma\tau}(g_1 - g_2)^\mu + \eta^{\tau\mu}(g_1 + 2g_2)^\sigma - \eta^{\mu\tau}(2g_1 + g_2)^\sigma \right] \\ & \times \left\{ \frac{\alpha_s}{4\pi} \left[\frac{4}{3} T_F n_f - \frac{(17 - 9\xi)}{12} C_A \right] \Delta_\epsilon + \begin{matrix} \text{U.V.} \\ \text{finite} \end{matrix} \right\} . \end{aligned} \tag{3.139}$$

The first term is given by the n_f fermions which contribute to the quark loop. In QED, this term would vanish according to Furry's theorem (Furry, 1937), which states that any quark loop joined to an odd number of photons vanishes. This is essentially because QED's charge conjugation symmetry guarantees that

the contributions from a quark and an antiquark going round the loop in the opposite direction exactly cancel. Furry's theorem does not ensure the vanishing of this diagram because in QCD the order of the colour factors is important: $\mathrm{Tr}\left\{T^aT^bT^c\right\} \neq \mathrm{Tr}\left\{T^cT^bT^a\right\}$ so that the quark and antiquark contributions do not cancel. The second term in eqn (3.139) arises from the pure gauge field (gluon and ghost) diagrams.

As a result of these and other somewhat involved calculations we are able to write the one-loop corrections in terms of a divergent (in the $\epsilon \to 0$ limit) and a finite piece. Significantly, the coefficients of the divergent pieces follow the pattern established by the tree-level terms already present in the Lagrangian density — no new divergent interactions occur. This will prove to be of crucial importance in our approach to renormalization. It is also a very non-trivial statement. For example, a term of the form $\ln(p^2/\mu^2)/\epsilon$ appearing in a correction would certainly invalidate this statement. Fortunately, a theorem due to S. Weinberg states that the divergences may only be proportional to a polynomial in the external momenta and particle masses, of the order of the diagram's degree of divergence (Weinberg, 1960; 'tHooft, 1973; Weinberg, 1973*b*).

Before proceeding to consider the renormalization of the theory it is useful to collect our results so far. Beginning with the quark propagator, the sum of the tree and one-loop contributions may be written heuristically as

$$\begin{aligned} & S_F + S_F(-\mathrm{i}\,\Sigma)S_F + \mathcal{O}(\alpha_s^2) \\ &= S_F + S_F(-\mathrm{i}\,\Sigma)S_F + S_F(-\mathrm{i}\,\Sigma)S_F(-\mathrm{i}\,\Sigma)S_F + \cdots \\ &= \left(S_F^{-1} + \mathrm{i}\,\Sigma\right)^{-1} . \end{aligned} \tag{3.140}$$

Here $S_F^{-1} = -\mathrm{i}\,(\not{p} - m)$ is the inverse of the quark propagator and Σ is the quark self-energy. This should be calculated from one-particle irreducible diagrams, that is diagrams which cannot be split in two by cutting a single propagator, so as to avoid double counting in the series. Now the interpretation of the first expression is somewhat confused since its second term contains a double pole, $1/(p^2 - m^2)^2$, due to the two quark propagators. In order to obtain an expression containing only a simple pole we follow Dyson and sum the infinite set of terms given in the second line. The expression in the third line gives the sum of this geometric series. Even though S_F is a 4×4 spinor matrix (and S_B, below, is a two-index Lorentz tensor), the usual trick of considering the difference of the geometric series and $S_F(-\mathrm{i}\,\Sigma)$ times the series allows the sum to be calculated. The only proviso being that a little care is taken over the order of the non-commuting terms. Using the result eqn (3.132), the explicit expression for the summed (inverse) propagator is

$$\mathrm{i}\left\{\not{p}\left(1 + \frac{\alpha_s}{4\pi}C_F\left[\xi\Delta_\epsilon + \frac{\text{U.V.}}{\text{finite}}\right]\right) - m\left(1 + \frac{\alpha_s}{4\pi}C_F\left[(3+\xi)\Delta_\epsilon + \frac{\text{U.V.}}{\text{finite}}\right]\right) + \mathcal{O}(\alpha_s^2)\right\}^{-1} . \tag{3.141}$$

Similar considerations apply to the gluon propagator which can be summed in the same fashion to give

$$
\begin{aligned}
& S_B + S_B(-\mathrm{i}\,\Pi)S_B + S_B(-\mathrm{i}\,\Pi)S_B(-\mathrm{i}\,\Pi)S_B + \cdots \\
&= \left[(S_B^{-1} + \mathrm{i}\,\Pi)^{-1}\right]^{\mu\nu} \\
&= -\mathrm{i}\left[(1+\Pi_0)(p^2\eta^{\mu\nu} - p^\mu p^\nu) + \xi^{-1}p^\mu p^\nu\right]^{-1} \\
&= \frac{\mathrm{i}}{p^2}\left[\frac{1}{(1+\Pi_0)}\left(-\eta^{\mu\nu} + \frac{p^\mu p^\nu}{p^2}\right) - \xi\frac{p^\mu p^\nu}{p^2}\right] . \qquad (3.142)
\end{aligned}
$$

Here S_B^{-1} is the inverse of the gluon propagator, as found in eqn (3.17), and $\Pi^{\mu\nu} = \Pi_0(p^2\eta^{\mu\nu} - p^\mu p^\nu)$ is the gluon self-energy. We do not show the diagonal colour matrix. Observe that the 'gauge fixing', longitudinal, term is unaffected by the corrections which remain orthogonal to it to all orders. Using the results of eqns (3.134) and (3.137) we have the explicit expression

$$
1 + \Pi_0(p^2) = 1 + \frac{\alpha_s}{4\pi}\left(\left[\frac{4}{3}T_F n_f - \frac{(13-3\xi)}{6}C_A\right]\Delta_\epsilon + \begin{matrix}\text{U.V.}\\ \text{finite}\end{matrix}\right) + \mathcal{O}(\alpha_s^2) . \quad (3.143)
$$

Here, we allow for n_f flavours of quarks in the loop. The vertex corrections are simpler to treat. The sum of the tree- and one-loop level contributions to the quark–gluon vertex is

$$
-\mathrm{i}\,g_s\mu^\epsilon T^a_{ji}\gamma^\mu\left\{1 + \frac{\alpha_s}{4\pi}\left(\left[\xi C_F + \frac{(3+\xi)}{4}C_A\right]\Delta_\epsilon + \begin{matrix}\text{U.V.}\\ \text{finite}\end{matrix}\right) + \mathcal{O}(\alpha_s^2)\right\} , \quad (3.144)
$$

whilst the similar sum for the triple-gluon vertex is

$$
\begin{aligned}
& \mathrm{i}\,g_s\mu^\epsilon f_{abc}\left[\eta^{\sigma\tau}(g_1-g_2)^\mu + \eta^{\tau\mu}(g_1+2g_2)^\sigma - \eta^{\mu\tau}(2g_1+g_2)^\sigma\right] \qquad (3.145) \\
& \times\left\{1 + \frac{\alpha_s}{4\pi}\left(\left[-\frac{4}{3}T_F n_f + \frac{(17-9\xi)}{12}C_A\right]\Delta_\epsilon + \begin{matrix}\text{U.V.}\\ \text{finite}\end{matrix}\right) + \mathcal{O}(\alpha_s^2)\right\} .
\end{aligned}
$$

In the next section we discuss how to obtain physically meaningful results from these divergent expressions.

3.4.2 *Renormalization*

The basic analysis that led to eqn (3.132) can be applied to all the loop integrals encountered in pQCD. The loop integrals are first calculated in D dimensions, using analytic continuation, and then expanded in $\epsilon = (4-D)/2$. The ultraviolet divergences manifest themselves as poles in $1/\epsilon$ (Speer, 1974; Breitenlohner and Maison, 1977). An N-loop amplitude has the Laurent expansion

$$
I_N = \sum_{n=0}^{N}\left(\frac{\alpha_s}{4\pi}\right)^n\frac{C_n}{\epsilon^n} + \mathcal{O}(\epsilon) . \qquad (3.146)
$$

The coefficients $\{C_n\}$ depend on combinations of the external momenta, typically arising via integrals over Feynman parameters, and an arbitrary mass μ. Clearly, the physical limit of an expression such as eqn (3.146) is not well defined. To

make progress we must find a method of removing the $1/\epsilon$ poles, thus allowing the $D \to 4$ ($\epsilon \to 0$) limit to be taken: this is renormalization.

The procedure we adopt is a pragmatic one. Using the original Lagrangian's Feynman rules, the divergent diagrams are identified and evaluated. Then knowing which interactions contain divergences, supplementary Feynman rules are added to the theory, one for each divergent interaction. These have coefficients that are carefully chosen so that they completely cancel the divergent $1/\epsilon$ poles generated by the original terms. In essence, the Lagrangian is supplemented by a counterterm Lagrangian which, treated as a perturbation, generates the new interactions necessary to render the theory finite. Schematically, this can be written as

$$\begin{aligned}\mathcal{L}_{\text{renorm}} &= \mathcal{L} + \mathcal{L}^{(1)}_{\text{counter}} + \mathcal{L}^{(2)}_{\text{counter}} + \mathcal{L}^{(3)}_{\text{counter}} + \cdots \\ &= \mathcal{L} + \mathcal{L}_{\text{counter}} \,. \end{aligned} \tag{3.147}$$

The $\mathcal{O}(\alpha_s)$ term, $\mathcal{L}^{(1)}_{\text{counter}}$, is constructed to cancel the one-loop divergences generated by the original Lagrangian, $\mathcal{L}$. The $\mathcal{O}(\alpha_s^2)$ term, $\mathcal{L}^{(2)}_{\text{counter}}$, is constructed to cancel the 'two-loop' divergences generated by $\mathcal{L} + \mathcal{L}^{(1)}_{\text{counter}}$ etc.

Referring back to eqn (3.132) we see that two divergences occur in the quark propagator. One is associated with the quark's kinetic term, $\propto \not{p} \leftrightarrow \bar{\psi}\, i\not{\partial}\psi$, and one with its mass term, $\propto m \leftrightarrow m\bar{\psi}\psi$. Equations (3.134) and (3.137) show that another divergence is associated with the transverse part of the gluon's kinetic term, $\propto (p^2\eta^{\mu\nu} - p^\mu p^\nu) \leftrightarrow (\partial^\mu A^{a\nu} - \partial^\nu A^{a\mu})\partial_\mu A^a_\nu$; the longitudinal part of the gluon's kinetic energy term remains finite. Equation (3.138) contains a divergence of the same form as the quark–gluon vertex, $\propto T^a_{jk}\gamma^\mu \leftrightarrow T^a_{jk}\bar{\psi}_j \not{A}^{a\mu}\psi_k$, whilst eqn (3.139) contains a divergence of the same structure as the triple-gluon vertex, $\propto f_{abc}[\eta^{\sigma\tau}(g_1 - g_2)^\mu + \eta^{\tau\mu}(g_1 + 2g_2)^\sigma - \eta^{\mu\tau}(2g_1 + g_2)^\sigma] \leftrightarrow f_{abc}(\partial_\mu A^a_\nu)A^{b\mu}A^{c\nu}$. Proceeding in this way we find that the form for the $\mathcal{O}(\alpha_s)$ counterterm Lagrangian, in a general covariant gauge, is given by

$$\begin{aligned}\mathcal{L}^{(1)}_{\text{counter}} = {} & \delta Z^{(1)}_\psi \;\bar{\psi}_i\, i\not{\partial}\psi_i - \delta Z^{(1)}_{m\bar{\psi}\psi}\; m\bar{\psi}_i\psi_i - \delta Z^{(1)}_A\; \frac{1}{2}(\partial_\mu A^a_\nu - \partial_\nu A^a_\mu)\partial^\mu A^{a\nu} \\ & + \delta Z^{(1)}_\eta\; (\partial^\mu \eta^{a\dagger})(\partial_\mu \eta^a) \\ & - \delta Z^{(1)}_{A\bar{\psi}\psi}\; g_s\mu^\epsilon T^a_{jk}\bar{\psi}_j \not{A}^a \psi_k + \delta Z_{\eta^\dagger\eta A}\; g_s\mu^\epsilon f_{abc}(\partial_\mu \eta^{a\dagger})\eta^b A^{c\mu} \\ & + \delta Z^{(1)}_{A^3}\; g_s\mu^\epsilon f_{abc}(\partial_\mu A^a_\nu)A^{b\mu}A^{c\nu} - \delta Z^{(1)}_{A^4}\; g_s^2\mu^{2\epsilon}\frac{1}{4} f_{abc}f_{ade}A^{b\mu}A^{c\nu}A^d_\mu A^e_\nu \,. \end{aligned} \tag{3.148}$$

Here, we have also added terms to cancel divergences which arise in the corrections to the ghost propagator, the quartic-gluon vertex and the ghost–gluon vertex. We have chosen not to include a term proportional to $(\partial^\mu A^a_\mu)^2$, as the longitudinal part of the gluon propagator receives no corrections.

As indicated earlier, in eqn (3.148) each term should be regarded as a perturbation to which new Feynman rules can be associated. The coefficients $\delta Z^{(1)}$ are chosen so that the sum of their individual contributions plus those of the corresponding one-loop contributions from the original Lagrangian are finite. Using

the results from our earlier calculations, Section 3.4.1, and referring to the relationship between the quantum Lagrangian, eqn (3.21), and the Feynman rules derived from it, Appendix B, we can infer the values of six of the $\delta Z^{(1)}$ as

$$\begin{aligned}
\delta Z_{\psi}^{(1)} &= \frac{\alpha_s}{4\pi}\left[-\xi C_F \Delta_\epsilon + F_\psi\right] \\
\delta Z_{m\bar{\psi}\psi}^{(1)} &= \frac{\alpha_s}{4\pi}\left[-(3+\xi) C_F \Delta_\epsilon + F_{m\bar{\psi}\psi}\right] \\
\delta Z_{A}^{(1)} &= \frac{\alpha_s}{4\pi}\left[-\left(\frac{4}{3}T_F n_f - \frac{(13-3\xi)}{6}C_A\right)\Delta_\epsilon + F_A\right] \\
\delta Z_{A\bar{\psi}\psi}^{(1)} &= \frac{\alpha_s}{4\pi}\left[-\left(\xi C_F + \frac{(3+\xi)}{4}C_A\right)\Delta_\epsilon + F_{A\bar{\psi}\psi}\right] \\
\delta Z_{A^3}^{(1)} &= \frac{\alpha_s}{4\pi}\left[-\left(\frac{4}{3}T_F n_f - \frac{(17-9\xi)}{12}C_A\right)\Delta_\epsilon + F_{A^3}\right] .
\end{aligned} \tag{3.149}$$

The finite functions, F_ψ, $F_{m\bar{\psi}\psi}$, F_A, $F_{A\bar{\psi}\psi}$, F_{A^3} are arbitrary. Only the coefficients of the $1/\epsilon$ poles are prescribed. We shall return to the issue of how to choose the F_is later when we discuss renormalization schemes.

In eqn (3.148) we have the beginnings of a remarkable result which saves our approach from being merely *ad hoc*. Comparing eqn (3.21) and eqn (3.148) one is immediately struck by their similarity; a fact which has been proven to hold true to all orders in perturbation theory. We can make this similarity more manifest by rescaling, or if you will renormalizing, the fields, masses and couplings. To do this, introduce

$$Z = 1 + \delta Z \quad \text{where} \quad \delta Z = \delta Z^{(1)} + \delta Z^{(2)} + \delta Z^{(3)} + \cdots \tag{3.150}$$

and

$$\begin{aligned}
\psi_0 &= Z_\psi^{1/2}\psi \qquad & m_0 &= Z_{m\bar{\psi}\psi} Z_\psi^{-1} m \\
A_0^\mu &= Z_A^{1/2} A^\mu & &\equiv Z_m m \\
\eta_0 &= Z_\eta^{1/2}\eta & \xi_0 &= Z_A \xi \quad (Z_\xi = Z_A) .
\end{aligned} \tag{3.151}$$

This allows us to write the sum of eqns (3.148) and (3.21), with $g_s \to g_s \mu^\epsilon$ as appropriate for $D = 4 - 2\epsilon$ dimensions, as

$$\begin{aligned}
\mathcal{L}_{\text{renorm}} = {} & \bar{\psi}_0(\mathrm{i}\partial\!\!\!/ - m_0)\psi_0 - \frac{1}{2}\left[\left(\partial_\mu A_{0\nu}^a - \partial_\nu A_{0\mu}^a\right)\partial^\mu A_0^{a\nu} + \frac{1}{\xi_0}(\partial^\mu A_{0\mu}^a)^2\right] \\
& + (\partial^\mu \eta_0^a)(\partial_\mu \eta_0^a) \\
& - g_s\mu^\epsilon \frac{Z_{A\bar{\psi}\psi}}{Z_A^{1/2} Z_\psi} T_{jk}^a \bar{\psi}_{0j} A_0^a \psi_{0k} + g_s\mu^\epsilon \frac{Z_{A\eta^\dagger\eta}}{Z_A^{1/2} Z_\eta} f_{abc}(\partial_\mu \eta_0^{a\dagger})\eta_0^b A_0^{c\mu} \\
& + g_s\mu^\epsilon \frac{Z_{A^3}}{Z_A^{3/2}} f_{abc}(\partial_\mu A_{0\nu}^a) A_0^{b\mu} A_0^{c\nu} - g_s^2\mu^{2\epsilon}\frac{Z_{A^4}}{Z_A^2}\frac{1}{4} f_{abc} f_{ade} A_0^{b\mu} A_0^{c\nu} A_{0\mu}^d A_{0\nu}^e .
\end{aligned} \tag{3.152}$$

In a renormalizable theory all the ultraviolet divergences arising in loop diagrams can be cancelled by counterterms corresponding to the finite number of

interactions of mass dimension four or less. By contrast, in a non-renormalizable theory counterterms corresponding to new interactions must be added at each new order in perturbation theory.

Unfortunately, looking at eqn (3.152), we appear to have lost gauge invariance which, as we learnt in Section 3.3.3 for tree-level calculations, requires very particular relationships to hold between the various terms in the Lagrangian. This is potentially a calamitous situation because the formal proof of renormalizability relies on the gauge symmetry to guarantee certain relationships amongst the theory's Green's functions. Now, this apparent loss of gauge invariance already appeared at the classical level because of the necessity to introduce a gauge fixing (and ghost) term. Fortunately, Becchi, Rouet and Stora (BRS) (1974) have found a rather unusual, but nonetheless exact, symmetry of the 'broken Lagrangian'. Thus, a form of gauge invariance can be restored with the proviso that all the gauge couplings are equal. This symmetry then allows a number of relationships, known as Slavnov–Taylor (Taylor, 1971; Slavnov, 1972) identities (or Ward identities in the abelian QED case), to be established between the Green's functions of the Yang–Mills theory. A consequence of these relationships is the requirement for the following equations to hold:

$$\frac{Z_{A\bar{\psi}\psi}}{Z_A^{1/2}Z_\psi} = \frac{Z_{A\eta^\dagger\eta}}{Z_A^{1/2}Z_\eta} = \frac{Z_{A^3}}{Z_A^{3/2}} = \sqrt{\frac{Z_{A^4}}{Z_A^2}} \equiv Z_g = \frac{g_{s0}}{g_s\mu^\epsilon} \,. \tag{3.153}$$

This allows us to introduce a single renormalization factor Z_g and a unique gauge coupling g_{s0} in the quark–gluon, triple-gluon, quartic-gluon and ghost–gluon terms. Thus, the apparent proliferation of couplings in eqn (3.152) is illusory provided that we choose the finite parts of the counterterms in eqn (3.149) so as to respect eqn (3.153).

The renormalization prescription results in a finite Lagrangian, eqn (3.152), whose form is exactly the same as that of the original Lagrangian, eqn (3.21), written in terms of rescaled fields ψ_0, A_0 and η_0 and parameters g_{s0}, m_0 and ξ_0. These are often referred to as the bare Lagrangian and bare fields and parameters. In essence what we have are a remarkable series of cancellations, for example,

$$\begin{aligned} \psi &= \psi_0 - (Z_\psi^{1/2} - 1)\psi \\ m &= m_0 - (Z_m - 1)m \quad \text{etc.} \end{aligned} \tag{3.154}$$

Here both the bare quantities and the corresponding counter terms are divergent but their difference is finite.

We now return to the question of how to choose the finite terms, F_i, in eqn (3.149). First, we should not be alarmed by their arbitrariness. This reflects nothing more than the need to experimentally measure the actual masses and couplings, something which would be true of any theory, irrespective of the need for renormalization. Actually this cannot fix the wavefunction renormalizations, Z_ψ, Z_A and Z_η, as they do not appear in physical quantities, though this also

means that we could live without them. The different choices for the F_i functions constitute different renormalization schemes. The most important point to remember with choosing a renormalization scheme is to use it consistently throughout the calculation so as not to spoil the critical relationships between Green's functions.

Perhaps the simplest scheme is the minimal subtraction, or MS, scheme ('tHooft, 1973) in which the counterterms only cancel the $1/\epsilon$ poles. A variant of this is the modified minimal subtraction, or $\overline{\text{MS}}$, scheme (Bardeen *et al.*, 1978) in which the counterterms cancel the full $\Delta_\epsilon = 1/\epsilon + \ln(4\pi) - \gamma_{\text{E}}$ pieces. In eqn (3.149) this amounts to setting $F_i = 0$ in all the expressions. The difference between the two schemes is a difference in the finite parts proportional to $\ln(4\pi) - \gamma_{\text{E}} = 1.954$, equivalent to replacing the arbitrary μ^2 by $\overline{\mu}^2 = 4\pi\mu^2/\text{e}^{\gamma_{\text{E}}}$. Thus, in the $\overline{\text{MS}}$ scheme a potentially large contribution to radiative corrections is also removed, thereby aiding the convergence of the perturbative expansion. Despite its somewhat abstract nature the $\overline{\text{MS}}$ scheme's simplicity makes it the most popular one for pQCD calculations. A less manifest advantage of the scheme is the fact that the dimensionless Z_i do not depend on the combination m/μ. As we shall see, this mass independence simplifies the discussion of the renormalization group equations (RGEs). That this holds to all orders can be seen by the following heuristic argument. The counterterms are constructed to have just the bare bones necessary to remove the divergences which occur at high momentum. However, in this limit, we might expect any masses to be negligible so that they do not appear in the residues of the poles, and since $F_i = 0$, nor in the Z_i.

Other 'more physical' renormalization schemes may also be used. For example, when focusing on heavy quark properties the on mass-shell scheme may be used. Here F_ψ and F_m are adjusted so that the (real part) of the pole in the quark propagator occurs at the quark mass, $p^2 = m^2$, and has unit residue. In a similar fashion F_A and F_{A^3} may be adjusted so that the triple-gluon vertex, eqn (3.145), plus counterterm equals g_s at a particular external momentum configuration, typically chosen to be unphysical so as to avoid introducing extraneous singularities. In these schemes, it is common for a mass (m/μ) dependence to be introduced via the finite parts of the counterterms.

To finish this section we give the results of calculating the renormalization factors Z_i to two-loop approximation in pQCD. To be more specific, in a covariant gauge the $\overline{\text{MS}}$ prescription gives

$$Z_\psi = 1 - \frac{\alpha_{\text{s}}}{4\pi}\frac{1}{\epsilon}\xi C_F + \left(\frac{\alpha_{\text{s}}}{4\pi}\right)^2 \left\{ +\frac{1}{\epsilon}\left[T_F n_f + \frac{3}{4}C_F - \frac{(25+8\xi+\xi^2)}{8}C_A\right] - \frac{1}{\epsilon^2}\left[\frac{\xi^2}{2}C_F + \frac{(3+\xi)\xi}{4}C_A\right]\right\} C_F$$

$$Z_A = 1 - \frac{\alpha_{\text{s}}}{4\pi}\frac{1}{\epsilon}\left[\frac{4}{3}T_F n_f - \frac{(13-3\xi)}{6}C_A\right]$$

$$+\left(\frac{\alpha_s}{4\pi}\right)^2\left\{-\frac{1}{\epsilon}\left[\left(2C_F+\frac{5}{2}C_A\right)T_F n_f-\frac{(59-11\xi-2\xi^2)}{16}C_A^2\right]\right.$$
$$\left.+\frac{1}{\epsilon^2}\frac{(3+2\xi)}{3}\left[T_F n_f-\frac{(13-3\xi)}{8}C_A\right]C_A\right\}$$
$$Z_\eta=1+\frac{\alpha_s}{4\pi}\frac{1}{\epsilon}\frac{(3-\xi)}{4}C_A+\left(\frac{\alpha_s}{4\pi}\right)^2\left\{-\frac{1}{\epsilon}\left[\frac{5}{12}T_F n_f-\frac{(95+3\xi)}{96}C_A\right]\right.$$
$$\left.+\frac{1}{\epsilon^2}\left[\frac{1}{2}T_F n_f-\frac{(35-3\xi^2)}{32}C_A\right]\right\}C_A$$
$$Z_m=1-\frac{\alpha_s}{4\pi}\frac{1}{\epsilon}3C_F+\left(\frac{\alpha_s}{4\pi}\right)^2\left\{+\frac{1}{\epsilon}\left[\frac{5}{3}T_F n_f-\frac{3}{4}C_F-\frac{97}{12}C_A\right]\right.$$
$$\left.-\frac{1}{\epsilon^2}\left[2T_F n_f-\frac{9}{2}C_F-\frac{11}{2}C_A\right]\right\}C_F$$
$$Z_g=1+\frac{\alpha_s}{4\pi}\frac{1}{\epsilon}\left[\frac{2}{3}T_F n_f-\frac{11}{6}C_A\right]$$
$$+\left(\frac{\alpha_s}{4\pi}\right)^2\left\{\frac{1}{\epsilon}\left[\left(C_F+\frac{5}{3}C_A\right)T_F n_f-\frac{17}{6}C_A^2\right]+\frac{1}{\epsilon^2}\frac{1}{24}\left[4T_F n_f-11C_A\right]^2\right\}. \tag{3.155}$$

Here, we have done some work to derive the expression for Z_g, which cannot be obtained directly but is obtained indirectly using eqn (3.153). Typically, due to its relative simplicity, the correction to the ghost–gluon vertex is quoted to which one applies $Z_g = Z_{A\eta^\dagger\eta}/Z_A^{1/2}Z_\eta$; though any of the remaining three expressions in eqn (3.153) must lead to the same expression for Z_g. Also, you are reminded that the non-renormalization of the longitudinal part of the gluon propagator implies that $Z_\xi = Z_A$.

Before using these results we make a few observations. The choice of the (modified) minimal subtraction scheme leads to several simplifications which need not hold in other schemes. First, the leading terms in all the expressions are unity, $Z = 1 + \mathcal{O}(\alpha_s)$. Second, since all $F_i = 0$, there is no dependence on any external momentum scales. All the coefficients of α_s^n are made up of pure numbers, the gauge fixing parameter and group factors. Third, there is also no dependence on the quark mass scale, m/μ. The MS prescriptions are the archetypical examples of mass independent renormalization schemes ('tHooft, 1973; Weinberg, 1973*b*). Fourth, both Z_m and Z_g are independent of ξ, the gauge fixing parameter (Caswell and Wilczek, 1974; Gross, 1976). A more general observation is that both δZ_ψ and δZ_m are proportional to the quark colour charge C_F, whilst δZ_η is proportional to C_A. All the above observations hold to all orders in α_s. We also see that certain choices of ξ give simplifications. In particular, in the Landau gauge, $\xi = 0$, the $\mathcal{O}(\alpha_s)$ term in Z_ψ vanishes and the $\mathcal{O}(\alpha_s^2)$ term simplifies greatly.

3.4.3 *The renormalization group equations*

It should not have gone unnoticed that there appears to be a disturbingly large freedom in the application of the renormalization procedure. First is the freedom to select the finite parts of the counterterms, subject to respecting the Slavnov–Taylor identities. We have already exploited this freedom to absorb a numerically large coefficient in the change from the MS to $\overline{\rm MS}$ schemes. Second is the freedom in the choice of the unit mass, μ, which sets a scale for the problem. However, physical quantities can not depend on any of these arbitrary choices. All prescriptions are ultimately equivalent. For example, in two schemes the quark masses are related as $Z_m(R)m_R = m_0 = Z_m(R')m_{R'}$ so that $m_R = [Z_m(R')/Z_m(R')]m_{R'}$, where the ratio is finite, because so is each m_R, even though neither Z_m is individually finite. In this way the invariance can be encapsulated in the group structure of the transformations connecting quantities (g_s, m, ψ, etc.) in different schemes.

The seemingly simple invariance of physical quantities under changes in μ leads to a very powerful differential equation conecting g_s, m, ψ, etc., defined at one scale μ to those at a second scale. To see how this arises, suppose we calculate the amplitude, that is amputated Green's function, for an operator describing the 'scattering' of n_ψ (anti)quarks and n_A gluons (we need not consider external ghosts). This amplitude can be written in terms of either the bare or renormalized quantities. Here, we have assumed that the counterterm for the interaction is proportional to itself so that the renormalization is multiplicative,[3] that is,

$$\Gamma_0(\alpha_{s0}, m_0, \xi_0, Q) = Z_\psi^{-\frac{n_\psi}{2}} Z_A^{-\frac{n_A}{2}} \Gamma(\mu, \alpha_s, m, \xi, Q)\,. \tag{3.156}$$

Here, we use the single scale Q to characterize any external four-momenta present in the problem. For simplicity we only consider one quark mass, m. The left-hand side of eqn (3.156) is clearly independent of μ, as must be the right-hand side. Differentiating with respect to μ, using the chain rule, we obtain the following renormalization group equation

$$0 = \mu \frac{\mathrm{d}}{\mathrm{d}\mu}\left[Z_\psi^{-\frac{n_\psi}{2}} Z_A^{-\frac{n_A}{2}} \Gamma(\mu, \alpha_s, m, \xi, Q)\right] \tag{3.157}$$

$$\Longrightarrow \quad 0 = \left\{ \mu\frac{\partial}{\partial\mu} + \beta\frac{\partial}{\partial\alpha_s} + m\gamma_m\frac{\partial}{\partial m} + \xi\delta_\xi\frac{\partial}{\partial\xi} - n_\psi\gamma_\psi - n_A\gamma_A \right\}\Gamma\,.$$

The first term accounts for any explicit μ dependence, whilst the remainder takes care of any implicit dependences via $g_s(\mu)$, $m(\mu)$ and $\xi(\mu)$. Equation (3.157) serves to define the dimensionless coefficient functions

[3] In general the counterterm may involve other operators of the same mass dimension. An example is provided by the pQCD corrections to a weak decay. In the case of such operator mixing it is necessary to consider linear combinations of the operators which are diagonal.

$$\beta\left(\alpha_s, \frac{m}{\mu}; \epsilon\right) = \mu\frac{\partial\alpha_s}{\partial\mu} \qquad \gamma_\psi\left(\alpha_s, \frac{m}{\mu}, \xi; \epsilon\right) = \frac{1}{2}\frac{\mu}{Z_\psi}\frac{\partial Z_\psi}{\partial\mu}$$
$$\gamma_m\left(\alpha_s, \frac{m}{\mu}; \epsilon\right) = \frac{\mu}{m}\frac{\partial m}{\partial\mu} \qquad \gamma_A\left(\alpha_s, \frac{m}{\mu}, \xi; \epsilon\right) = \frac{1}{2}\frac{\mu}{Z_A}\frac{\partial Z_A}{\partial\mu} \tag{3.158}$$
$$\delta_\xi\left(\alpha_s, \frac{m}{\mu}, \xi; \epsilon\right) = \frac{\mu}{\xi}\frac{\partial\xi}{\partial\mu}$$

which are all finite as $\epsilon \to 0$. You are warned that variants of these definitions, differing slightly in signs and normalizations, occur in the literature. Observe that β and γ_m, like Z_g and Z_m, are both independent of ξ.

A linear partial differential equation such as eqn (3.157) can be solved using the method of characteristics. To do this we introduce the functions $\overline{\mu}(t)$, $\overline{\alpha}_s(t)$, $\overline{m}(t)$ and $\overline{\xi}(t)$ which satisfy the differential equations

$$\mathrm{d}t = \frac{\mathrm{d}\overline{\mu}}{\overline{\mu}} = \frac{\mathrm{d}\overline{\alpha}_s}{\beta(\overline{\alpha}_s, \overline{m}/\overline{\mu})} = \frac{\mathrm{d}\overline{m}}{\overline{m}}\frac{1}{\gamma_m(\overline{\alpha}_s, \overline{m}/\overline{\mu})} = \frac{\mathrm{d}\overline{\xi}}{\overline{\xi}}\frac{1}{\delta_\xi(\overline{\alpha}_s, \overline{m}/\overline{\mu}, \overline{\xi})} \tag{3.159}$$

and pass through the point $\overline{\mu}(0) = \mu$, $\overline{\alpha}_s(0) = \alpha_s$, $\overline{m}(0) = m$ and $\overline{\xi}(0) = \xi$. These functions connect the parameters defined at the scale μ to those defined at a second scale $\overline{\mu} = \mu\mathrm{e}^t$. The 'bar-notation' serves to highlight that we are now thinking of α_s, etc. as running parameters. Later on, except for $\overline{m}$, we will drop the special notation. The functions in eqn (3.159) define a characteristic parameterized by t. Since $\mathrm{d}\overline{\xi} \propto \overline{\xi}$, for $\delta_\xi \neq 0$, then $\overline{\xi}$ will remain identically zero if $\overline{\xi}(0) = 0$ and we can ignore any ξ-dependence in eqn (3.157): $\xi = 0$ is the Landau gauge which we adopt. The solution of these equations is straightforward if β, γ_m (and δ_ξ) do not depend on $\overline{m}/\overline{\mu}$. In a minimal subtraction scheme, or more generally a mass independent scheme, all the functions in eqn (3.158) are independent of m/μ. Adopting this further restriction we have

$$t = \ln\left(\frac{\overline{\mu}}{\mu}\right) = \int_{\alpha_s}^{\overline{\alpha}_s(t)}\frac{\mathrm{d}x}{\beta(x)} \quad \text{and} \quad \ln\left(\frac{\overline{m}(t)}{m}\right) = \int_{\alpha_s}^{\overline{\alpha}_s(t)}\mathrm{d}x\frac{\gamma_m(x)}{\beta(x)}\,. \tag{3.160}$$

Explicit solutions for $\overline{\alpha}_s$ and $\overline{m}$ require the actual expressions for β and γ_m. We shall derive these shortly but for the moment we assume that the solutions have been found. This allows us to rewrite eqn (3.157) as

$$\left\{\frac{\mathrm{d}}{\mathrm{d}t} - n_\psi\gamma_\psi(\overline{\alpha}_s(t)) - n_A\gamma_A(\overline{\alpha}_s(t))\right\}\Gamma(\overline{\mu}(t), \overline{\alpha}_s(t), \overline{m}(t), Q) = 0\,. \tag{3.161}$$

This ordinary differential equation is easily solved using an integrating factor:

$$\Gamma(\mu, \alpha_s, m, Q) = \exp\left(-n_\psi\int_{\alpha_s}^{\overline{\alpha}_s}\mathrm{d}x\frac{\gamma_\psi(x)}{\beta(x)} - n_A\int_{\alpha_s}^{\overline{\alpha}_s}\mathrm{d}x\frac{\gamma_A(x)}{\beta(x)}\right)\Gamma(\overline{\mu}, \overline{\alpha}_s, \overline{m}, Q)\,. \tag{3.162}$$

The solution is a constant along our characteristic which we evaluate at $t = 0$. What it says is that the theory defined at (μ, α_s, m) is equivalent to the

theory defined at $\overline{\mu}$, provided that the coupling and mass are changed to take the effective values $\overline{\alpha}_s(\overline{\mu})$ and $\overline{m}(\overline{\mu})$ and the fields present are scaled appropriately.

It is useful to make explicit the dimensionality of the Green's function. The mass dimension of Γ is given by $d_\Gamma = D - n_\psi d_\psi - n_A d_A$, where again D is the dimensionality of space–time, and $d_\psi = (D-1)/2$ and $d_A = (D-2)/2$ are the mass dimensions of the quark and gluon fields. The significance of this dimension is that if $\{\mu, m, Q\}$ are all scaled by the same factor s, then Γ scales as s^{d_Γ}, that is, $\Gamma(s\mu, \alpha_s, sm, sQ) = s^{d_\Gamma}\Gamma(\mu, \alpha_s, m, Q)$. This allows us to write,

$$\begin{aligned}\Gamma(\mu, \alpha_s, m, sQ) &= s^{d_\Gamma}\Gamma\left(\frac{\mu}{s}, \alpha_s, \frac{m}{s}, Q\right) \qquad (3.163)\\ &= s^{d_\Gamma}\exp\left(-\int_{\alpha_s}^{\overline{\alpha}_s} \mathrm{d}x \frac{n_\psi\gamma_\psi(x) + n_A\gamma_A(x)}{\beta(x)}\right)\Gamma\left(\frac{\overline{\mu}}{s}, \overline{\alpha}_s, \frac{\overline{m}}{s}, Q\right).\end{aligned}$$

In the second form we have employed eqn (3.162). If we now choose $\overline{\mu} = s\mu$ then we can determine how the Green's function changes under a scaling of the external four-momenta.

$$\begin{aligned}\Gamma(\mu, \alpha_s, m, sQ) &= s^{d_\Gamma}\exp\left(-\int_{\alpha_s}^{\overline{\alpha}_s} \mathrm{d}x \frac{n_\psi\gamma_\psi(x) + n_A\gamma_A(x)}{\beta(x)}\right)\Gamma\left(\mu, \overline{\alpha}_s, \frac{\overline{m}}{s}, Q\right)\\ &= s^{(d_\gamma - n_\psi\gamma_\psi - n_A\gamma_A)}\Gamma\left(\mu, \overline{\alpha}_s, \frac{\overline{m}}{s}, Q\right) \qquad (3.164)\end{aligned}$$

In the second form we make the simplifying assumption that the γ_i are constant. Thus, the dependence on the scaling factor s can be taken into account by evaluating the Green's function at an effective coupling, $\overline{\alpha}_s(s\mu)$, and a scaled effective mass, $\overline{m}(s\mu)/s$, together with an overall scaling of the Green's function. However, the overall scaling dimension differs from the canonical dimension, d_Γ, by the presence of the γ_i term. Reflecting this discrepancy with the naïve expectation, the γ_i are known as anomalous dimensions. As we shall see shortly, in practice one often uses $\mu \sim Q$. Note that even if $m = 0$, so that the classical theory were scale invariant, the anomalous dimensions and non-zero β-function would still imply a breaking of this classical scale invariance in the quantum theory. This is possible because the renormalization procedure necessarily introduces a mass/momentum scale, here μ.

As the next section will show, in QCD both β and γ_m are negative. This means that the effective, or running, coupling, $\overline{\alpha}_s(Q)$, decreases logarithmically as the scale Q increases, eqn (3.22). This weakening of the strong force is the essence of asymptotic freedom (Gross and Wilczek, 1973; Politzer, 1974) and lies behind the success of perturbative QCD. The solution for $\overline{m}(Q)$ shows that it is also logarithmically suppressed; this is in addition to the factor $1/Q$ which appears in eqn (3.164). At this point it might be tempting to neglect quark masses, $m = 0$ in eqn (3.164), at high energies, $Q \gg \overline{m}(Q)$, so that all Q

dependence occurs via $\overline{\alpha}_s(Q)$. However, this can lead to problems with low-energy or near collinear gluons so that for this approximation to make sense we must restrict ourselves to infrared safe quantities as discussed in Section 3.5.

Before moving on, we mention that a number of similar renormalization group equations have been derived in the literature. Foremost is the Callan–Symanzik equation (Symanzik, 1971; Callan, 1972) which is obtained by studying the Green's function's dependence on the physical mass m. The equation takes the form of eqn (3.157) with coefficient functions that only depend on g_s ($\gamma_m = 1$) and with the $\mu\partial/\partial\mu$ term replaced by an inhomogeneous term which may be neglected in the $m/Q \to 0$ limit.

3.4.4 *Calculating the RGE coefficient functions*

The values of the coefficient functions β, γ_m, γ_A, etc. defined in eqn (3.158) can be calculated as power series in α_s using our previous results. Here, we illustrate the method for the β-function. Consider the relationship, eqn (3.153), between the bare and renormalized couplings, $g_{s0} = \mu^\epsilon g_s Z_g$. Since the bare coupling g_{s0} can know nothing of the arbitrary scale μ, which was introduced only to facilitate renormalization, we must have

$$\mu\frac{\mathrm{d}g_{s0}}{\mathrm{d}\mu} = 0 \quad \Longrightarrow \quad 0 = \mu^\epsilon\left[\epsilon g_s Z_g + \beta_g\left(Z_g + g_s\frac{\partial Z_g}{\partial g_s}\right)\right]. \tag{3.165}$$

From this we can obtain $\beta = (g_s/2\pi)\beta_g$. In applying the chain rule we have made the simplifying assumption that we use a mass independent renormalization scheme such as $\overline{\text{MS}}$. Thus Z_g only depends on the renormalized coupling g_s and not on $\overline{m}(\mu)/\mu$ (nor on ξ). Equation (3.165) determines how much $g_s(\mu)$ must change by when μ changes in order that g_{s0} stays constant. Referring to eqn (3.155) we can write Z_g as a Laurent series in inverse powers of ϵ,

$$Z_g = 1 + \sum_{n\geq 1}\frac{a_n(g_s)}{\epsilon^n}. \tag{3.166}$$

On the other hand, we want both g_s and β_g to be well defined in the limit $\epsilon \to 0$, that is to contain no poles in $1/\epsilon$. Thus, we write $\beta_g = A + B\epsilon$; it is easily confirmed that all higher powers of ϵ must vanish. Substituting this into eqn (3.165) and collecting powers of ϵ gives

$$0 = (B+g_s)\epsilon + A + g_s B a_1' + \cdots \frac{\left[A a_{n-1} + (B+g_s)a_n + g_s A a_{n-1}' + g_s B a_n'\right]}{\epsilon^{n-1}} + \cdots, \tag{3.167}$$

where the prime indicates differentiation with respect to g_s. Setting the coefficients of ϵ^m, $m \leq 1$, to zero gives

$$\beta_g(g_s) = \lim_{\epsilon\to 0}\{g_s^2 a_1' - \epsilon g_s\} \quad \text{and} \quad a_n' = a_1'(a_{n-1} + g_s a_{n-1}'), \quad n \geq 2$$

$$= g_s^2 a_1' \,. \tag{3.168}$$

At first sight, it may seem odd that we can calculate the β-function from just the residue of the $1/\epsilon$ pole. However, the conditions on the $a_{n\geq 2}$ ('tHooft, 1973), which ensure the absence of pole terms in β, together with the boundary conditions $a_n(0) = 0$ allow all the $a_{n\geq 2}$ to be calculated in terms of a_1.

Referring to eqn (3.155) the coefficient a_1 is easily read off, allowing us to infer the first two terms in the expansion of the β-function.

$$\begin{aligned}\beta = 2\Bigg\{ & \frac{\alpha_s^2}{4\pi}\left[\frac{4}{3}T_F n_f - \frac{11}{3}C_A\right] + \frac{\alpha_s^3}{(4\pi)^2}\left[\left(4C_F + \frac{20}{3}C_A\right)T_F n_f - \frac{34}{3}C_A^2\right] \\ & + \frac{\alpha_s^4}{(4\pi)^3}\left[\left(\frac{44}{9}C_F + \frac{158}{27}C_A\right)T_F^2 n_f^2 \right. \\ & \left. + \left(2C_F^2 - \frac{205}{9}C_F C_A - \frac{1415}{27}C_A^2\right)T_F n_f + \frac{2857}{54}C_A^3\right] + \cdots\Bigg\}\,.\end{aligned} \tag{3.169}$$

The third term is given in (Tarasov *et al.*, 1980) for the $\overline{\rm MS}$ scheme and the $\mathcal{O}(\alpha_s^5)$ (four loop) term is available in (Larin *et al.*, 1997), again for the $\overline{\rm MS}$ scheme. Similar analyses to the above can be applied to $m_0 = mZ_m(g_s)$ to obtain γ_m, to obtain γ_A from $Z_A(g_s, \xi)$ and likewise γ_ψ and γ_η; see Ex. (3-20). Here we simply quote the results:

$$\begin{aligned}\gamma_m &= -\frac{\alpha_s}{4\pi}6C_F + \left(\frac{\alpha_s}{4\pi}\right)^2\left[\frac{20}{3}T_F n_f - 3C_F - \frac{97}{3}C_A\right]C_F + \cdots \\ \gamma_\psi &= +\frac{\alpha_s}{4\pi}\xi C_F - \left(\frac{\alpha_s}{4\pi}\right)^2\left[2T_F n_f + \frac{3}{2}C_F - \frac{(25+8\xi+\xi^2)}{4}\right]C_F + \cdots \\ \gamma_A &= +\frac{\alpha_s}{4\pi}\left[\frac{4}{3}T_F n_f - \frac{(13-3\xi)}{6}C_A\right] \\ &\quad + \left(\frac{\alpha_s}{4\pi}\right)^2\left[(4C_F + 5C_A)T_F n_f - \frac{(59-11\xi-2\xi^2)}{8}C_A^2\right] + \cdots \\ \gamma_\eta &= -\frac{\alpha_s}{4\pi}\frac{(3-\xi)}{4}C_A + \left(\frac{\alpha_s}{4\pi}\right)^2\left[\frac{5}{6}T_F n_f - \frac{(95+3\xi)}{48}C_A\right]C_A + \cdots\,.\end{aligned} \tag{3.170}$$

Observe that both β and γ_m are independent of the gauge parameter ξ, a fact which can be traced to the ξ-independence of Z_g and Z_m in a mass independent renormalization scheme. This is not so for the wavefunction anomalous dimensions γ_ψ, γ_A and γ_η. This raises the issue of the scheme (in)dependence of our results. If we restrict ourselves to mass independent schemes (and neglect possible non-perturbative effects) then the first two terms in β and the first terms in γ_m, γ_ψ and γ_A are independent of the specific choices of counterterms. Beyond these leading terms the results are scheme dependent and, for example, the third and higher order terms in eqn (3.169) can be set equal to arbitrary values.

In eqn (3.165) we assumed a mass independent renormalization scheme had been used. If this is not the case, then the presence of m/μ dependences in the Z_i

significantly complicates the RGEs. First, the evaluation of β and the γ_i is made harder by, for example, the extra term, $\frac{m}{\mu}(\gamma_m - 1)\partial Z_g/\partial(\frac{m}{\mu})$, in eqn (3.165). Second, the solution of the coupled, linear, differential equations for the effective coupling and mass, eqn (3.159), is made harder. Here, a possible approach to avoiding these problems is to go to a regime where the mass(es) are negligible compared to μ and all other scales (Q).

3.4.5 *The running coupling and quark masses*

A key lesson from our study of the RGEs is the need to express our results in terms of the running, or effective, coupling and mass. If we use as argument Q^2, the evolution equations in a mass independent scheme are

$$Q^2\frac{\mathrm{d}\alpha_s(Q^2)}{\mathrm{d}Q^2} = \beta\big(\alpha_s(Q^2)\big) = -\alpha_s^2(\beta_0 + \beta_1\alpha_s + \beta_2\alpha_s^2 + \cdots) \quad \text{and} \tag{3.171}$$

$$\frac{Q^2}{\overline{m}(Q^2)}\frac{\mathrm{d}\overline{m}(Q^2)}{\mathrm{d}Q^2} = \gamma_m\big(\alpha_s(Q^2)\big) = -\alpha_s(\gamma_0 + \gamma_1\alpha_s + \gamma_2\alpha_s^2 + \cdots)\,, \tag{3.172}$$

c.f. eqn (3.159). Here, we have in mind that $\beta_0, \gamma_0 > 0$ so that $\beta, \gamma_m < 0$. Taking into account that $Q^2\,\mathrm{d}/\mathrm{d}Q^2 = (1/2)Q\,\mathrm{d}/\mathrm{d}Q$, the coefficients in the series expansions for the $\overline{\mathrm{MS}}$ scheme can be read off from eqns (3.169) and (3.170).

$$\begin{aligned}
\beta_0 &= \frac{11C_A - 4T_F n_f}{12\pi} &&= \frac{(33 - 2n_f)}{12\pi}\\
\beta_1 &= \frac{17C_A^2 - (6C_F + 10C_A)T_F n_f}{24\pi^2} &&= \frac{(153 - 19n_f)}{24\pi^2}\\
\gamma_0 &= \frac{3C_F}{4\pi} &&= \frac{1}{\pi}\\
\gamma_1 &= \frac{C_F(97C_A + 9C_F - 20T_F n_f)}{96\pi^2} &&= \frac{(303 - 10n_f)}{72\pi^2}
\end{aligned} \tag{3.173}$$

Here β_0, β_1 and γ_0 are common to any mass independent renormalization scheme, whilst γ_1 is specific to the $\overline{\mathrm{MS}}$ scheme. The terms quoted above are given as function of the colour factors C_F, C_A and T_F and thus are valid for any gauge theory with an unbroken gauge symmetry. Note that T_F always appears in a product with n_f, the number of active quark flavours. The coefficients on the right-hand side apply for the case of colour SU(3), that is, they are specific to QCD.

Referring to eqn (3.160) and working to next-to-leading order the solution for $\alpha_s(Q^2)$ is given implicitly by

$$\begin{aligned}
\ln\left(\frac{Q^2}{Q_0^2}\right) &= +\int_{\alpha_s(Q_0^2)}^{\alpha_s(Q^2)}\frac{\mathrm{d}x}{\beta(x)}\\
&= -\frac{1}{\beta_0^2}\int_{\alpha_s(Q_0^2)}^{\alpha_s(Q^2)}\mathrm{d}x\left[\frac{\beta_0^2}{x^2(\beta_0 + x\beta_1)} = \frac{\beta_0}{x^2} - \frac{\beta_1}{x} + \frac{\beta_1^2}{\beta_0 + x\beta_1}\right]
\end{aligned}$$

$$\Longrightarrow \quad \beta_0 \ln\left(\frac{Q^2}{Q_0^2}\right) = \frac{1}{\alpha_s(Q^2)} + \frac{\beta_1}{\beta_0} \ln\left(\frac{\alpha_s(Q^2)}{\beta_0 + \beta_1 \alpha_s(Q^2)}\right)\Bigg|_{Q_0^2}^{Q^2} . \tag{3.174}$$

Thus, given the value of $\alpha_s(Q_0^2)$ at one scale Q_0, it is possible to solve for $\alpha_s(Q^2)$ at a second scale Q; the one proviso being that we remain in the perturbative domain where eqn (3.171) is valid. An alternative and slightly simpler form of eqn (3.174) can be obtained using the boundary condition $\alpha_s(\Lambda_{\rm QCD}^2) = \infty$.

$$\beta_0 \ln\left(\frac{Q^2}{\Lambda_{\rm QCD}^2}\right) = \frac{1}{\alpha_s(Q^2)} + \frac{\beta_1}{\beta_0} \ln\left(\frac{\alpha_s(Q^2)}{\beta_0 + \beta_1 \alpha_s(Q^2)}\right) . \tag{3.175}$$

Here the parameter $\Lambda_{\rm QCD}$ is equivalent to giving the coupling $\alpha_s(Q^2)$ at a specific scale Q. At the quantum-level, QCD is specified by a dimensionful parameter. This is even true in the absence of any quark masses to set a classical-level scale. The appearance of such a scale at the quantum-level is known as dimensional transmutation. In eqn (3.175) $\alpha_s(Q^2)$ is given implicitly. By expanding in inverse powers of $\ln(Q^2/\Lambda_{\rm QCD}^2)$ an approximate explicit form can be derived.

$$\alpha_s(Q^2) = \frac{1}{\beta_0 \ln(Q^2/\Lambda_{\rm QCD}^2)} \left\{ 1 - \frac{\beta_1}{\beta_0^2} \frac{\ln\left[\ln(Q^2/\Lambda_{\rm QCD}^2)\right]}{\ln(Q^2/\Lambda_{\rm QCD}^2)} \right. \tag{3.176}$$
$$\left. + \frac{\beta_1^2}{\beta_0^4 \ln^2(Q^2/\Lambda_{\rm QCD}^2)} \left[\left(\ln\left[\ln(Q^2/\Lambda_{\rm QCD}^2)\right] - \frac{1}{2} \right)^2 - \frac{5}{4} \right] \right\} .$$

In practice the last $(-5/4)$ term in this expression is often neglected. This is equivalent to a redefinition of $\Lambda_{\rm QCD}$ by $\mathcal{O}(+10\%)$ (Buras *et al.*, 1977).

If we had worked at leading order, $\beta_1 = 0$, then eqn (3.174) can be solved to give

$$\alpha_s(Q^2) = \frac{\alpha_s(Q_0^2)}{1 + \beta_0 \alpha_s(Q_0^2) \ln(Q^2/Q_0^2)} \tag{3.177}$$

and the inverse of eqn (3.175) is given exactly by eqn (3.22) with $\Lambda_{\rm QCD}^2 = Q_0^2 \exp[-1/\beta_0 \alpha_s(Q_0^2)]$. As this expression for $\Lambda_{\rm QCD}$ suggests, changing the value of $\alpha_s(Q^2)$ for a fixed Q does not really alter the theory but gives the same theory with its unit of momentum rescaled. In this sense (massless) QCD is parameter free (Coleman and Weinberg, 1973). Equation (3.176) makes the asymptotic behaviour of $\alpha_s(Q^2)$ manifest — the QCD coupling decreases as $1/\ln(Q/\Lambda_{\rm QCD})$ for $Q \to \infty$. It is important to realize that this decrease in α_s justifies the use of pQCD, in particular the solution based on the first few terms in eqn (3.171). As Q decreases the converse is expected and indeed a strong growth of $\alpha_s(Q^2)$ is confirmed experimentally. However, the singularity at $Q = \Lambda_{\rm QCD}$ should not be taken too seriously as large values of α_s invalidate eqn (3.171) and any solutions based upon it. In this low-Q regime QCD is non-perturbative and no one knows yet how $\alpha_s(Q^2)$ behaves in reality, nor can it be claimed that this is a proof of confinement in QCD, though it does make it more plausible. It is safer to regard

$\Lambda_{\rm QCD} \sim 200\,{\rm MeV}$, roughly an inverse hadron size, as the scale at which non-perturbative physics becomes important. Finally, returning to eqn (3.176), if we substitute $\Lambda^2_{\rm QCD} = Q_0^2 \exp[-1/\beta_0 \alpha_{\rm s}(Q_0^2)]$ we can derive an explicit expression relating the strong coupling at two scales,

$$\alpha_{\rm s}(Q^2) = \frac{\alpha_{\rm s}(Q_0^2)}{\omega}\left(1 - \frac{\beta_1}{\beta_0}\alpha_{\rm s}(Q_0^2)\frac{\ln\omega}{\omega}\right) \qquad (3.178)$$

$$\text{with} \quad \omega = 1 + \beta_0 \alpha_{\rm s}(Q_0^2)\ln\left(\frac{Q^2}{Q_0^2}\right) ,$$

which is accurate to next-to-leading order.

The crucial fact for asymptotic freedom is that β is negative, that is $\beta_0 > 0$. Referring to eqn (3.173) we see that quarks, and fermions in general, give a positive contribution, whilst non-abelian interactions amongst gluons, proportional to C_A, lead to an overall negative β, provided $n_f < 17$. In QED with abelian photons the β-function is positive and consequently electric charges grow as the scale of a measurement grows. How various particles contribute to the β-function has been extensively studied and it is now known that only theories containing non-abelian gauge bosons give negative contributions (Coleman and Gross, 1973). Since many extensions to the Standard Model have been proposed, it is interesting to see how a new particle would contribute to the β-function; see Ex. (3-22). At leading order only coloured particles can contribute to the QCD β-function, though in higher orders all particles contribute. The contributions to β_0 consist of two components related to the particles' colour and Poincaré group representations. The general expression is

$$\beta_0 = -\frac{1}{12\pi}\sum_{\substack{\text{coloured}\\ \text{particles}}} D_i T_R , \qquad (3.179)$$

Here D_i equals -11 for a vector boson, $+4$ for a Dirac fermion, $+2$ for a Weyl fermion, $+1$ for a complex scalar and $+1/2$ for a real scalar field, whilst T_R is a colour charge determined by the particle's SU(N_c) representation. For example, $T_F = 1/2$ (by convention) for the fundamental (triplet) representation, $T_A = 2N_cT_F$ for the adjoint (octet) representation, $(2N_c - 1)T_F$ for the sextet representation etc. For QCD with a colour SU(3) octet of vector bosons and n_f triplets of Dirac fermions this gives eqn (3.169).

The next-to-leading order solution for $\overline{m}(Q^2)$ follows similar lines to that for $\alpha_{\rm s}(Q^2)$. One finds

$$\ln\left(\frac{\overline{m}(Q^2)}{\overline{m}(Q_0^2)}\right) = \int_{\alpha_{\rm s}(Q_0^2)}^{\alpha_{\rm s}(Q^2)} {\rm d}x \frac{\gamma_m(x)}{\beta(x)}$$

$$= \frac{1}{\beta_0}\int_{\alpha_{\rm s}(Q_0^2)}^{\alpha_{\rm s}(Q^2)} {\rm d}x \left[\frac{\beta_0(\gamma_0 + \gamma_1 x)}{x(\beta_0 + \beta_1 x)} = \frac{\gamma_0}{x} + \frac{\gamma_1\beta_0 - \beta_1\gamma_0}{\beta_0 + \beta_1 x}\right]$$

$$\Longrightarrow \quad \overline{m}(Q^2) = \overline{m}(Q_0^2)\left(\frac{\alpha_s(Q^2)}{\alpha_s(Q_0^2)}\right)^{\frac{\gamma_0}{\beta_0}}\left(\frac{\beta_0+\beta_1\alpha_s(Q^2)}{\beta_0+\beta_1\alpha_s(Q_0^2)}\right)^{\frac{(\beta_0\gamma_1-\beta_1\gamma_0)}{\beta_0\beta_1}}$$

$$\text{or} \quad \overline{m}(Q^2) = \overline{m}_0\left(\alpha_s(Q^2)\right)^{\frac{\gamma_0}{\beta_0}}\left[1+\frac{\beta_1}{\beta_0}\alpha_s(Q^2)\right]^{\frac{(\beta_0\gamma_1-\beta_1\gamma_0)}{\beta_0\beta_1}} . \tag{3.180}$$

Again, given $\overline{m}(Q_0^2)$ at one scale Q_0 we can calculate $\overline{m}(Q^2)$ at a second scale Q, provided that pQCD, and in particular eqn (3.172), remains valid. This offers a concise way of specifying a running quark mass as the mass when the scale equals its mass: $m = \overline{m}(m^2)$. In the second form of the solution $\overline{m}_0$ plays a similar rôle to $\Lambda_{\rm QCD}$. Specializing to the leading order result, $\gamma_1 = 0 = \beta_1$, we have

$$\overline{m}(Q^2) = \overline{m}(Q_0^2)\left(\frac{\alpha_s(Q^2)}{\alpha_s(Q_0^2)}\right)^{\frac{\gamma_0}{\beta_0}} = \overline{m}(Q_0^2)\left(\frac{\ln(Q_0/\Lambda_{\rm QCD})}{\ln(Q/\Lambda_{\rm QCD})}\right)^{\frac{\gamma_0}{\beta_0}} . \tag{3.181}$$

Thus, we see that the quark mass falls as an inverse power of a logarithm as Q^2 increases. This quantum scaling violation, in addition to the classical $\overline{m}(Q^2)/Q$ suppression, adds justification to dropping light quark masses from our calculations.

Up to this point we have left unresolved the issue of how many quarks, n_f, to include in our calculations. The critical issue is the relative magnitude of a quark's mass to the overall scale Q. If the quark has $\overline{m}(Q^2) \gg Q$ then it can only make its presence felt via internal loops and it is possible to remove these contributions by suitable choices of the counterterms. This decoupling theorem (Symanzik, 1973; Appelquist and Carazzone, 1975) means that we can ignore a quark if $\overline{m}(Q^2) \gg Q$. On the other hand, if the quark has $\overline{m}(Q^2) \ll Q$, then we should include its contributions and infrared safe quantities can be evaluated using the approximation $m_{\rm q} = 0$. The so-called light quarks, d, u and s, have $m_{\rm q} < \Lambda_{\rm QCD}$ so that in a pQCD calculation, characterized by $Q \gg \Lambda_{\rm QCD}$, we always have $n_f \geq 3$. The issue is more delicate for the so-called heavy quarks, c, b and t, in situations where $\overline{m}_{\rm Q}(Q^2) \sim Q$. Here we expect significant, process dependent contributions from the quark mass which we must therefore include in our calculations. Furthermore, we have to decide how to cope with the change in the β-function above and below the quark mass threshold.

Well above $\overline{m}_{\rm Q}$ we can use the 'full' theory containing $n_f + 1$ quarks and $\alpha_s^+(Q^2)$, whilst well below $\overline{m}_{\rm Q}$ we can use an 'effective' theory with n_f light quarks and $\alpha_s^-(Q^2)$. At intermediate scales, $Q \sim \overline{m}_{\rm Q}(Q^2)$, we must match the two versions of the theory so as to ensure that they give consistent results. This matching has been carried out to next-to-next-to-leading order for SU(3) in the $\overline{\rm MS}$ scheme (Bernreuther, 1983) and results in a relationship between the two running couplings given by

$$\alpha_s^+(Q^2) = \alpha_s^-(Q^2)\left[1+\frac{x}{6\pi}\alpha_s^-(Q^2)+\frac{(2x^2+33x-11)}{72\pi^2}\left(\alpha_s^-(Q^2)\right)^2\right]$$

$$\text{with} \quad x = \ln\left(\frac{Q^2}{\overline{m}_{\rm Q}^2(Q^2)}\right) . \tag{3.182}$$

If we evaluate this expression at the point at which the scale equals the running quark mass, $m_{\rm Q} = \overline{m}(m_{\rm Q}^2)$, that is $x = 0$, then eqn (3.182) almost reduces to requiring $\alpha_{\rm s}$ to be continuous at the scale $m_{\rm Q}$ (Marciano, 1984),

$$\alpha_{\rm s}^{+}(m_{\rm Q}^2) = \alpha_{\rm s}^{-}(m_{\rm Q}^2) - \frac{11}{72\pi^2}\left(\alpha_{\rm s}^{-}(m_{\rm Q}^2)\right)^3 . \tag{3.183}$$

This explains why it is common to require $\alpha_{\rm s}$ to be continuous at $Q = m_{\rm Q}$ rather than at the production threshold $Q = 2m_{\rm Q}$. Of course, imposing continuity on $\alpha_{\rm s}$ implies a discontinuity in $\Lambda_{\rm QCD}$, which subsequently becomes dependent on the number of active flavours, n_f. For example, at leading order it is easy to verify that the continuity of $\alpha_{\rm s}(m_{\rm Q})$ as $n_f \to n_f + 1$ requires

$$\Lambda_{\rm QCD}^{(n_f+1)} = \Lambda_{\rm QCD}^{(n_f)}\left(\frac{\Lambda_{\rm QCD}^{(n_f)}}{m_{\rm Q}}\right)^{\frac{\beta_0^{(n_f)} - \beta_0^{(n_f+1)}}{\beta_0^{(n_f+1)}}} = \Lambda_{\rm QCD}^{(n_f)}\left(\frac{\Lambda_{\rm QCD}^{(n_f)}}{m_{\rm Q}}\right)^{\frac{2}{31-2n_f}} . \tag{3.184}$$

Similar expressions can be derived at next-to-leading order given a specific equation for $\alpha_{\rm s}$, equivalent to a definition for $\Lambda_{\rm QCD}$.

This raises the issue of how to quote a measurement of the running coupling, $\alpha_{\rm s}$. Two conventions in popular usage are to quote $\alpha_{\rm s}(M_{\rm Z}^2)$ or $\Lambda_{\rm QCD}^{(5)}$. In both cases, this will typically involve having either to evolve $\alpha_{\rm s}$ or to match $\Lambda_{\rm QCD}$ at flavour thresholds. In the case of $\Lambda_{\rm QCD}$ it is important to be specific as to which next-to-leading order equation is being used, for example, eqn (3.175) or (3.176) with or without the last term. The value of $\Lambda_{\rm QCD}$ also depends on the renormalization scheme, for example, $\Lambda_{\overline{\rm MS}}^2 = 4\pi {\rm e}^{-\gamma_E}\Lambda_{\rm MS}^2$. Since there are more traps involved in specifying $\Lambda_{\rm QCD}$, the preferred option has become to quote $\alpha_{\rm s}$ at the scale of the Z mass.

An interesting aspect of converting a measurement at Q^2 to an $\alpha_{\rm s}$ value at $M_{\rm Z}^2$ is the effect on the measurement's error. By differentiating eqn (3.160) we find

$$\Delta\alpha_{\rm s}(Q^2) = \frac{\beta\left(\alpha_{\rm s}(Q^2)\right)}{\beta\left(\alpha_{\rm s}(M_{\rm Z}^2)\right)}\Delta\alpha_{\rm s}(M_{\rm Z}^2) \approx \left(\frac{\alpha_{\rm s}(Q^2)}{\alpha_{\rm s}(M_{\rm Z}^2)}\right)^2 \Delta\alpha_{\rm s}(M_{\rm Z}^2) . \tag{3.185}$$

So that, if $Q^2 < M_{\rm Z}^2$, then the error will shrink as we evolve from Q to $M_{\rm Z}$. A second consequence of eqn (3.185) is that a change in $\alpha_{\rm s}(M_{\rm Z}^2)$ only causes an $\mathcal{O}(\alpha_{\rm s}^2)$ change in $\alpha_{\rm s}(Q^2)$. Thus, an experimentally determined quantity, $\sigma \pm \Delta\sigma$, at Q^2 must be compared to at least a next-to-leading order theoretical prediction in order to be able to meaningfully measure $\alpha_{\rm s}(M_{\rm Z}^2)$,

$$\sigma \pm \Delta\sigma = A\alpha_{\rm s}^N\left[1 + B\alpha_{\rm s} \pm \Delta C\alpha_{\rm s}^2 \pm \frac{\Delta D}{Q^p}\right] . \tag{3.186}$$

That is, in addition to the leading $\mathcal{O}(\alpha_s^N)$ term we require the $\mathcal{O}(\alpha_s^{N+1})$ term to measure $\alpha_s(M_Z^2)$. In eqn (3.186) we also included an estimate of the next-to-next-to-leading order perturbative correction and a non-perturbative contribution that is parameterized as a power law correction. The measurement error on $\alpha_s(M_Z^2)$ can be estimated as

$$\frac{\Delta\alpha_s(M_Z^2)}{\alpha_s(M_Z^2)} = \frac{\alpha_s(M_Z^2)}{\alpha_s(Q^2)}\frac{1}{N}\left[\frac{\Delta\sigma}{\sigma} \pm \Delta C\alpha_s^2(Q^2) \pm \frac{\Delta D}{Q^p}\right] . \tag{3.187}$$

Looking at the first term, the 'error telescoping effect' suggests using a small value of Q^2 together with an intrinsically higher order process, large N. However, the error associated with missing the second two terms favours using larger values of Q^2, where their contributions are smaller. It is also possible that $\Delta C, \Delta D \propto N$ so that there is no advantage to larger N.

3.4.6 *An explicit example*

In the previous sections we learnt that physical quantities are independent of the arbitrary renormalization scale μ if they are made functions of the running coupling and mass. We now repeat this rather formal analysis in a particular case. We focus on QCD corrections to the dimensionless R parameter defined in e^+e^- annihilation, eqn (2.30). Suppose we have calculated a perturbative series for R,

$$R\left(\frac{Q^2}{\mu^2}, \alpha_s(\mu^2)\right) = 1 + \sum_{n=1}^{\infty} r_n(Q^2/\mu^2)\alpha_s^n(\mu^2) . \tag{3.188}$$

We have removed an inessential factor $N_c e_q^2$ from eqn (3.188) with respect to the usual definition and assumed that all quark masses are zero. We comment shortly on the case of only a finite number of terms. Demanding that R, a physically measurable quantity, is independent of μ leads to a series of differential equations

$$\begin{aligned} 0 &= \mu^2\frac{\mathrm{d}}{\mathrm{d}\mu^2}R\left(\frac{Q^2}{\mu^2}, \alpha_s(\mu^2)\right) \\ &= \left[\mu^2\frac{\partial}{\partial\mu^2} + \beta(\alpha_s)\frac{\partial}{\partial\alpha_s}\right]R\left(\frac{Q^2}{\mu^2}, \alpha_s\right) \\ &= \sum_{n=1}\sum_{m=0}\left(\mu^2\frac{\mathrm{d}r_n}{\mathrm{d}\mu^2}\alpha_s^n - nr_n\beta_m\alpha_s^{n+m+1}\right) . \end{aligned} \tag{3.189}$$

The first few terms are given explicitly by

$$0 = \mu^2\frac{\mathrm{d}r_1}{\mathrm{d}\mu^2}\alpha_s + \left(\mu^2\frac{\mathrm{d}r_2}{\mathrm{d}\mu^2} - 1r_1\beta_0\right)\alpha_s^2 + \left(\mu^2\frac{\mathrm{d}r_3}{\mathrm{d}\mu^2} - 2r_2\beta_0 - 1r_1\beta_1\right)\alpha_s^3 + \cdots . \tag{3.190}$$

Since each coefficient must vanish individually we obtain a series of differential equations which are solved easily to give

$$r_1(t) = c_1$$

$$
\begin{aligned}
r_2(t) &= c_2 + c_1\beta_0 t \\
r_3(t) &= c_3 + (2c_2\beta_0 + c_1\beta_1)t + c_1\beta_0^2 t^2 \\
r_n(t) &= c_n + \cdots + c_1(\beta_0 t)^{n-1} \, .
\end{aligned} \tag{3.191}
$$

Here the μ-dependence is via $t = \ln(\mu^2/Q^2)$ and the $\{c_i\}$ are numerical constants. In general, $r_n(t) \propto t^{n-1}$, so that the series contains terms of the form $(\alpha_s t)^n$. This raises a potentially embarrassing problem, for when $\alpha_s(\mu^2)\ln(\mu^2/Q^2) \geq 1$, which is inevitable for sufficiently large Q, the series appears not to be convergent. This problem is easily finessed if we rearrange eqn (3.191) to take account of these so-called leading logarithmic terms,

$$
\begin{aligned}
R(t,\alpha_s) &= 1 + c_1[1 + \beta_0\alpha_s t + (\beta_0\alpha_s t)^2 + \cdots]\alpha_s \\
&\quad + c_2\alpha_s^2 + [c_3 + (2c_2\beta_0 + c_1\beta_1)t]\alpha_s^3 + \cdots \\
&= 1 + c_1\frac{\alpha_s(\mu^2)}{1 + \beta_0\alpha_s(\mu^2)\ln(Q^2/\mu^2)} + \cdots \, .
\end{aligned} \tag{3.192}
$$

It is then apparent that the leading logarithms can be summed by the use of the one-loop running coupling $\alpha_s(Q^2)$. You may wonder if this just means that the convergence problem has been shifted to the next-to-leading logarithmic terms $\propto (\alpha_s t)^n\alpha_s$. However, using the two-loop running coupling sums both the leading and next-to-leading logarithms and shows that the NLL terms are genuinely suppressed by α_s. In fact we already know the result of carrying this program to completion. It is given by eqn (3.162),

$$
R\big(1,\alpha_s(Q^2)\big) = 1 + c_1\alpha_s(Q^2) + c_2'\alpha_s^2(Q^2) + c_3'\alpha_s^3(Q^2)\cdots \, , \tag{3.193}
$$

a series whose convergence actually improves as $Q \to \infty$. The coefficients in eqn (3.193) have been calculated to $\mathcal{O}(\alpha_s^3)$ (Chetyrkin *et al.*, 1996*a*). The coefficient c_1 is renormalization scheme independent, whereas c_n' for $n \geq 2$ depends on the scheme. We calculate the one-loop correction in Section 3.5.

It is useful to review the above calculation from a different perspective which gives an insight into how the RGEs work. Earlier, we encountered Weinberg's theorem when discussing the form of the counterterms needed to remove ultraviolet divergences (Weinberg, 1960). Once a diagram is rendered finite he went on to investigate its asymptotic behaviour as the scale of the external momenta becomes large. A typical behaviour is a dimensionful factor, Q^d, times a polynomial in $\ln(Q^2/\mu^2)$ (Mueller, 1981). Thus, we expect a typical cross section to have the form

$$
\sigma = Q^d \sum_n \alpha_s^n S_n\Big(\ln(Q^2/\mu^2)\Big) \quad \text{with} \quad S_n(x) = a_{n0} + a_{n1}x + \cdots + a_{nm}x^m \, . \tag{3.194}
$$

c.f. eqns (3.188) and (3.191). Now, because the terms in the RGE eqn (3.157) are of different orders in α_s, it interrelates S_n of different n and their coefficients a_{nm}. Indeed these constraints allow the S_n to be partially reconstructed. The

resulting structure contains series of leading and next-to-leading logarithms etc., which correspond to expansions of the running coupling. Thus, the RGE enforces relationships between the coefficients such that all the large logarithms can be summed by using an effective coupling with a scale appropriate to the problem.

Before leaving eqn (3.188) we comment on two features of eqn (3.191). First is the seemingly trivial observation that $r_1(Q^2/\mu^2)$ is a constant, c_1. Since any μ dependence in r_n arises from the treatment of ultraviolet divergences, this means that at one-loop the QCD correction to the $\gamma^*\mathrm{q\bar{q}}$ vertex is finite; a result which must in fact hold at all orders if QCD is not to spoil electric charge conservation.

Second is the effect of truncating the series eqn (3.188). As we have noted the coefficient of the $\mathcal{O}(\alpha_s^{n+1})$ term is related to coefficients of the $\mathcal{O}(\alpha_s^n)$, $\mathcal{O}(\alpha_s^{n-1})$, ..., $\mathcal{O}(\alpha_s^1)$ terms in such a way as to remove the μ-dependence to $\mathcal{O}(\alpha_s^n)$. For example, to two-loops one has

$$R^{(2)}\left(\frac{Q^2}{\mu^2},\alpha_s\right) = 1 + c_1\alpha_s(\mu^2) + \left[c_2 - c_1\beta_0 \ln\left(\frac{Q^2}{\mu^2}\right)\right]\alpha_s^2(\mu^2)\,, \qquad (3.195)$$

which is μ-independent to $\mathcal{O}(\alpha_s)$ but μ-dependent at $\mathcal{O}(\alpha_s^2)$. Thus, a truncated series is μ-dependent and in practice we must decide what value(s) to use for μ. This is the scale setting problem. A conservative approach is to vary μ in a range centred on the characteristic scale $[Q/\lambda, Q\lambda]$. This should cover more specific prescriptions whilst, if λ is kept modest, avoid making the logarithm large and spoiling the validity of eqn (3.195). In this sense the measurement can be said to be of α_s at the scale Q^2. A word of caution: it is sometimes claimed that by varying μ one can estimate the size of the next (uncalculated) term in a series. For example, the α_s^2 term from the α_s term in eqn (3.195), but since c_2 is arbitrary (until calculated) this procedure is not without risk. Other more ambitious proposals for scale setting are available. The principle of minimum sensitivity (PMS) (P.M. Stevenson 1981) chooses μ so as to make the truncated series locally independent of μ. Applied to eqn (3.195) this yields

$$\mu^2\frac{\mathrm{d}R^{(n)}}{\mathrm{d}\mu^2}(\mu^2)\bigg|_{\mu^2_{\mathrm{PMS}}} = 0 \implies \mu^2_{\mathrm{PMS}} = Q^2\exp\left(-\frac{c_2}{\beta_0 c_1} - \frac{\beta_1}{2\beta_0^2}\right)\,. \qquad (3.196)$$

The application is to eqn (3.195). Fastest apparent convergence (FAC) chooses μ so that the first non-trivial term gives the same result as the sum of the known terms. Applying this prescription to eqn (3.195) gives

$$R^{(1)}(\mu^2_{\mathrm{FAC}}) = R^{(n)}(\mu^2_{\mathrm{FAC}}) \implies \mu^2_{\mathrm{FAC}} = Q^2\exp\left(-\frac{c_2}{\beta_0 c_1}\right)\,. \qquad (3.197)$$

Again the application is to eqn (3.195). A third proposal by Brodsky, Lepage and Mackenzie (BLM) (1983) determines μ from the requirement that the n_f-dependence of the coefficients c_i vanishes. In all cases, by going to higher orders in α_s, the dependence on μ is reduced and the scale setting problem diminished.

3.5 Infrared safety

Ultraviolet divergences are not the only complication which arises in QCD, divergences also occur when real gluons are emitted with either very low energy or nearly collinear to the emitter. We already noticed this problem at tree level with the $e^+e^- \to q\bar{q}g$ calculation in Section 3.3.2. Throughout this section we will illustrate the basic methods and ideas used to deal with these infrared divergences using the important example of the $\mathcal{O}(\alpha_s)$ correction to electron–positron annihilation to hadrons. The underlying process is $e^+e^- \to \gamma^*(Q) \to q\bar{q}$ which, as we have seen, is also closely related to both deep inelastic scattering and the Drell–Yan process. The $\mathcal{O}(\alpha_s)$ correction is given by gluon emission off the final state quark or antiquark, though the following discussion applies with minimal modification for emission off a gluon. Recall the behaviour of the quark propagator prior to emission, eqn (3.105),

$$\frac{1}{(q+g)^2 - m_q^2} = \frac{1}{2E_g E_q(1-\beta_q \cos\theta_{qg})} \quad \text{with} \quad \beta_q = \frac{|q|}{E_q} = \sqrt{1 - \frac{m_q^2}{E_q^2}}\,. \tag{3.198}$$

Here we see that there are basically two singular regions, which may overlap:

$$(\text{Propagator})^{-1} \longrightarrow \begin{cases} 0 & E_g \to 0 \quad \text{soft} \\ 2E_g E_q(1-\beta_q) \xrightarrow{m_q \to 0} 0 & \theta_{qg} \to 0 \quad \text{collinear}\,. \end{cases} \tag{3.199}$$

The collinear singularity is also known as a mass singularity since the propagator is strictly only divergent for gluon emission off a massless parton, quark or gluon. In both limits the virtuality of the emitter tends to zero, so that it travels a large space–time distance prior to the gluon emission. These divergences are therefore associated with the long distance, infrared behaviour of the theory. Similar infrared divergences occur also in virtual processes. This is because the integrals over loop momenta include phase space regions corresponding to the emission of both collinear and low-energy, real gluons for which the propagators are singular. This leads to very long-lived virtual fluctuations. It must now be admitted that we glossed over this issue in our earlier discussions of ultraviolet divergences. Since our calculations are perturbative, based on quarks and gluons, they will break down in these limits where non-perturbative contributions enter. In this section we shall consider how to cope with these divergences and under what circumstances they cancel.

3.5.1 *Infrared cancellations and dimensional regularization*

The key to treating infrared divergences lies in two observations. First, whilst real diagrams squared always give positive contributions to a cross section, interference involving virtual diagrams can give negative contributions. This opens up the possibility of arranging a cancellation between the singularities in the two sets of diagrams at the level of the amplitudes squared. Second, there is a striking similarity between the two singular configurations, soft and near-collinear gluon

emission, and the situation where no emission at all occurs. In practical situations a detector's energy resolution and granularity will not allow a sufficiently soft or collinear emission to be distinguished from no emission. If this is to be reflected in the corresponding theoretical calculation then the two contributions need to be added to give a useful result. In the case of electron–positron annihilation to hadrons the lowest order terms in the matrix element squared are given by

$$\mathcal{M}_{q\bar{q}} = \mathcal{M}^{(0)}_{q\bar{q}} + \alpha_s \mathcal{M}^{(1)}_{q\bar{q}} + \cdots ; \qquad \mathcal{M}_{q\bar{q}g} = \sqrt{\alpha_s}\mathcal{M}^{(0)}_{q\bar{q}g} + \cdots$$
$$|\mathcal{M}|^2 = \left|\mathcal{M}^{(0)}_{q\bar{q}}\right|^2 + \alpha_s \left(\left|\mathcal{M}^{(0)}_{q\bar{q}g}\right|^2 + 2\mathcal{R}e\left\{ \mathcal{M}^{(0)}_{q\bar{q}} \mathcal{M}^{(1)*}_{q\bar{q}} \right\} \right) + \cdots . \quad (3.200)$$

There is no $\sqrt{\alpha_s}$ cross-term in the squared result as there is no common final state: $|q\bar{q}\rangle \neq |q\bar{q}g\rangle$. At next-to-leading order we should take into account both the real process $e^+e^- \to q\bar{q}g$ and the interference between the tree-level and one-loop, virtual corrections to the process $e^+e^- \to q\bar{q}$. In eqn (3.200) we anticipate that the first and second terms at $\mathcal{O}(\alpha_s)$ will contain '$+\infty$' and '$-\infty$' infrared divergences and that these will cancel when added to leave a finite result.

As with the treatment of ultraviolet divergences, before we can manipulate any matrix elements we need to regulate any infrared divergences and make them finite. It is rather pleasing that dimensional regularization again provides a suitable method. To see how this works we shall consider the tree-level process $\gamma^* \to q\bar{q}g$, for massless quarks. In the soft gluon limit the dominant contribution to the matrix element squared comes from the cross-term, eqn (3.106),

$$|\mathcal{M}|^2 \propto \frac{q\cdot\bar{q}}{(q\cdot g)(\bar{q}\cdot g)} \sim \frac{1}{E_g^2}\frac{1}{(1-\cos\theta_{qg})} , \quad (3.201)$$

which behaves as E_g^{-2}. This expression, describing radiation off a colour–anti-colour dipole, also contains collinear singularities for $g \to\!\parallel q$, where it behaves as θ_{qg}^{-2}, and for $g \to\!\parallel \bar{q}$, where it behaves as θ_{qg}^{-2}. As we shall learn in Sections 3.7 and 3.6.7, this simplification of a matrix element squared in the soft and collinear limits is generic. Thus the contribution to the cross section from a soft gluon emitted nearly parallel to the quark is given by the following D-dimensional phase space integral

$$\int \frac{\mathrm{d}^D g}{(2\pi)^D}\Theta^{(+)}(g^2)\frac{q\cdot\bar{q}}{(q\cdot g)(\bar{q}\cdot g)} \quad (3.202)$$
$$= \int \frac{\mathrm{d}^{D-3}\Omega}{(2\pi)^D}\int_0 \frac{\mathrm{d}g_\parallel \mathrm{d}g_\perp g_\perp^{D-3}}{2E_g}\frac{1}{E_g\left[E_g - g_\parallel\right] f(\Omega)}\bigg|_{E_g=\sqrt{g_\parallel^2+g_\perp^2}}$$
$$= \int_0 \mathrm{d}E_g E_g^{D-5}\int_0^\pi \mathrm{d}\theta_{qg}\frac{\sin^{D-3}\theta_{qg}}{2(1-\cos\theta_{qg})}\int\frac{\mathrm{d}^{D-3}\Omega}{(2\pi)^D}\frac{1}{f(\Omega)}$$

$$= \int_0 \mathrm{d}E_\mathrm{g} E_\mathrm{g}^{D-5} \int_0^\pi \mathrm{d}\theta_\mathrm{qg} \sin^{D-5}(\theta_\mathrm{qg}/2)\, \cos^{D-3}(\theta_\mathrm{qg}/2) \int \frac{\mathrm{d}^{D-3}\Omega}{(2\pi)^D} \frac{2^{D-5}}{f(\Omega)} .$$

In the first line we isolate the component of the gluon's momentum parallel to the quark; $f(\Omega)$ describes the (non-singular) angular dependence of the dimensionless combination $(q \cdot \bar{q}/\bar{q} \cdot g) \times (E_\mathrm{g}/E_\mathrm{q})$. In the second line we have introduced polar coordinates oriented along the direction q. As the third line makes clear, it is apparent that the soft, $E_\mathrm{g} \to 0$, singularity is integrable provided $D > 4$, as is the collinear, $\theta_\mathrm{qg} \to 0$, singularity. Thus to tame infrared divergences we work in $D = 4 - 2\epsilon$ dimensions, but now with $\epsilon < 0$ so that $D > 4$.

Readers may be aware that another method for regulating infrared divergences is to add a small mass to the gluon in intermediate calculations which can be removed in the final result. However, this is a 'short-sighted' solution as a gluon mass term violates gauge invariance at $\mathcal{O}(\alpha_\mathrm{s})$. As soon as two gluons are involved in a situation, a gluon mass cannot be used without destroying the basis for the theory. You may wonder if it is possible to extend the BRS symmetry even further to accommodate a gluon (or ghost) mass term as well as the gauge fixing term. Unfortunately, this is only known to be possible for an abelian theory such as QED.

3.5.2 $\mathrm{e}^+\mathrm{e}^-$ *annihilation to hadrons at NLO*

We can now start to calculate the cross section for electron–positron annihilation to hadrons including our infrared regulator. This is given schematically as the product of a lepton tensor and a hadron tensor which is integrated over the final state phase space, c.f. eqn (3.85),

$$\sigma = \frac{1}{2Q^2} L_{\mu\nu} \frac{1}{Q^4} \int \mathrm{d}\Phi H^{\mu\nu} . \tag{3.203}$$

Observe that in the photon propagator any terms proportional to $(1 - \xi)Q^\mu Q^\nu$ do not contribute thanks to electromagnetic gauge invariance which requires that both $Q^\mu L_{\mu\nu} = 0 = Q^\nu L_{\mu\nu}$ and $Q_\mu H^{\mu\nu} = 0 = Q_\nu H^{\mu\nu}$. Now, the only available objects that can carry the integrated hadron tensor's Lorentz indices are $\eta^{\mu\nu}$ and $Q^\mu Q^\nu$. Add to this the gauge invariance requirement, and we can restrict the integrated hadron tensor to the form

$$\int \mathrm{d}\Phi H^{\mu\nu}(Q) = \frac{1}{(D-1)} \left(-\eta^{\mu\nu} + \frac{Q^\mu Q^\nu}{Q^2} \right) H(Q^2) \tag{3.204}$$

$$\text{with} \quad H(Q^2) = -\eta_{\mu\nu} \int \mathrm{d}\Phi H^{\mu\nu}(Q^2) .$$

You may recognize the pre-factor as the appropriate form of the spin averaged polarization sum for an off mass-shell photon in D dimensions, c.f. eqn (3.111). Substituting eqn (3.204) into eqn (3.203) and using the standard form of the (massless) lepton tensor, eqn (3.85), then gives

$$\sigma = \frac{e^2}{4Q^4} \frac{(D-2)}{(D-1)} H(Q^2) . \tag{3.205}$$

In this way we have reduced the problem to the simpler one of calculating the contraction of the hadronic tensor with $-\eta_{\mu\nu}$ and integrating it over its phase space. To confirm eqn (3.205) we apply it to the underlying, lowest order subprocess for a single, massless quark flavour,

$$\begin{aligned}\sigma_0^{(\epsilon)} &= \frac{e^2}{4Q^4}\frac{2(1-\epsilon)}{(3-2\epsilon)}(ee_q\mu^\epsilon)^2 N_c \times -\eta_{\mu\nu}\int \mathrm{d}\Phi_2 \mathrm{Tr}\left\{\not{q}\gamma^\mu \not{\bar{q}}\gamma^\nu\right\} \\ &= \frac{e^2}{4Q^4}\frac{2(1-\epsilon)}{(3-2\epsilon)}(ee_q\mu^\epsilon)^2 N_c \frac{1}{4\pi}\frac{1}{2}\left(\frac{4\pi}{Q^2}\right)^\epsilon \frac{\Gamma(1-\epsilon)}{\Gamma(2-2\epsilon)} 4(1-\epsilon)Q^2 \\ &= \frac{4\pi\alpha_{\mathrm{em}}^2}{Q^2}e_q^2 N_c \frac{(1-\epsilon)^2}{(3-2\epsilon)}\frac{\Gamma(1-\epsilon)}{\Gamma(2-2\epsilon)}\left(\frac{4\pi\mu^2}{Q^2}\right)^\epsilon . \end{aligned} \tag{3.206}$$

The evaluation of the hadron tensor essentially follows the earlier treatment, Section 3.3.1, however, we now work in D dimensions. This means adding a factor μ^ϵ to the quark's coupling and remembering that $\eta_\mu{}^\mu = D = 4-2\epsilon$ when doing the γ-matrix algebra: see Ex. (3-19). We used eqn (C.22) for the phase space. The result coincides with eqn (3.93) in the limit $D \to 4$.

3.5.2.1 *The real $\mathcal{O}(\alpha_s)$ contribution* At $\mathcal{O}(\alpha_s)$ the most straightforward contributions to evaluate come from the real emission process $\gamma^* \to q\bar{q}g$; see Fig. 3.11 and the earlier discussion of Section 3.3.2. Working with massless quarks in D dimensions the projection of the $q\bar{q}g$ matrix element squared is

$$\begin{aligned}&\frac{-\eta_{\mu\nu}H_{\mathrm{R}}^{\mu\nu}}{(ee_q g_s \mu^{2\epsilon})^2 C_F N_c} \\ &= 2(1-\epsilon)\mathrm{Tr}\{\mathbf{1}\}\left[(1-\epsilon)\left(\frac{g\cdot\bar{q}}{g\cdot q} + \frac{g\cdot q}{g\cdot\bar{q}}\right) + \frac{(q\cdot\bar{q})Q^2}{(g\cdot q)(g\cdot\bar{q})} - 2\epsilon\right] \\ &= 2(1-\epsilon)\mathrm{Tr}\{\mathbf{1}\}\left[(1-\epsilon)\left(\frac{(1-x_{\mathrm{q}})}{(1-x_{\mathrm{q}})} + \frac{(1-x_{\mathrm{q}})}{(1-x_{\mathrm{q}})}\right) + \frac{2(1-x_g)}{(1-x_{\mathrm{q}})(1-x_{\mathrm{q}})} - 2\epsilon\right] \\ &= 2(1-\epsilon)\mathrm{Tr}\{\mathbf{1}\}\left[\frac{x_{\mathrm{q}}^2 + x_{\bar{\mathrm{q}}}^2 - \epsilon x_g^2}{(1-x_{\mathrm{q}})(1-x_{\bar{\mathrm{q}}})}\right] . \end{aligned} \tag{3.207}$$

Here we employ the usual energy fractions, x_i, defined in eqn (3.113). In the first two lines it is easy to identify the individual contributions from the diagrams corresponding to gluon emission off the quark, emission off the antiquark and their interference. In this expression the collinear singularities appear as single poles in the limits $g\cdot q \to 0$ ($x_{\mathrm{q}} \to 1$) or $g\cdot\bar{q} \to 0$ ($x_{\bar{\mathrm{q}}} \to 1$). The soft singularity appears as poles in the limit $g\cdot q \to 0$ and $g\cdot\bar{q} \to 0$ ($x_{\mathrm{q}} \to 1$ and $x_{\bar{\mathrm{q}}} \to 1$). Observe that in this limit the interference term has a double pole. The appropriate D-dimensional, three-body phase space integral is given by eqn (C.23), so that $H_{\mathrm{R}}(Q^2)$ is given by

$$H_{\mathrm{R}}(Q^2) = -\eta_{\mu\nu}\int \mathrm{d}\Phi_3 H^{\mu\nu}(Q^2) = \alpha_{\mathrm{em}}e_q^2\frac{\alpha_s}{2\pi}C_F N_c 2Q^2\left(\frac{4\pi\mu^2}{Q^2}\right)^{2\epsilon}\frac{(1-\epsilon)}{\Gamma(2-2\epsilon)}$$

$$\times \int_0^1 \mathrm{d}x_{\bar{\mathrm{q}}} \int_{1-x_{\bar{\mathrm{q}}}}^1 \mathrm{d}x_{\mathrm{q}} \frac{1}{[(1-x_{\mathrm{q}})(1-x_{\bar{\mathrm{q}}})(x_{\mathrm{q}}+x_{\bar{\mathrm{q}}}-1)]^{\epsilon}}$$
$$\times \left[(1-\epsilon)\left(\frac{(1-x_{\mathrm{q}})}{(1-x_{\bar{\mathrm{q}}})}+\frac{(1-x_{\bar{\mathrm{q}}})}{(1-x_{\mathrm{q}})}\right)+\frac{2(x_{\mathrm{q}}-x_{\bar{\mathrm{q}}}-1)}{(1-x_{\mathrm{q}})(1-x_{\bar{\mathrm{q}}})}-2\epsilon\right] . \qquad (3.208)$$

This phase space integral looks very daunting, but can in fact be rendered quite simple by means of a change of variables, $x_{\bar{\mathrm{q}}} = 1 - vx_{\mathrm{q}}$, and $x_{\mathrm{q}} = x$,

$$\int_0^1 \mathrm{d}x \int_0^1 \mathrm{d}v \frac{x}{[x^2(1-x)v(1-v)]^{\epsilon}}$$
$$\times \left\{(1-\epsilon)\left(\frac{(1-x)}{xv}+\frac{xv}{(1-x)}\right)+2\frac{(1-v)}{(1-x)v}-2\epsilon\right\}$$
$$= 2\left\{(1-\epsilon)\frac{\Gamma(2-\epsilon)\Gamma(1-\epsilon)\Gamma(-\epsilon)}{\Gamma(3-3\epsilon)}+\frac{\Gamma(2-\epsilon)\Gamma^2(-\epsilon)}{\Gamma(2-3\epsilon)}-\epsilon\frac{\Gamma^3(1-\epsilon)}{\Gamma(3-3\epsilon)}\right\}$$
$$= \frac{\Gamma^3(1-\epsilon)}{\Gamma(1-3\epsilon)}\frac{1}{(1-3\epsilon)}\left(\frac{2}{\epsilon^2}-\frac{3}{\epsilon}+\frac{(1-4\epsilon)}{(2-3\epsilon)}\right)$$
$$= \frac{\Gamma^3(1-\epsilon)}{\Gamma(1-3\epsilon)}\left(\frac{2}{\epsilon^2}+\frac{3}{\epsilon}+\frac{19}{2}+\mathcal{O}(\epsilon)\right) . \qquad (3.209)$$

The x and v integrals are of the standard Euler β-function form, eqn (C.27), and the resulting Γ-functions have been manipulated using eqn (C.25). Here we see a double, $1/\epsilon^2$, pole which comes from the interference term and is associated with the soft gluon singularity. There is also a single, $1/\epsilon$, pole associated with the collinear/soft divergences. Combining eqns (3.209), (3.208) and (3.205) gives the real gluon emission cross section at $\mathcal{O}(\alpha_{\mathrm{s}})$,

$$\sigma_{\mathrm{R}}^{(\epsilon)} = \sigma_0^{(\epsilon)}\frac{\alpha_{\mathrm{s}}}{2\pi}C_F\left(\frac{4\pi\mu^2}{Q^2}\right)^{\epsilon}\frac{\Gamma^2(1-\epsilon)}{\Gamma(1-3\epsilon)}\left(\frac{2}{\epsilon^2}+\frac{3}{\epsilon}+\frac{19}{2}+\mathcal{O}(\epsilon)\right) . \qquad (3.210)$$

3.5.2.2 *The virtual $\mathcal{O}(\alpha_{\mathrm{s}})$ contribution* We now turn our attention to the $\mathcal{O}(\alpha_{\mathrm{s}})$ contribution coming from the interference of the virtual, one-loop corrections, shown in Fig. 3.20, and the tree-level process $\gamma^* \to \mathrm{q}\bar{\mathrm{q}}$.

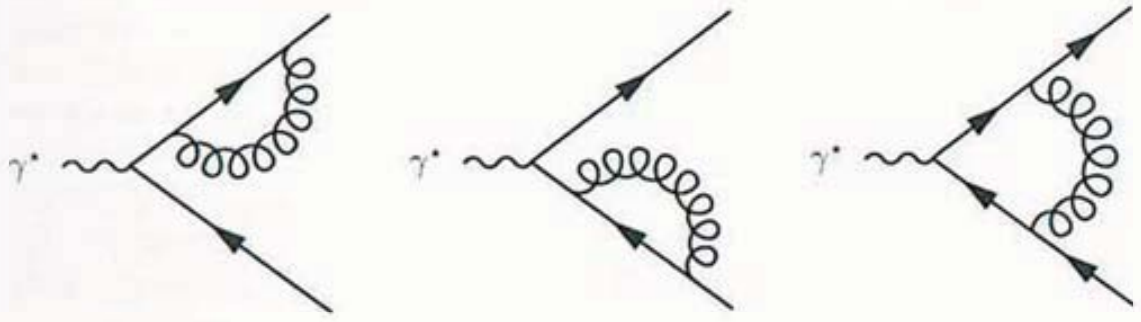

FIG. 3.20. The virtual, one-loop, QCD corrections to the $\gamma^* \to \mathrm{q}\bar{\mathrm{q}}$ vertex at $\mathcal{O}(\alpha_{\mathrm{s}})$

Recalling our earlier discussion of renormalization, Section 3.4.1, we anticipate that these virtual corrections contain both infrared and ultraviolet divergences. We begin by investigating the ultraviolet behaviour of the corrections. The divergence in the quark self-energy can be read off from eqn (3.132). To obtain the divergent part of the vertex correction we note its similarity to the first, 'QED-like' graph in Fig. 3.18 which is identical upon making the replacement $g_s(T^bT^aT^b)_{ij} \to ee_q(T^bT^b)_{ij} = ee_qC_F\delta_{ij}$. Thus, the divergence can be read off from the first term in eqn (3.138). Temporarily abandoning our restriction to massless, on mass-shell (anti)quarks, the one-loop contribution to the $\gamma q\bar{q}$ vertex is given by

$$
\begin{aligned}
&-\mathrm{i}ee_q\mu^{\epsilon}\delta_{ij}\frac{1}{2}\left[\Sigma(q)\frac{(\not{q}+m)}{q^2-m^2}\gamma^\mu+\gamma^\mu\frac{(-\not{\bar{q}}+m)}{\bar{q}^2-m^2}\Sigma(-\bar{q})\right]+\Gamma_{ij}(Q,q)^\mu\\
&=-\mathrm{i}ee_q\mu^{\epsilon}\delta_{ij}\frac{\alpha_s}{4\pi}C_F\left\{\left(-\frac{1}{2}\left[\left(\xi-3m\frac{(\not{q}+m)}{q^2-m^2}\right)\gamma^\mu\right.\right.\right.\\
&\qquad\left.\left.\left.+\gamma^\mu\left(\xi+3m\frac{(\not{\bar{q}}-m)}{\bar{q}^2-m^2}\right)\right]+\xi\gamma^\mu\right)\Delta_\epsilon+\text{U.V. finite}\right\}\\
&=-\mathrm{i}ee_q\delta_{ij}\frac{\alpha_s}{4\pi}C_F\times(\text{U.V. finite})\,. \qquad (3.211)
\end{aligned}
$$

Note that we only absorb half of the self-energy corrections into the renormalized coupling appearing in the third line. The other half goes into the wavefunction renormalization. We also use the Dirac equation acting on quark, $\bar{u}(q)$, and antiquark, $v(\bar{q})$, basis states to eliminate the two remaining divergent terms. The sum is then free of ultraviolet divergences. This result for the $\gamma q\bar{q}$ vertex should be compared to that for the $gq\bar{q}$ vertex, Ex. (3-23).

The absence of ultraviolet divergent QCD corrections to the $\gamma q\bar{q}$ vertex is not an accident but an important requirement for the acceptability of QCD. Its significance lies in the fact that QCD does not affect the renormalization of electric charges or, if you wish, does not spoil electromagnetic gauge invariance. More formally, the electric charge operator commutes with the QCD Hamiltonian. If it did not, then electric charges would not be conserved. For example, consider an antineutrino interacting with an electron to give hadrons, $\bar{\nu}_e e^- \to W^- \to d\bar{u}$. The initial state has charge $-e$ and is unaffected by strong corrections, whereas the final state is potentially affected by them and so might have a renormalized charge $-e' \neq -e$ which is unacceptable. The $\gamma q\bar{q}$, $Zq\bar{q}$ and $Wq\bar{q}'$ vertices are free of strong interaction divergences to all orders. This is the reason why we can calculate the charge on a hadron from the sum of charges on its constituent quarks without regard to any complex, non-perturbative, strong interaction dynamics.

Since we are focusing on the case of massless, on mass-shell (anti)quarks a number of the virtual diagrams do not contribute. Recall eqn (3.131) for the quark self-energy, which in the case of $p^2 = m^2 = 0$ reduces to

$$
-\mathrm{i}\Sigma(p) = -(g_s\mu^{\epsilon})^2C_F\delta_{ij}\int\frac{\mathrm{d}^Dk}{(2\pi)^D}\frac{\gamma_\mu(\not{k}+\not{p})\gamma_\nu}{[k^2+2k\cdot p]k^2}\left[\eta^{\mu\nu}-(1-\xi)\frac{k^\mu k^\nu}{k^2}\right]
$$

$$= -(g_s\mu^\epsilon)^2 C_F \delta_{ij} \not{p} \int \frac{\mathrm{d}^D k}{(2\pi)^D} f(k) = 0 \,. \tag{3.212}$$

In the second line, we have made explicit the fact that the resulting loop integral is independent of any scale ($p^2 = 0$). This is the same situation that we encountered previously with the tadpole diagrams where the integral cannot be defined for any dimension D. In dimensional regularization these integrals are defined to be zero. Thus, the only one-loop diagram which can contribute is the vertex correction where the scale is set by $Q^2 = 2q \cdot \bar{q}$.

The contraction of the hadron tensor describing the interference between the vertex correction and tree-level diagrams is given by the real part of the following expression,

$$-\eta_{\mu\nu} H_{\mathrm{V}}^{\mu\nu} = +\mathrm{i}\, 2(e e_{\mathrm{q}} g_s \mu^{2\epsilon})^2 \mathrm{Tr}\left\{T^b T^b\right\} \int \frac{\mathrm{d}^D k}{(2\pi)^D} \frac{1}{k^2 (k+q)^2 (k-\bar{q})^2}$$
$$\times \left\{ \mathrm{Tr}\left\{ \not{q}\gamma_\sigma (\not{k} + \not{q}) \gamma_\mu (\not{k} - \not{\bar{q}}) \gamma^\sigma \not{\bar{q}} \gamma^\mu \right\} - \frac{(1-\xi)}{k^2} \mathrm{Tr}\left\{ \not{q}\not{k} (\not{k} + \not{q}) \gamma_\mu (\not{k} - \not{\bar{q}}) \not{k} \not{\bar{q}} \gamma^\mu \right\} \right\} . \tag{3.213}$$

Evaluating the two traces is a straightforward if tedious exercise,

$$\begin{aligned} &\mathrm{Tr}\left\{ \not{q}\gamma_\sigma (\not{k} + \not{q}) \gamma_\mu (\not{k} - \not{\bar{q}}) \gamma^\sigma \not{\bar{q}} \gamma^\mu \right\} \\ &\quad = +8(1-\epsilon)\left[Q^4 - 4(k\cdot q)(k\cdot \bar{q}) - 2k\cdot(q-\bar{q})Q^2 + \epsilon k^2 Q^2 \right] \\ &\mathrm{Tr}\left\{ \not{q}\not{k} (\not{k} + \not{q}) \gamma_\mu (\not{k} - \not{\bar{q}}) \not{k} \not{\bar{q}} \gamma^\mu \right\} \\ &\quad = -4(1-\epsilon)(k+q)^2 (k-\bar{q})^2 Q^2 \,. \end{aligned} \tag{3.214}$$

The second result implies that the gauge dependent contribution is of the same type as the integral in eqn (3.212) and therefore vanishes. There is no ξ-dependence. In order to treat the remaining loop momentum integral we first combine the propagators using Feynman parameters,

$$\begin{aligned} \frac{1}{k^2 (k+q)^2 (k-\bar{q})^2} &= \int_0^1 \mathrm{d}\alpha \int_0^{1-\alpha} \mathrm{d}\beta \frac{1}{\left[\alpha(k+q)^2 + \beta(k-\bar{q})^2 + (1-\alpha-\beta)k^2\right]^3} \\ &= \int_0^1 \mathrm{d}\alpha \int_0^{1-\alpha} \mathrm{d}\beta \frac{1}{\left[(k + \alpha q - \beta\bar{q})^2 + \alpha\beta Q^2\right]^3} \,. \end{aligned} \tag{3.215}$$

This suggests the change of variables $k^\mu \to k^\mu - \alpha q^\mu + \beta \bar{q}^\mu$ in the integral. Making this substitution in the integral's numerator the first trace, eqn (3.214), gives

$$\begin{aligned} \mathrm{Tr}\{\} &= 8(1-\epsilon)\, \left\{ Q^4 - 4\left[(k\cdot q)(k\cdot\bar{q}) - \alpha\beta (q\cdot\bar{q})^2 \right] \right. \\ &\qquad \left. -2\left[\beta q\cdot\bar{q} + \alpha q\cdot\bar{q}\right] Q^2 + \epsilon\left[k^2 - 2\alpha\beta q\cdot\bar{q}\right] Q^2 \right\} \\ &= 8(1-\epsilon) Q^2 \left\{ \left[1 - \alpha - \beta + (1-\epsilon)\alpha\beta\right] Q^2 - (1-\epsilon)^2 (2-\epsilon)^{-1} k^2 \right\} . \end{aligned} \tag{3.216}$$

In the first line we have discarded any terms that are linear in k and so give vanishing contributions in an isotropic integral. Whilst in the second line we

have replaced $k^\mu k^\nu$ by $k^2\eta^{\mu\nu}/D$, again by virtue of the integral's isotropy. When we substitute eqns (3.215) and (3.216) into (3.213) we see that we have an expression which only depends on Q^2. This makes the evaluation of the two-body phase space integral in eqn (3.204) trivial and we can go straight to eqn (3.205) for the result,

$$\begin{aligned}\sigma_{\rm V}^{(\epsilon)} &= +{\rm i}\,\sigma_0^{(\epsilon)} 4(g_s\mu^\epsilon)^2 C_F \int_0^1 {\rm d}\alpha \int_0^{1-\alpha} {\rm d}\beta \int \frac{{\rm d}^D k}{(2\pi)^D} \frac{1}{[k^2+\alpha\beta Q^2]^3} \\ &\qquad \times \left\{ \left[1-\alpha-\beta+(1-\epsilon)\alpha\beta\right] Q^2 - (1-\epsilon)^2(2-\epsilon)^{-1}k^2 \right\} \\ &= -\sigma_0^{(\epsilon)} \frac{\alpha_{\rm s}}{2\pi} C_F \left(\frac{4\pi\mu^2}{-Q^2}\right)^\epsilon \Gamma(1+\epsilon) \int_0^1 {\rm d}\alpha \int_0^{1-\alpha} {\rm d}\beta \frac{1}{(\alpha\beta)^\epsilon} \\ &\qquad \times \left\{ \frac{\left[1-\alpha-\beta+(1-\epsilon)\alpha\beta\right]}{\alpha\beta} - \frac{(1-\epsilon)^2}{\epsilon} \right\} . \end{aligned} \tag{3.217}$$

The loop momentum integrals are evaluated using eqn (C.11). The integral over the Feynman parameters is simplified by means of the change of variable $\beta = (1-\alpha)v$ which decouples the integrals and allows the use of eqn (C.27) to obtain

$$\begin{aligned}&\int_0^1 {\rm d}\alpha \int_0^{1-\alpha} {\rm d}\beta \frac{1}{(\alpha\beta)^\epsilon} \left\{ \frac{\left[1-\alpha-\beta+(1-\epsilon)\alpha\beta\right]}{\alpha\beta} - \frac{(1-\epsilon)^2}{\epsilon} \right\} \\ &= \int_0^1 {\rm d}\alpha \int_0^1 {\rm d}v \frac{(1-\alpha)}{[\alpha(1-\alpha)v]^\epsilon} \left\{ \frac{\left[(1-\alpha)(1-v)+(1-\epsilon)\alpha(1-\alpha)v\right]}{\alpha(1-\alpha)v} - \frac{(1-\epsilon)^2}{\epsilon} \right\} \\ &= \frac{\Gamma^2(1-\epsilon)}{\Gamma(2-2\epsilon)} \left[\frac{1}{\epsilon^2} + \frac{1}{2} - \frac{(1-\epsilon)}{2\epsilon} \right] \\ &= \frac{\Gamma^2(1-\epsilon)}{\Gamma(1-2\epsilon)} \frac{1}{2} \left[\frac{2}{\epsilon^2} + \frac{3}{\epsilon} + \frac{8}{(1-2\epsilon)} \right] . \end{aligned} \tag{3.218}$$

Substituting this result into eqn (3.217) gives us our final result,

$$\begin{aligned}\sigma_{\rm V}^{(\epsilon)} &= -\sigma_0^{(\epsilon)} \frac{\alpha_{\rm s}}{2\pi} C_F \left(\frac{4\pi\mu^2}{-Q^2}\right)^\epsilon \frac{\Gamma(1+\epsilon)\Gamma^2(1-\epsilon)}{\Gamma(1-2\epsilon)} \left(\frac{2}{\epsilon^2} + \frac{3}{\epsilon} + \frac{8}{(1-2\epsilon)} \right) \\ &= -\sigma_0^{(\epsilon)} \frac{\alpha_{\rm s}}{2\pi} C_F \left(\frac{4\pi\mu^2}{-Q^2}\right)^\epsilon \frac{\Gamma(1+\epsilon)\Gamma^2(1-\epsilon)}{\Gamma(1-2\epsilon)} \left(\frac{2}{\epsilon^2} + \frac{3}{\epsilon} + 8 + \mathcal{O}(\epsilon) \right) . \end{aligned} \tag{3.219}$$

Here, it is important to remember that the real part is understood.

3.5.2.3 *The combined $\mathcal{O}(\alpha_{\rm s})$ contribution* After having calculated the real, eqn (3.210), and the virtual, eqn (3.219), gluon corrections to the lowest order expression, eqn (3.206), we can combine them to give the complete, $\mathcal{O}(\alpha_{\rm s})$ cross section for electron–positron annihilation to hadrons,

$$\sigma = \sigma_0^{(\epsilon)} \left\{ 1 + \frac{\alpha_{\rm s}}{2\pi} C_F \left(\frac{4\pi\mu^2}{Q^2}\right)^\epsilon \frac{\Gamma^2(1-\epsilon)}{\Gamma(1-3\epsilon)} \left[\left(\frac{2}{\epsilon^2} + \frac{3}{\epsilon} + \frac{19}{2} + \mathcal{O}(\epsilon) \right) \right. \right.$$

$$+\mathcal{R}e\{(-1)^\epsilon\}\frac{\Gamma(1+\epsilon)\Gamma(1-3\epsilon)}{\Gamma(1-2\epsilon)}\left(-\frac{2}{\epsilon^2}-\frac{3}{\epsilon}-8+\mathcal{O}(\epsilon)\right)\Bigg]\Bigg\}$$

$$= [\sigma_0+\mathcal{O}(\epsilon)]\left\{1+\frac{\alpha_s}{2\pi}C_F[1+\mathcal{O}(\epsilon)]\left[\left(\frac{2}{\epsilon^2}+\frac{3}{\epsilon}+\frac{19}{2}+\mathcal{O}(\epsilon)\right)\right.\right.$$

$$\left.\left.-[1+\mathcal{O}(\epsilon^4)]\left(\frac{2}{\epsilon^2}+\frac{3}{\epsilon}+8+\mathcal{O}(\epsilon)\right)\right]\right\}$$

$$= \sigma_0\left\{1+\frac{3}{4}C_F\frac{\alpha_s}{\pi}+\mathcal{O}(\alpha_s^2)\right\}. \qquad (3.220)$$

In the second line we made use of the expansion $\mathcal{R}e\{(-1)^\epsilon\} = \mathcal{R}e\{e^{i\pi\epsilon}\} = 1-(\pi^2/2)\epsilon^2+\mathcal{O}(\epsilon^4)$ and eqn (C.26). As a result, it becomes clear that both the $1/\epsilon^2$ and $1/\epsilon$ poles cancel to leave a finite result. As a consequence we can safely take $\epsilon \to 0$ and obtain the $D = 4$ limit. Thus, for a suitably inclusive definition of the hadronic cross section we avoid the potential infrared catastrophe associated with soft gluons.

Before going on to identify the general characteristics of infrared safe observables we mention a succinct way of organizing the above cancellation using cut-diagrams. The $\mathcal{O}(\alpha_s)$ cross section is represented by the diagrams shown in Fig. 3.21. The two basic diagrams have each been 'cut' in two ways. On the left-hand side of the cut we view it as the usual Feynman diagram corresponding to $\mathcal{M}$. On the right-hand side of the cut we view it as a 'reversed' Feynman diagram corresponding to $\mathcal{M}^*$. Thus, the top-left diagram represents the interference between the two tree-level Feynman diagrams, whilst the bottom-left diagram represents the interference between the tree-level and one-loop correction to the basic $\gamma q\bar{q}$ vertex. You should notice that these are the same diagram cut in two different places. This one diagram encapsulates the contributions which must be taken into account to ensure the cancellation of infrared divergences.

3.5.3 *Infrared safe observables*

Our calculation of the cross section for electron–positron annihilation to hadrons demonstrates that it is free of infrared divergences to at least $\mathcal{O}(\alpha_s)$. In fact, the KLN-theorem (Kinoshita, 1962; Lee and Nauenberg, 1964), and its generalization to QCD (Poggio and Quinn, 1976; Sterman, 1976), guarantees that such a fully inclusive observable is infrared finite to all orders. This theorem can be extended so as to apply to other observables (Sterman and Weinberg, 1977; Dokshitzer *et al.*, 1980). The key requirement for the cancellation is that a quark and a quark accompanied by any number of soft gluons and/or collinear gluons and $q\bar{q}$-pairs are treated the same. Likewise, $|g\rangle$ and $|g+n_1g_s+n_2g_\parallel+n_3(q\bar{q})_\parallel\rangle$ must give the same contribution to an observable. Now, in practice cross sections are often weighted by functions corresponding to physical measurements on the parton final states. In general a measurement is described by an expression of the form

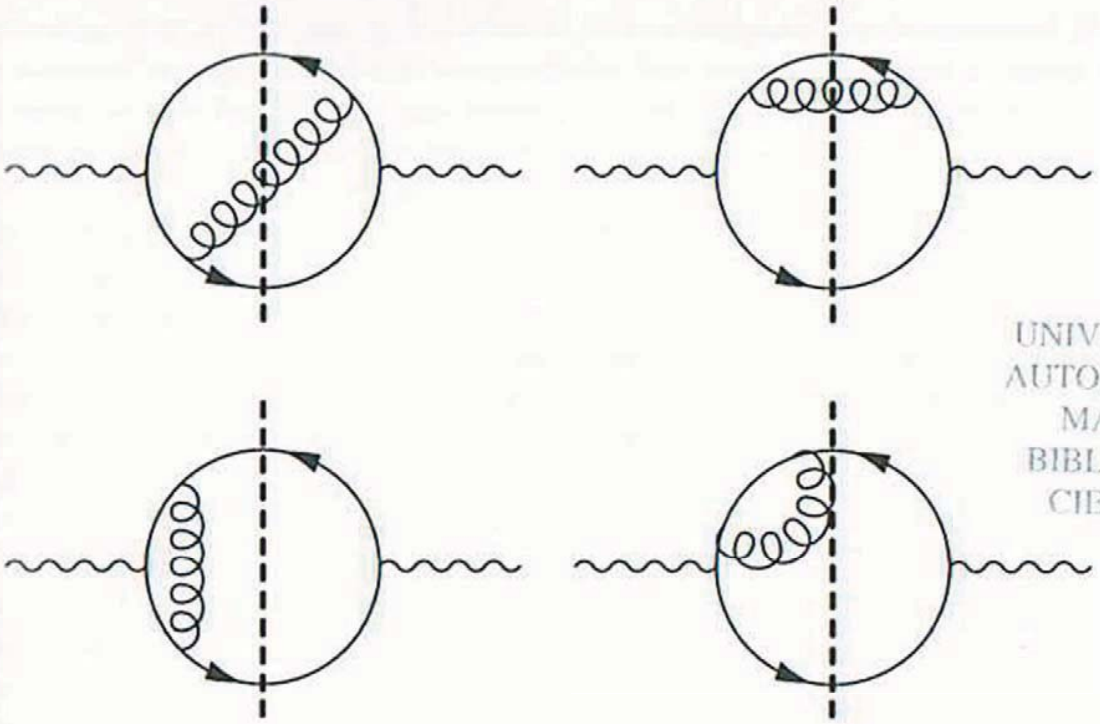

FIG. 3.21. The cut-diagrams which describe the contributions to the amplitude squared for $\gamma^* \to$ hadrons at $\mathcal{O}(\alpha_s)$

$$I = \frac{1}{\text{flux}} \sum_n \frac{1}{n!} \int \mathrm{d}\Phi^n \overline{\sum} \left| \mathcal{M}^{(n)}(p_i) \right|^2 \rho_n(p_i) \tag{3.221}$$

$$\text{with} \quad \begin{cases} \rho_n = 1 & I = \sigma \quad \text{(total cross section)} \\ \rho_n = \delta\big(X - \mathcal{X}_n(p_i)\big) & I = \dfrac{\mathrm{d}\sigma}{\mathrm{d}X} \quad \text{(differential cross section)} \,. \end{cases}$$

The sum includes the contributions from all n-parton final states and, on the assumption that quarks, antiquarks and gluons are not distinguished, we include the symmetrization factor $1/n!$. The weight functions of the n final state partons, $\rho_n(p_1, \ldots, p_n)$, define the measurement. For example, to obtain the total cross section, $I = \sigma$, we simply use $\rho_n(p_i) = 1$. Often, we are interested in the distribution of some variable X which is given by the function $\mathcal{X}_n(p_i)$ for n partons. Typical observables discussed later include the event's Thrust, see eqn (6.2), or a jet resolution parameter, see eqn (6.3) or (6.4). To obtain $I = \mathrm{d}\sigma/\mathrm{d}X$ we have to use $\rho_n = \delta(X - \mathcal{X}_n(p_i))$. However, in view of the cancellations required for infrared safety, the functions $\mathcal{X}_{n+1}$ and $\mathcal{X}_n$ must become equal in the soft and collinear limits,

$$\left.\begin{matrix} \mathcal{X}_{n+1}(p_1, \ldots, \lambda p_n, (1-\lambda)p_n) \\ \mathcal{X}_{n+1}(p_1, \ldots, p_n, 0) \end{matrix}\right\} = \mathcal{X}_n(p_1, \ldots, p_n) \,. \tag{3.222}$$

Whilst this is a requirement imposed on theoretical grounds, you are reminded that it also has a basis in experimental reality. The results of a measurement

should be insensitive to changes in a detector's energy resolution or granularity. As a result of this requirement any observable which is not a linear function of the parton four-momenta will not be infrared safe and should not be used in experiment or theory. If you do not heed this restriction then you will be sensitive to long-distance physics. This means either introducing a non-perturbative model, upon which your results will depend, or accepting that using pQCD will give infinity at NLO. Despite this established wisdom it is still too common to see variables such as Sphericity (not to be confused with spherocity) or (some) cone based jet finders which are infrared unsafe!

A special situation arises for observables such as structure functions and fragmentation functions. By their nature the inclusive summation over initial or final states is restricted by the requirement to contain a specific particle. This results in residual collinear singularities which can be treated in a manner which is reminiscent of renormalization: see Section 3.6.

The first example of an observable specifically designed to satisfy the infrared finiteness requirement is the Sterman–Weinberg jet definition (Sterman and Weinberg, 1977). Other examples of early variables are given in (Basham *et al.*, 1978*a*) and (Fox and Wolfram, 1978). A hadronic e^+e^- event is defined to be a two-jet event if a fraction $(1-\epsilon)$ of the total C.o.M. energy is contained within two back-to-back cones of half angle δ. Whilst this clearly satisfies eqn (3.222), in practice it is rarely used at e^+e^- colliders, though such 'cone based' definitions are still used at hadron colliders. A more popular jet definition is based on the minimum invariant mass of particle pairs. At leading order all events are two-jet events. At $\mathcal{O}(\alpha_s)$, an event is only classified as two-jet if one of the three possible pairs of partons has $(p_i+p_j)^2/Q^2 < y$ for a given value of the resolution parameter y. By construction we have $y < 1/3$. A two-jet event occurs for two basic phase space configurations. Either, the gluon is radiated sufficiently close in direction to the quark or with sufficiently low energy that $(q+g)^2/Q^2 < y$ and the qg-pair forms a jet recoiling against the $\bar{q}$ (or with q and $\bar{q}$ interchanged). Or, much less likely, the gluon has high energy and the $q\bar{q}$-pair forms a jet recoiling against the gluon. Using $(p_i+p_j)^2/Q^2 = 1-x_k > y$ we see that the three-jet region of phase space is confined to a triangular region, $2y < x_i < 1-y$, in the centre of the $x_q - x_{\bar{q}}$ plane away from the collinear and soft singularities, see Fig. 3.12 where $y = 1-T$. This means that calculating the $\mathcal{O}(\alpha_s)$, three-jet cross section is relatively straightforward as, unlike the two-jet cross section, it does not involve any infrared cancellations and therefore it does not require a regulator. One can then use the known result $\sigma_2 + \sigma_3 = \sigma_0[1 + (3C_F\alpha_s/(4\pi)]$, eqn (3.220), to infer the two-jet cross section. Rather than do this in one step we first use eqn (3.221) with $X_{n=3} = \min\{1-x_1, 1-x_2, 1-x_3\}$, $X = y$ and the matrix element squared given by eqn (3.112),

$$\frac{\mathrm{d}\sigma_3}{\mathrm{d}y} = \sigma_0 \frac{\alpha_s}{2\pi} C_F \int_{2y}^{1-y} \mathrm{d}x \left\{ 2\, \frac{x^2+\bar{x}^2}{(1-x)(1-\bar{x})}\bigg|_{\bar{x}=1-y} + \frac{x^2+\bar{x}^2}{(1-x)(1-\bar{x})}\bigg|_{\bar{x}=1+y-x} \right\}$$

$$= \sigma_0 \frac{\alpha_s}{2\pi} C_F \int_{2y}^{1-y} \mathrm{d}x \left\{ 2\frac{(1-y)^2 + 1 - (1-x)(1+x)}{y(1-x)} + \frac{1}{1-y}\left(\frac{1}{1-x} + \frac{1}{x-y}\right)\left[1 + y^2 - 2(1-x)(x-y)\right]\right\}$$

$$= \sigma_0 \frac{\alpha_s}{2\pi} C_F \left[2\frac{(3y^2 - 3y + 2)}{y(1-y)} \ln\left(\frac{1-2y}{y}\right) - 3\frac{(1-3y)(1+y)}{y}\right] . \qquad (3.223)$$

This expression shows a characteristic logarithmic divergence as $y \to 0$, that is, as the singular regions are approached. In passing, we mention that this expression gives the Thrust distribution with $T = 1 - y$. Integrating this expression from y to the phase space limit $1/3$, we can calculate σ_3 and hence the n-jet rates defined by $f_n = \sigma_n/\sigma_{\mathrm{tot}}$ as

$$f_3(y) = \frac{\alpha_s}{2\pi} C_F \left\{ \frac{5}{2} - \frac{\pi^2}{3} - 6y - \frac{9}{2}y^2 + (3 - 6y)\ln\left(\frac{y}{1-2y}\right) + 4\mathrm{Li}_2\left(\frac{y}{1-y}\right) + 2\ln^2\left(\frac{y}{1-y}\right)\right\}$$

$$\text{and} \quad f_2(y) = 1 - f_3(y) . \qquad (3.224)$$

Here, the dilogarithm or Spence function is defined by

$$\mathrm{Li}_2(x) = -\int_0^x \mathrm{d}z \frac{\ln(1-z)}{z} . \qquad (3.225)$$

It arises frequently in QCD calculations. Equation (3.224) shows that in the limit $y \to 0$, $f_3(y)$ diverges as $(\alpha_s C_F/\pi)\ln^2 y$. This can give the counter-intuitive result $f_2(y) < f_3(y)$ and worse $f_2(y) < 0$. Whilst this is unsettling, it is possible because $f_2(y)$ receives contributions from an interference term. In calculating $f_3(y)$ we restrict ourselves to a subregion of the real phase space so that the full cancellation of divergences which occurred in eqn (3.220) is now only partially complete and residual logarithms remain. At higher orders we may anticipate terms of the form $[\alpha_s C_F/(2\pi)\ln^2 y]^m$. Such large enhancements have obvious implications for the convergence of cross sections. Consequently a significant effort is dedicated to identifying and 'resumming' such contributions. For reference we also give the $\mathcal{O}(\alpha_s)$, three-jet rate for the Sterman–Weinberg jet definition,

$$f_3(\epsilon, \delta) = \frac{\alpha_s}{2\pi} C_F 8 \left\{ \ln\left(\frac{1}{\delta}\right)\left[\ln\left(\frac{1}{2\epsilon} - 1\right) - \frac{3}{4}\right] + \frac{\pi^2}{12} - \frac{7}{16} + \mathcal{O}(\epsilon\ln\delta, \delta^2\ln\epsilon)\right\} . \qquad (3.226)$$

Here, it is clear that the most singular term is associated with overlapping collinear, $\delta \to 0$, and soft, $\epsilon \to 0$, singularities.

3.6 The QCD improved parton model

The naïve (quark) parton model is independent of QCD as such and indeed was invented before QCD existed (Bjorken and Paschos, 1969; Feynman, 1972). It

began as a quasi-classical model for DIS, based upon the idea that a hadron can be described as a collection of independent partons, with little transverse momentum, off which a lepton can scatter via the exchange of a vector boson. The constituent quark model supplies quantum numbers to these partons and thereby suggests relationships between the various structure functions (Close, 1979). At this tree level all that pQCD supplies is support for treating the partons as independent, via asymptotic freedom, and candidates, the gluons, for the electroweak neutral partons inferred from the apparent violation of the momentum sum rule (Llewellyn-Smith, 1972). This parton model picture of DIS is easily generalized to hadron–hadron collisions.

The parton model comes to life when we add pQCD corrections (Altarelli, 1982). This brings to the fore quantum effects and changes our picture of the partons within a hadron. An essential feature of the parton model is the separation of a cross section into hadron independent coefficient functions, which describe the parton scatterings, and scattering independent p.d.f.s, which characterize the hadrons; see, for example, eqn (3.227). In order to maintain this separation in the presence of QCD corrections, we are obliged to make the p.d.f.s scale dependent, that is, functions of both x and Q^2. This introduces the idea that a parton contains within it further 'daughter' partons and that these are revealed when the Q^2 of the probing vector boson is increased. This scale dependence is governed by the famous DGLAP equations and whilst it remains true that, in the absence of suitable non-perturbative techniques for QCD, we cannot calculate the p.d.f.s from first principles, we can deduce the p.d.f.s at one scale from a given set at another scale. Introducing pQCD also forces us to give a precise meaning to the idea of factorization, which has now been proved to hold in pQCD (Collins and Soper, 1987). In doing so we give greater legitimacy to the QCD improved parton model; so much so that the QCD improved parton model provides the conventional framework for carrying out pQCD calculations.

Inevitably, when we add pQCD corrections to the naïve parton model, the necessary mathematics becomes more involved. However, we believe that the underlying ideas are not that complicated. Therefore, after repeating the tree-level treatment of DIS we give a heuristic development of the NLO pQCD corrections to DIS and factorization. This is followed by the complete $\mathcal{O}(\alpha_s)$ calculation. After this we switch attention to the DGLAP evolution equations and their generalizations. This is followed by a discussion of how these equations take account of large logarithmic enhancements to a cross section. Finally, we show how the factorization formalism is applied to the Drell–Yan process in hadron–hadron collisions.

3.6.1 *DIS at the parton level*

The formal description of lepton–parton scattering follows that for lepton–hadron scattering. The partonic cross section, $d\hat{\sigma}^{\ell f}$, is given by eqn (3.32) with two modifications: the hadron momentum p^μ is replaced by the parton momentum yp^μ and in the hadron tensor the state $|h\rangle$ is replaced by $|f\rangle$, $f = \{q, \bar{q}, g\}$, to

give $\hat{H}_{\mu\nu}^{(Vf)}$. Again gauge invariance ensures that this partonic tensor retains the form given in eqn (3.36) but with partonic structure functions. These partonic structure functions are functions of yp^μ and q_V^μ which, thanks to Bjorken scaling (Bjorken, 1969), occur in the combination $-q_V^2/(y2p\cdot q_V) = x/y$. Since we use the name of a particle to represent its four-momentum, we use q_V^μ for the four-momentum of the exchanged boson to avoid any confusion with the momentum of a quark, q^μ. The lepton tensor is, as before, given by eqn (3.33). This parton cross section is related to the hadron cross section by weighting it by the hadron's p.d.f.s,

$$\mathrm{d}\sigma^{(\mathrm{lh})} = \sum_{f=q,\bar{q},g} \int_0^1 \mathrm{d}y f_{\mathrm{h}}(y) \mathrm{d}\hat{\sigma}^{(\mathrm{lf})}\left(\frac{x}{y}\right) . \tag{3.227}$$

This implies

$$H_{\mu\nu}^{(V\mathrm{h})}(p,q_V) = \sum_{f=q,\bar{q},g} \int_0^1 \frac{\mathrm{d}y}{y} f_{\mathrm{h}}(y) \hat{H}_{\mu\nu}^{(Vf)}(yp,q_V) , \tag{3.228}$$

where the factor $1/y$ can be traced to the scaling $p^\mu \to yp^\mu$ used to obtain the lepton–parton flux factor.

Rather than work with the full hadronic tensor, it is helpful to project out two combinations of structure functions,

$$\begin{aligned} H_\Sigma^{(V\mathrm{h})} &\equiv -\eta^{\mu\nu} H_{\mu\nu}^{(V\mathrm{h})} \\ &= (D-2)\frac{F_2}{2x}\left(1+\frac{(2xM_{\mathrm{h}})^2}{Q^2}\right) - (D-1)\left[\frac{F_2}{2x}\left(1+\frac{(2xM_{\mathrm{h}})^2}{Q^2}\right) - F_1\right] \\ H_L^{(V\mathrm{h})} &\equiv p^\mu p^\nu H_{\mu\nu}^{(V\mathrm{h})} \\ &= \frac{Q^2}{(2x)^2}\left[\frac{F_2}{2x}\left(1+\frac{(2xM_{\mathrm{h}})^2}{Q^2}\right) - F_1\right]\left(1+\frac{(2xM_{\mathrm{h}})^2}{Q^2}\right) . \end{aligned} \tag{3.229}$$

This will simplify the expressions with which we have to work. Here, with a view to future use, we have chosen to work in $D = 4 - 2\epsilon$ dimensions. Similar projections can be defined at the parton level. In the case of $\hat{H}_\Sigma$ this is straightforward but for $\hat{H}_L$ we have to use the parton momentum, yp, in the equivalent of eqn (3.229). Referring to eqn (3.228) we then have

$$\begin{aligned} H_\Sigma^{(V\mathrm{h})} &= \sum_{f=q,\bar{q},g} \int_0^1 \frac{\mathrm{d}y}{y} f_{\mathrm{h}}(y) \hat{H}_\Sigma^{(Vf)}(yp,q_\gamma) = \sum_{f=q,\bar{q},g} \int_x^1 \frac{\mathrm{d}z}{z} f_{\mathrm{h}}\left(\frac{x}{z}\right) \hat{H}_\Sigma^{(Vf)}(z) \\ H_L^{(V\mathrm{h})} &= \sum_{f=q,\bar{q},g} \int_0^1 \frac{\mathrm{d}y}{y^3} f_{\mathrm{h}}(y) \hat{H}_L^{(Vf)}(yp,q_\gamma) = \sum_{f=q,\bar{q},g} \frac{1}{x^2} \int_x^1 \frac{\mathrm{d}z}{z} f_{\mathrm{h}}\left(\frac{x}{z}\right) z^2 \hat{H}_L^{(Vf)}(z) . \end{aligned} \tag{3.230}$$

Remember that scaling implies that the $\hat{H}_i^{(Vf)}$ are functions of $Q^2/(y2p\cdot q_\gamma) = x/y$. The advantage of the 'total' structure function, $\hat{H}_\Sigma^{(Vf)}$, is that it is essentially the matrix element squared for the vector boson–parton subprocess.

The 'longitudinal' structure function, $\hat{H}_L^{(Vf)}$, is particularly nice because many diagrams give vanishing contributions and those that do not vanish at $\mathcal{O}(\alpha_s)$ are free of infrared singularities. In eqn (3.229) we recognise the combination in square brackets as the longitudinal structure function; see Ex. (3-5). Once we have calculated H_Σ and H_L we can invert eqn (3.229) to give us the structure functions F_2 and F_1,

$$\begin{aligned}\frac{F_2(x)}{x} &= \frac{1}{(1-\epsilon)} H_\Sigma^{(Vh)} + \frac{(3-2\epsilon)}{(1-\epsilon)} \frac{4x^2}{Q^2} H_L^{(Vh)} \\ &= \sum_{f=q,\bar{q},g} \int_x^1 \frac{\mathrm{d}z}{z} f\left(\frac{x}{z}\right) \left[\frac{1}{(1-\epsilon)} \hat{H}_\Sigma^{(Vf)}(z) + \frac{(3-2\epsilon)}{(1-\epsilon)} \frac{4z^2}{Q^2} \hat{H}_L^{(Vf)}(z) \right] \\ F_1(x) - \frac{F_2(x)}{2x} &= -\frac{4x^2}{Q^2} H_L^{(Vh)} \\ &= -\sum_{f=q,\bar{q},g} \int_x^1 \frac{\mathrm{d}z}{z} f\left(\frac{x}{z}\right) \frac{4z^2}{Q^2} \hat{H}_L^{(Vf)}(z) \,. \end{aligned} \tag{3.231}$$

Here we have made the simplifying assumption that the $2xM_h/Q$ terms are negligible. In what follows we shall also neglect all quark masses. This makes the algebra simpler and will cast into sharper relief any collinear singularities.

3.6.2 *DIS at leading order*

We now calculate the leading order contributions to DIS in the parton model. We will focus on electromagnetic exchange in which a photon couples to the electrically charged partons: quarks and antiquarks. The charge conjugation symmetry of QED and QCD ensures that quarks and antiquarks give the same contribution. Thus at $\mathcal{O}(\alpha_s^0)$ we need only consider the one tree-level subprocess $\gamma^* \mathrm{q} \to \mathrm{q}'$. The treatment of Z and $\mathrm{W}^\pm$ exchange involves only minor modifications.

To calculate $\hat{H}_\Sigma^{(\gamma \mathrm{q})}$ we first require the matrix element squared. This is easily evaluated in D dimensions,

$$\sum |\mathcal{M}(\gamma^* \mathrm{q} \to \mathrm{q}')|^2 = e^2 e_\mathrm{q}^2 N_c (1-\epsilon) \mathrm{Tr}\{1\} Q^2 \,. \tag{3.232}$$

Here $Q^2 = -(q'-q)^2 = 2q \cdot q' > 0$. Next, we average over the spin and colour polarizations of the incoming quark, $2N_c$, and include the one-body phase space integral, eqn (C.19), to obtain

$$\int \mathrm{d}\Phi_1 \overline{\sum} |\mathcal{M}(\gamma^* \mathrm{q} \to \mathrm{q}')|^2 = 2e^2 e_\mathrm{q}^2 (1-\epsilon) Q^2 \times 2\pi \delta(q'^2) \,. \tag{3.233}$$

Here we have used $\mathrm{Tr}\{1\} = 4$. Since the struck quark carries a fraction y of the parent hadron's momentum, $q^\mu = y p^\mu$, the δ-function, which constrains the scattered quark to be on mass-shell, can be rewritten as

$$q'^2 = (yp + q_\gamma)^2 = y 2p \cdot q^\gamma - Q^2 = 2p \cdot q^\gamma (y - x)$$

$$\Longrightarrow \quad \delta(q'^2) = \frac{1}{2p\cdot q}\delta(y-x)\,. \tag{3.234}$$

Here x is the usual Bjorken-x, eqn (3.39). At this point we pause to observe that the origin of this $\delta(y-x)$ factor is purely kinematical and therefore we may anticipate that all the one-loop corrections to the $\gamma^*\mathrm{q}\to\mathrm{q}'$ vertex will also be proportional to $\delta(y-x)$. Finally, following convention, we divide out a factor $4\pi e^2$ to obtain

$$\begin{aligned}\hat{H}_\Sigma^{(\gamma\mathrm{q})} \equiv \frac{1}{4\pi e^2}\int \mathrm{d}\Phi_1 \overline{\sum}\,|\mathcal{M}(\gamma^*\mathrm{q}\to\mathrm{q}')|^2 &= e_\mathrm{q}^2(1-\epsilon)\frac{Q^2}{2p\cdot q}\delta(y-x)\\ &= e_\mathrm{q}^2(1-\epsilon)x\delta(y-x)\,. \end{aligned}\tag{3.235}$$

The effect of the δ-function in eqn (3.235) is to select only those (anti)quarks with momentum fraction x. The presence of a δ-function also means that the partonic structure functions are formally distribution functions (in the mathematical sense) and so only have meaning when integrated with a sufficiently smooth ordinary function. The calculation of $\hat{H}_L^{(\gamma\mathrm{q})}$, eqn (3.229), is even easier as it vanishes. This follows because, assuming massless quarks so that $\not{q}u(q)=0$, we have

$$q_\mu \mathcal{M}^\mu(\gamma^{*\mu}\mathrm{q}\to\mathrm{q}') \propto \bar{u}(q')\not{q}u(q) = 0\,. \tag{3.236}$$

Given $\hat{H}_\Sigma^{(\gamma\mathrm{q})}$, together with $\hat{H}_L^{(\gamma\mathrm{q})}=0$, we use eqn (3.231) to obtain the lowest order electromagnetic structure functions

$$2xF_1^{(\gamma\mathrm{h})}(x) = F_2^{(\gamma\mathrm{h})}(x) = x\sum_{f=q,\bar{q}} e_f^2 f_\mathrm{h}(x)\,. \tag{3.237}$$

This confirms the Callan–Gross relationship between F_1 and F_2 which holds at lowest order for scattering off a spin-1/2 parton. As we will see at $\mathcal{O}(\alpha_s)$ and beyond $F_2(x) \neq 2xF_1(x)$ and the two structure functions can no longer be regarded as equivalent. In Ex. (3-24) the same result is obtained using the explicit hadron tensor. This also demonstrates, as one might expect of the parity conserving QED, that $F_3^{(\gamma\mathrm{h})}=0$.

This calculation has familiarized us with our notation and proved the Callan–Gross relationship between the structure functions appearing in the parton model at tree-level. We now wish to investigate how this picture changes with the inclusion of pQCD corrections.

3.6.3 *A heuristic treatment of factorization*

A number of processes contribute to the structure functions at $\mathcal{O}(\alpha_s)$. If the struck parton is a(n anti)quark we have the tree-level scattering $\gamma^*\mathrm{q}\to\mathrm{q}'\mathrm{g}$, the so-called QCD Compton process, shown in Fig. 3.22. To this must be added the interference between the tree-level and the one-loop corrections to the basic scattering $\gamma^*\mathrm{q}\to\mathrm{q}'$. The situation here is similar to that encountered in the treatment of the pQCD corrections to the process $\gamma^*\to\mathrm{q}\bar{\mathrm{q}}$; see Section 3.5.

There, both the ultraviolet and infrared singularities in the two sets of contributions cancelled to leave a finite result. Electroweak vector bosons do not directly couple to gluons. In order for gluons to contribute to the structure functions they must first split into a charged $q\bar{q}$-pair. Thus their contribution is at least $\mathcal{O}(\alpha_s)$. The lowest order contribution comes from the tree-level process $\gamma^* g \to q\bar{q}$, the so-called boson–gluon fusion process, shown in Fig. 3.23.

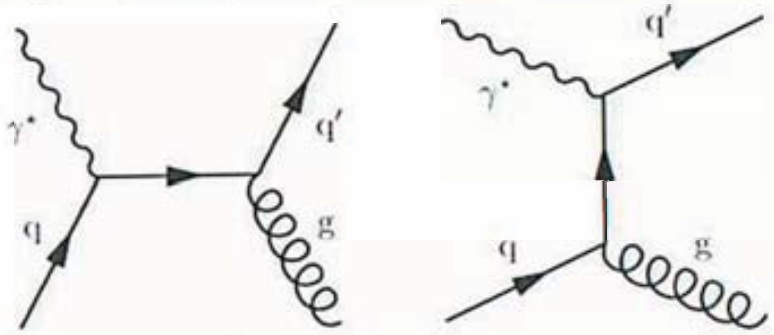

FIG. 3.22. The two diagrams contributing to the QCD Compton process, $\gamma^* q \to q' g$, at leading $\mathcal{O}(\alpha_s)$ and, reading right to left, $g\bar{q}' \to \gamma^* \bar{q}$

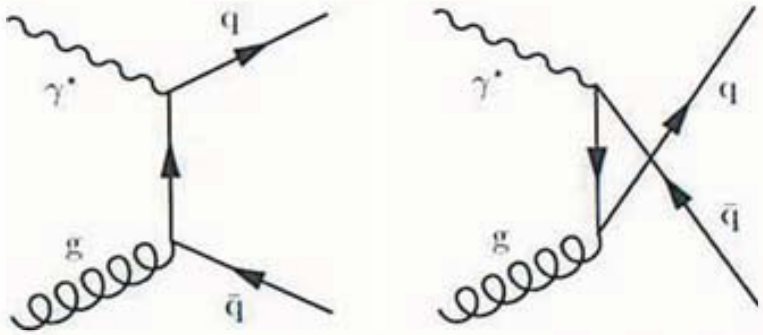

FIG. 3.23. The two diagrams contributing to the boson–gluon fusion process, $\gamma^* g \to q\bar{q}$, at leading $\mathcal{O}(\alpha_s)$ and, reading right to left, $q\bar{q} \to \gamma^* g$

We shall concentrate on the tree-level, $\mathcal{O}(\alpha_s)$, process $\gamma^* q \to q' g$ and in particular the partonic structure function $\hat{H}_\Sigma^{(\gamma q)}$, since this contains examples of all the singularities with which we shall have to deal. As noted, $\hat{H}_\Sigma^{(\gamma q)}$ is proportional to the matrix element squared for the hard subprocess. This can be obtained from that for the process $\gamma^* \to q\bar{q}g$, eqn (3.207), using crossing, eqn (3.95). That is, making the substitutions $q^\mu \to q'^\mu$, $\bar{q}^\mu \to -q^\mu$ and $Q^2 \to -Q^2$, reflecting the space-like nature of the photon's virtuality, one finds

$$\sum |\mathcal{M}(\gamma^* q \to q' g)|^2 = 8e^2 e_q^2 g_s^2 \mathrm{Tr}\left\{T^a T^a\right\} \left[\frac{g\cdot q'}{g\cdot q} + \frac{g\cdot q}{g\cdot q'} + \frac{Q^2(q\cdot q')}{(g\cdot q)(g\cdot q')}\right]. \tag{3.238}$$

The three terms correspond to emission of the gluon off the outgoing quark,

off the incoming quark and the interference between the two contributions. To obtain $\hat{H}_\Sigma^{(\gamma q)}$ we need to average over the incoming quark spins and colours, $2N_c$, divide by the conventional factor $4\pi e^2$ and integrate over the two-body phase space of the final state particles,

$$\begin{aligned}\hat{H}_\Sigma^{(\gamma q)} &= \frac{1}{4\pi e^2}\int d\Phi_2 \overline{\sum} |\mathcal{M}(\gamma^* q \to q'g)|^2 \\ &= 4e_q^2 \alpha_s C_F \int d\Phi_2 \left[\frac{g\cdot q'}{g\cdot q} + \frac{g\cdot q}{g\cdot q'} + \frac{Q^2(q\cdot q')}{(g\cdot q)(g\cdot q')}\right] . \end{aligned} \tag{3.239}$$

Here we used $\mathrm{Tr}\{T^a T^a\} = C_F N_c$. Looking at the propagators, $\propto [E_g(1-\cos\theta)]^{-1}$, we see that this expression has a number of singular regions; c.f. Section 3.3.2. There are collinear singularities when the gluon is emitted parallel to the incoming quark, $g\cdot q \to 0$, or the outgoing quark, $g\cdot q' \to 0$. There is also a soft singularity when the energy of the gluon vanishes. The collinear singularities are associated with the vanishing of the quark propagators just prior to or just after the interaction with the photon. Such a low-virtuality intermediate quark will travel a large distance, $x^\mu = k^\mu/k^2$, so that the gluon is emitted either well before or well after the hard subprocess. We may therefore anticipate that the initial state collinear singularity can be naturally associated with the incoming hadron and into which it might be absorbed. The final state collinear and soft gluon singularities both imply a zero mass particle in the final state,

$$\begin{aligned}\hat{s} &= (g+q')^2 = 2g\cdot q' \\ &= (q+q_\gamma)^2 = y 2p\cdot q_\gamma - Q^2 = Q^2\left(\frac{y}{x}-1\right) = Q^2\frac{(1-z)}{z} .\end{aligned} \tag{3.240}$$

In the second form we let the incoming quark carry a momentum fraction y, that is, $q^\mu = yp^\mu$ and we introduced $z = x/y$ where x has its usual meaning, eqn (3.39). Thus, $\hat{s} = 2g\cdot q' \to 0$ is equivalent to $Q^2(y/x-1) \to 0$ so that these singularities involve the kinematics of the lowest order hard scattering to which they must consequently be associated. They also raise the spectre of infrared singular cross sections.

Fortunately, for the analogous process $\gamma^* \to q\bar{q}g$ we learnt that including the contribution from the interference between the tree-level and one-loop corrections to the process $\gamma^* \to q\bar{q}$ ensured that all the singularities cancelled in the infrared safe total cross section, eqn (3.220); see Section 3.5. Hence we might expect that the singularities present in eqn (3.239) will cancel when we include the contribution coming from the interference between the tree-level and one-loop corrections to the process $\gamma^* q \to q'$. Unfortunately, in DIS the probing photon can tell the difference between the charged quark in a collinear qg-pair and a quark q with equal momentum. Thus, the equivalent cancellation for DIS is incomplete. In particular the final state collinear and soft gluon singularities cancel but the collinear singularity associated with the incoming quark remains. This removes the danger of a singular DIS cross section, provided we have a means of dealing with the remaining initial state singularity.

In view of the above discussion we will analyse the initial state, collinear singularity present in eqn (3.239). Equation (3.240) gives us one of the Lorentz invariants. To evaluate $g \cdot q$ and $q \cdot q'$ it is helpful to specialize to the C.o.M. frame. Here the momenta of the massless q, q′ and g can be written as

$$\begin{aligned} q^\mu &= \hat{p}_{\text{in}}(1,0,0,1) & \hat{p}_{\text{in}} &= \frac{(\hat{s}+Q^2)}{2\sqrt{\hat{s}}} \\ q'^\mu &= \hat{p}_{\text{out}}(1,-\sin\theta^\star,0,-\cos\theta^\star) & & \\ g^\mu &= \hat{p}_{\text{out}}(1,+\sin\theta^\star,0,+\cos\theta^\star) & \hat{p}_{\text{out}} &= \frac{\sqrt{\hat{s}}}{2}\,. \end{aligned} \tag{3.241}$$

These allow us to infer that

$$\begin{aligned} 2g\cdot q &= 2\frac{\sqrt{\hat{s}}}{2}\frac{(\hat{s}+Q^2)}{2\sqrt{\hat{s}}}(1-\cos\theta^\star) & 2q\cdot q' &= 2\frac{(\hat{s}+Q^2)}{2\sqrt{\hat{s}}}\frac{\sqrt{\hat{s}}}{2}(1+\cos\theta^\star) \\ &= \frac{Q^2}{2z}(1-\cos\theta^\star) & &= \frac{Q^2}{2z}(1+\cos\theta^\star)\,. \end{aligned} \tag{3.242}$$

The two-body phase space integral is given by eqn (C.21) with, for the moment, $\epsilon = 0$. In terms of these C.o.M. variables eqn (3.239) becomes

$$\begin{aligned} \hat{H}_\Sigma^{(\gamma q)} = 4e_q^2\alpha_s C_F \frac{1}{8\pi}\frac{\hat{p}_{\text{out}}}{\sqrt{\hat{s}}}\int_{-1}^{+1} \mathrm{d}\cos\theta^\star \\ \times\left[\frac{2(1-z)}{(1-\cos\theta^\star)} + \frac{(1-\cos\theta^\star)}{2(1-z)} + \frac{2z(1+\cos\theta^\star)}{(1-z)(1-\cos\theta^\star)}\right]\,. \end{aligned} \tag{3.243}$$

Referring to eqn (3.241) we see that the $\cos\theta^\star \to 1$ singularity in eqn (3.243) arises when the gluon direction approaches that of the incoming quark. The soft gluon and final state collinear singularities manifest themselves as the $z \to 1$ singularity, see eqn (3.240). Now, rather than work with $\cos\theta^\star$, we choose to use the transverse momentum of the gluon measured with respect to the incoming quark direction,

$$\begin{aligned} k_T^2 &= \hat{p}_{\text{out}}^2 \sin^2\theta^\star \\ &= \frac{Q^2}{4}\frac{(1-z)}{z}(1-\cos^2\theta^\star) \quad\Longrightarrow\quad \frac{\mathrm{d}k_T^2}{k_T^2} = -\frac{2\cos\theta^\star}{(1+\cos\theta^\star)}\frac{\mathrm{d}\cos\theta^\star}{(1-\cos\theta^\star)}\,. \end{aligned} \tag{3.244}$$

The limit $\cos\theta^\star \to 1$ now becomes $k_T^2 \to 0$. Making this change of variables in eqn (3.243) gives

$$\begin{aligned} &\hat{H}_\Sigma^{(\gamma q)} = \\ &e_q^2\frac{\alpha_s}{2\pi}C_F\int_{\kappa^2}^{Q^2\frac{(1-z)}{4z}}\frac{\mathrm{d}k_T^2}{k_T^2}\frac{2\cos\theta^\star}{(1+\cos\theta^\star)}\left[\frac{(1-z)^2+(1+\cos\theta^\star)z}{(1-z)} + \frac{1-\cos\theta^\star}{4(1-z)}\right]\,, \end{aligned} \tag{3.245}$$

where $\cos\theta^\star$ is now implicitly given in terms of k_T. Notice that we have introduced a cut-off, κ^2, on the transverse momentum in order to regulate the

collinear singularity. At small opening angles, $\cos\theta^* \to 1$, the virtuality of the intermediate quark, $2g\cdot q$ in eqn (3.242), and the gluon's transverse momentum, eqn (3.244), are related by $2(g\cdot q) = k_T^2/(1-z)$. Thus, κ^2 is also a lower bound on the minimum virtuality of the intermediate quark, equivalent to an upper bound on the distance it travels. This *ad hoc* prescription will be replaced by dimensional regularization in Section 3.6.4. Focussing on the collinear region we obtain

$$\tilde{H}_\Sigma^{(\gamma q)} = e_q^2 \frac{\alpha_s}{2\pi} C_F \left\{ \int_{\kappa^2}^{Q^2\frac{(1-z)}{4z}} \frac{dk_T^2}{k_T^2} \left(\frac{1+z^2}{1-z} \right) + R''(z) + \mathcal{O}(\kappa^2/Q^2) \right\} . \quad (3.246)$$

The final state, $z \to 1$, singularity is still present in this result. Invoking the $\mathcal{O}(\alpha_s)$ corrections to the $\gamma^* q \to q'$ vertex, which are proportional to $\delta(1-z)$, this singularity is removed. A more proper treatment would show us that the coefficient is actually a distribution,

$$\begin{aligned} \tilde{H}_\Sigma^{(\gamma q)} &= e_q^2 \frac{\alpha_s}{2\pi} C_F \left\{ \int_{\kappa^2}^{Q^2\frac{(1-z)}{4z}} \frac{dk_T^2}{k_T^2} \left[\frac{1+z^2}{(1-z)_+} + C_{qq}\delta(1-z) \right] + R'(z) \right\} \\ &\equiv e_q^2 \frac{\alpha_s}{2\pi} \left\{ P_{qq}^{(0)}(z) \ln\left(\frac{Q^2}{\kappa^2}\right) + R(z) \right\} . \end{aligned} \quad (3.247)$$

Here, we introduced $1/(1-z)_+$ as a shorthand for $(1/(1-z))_+$, where the plus-prescription is defined by

$$F(z)_+ = F(z) - \delta(1-z) \int_0^1 dy\, F(y) . \quad (3.248)$$

Distributions only make sense when integrated with a suitable smooth function. We typically encounter the plus-prescription in a situation such as

$$\int_x^1 dz\, g(z) \left[\frac{f(z)}{(1-z)} \right]_+ \equiv \int_x^1 dz \big[g(z) - g(1) \big] \frac{f(z)}{(1-z)} - g(1) \int_0^x dz \frac{f(z)}{(1-z)} \quad (3.249)$$

which is free of divergences provided $g(z)$, and $f(z)$, are non-singular.

The full calculation would also have given us the form of the unspecified coefficients C_{qq} and $R(z)$. Later we shall use a physical argument to extract $C_{qq} = 3/2$. Given C_{qq}, then eqn (3.247) fully specifies the regularized, lowest order, Altarelli–Parisi splitting function $P_{qq}^{(0)}(z)$, eqn (3.50). Finally, given a similar result for $\hat{H}_L^{(\gamma q)}$, which is non-singular, we can use eqn (3.231) to derive F_2 and F_1. Including the lowest order contribution, eqn (3.237), and, for simplicity omitting the sum over quark flavours, gives

$$\frac{F_2(x,Q^2;\kappa)}{x e_q^2} = \int_x^1 \frac{dz}{z} q\left(\frac{x}{z}\right) \left\{ \delta(1-z) + \frac{\alpha_s}{2\pi} \left[P_{qq}^{(0)}(z) \ln\left(\frac{Q^2}{\kappa^2}\right) + R_{qq}(z) \right] \right\}$$

$$= q(x) + \int_x^1 \frac{\mathrm{d}z}{z} q\left(\frac{x}{z}\right) \frac{\alpha_s}{2\pi} \left[P_{qq}^{(0)}(z) \ln\left(\frac{Q^2}{\kappa^2}\right) + R_{qq}(z) \right] . \quad (3.250)$$

In this expression we do not show explicitly any dependence on the renormalization scale μ_R which anyway does not enter at $\mathcal{O}(\alpha_s)$. Now, having identified and isolated the initial state singularity in F_2, we must decide how to deal with it.

Equation (3.250) exhibits a large logarithm coming from the collinear singularity which we have identified with long-distance physics. What we would like to do is to factorize eqn (3.250) in such a way that all long-distance physics is contained within the hadron specific p.d.f., whilst all short-distance physics is contained within a hard-subprocess specific coefficient function. In order to facilitate the separation of the long- and short-distance contributions we introduce a new factorization scale, μ_F, into eqn (3.250). Our aim is to move the logarithmic singularity into $q(x)$, but we are also free to move none, part or all of the finite term, R_{qq}, into $q(x)$. Reflecting this freedom we also introduce a finite, arbitrary function, $R_q^F(z)$, into eqn (3.250). The prescription for choosing R_q^F constitutes a factorization scheme. Introducing μ_F and R_q^F we rewrite eqn (3.250) as

$$\frac{F_2(x,Q^2;\kappa)}{xe_q^2} = q(x) + \int_x^1 \frac{\mathrm{d}z}{z} q\left(\frac{x}{z}\right) \frac{\alpha_s}{2\pi} \left[P_{qq}^{(0)}(z) \ln\left(\frac{\mu_F^2}{\kappa^2}\right) + R_q^F(z) \right] \quad (3.251)$$

$$+ \int_x^1 \frac{\mathrm{d}z}{z} q\left(\frac{x}{z}\right) \frac{\alpha_s}{2\pi} \left[P_{qq}^{(0)}(z) \ln\left(\frac{Q^2}{\mu_F^2}\right) + R_{qq}(z) - R_q^F(z) \right] .$$

This form suggests defining a factorization scale and scheme dependent p.d.f. which absorbs fully the collinear singularity

$$q^F(x,\mu_F^2,R_q^F;\kappa) = q(x) + \int_x^1 \frac{\mathrm{d}z}{z} q\left(\frac{x}{z}\right) \frac{\alpha_s}{2\pi} \left[P_{qq}^{(0)}(z) \ln\left(\frac{\mu_F^2}{\kappa^2}\right) + R_q^F(z) \right] . \quad (3.252)$$

The second term on the right-hand side of eqn (3.252) is logarithmically divergent as $\kappa^2 \to 0$, but we expect the p.d.f. on the left-hand side to be finite. In an argument that is very reminiscent of renormalization we claim that the 'bare' p.d.f., $q(x)$, contains a compensating logarithmic divergence in κ^2 in just such a way that their sum is finite and independent of κ^2 in the $\kappa^2 \to 0$ limit.

$$q^F(x,\mu_F^2,R_q^F) = q(x;\kappa) + \int_x^1 \frac{\mathrm{d}z}{z} q\left(\frac{x}{z};\kappa\right) \frac{\alpha_s}{2\pi} \left[P_{qq}^{(0)}(z) \ln\left(\frac{\mu_F^2}{\kappa^2}\right) + R_q^F(z) \right] . \quad (3.253)$$

This 'physical' p.d.f. is now finite and so we may drop any reference to the κ regulator. In terms of eqn (3.253) we can rewrite eqn (3.250) to $\mathcal{O}(\alpha_s)$ as

$$\frac{F_2(x,Q^2)}{xe_q^2} = q^F(x,\mu_F^2,R_q^F)$$

$$+ \int_x^1 \frac{\mathrm{d}z}{z} q^F\left(\frac{x}{z},\mu_F,R_q^F\right) \frac{\alpha_s}{2\pi} \left[P_{qq}^{(0)}(z) \ln\left(\frac{Q^2}{\mu_F^2}\right) + R_{qq}(z) - R_q^F(z) \right]$$

$$= \int_x^1 \frac{\mathrm{d}z}{z} q^F\left(\frac{x}{z}, \mu_F, R_{\mathrm{q}}^F\right) \tag{3.254}$$
$$\times \left\{\delta(1-z) + \frac{\alpha_{\mathrm{s}}}{2\pi}\left[P_{\mathrm{qq}}^{(0)}(z) \ln\left(\frac{Q^2}{\mu_F^2}\right) + R_{\mathrm{qq}}(z) - R_{\mathrm{q}}^F(z)\right]\right\} .$$

The right-hand side of these equations appears to depend on μ_F and R_{q}^F. However, all dependence on μ_F and R_{q}^F cancels to the calculated order, $\mathcal{O}(\alpha_{\mathrm{s}})$, and any dependence at $\mathcal{O}(\alpha_{\mathrm{s}}^2)$ would also cancel if we included the neglected $\mathcal{O}(\alpha_{\mathrm{s}}^2)$ terms in eqn (3.254). As the original expression, eqn (3.250), makes clear, the physical $F_2(x, Q^2)$ is independent of both the arbitrary factorization scale and scheme. What we have gained, as the second form in eqn (3.254) makes clear, is that all the long-distance behaviour is contained within the finite p.d.f. whilst the process dependent coefficient function only contains short-distance physics. The significance of μ_F is that it delimits the boundary between short, $Q > \mu_F$, and long, $Q < \mu_F$, distance physics.

In eqn (3.254) both the choice of μ_F and R_{q}^F are arbitrary. For the scale, choosing $\mu_F = Q$ is clearly advantageous, as it yields the simple expression

$$\frac{F_2(x, Q^2)}{x e_{\mathrm{q}}^2} = \int_x^1 \frac{\mathrm{d}z}{z} q^F\left(\frac{x}{z}, Q^2, R_{\mathrm{q}}^F\right)\left\{\delta(1-z) + \frac{\alpha_{\mathrm{s}}}{2\pi}\left[R_{\mathrm{qq}}(z) - R_{\mathrm{q}}^F(z)\right]\right\} . \tag{3.255}$$

The choice of which finite terms from R_{qq} in eqn (3.250) to absorb into R_{q}^F defines the factorization scheme. Two schemes are in popular usage. In the (modified) minimal subtraction scheme only the singular term is absorbed into the parton density function, that is, $R_{\mathrm{q}}^{\overline{\mathrm{MS}}} = 0$. In the DIS scheme all of the finite term, together with the singular term, are absorbed into the p.d.f., that is, $R_{\mathrm{q}}^{\mathrm{DIS}} = R_{\mathrm{qq}}$. This scheme results in a particularly simple form for the structure function,

$$F_2(x, Q^2) = x e_{\mathrm{q}}^2 q^{\mathrm{DIS}}(x, Q^2) . \tag{3.256}$$

The above reasoning which leads to factorization applies equally well to $F_1(x, Q^2)$. One might therefore be tempted to define DIS p.d.f.s according to the equivalent of eqn (3.256) for F_1. However, you should be aware that at $\mathcal{O}(\alpha_{\mathrm{s}})$ $F_2 \neq 2xF_1$ and the two schemes will not be equivalent. Equation (3.256) is the conventional definition. It is significant that $F_L = F_2/(2x) - F_1$ is infrared finite and in particular contains no collinear, initial state singularities. This means that the same redefinition of the p.d.f.s used to render F_2 finite will also render F_1 finite. Although we will not demonstrate it, this is also true for F_3.

As the discussion of factorization schemes makes clear, the p.d.f.s should not be regarded as physical quantities, since they depend on the scheme used to define them. However, when convoluted with the appropriate coefficient function, eqn (3.254), they give rise to physical, measurable structure functions.

The crucial point to remember with regard to factorization schemes is that the same scheme must be used for both the p.d.f.s and the coefficient functions. If this is not the case then the cancellation implicit in eqn (3.254) will not

occur and it will not be equivalent to eqn (3.250). Since the p.d.f.s in the $\overline{\text{MS}}$ scheme carry no information that is specific to lepton–hadron scattering, they are easier to use in applications to hadron–hadron scattering and thus often are the preferred choice. If DIS p.d.f.s were used to describe another process, then the new coefficient functions, describing that process's short-distance physics, would have to include a compensating factor of R_q^{DIS} taken from the unrelated DIS process.

3.6.4 *DIS at next-to-leading order*

The above discussion of factorization avoided technical details so as to concentrate on the core ideas. We now explicitly carry out this process for the case of DIS. We will use dimensional regularization throughout to deal with all the singularities.

3.6.4.1 *The process $\gamma^* q \to q'$ at $\mathcal{O}(\alpha_s)$* There are two contributions to the process $\gamma^* q \to q'$ which need to be considered at $\mathcal{O}(\alpha_s)$. The real, tree-level scattering $\gamma^* q \to q'g$, Fig. 3.22, and the virtual, one-loop corrections to $\gamma^* q \to q'$. These are both very similar to the pQCD corrections to the process $\gamma^* \to q\bar{q}$ which we have already calculated; see Section 3.5. In fact, to obtain $-\eta_{\mu\nu}\tilde{H}^{\mu\nu}$ we can use crossing, eqn (3.95), for the required matrix elements without any further calculation. The D-dimensional amplitude squared for the process $\gamma^* \to q\bar{q}g$ is given by eqn (3.207). To obtain the amplitude squared for the process $\gamma^* q \to q'g$ we need to make the substitutions $\bar{q}^\mu \to -q^\mu$, relabel the original q as q′, replace Q^2 by $-Q^2$ and add an overall minus sign since we now have a closed quark loop. This gives

$$\sum |\mathcal{M}(\gamma^* q \to q'g)|^2 = e^2 e_q^2 (g_s \mu^\epsilon)^2 C_F N_c 2\text{Tr}\{\mathbf{1}\}(1-\epsilon) \times \left\{ (1-\epsilon)\left[\frac{g\cdot q}{g\cdot q'} + \frac{g\cdot q'}{g\cdot q}\right] + \frac{Q^2(q\cdot q')}{(g\cdot q)(g\cdot q')} + 2\epsilon \right\}. \tag{3.257}$$

Here we have replaced $\text{Tr}\{T^a T^a\}$ by $C_F N_c$. As before we chose to use the C.o.M. variables

$$2g\cdot q' = \frac{Q^2}{z}(1-z)\,, \quad 2g\cdot q = \frac{Q^2}{z}v \quad \text{and} \quad 2q\cdot q' = \frac{Q^2}{z}(1-v)\,, \tag{3.258}$$

which differ from eqn (3.240) and eqn (3.242) only in the replacement of $\cos\theta^*$ by $v = (1+\cos\theta^*)/2$. In terms of these variables eqn (3.257) becomes

$$\sum |\mathcal{M}(\gamma^* q \to q'g)|^2 = e^2 e_q^2 (g_s \mu^\epsilon)^2 C_F N_c 2\text{Tr}\{\mathbf{1}\}(1-\epsilon) \times \left\{ (1-\epsilon)\left[\frac{v}{(1-z)} + \frac{(1-z)}{v}\right] + \frac{2z}{(1-z)}\frac{(1-v)}{v} + 2\epsilon \right\}. \tag{3.259}$$

To this expression we should add an average over the spin and colour of the incoming quark, $2N_c$, divide by the conventional factor $4\pi e^2$ and include the two-body phase space integral, eqn (C.21). This gives

$$
\begin{aligned}
&\hat{H}^{(\gamma q)}_{\Sigma,R} \\
&= \frac{1}{4\pi e^2}\overline{\sum}|\mathcal{M}(\gamma^* q \to q' g)|^2 \qquad (3.260)\\
&= e_q^2 \alpha_s C_F 4 \frac{1}{4\pi}\frac{\hat{p}_{out}}{\sqrt{\hat{s}}}\left(\frac{\pi\mu^2}{\hat{p}^2_{out}}\right)^{\epsilon}\frac{(1-\epsilon)}{\Gamma(1-\epsilon)} \\
&\quad \times \int_0^1 dv\, v^{-\epsilon}(1-v)^{-\epsilon}\left\{(1-\epsilon)\left[\frac{v}{(1-z)}+\frac{(1-z)}{v}\right]+\frac{2z}{(1-z)}\frac{(1-v)}{v}+2\epsilon\right\}.
\end{aligned}
$$

The v-integral is of the standard Euler β-function type, eqn (C.27), and is evaluated to yield

$$
\begin{aligned}
&\int_0^1 dv\, v^{-\epsilon}(1-v)^{-\epsilon}\{\cdots\} \\
&= \left\{(1-\epsilon)\left[\frac{1}{(1-z)}\frac{\Gamma(2-\epsilon)\Gamma(1-\epsilon)}{\Gamma(3-2\epsilon)}+(1-z)\frac{\Gamma(-\epsilon)\Gamma(1-\epsilon)}{\Gamma(1-2\epsilon)}\right]\right. \\
&\quad \left.+\frac{2z}{(1-z)}\frac{\Gamma(-\epsilon)\Gamma(2-\epsilon)}{\Gamma(2-2\epsilon)}+2\epsilon\frac{\Gamma^2(1-\epsilon)}{\Gamma(2-2\epsilon)}\right\} \\
&= \frac{\Gamma^2(1-\epsilon)}{\Gamma(1-2\epsilon)}\left\{-\frac{(1-\epsilon)}{\epsilon}\left[(1-z)+\frac{1}{(1-2\epsilon)}\frac{2z}{(1-z)}\right]\right. \\
&\qquad \left.+\frac{1}{2(1-z)}\frac{(1-\epsilon)}{(1-2\epsilon)}+\frac{2\epsilon}{(1-2\epsilon)}\right\} \\
&= \frac{\Gamma^2(1-\epsilon)}{\Gamma(1-2\epsilon)}\left\{-\frac{1}{\epsilon}\frac{1+z^2}{(1-z)}-\frac{3}{2}\frac{1}{(1-z)}+3-z+\left(6-\frac{7}{2(1-z)}\right)\epsilon+\mathcal{O}(\epsilon^2)\right\}.
\end{aligned}
\qquad (3.261)
$$

The simplifications in the second line have been achieved using eqn (C.25) whilst in the third line we have expanded out the expression in curly braces. Substituting eqn (3.261) into eqn (3.260) gives

$$
\begin{aligned}
\hat{H}^{(\gamma q)}_{\Sigma,R} &= e_q^2\frac{\alpha_s}{2\pi}C_F\left(\frac{4\pi\mu^2}{Q^2}\frac{z}{(1-z)}\right)^{\epsilon}(1-\epsilon)\frac{\Gamma(1-\epsilon)}{\Gamma(1-2\epsilon)} \\
&\quad \times\left\{-\frac{1}{\epsilon}\frac{1+z^2}{(1-z)}-\frac{3}{2}\frac{1}{(1-z)}+3-z+\left(6-\frac{7}{2(1-z)}\right)\epsilon+\mathcal{O}(\epsilon^2)\right\}.
\end{aligned}
\qquad (3.262)
$$

Identifying the $\epsilon \to 0$ limit in eqn (3.262) is a little tricky but using the identity

$$
\frac{z^{\epsilon}}{(1-z)^{1+\epsilon}} = -\frac{1}{\epsilon}\delta(1-z)+\frac{1}{(1-z)_+}-\epsilon\left(\frac{\ln(1-z)}{1-z}\right)_+ +\epsilon\frac{\ln z}{1-z}, \qquad (3.263)
$$

see Ex. (3-26), we finally obtain

$$\hat{H}^{(\gamma q)}_{\Sigma,R} = e_q^2 \frac{\alpha_s}{2\pi} C_F \left(\frac{4\pi\mu^2}{Q^2}\right)^\epsilon (1-\epsilon)\frac{\Gamma(1-\epsilon)}{\Gamma(1-2\epsilon)} \left\{ \left(\frac{2}{\epsilon^2}+\frac{3}{2\epsilon}+\frac{7}{2}\right)\delta(1-z) - \frac{1}{\epsilon}\frac{1+z^2}{(1-z)_+} + (1+z^2)\left(\frac{\ln(1-z)}{1-z}\right)_+ - \frac{1+z^2}{(1-z)}\ln z - \frac{3}{2}\frac{1}{(1-z)_+} + 3 - z + \mathcal{O}(\epsilon)\right\} . \tag{3.264}$$

The double pole, $1/\epsilon^2$, is due to the soft gluon singularity.

A second contribution to the total structure function at $\mathcal{O}(\alpha_s)$ comes from the interference between the process $\gamma^* q \to q'$ at one-loop and at tree-level. The structures of the one-loop vertex and tree-level diagram are the same, so that we can combine them into an effective vertex

$$\begin{aligned} i\Gamma^\mu &= -i e e_q \gamma^\mu \left[1 - \frac{\alpha_s}{4\pi} C_F \left(\frac{4\pi\mu^2}{Q^2}\right)^\epsilon \frac{\Gamma(1+\epsilon)\Gamma^2(1-\epsilon)}{\Gamma(1-2\epsilon)}\left(\frac{2}{\epsilon^2}+\frac{3}{\epsilon}+8\right)\right] \\ &= -i e e_q \gamma^\mu \left[1 - \frac{\alpha_s}{4\pi} C_F \left(\frac{4\pi\mu^2}{Q^2}\right)^\epsilon \frac{\Gamma(1-\epsilon)}{\Gamma(1-2\epsilon)}\left(\frac{2}{\epsilon^2}+\frac{3}{\epsilon}+8+\frac{\pi^2}{3}+\mathcal{O}(\epsilon)\right)\right] . \end{aligned} \tag{3.265}$$

Here, the one-loop contribution has been inferred from eqn (3.219), the only difference being the absence of the $(-1)^\epsilon$ factor, reflecting the space-like nature of q_γ^μ in DIS. In the second line we used $\Gamma(1+\epsilon)\Gamma(1-\epsilon) = 1 + (\pi^2/6)\epsilon^2 + \mathcal{O}(\epsilon^4)$. Equation (3.265) has infrared singularities but is ultraviolet finite. The calculation of this additional contribution to $\hat{H}^{(\gamma q)}_\Sigma$ is straightforward, giving

$$\begin{aligned} \hat{H}^{(\gamma q)}_{\Sigma,V} &= e_q^2(1-\epsilon)\delta(1-z) \\ &\quad \times \left\{1 - 2\frac{\alpha_s}{4\pi} C_F \left(\frac{4\pi\mu^2}{Q^2}\right)^\epsilon \frac{\Gamma(1-\epsilon)}{\Gamma(1-2\epsilon)}\left(\frac{2}{\epsilon^2}+\frac{3}{\epsilon}+8+\frac{\pi^2}{3}+\mathcal{O}(\epsilon)\right)\right\} . \end{aligned} \tag{3.266}$$

Adding eqn (3.264) and (3.266) together we see that the $1/\epsilon^2$ terms, the soft gluon pole, cancel,

$$\begin{aligned} \hat{H}^{(\gamma q)}_\Sigma = e_q^2 \frac{\alpha_s}{2\pi} C_F (1-\epsilon) \Bigg\{ &- \left[\frac{1+z^2}{(1-z)_+} + \frac{3}{2}\delta(1-z)\right] \frac{1}{\epsilon}\frac{\Gamma(1-\epsilon)}{\Gamma(1-2\epsilon)}\left(\frac{4\pi\mu^2}{Q^2}\right)^\epsilon \\ &+ (1+z^2)\left(\frac{\ln(1-z}{1-z}\right)_+ - \frac{1+z^2}{1-z}\ln z - \frac{3}{2}\frac{1}{(1-z)_+} \\ &+ 3 - z - \left(\frac{9}{2}+\frac{\pi^2}{3}\right)\delta(1-z)\Bigg\} . \end{aligned} \tag{3.267}$$

The remaining $1/\epsilon$ pole is associated with the collinear singularity for gluon emission off the incoming quark, its coefficient is the regularized, one-loop, Altarelli–Parisi splitting function

$$P_{\mathrm{qq}}^{(0)}(z) = C_F\left[\frac{1+z^2}{(1-z)_+} + \frac{3}{2}\delta(1-z)\right] = C_F\left(\frac{1+z^2}{1-z}\right)_+ . \tag{3.268}$$

This calculation supplies us with the value of $C_{\mathrm{qq}} = 3/2$ in eqn (3.247).

We also need to calculate the longitudinal part of the hadronic tensor. This is particularly easy to $\mathcal{O}(\alpha_s)$ since many of the potential contributions vanish in the massless quark limit. We have already seen, in eqn (3.236), that the tree-level diagram, and by virtue of eqn (3.265) its one-loop virtual correction, give no contribution. This implies that the longitudinal structure function, $F_L \propto H_L$, is at least $\mathcal{O}(\alpha_s)$. Turning to the $\mathcal{O}(\alpha_s)$ tree-level contribution and again assuming massless quarks, so that $\not{q}u(q) = 0$, we have

$$\begin{aligned} q_\mu \mathcal{M}(\gamma^{*\mu}\mathrm{q} \to \mathrm{q}'\mathrm{g}) &\propto \bar{u}(q')\left[\gamma_\sigma \frac{(\not{q}' + \not{g})}{(q'+g)^2}\not{\epsilon} + \not{\epsilon}\frac{(\not{q} - \not{g})}{(q-g)^2}\gamma_\sigma\right] u(q)\epsilon^\sigma(g)^* \\ &\propto \bar{u}(q')\frac{\not{\epsilon}\not{g}}{2q\cdot g}\gamma_\sigma u(q)\epsilon^\sigma(g)^* . \end{aligned} \tag{3.269}$$

Thus, the diagram describing gluon radiation off the scattered quark gives no contribution, leaving only the diagram describing gluon radiation off the incoming quark. Squaring this diagram and summing over spins, where we can use $-\eta^{\sigma\sigma'}$ for the lone gluon's polarization tensor, gives

$$\begin{aligned} \sum |q_\mu \mathcal{M}(\gamma^{*\mu}\mathrm{q} \to \mathrm{q}'\mathrm{g})|^2 &= -e^2 e_{\mathrm{q}}^2 (g_s\mu^\epsilon)^2 C_F N_c \frac{1}{(2q\cdot g)^2}\mathrm{Tr}\left\{\not{q}'\not{\epsilon}\not{g}\gamma_\sigma\not{\epsilon}\gamma^\sigma\not{g}\not{q}\right\} \\ &= e^2 e_{\mathrm{q}}^2 (g_s\mu^\epsilon)^2 C_F N_c \frac{1}{(2q\cdot g)^2} 2(1-\epsilon)\mathrm{Tr}\left\{\not{q}'\not{\epsilon}\not{g}\not{\epsilon}\not{g}\not{q}\right\} \\ &= e^2 e_{\mathrm{q}}^2 (g_s\mu^\epsilon)^2 C_F N_c \frac{1}{2q\cdot g} 2(1-\epsilon)\mathrm{Tr}\left\{\not{q}'\not{\epsilon}\not{g}\not{q}\right\} \\ &= e^2 e_{\mathrm{q}}^2 (g_s\mu^\epsilon)^2 C_F N_c 2(1-\epsilon)\mathrm{Tr}\left\{\not{q}'\not{q}\right\} \\ &= e^2 e_{\mathrm{q}}^2 (g_s\mu^\epsilon)^2 C_F N_c (1-\epsilon) 2q'\cdot q\,\mathrm{Tr}\left\{\mathbf{1}\right\} . \end{aligned} \tag{3.270}$$

Here, we have used the trick in Ex. (3-19) and repeatedly used $\not{g}\not{q} = 2g\cdot q - \not{q}\not{g}$ together with $\not{q}\not{q} = q^2 = 0$. The result is non-zero and free of singularities and so we need not have used a regulator. Next, we average over the incoming quark's spin and colour polarizations, $2N_c$, use $\mathrm{Tr}\{\mathbf{1}\} = 4$, adopt the choice of variables in eqn (3.242) and include the integral over two-body phase space, eqn (C.20), to obtain

$$\begin{aligned} \hat{H}_L^{(\gamma\mathrm{q})} &= \frac{1}{4\pi e^2}\int \mathrm{d}\Phi_2 \overline{\sum} |q_\mu \mathcal{M}(\gamma^{*\mu}\mathrm{q} \to \mathrm{q}'\mathrm{g})|^2 \\ &= \frac{1}{2\pi} e_{\mathrm{q}}^2 (g_s\mu^\epsilon)^2 C_F \frac{Q^2}{z}(1-\epsilon)\frac{1}{4\pi}\frac{\hat{p}_{\mathrm{out}}}{\sqrt{\hat{s}}}\left(\frac{\pi}{\hat{p}_{\mathrm{out}}^2}\right)^\epsilon \frac{1}{\Gamma(1-\epsilon)}\int_0^1 \mathrm{d}v\, v^{-\epsilon}(1-v)^{1-\epsilon} \\ &= \frac{1}{4} e_{\mathrm{q}}^2 \frac{\alpha_s}{2\pi} C_F \frac{Q^2}{z}\left(\frac{4\pi\mu^2}{Q^2}\frac{z}{1-z}\right)^\epsilon \frac{\Gamma(2-\epsilon)}{\Gamma(2-2\epsilon)} \end{aligned}$$

$$= \frac{1}{4} e_q^2 \frac{\alpha_s}{2\pi} C_F \frac{Q^2}{z} + \mathcal{O}(\epsilon) \,. \tag{3.271}$$

Given eqns (3.267) and (3.271) we can convolute them with the p.d.f. to reconstruct H_Σ and H_L and hence obtain the $\mathcal{O}(\alpha_s)$ (anti)quark's contribution to F_2 and F_1, c.f. eqn (3.231), as

$$\begin{aligned}
\frac{F_2^{\gamma q}(x)}{x e_q^2} &= \frac{\alpha_s}{2\pi} \int_x^1 \frac{dz}{z} q\left(\frac{x}{z}\right) \left\{ -P_{qq}^{(0)}(z) \frac{1}{\epsilon} \frac{\Gamma(1-\epsilon)}{\Gamma(1-2\epsilon)} \left(\frac{4\pi\mu^2}{Q^2}\right)^\epsilon \right. \\
&\qquad + C_F \left[(1+z^2) \left(\frac{\ln(1-z)}{1-z} \right)_+ - \frac{1+z^2}{(1-z)} \ln z \right. \\
&\qquad \left. \left. - \frac{3}{2} \frac{1}{(1-z)_+} + 3 + 2z - \left(\frac{9}{2} + \frac{\pi^2}{2} \right) \delta(1-z) \right] \right\} \\
&= \frac{\alpha_s}{2\pi} \int_x^1 \frac{dz}{z} q\left(\frac{x}{z}\right) \left\{ -P_{qq}^{(0)}(z) \left[\frac{1}{\epsilon} - \gamma_E + \ln(4\pi) - \ln\left(\frac{Q^2}{\mu^2}\right) \right] \right. \\
&\qquad \left. + C_F \left[\frac{1+z^2}{1-z} \left(\ln\left(\frac{1-z}{z}\right) - \frac{3}{4} \right) + \frac{5z+9}{4} \right]_+ \right\} \\
F_1^{\gamma q}(x) &= \frac{F_2^{\gamma q}(x)}{2x} - e_q^2 \frac{\alpha_s}{2\pi} \int_x^1 \frac{dz}{z} q\left(\frac{x}{z}\right) C_F z \,.
\end{aligned} \tag{3.272}$$

In the second expression for F_2 we have expanded out the coefficient of the splitting function and introduced a more compact form for the remainder term. The $1/\epsilon$ pole naturally arises in the combination Δ_ϵ, eqn (C.16). If we add in the leading order result, eqn (3.237), then eqn (3.272) takes the form of eqn (3.250) with ϵ acting as regulator. If the factorization procedure removes just the $1/\epsilon$ term we have the minimal subtraction scheme, if it removes the additional terms, Δ_ϵ, we have the modified minimal subtraction scheme, $\overline{\text{MS}}$. In the DIS scheme both the Δ_ϵ and finite terms are removed.

3.6.4.2 *The $\mathcal{O}(\alpha_s)$ process $\gamma^* g \to q\bar{q}$* The calculation of the terms $-\eta_{\mu\nu}\hat{H}^{\mu\nu}$ and $g_\mu g_\nu \hat{H}^{\mu\nu}$ for the process $\gamma^* g \to q\bar{q}$ follows the same lines as that for $\gamma^* q \to q' g$ but is a little simpler in practice due to the lack of soft gluon singularities. Here, we just quote the results and leave their computation to the adventurous/diligent reader; see Ex. (3-27).

$$\begin{aligned}
\hat{H}_\Sigma^{(\gamma g)} &\equiv -\eta_{\mu\nu}\hat{H}^{\mu\nu} = 2e_q^2 \frac{\alpha_s}{2\pi} T_F \left[z^2 + (1-z)^2 \right] \\
&\qquad \times \left\{ -\frac{1}{\epsilon} \left(\frac{4\pi\mu^2}{Q^2} \right)^\epsilon \frac{\Gamma(1-\epsilon)}{\Gamma(1-2\epsilon)} + \ln\left(\frac{1-z}{z}\right) + \mathcal{O}(\epsilon) \right\} \\
\hat{H}_L^{(\gamma g)} &\equiv g_\mu g_\nu \hat{H}^{\mu\nu} = e_q^2 \frac{\alpha_s}{2\pi} T_F Q^2 \frac{(1-z)}{z} + \mathcal{O}(\epsilon)
\end{aligned} \tag{3.273}$$

Using eqn (3.231) applied to the above results, which contain both the quark and antiquark terms, we obtain the $\mathcal{O}(\alpha_s)$ gluon's contribution to F_2 and F_1.

$$\frac{F_2^{\gamma g}}{x} = \frac{\alpha_s}{2\pi} T_F \sum_q e_q^2 \int_x^1 \frac{dz}{z} g\left(\frac{x}{z}\right)$$
$$\times \left\{ \frac{[z^2 + (1-z)^2]}{(1-\epsilon)} \left[-\frac{1}{\epsilon} \left(\frac{4\pi\mu^2}{Q^2} \right)^{\epsilon} \frac{\Gamma(1-\epsilon)}{\Gamma(1-2\epsilon)} + \ln\left(\frac{1-z}{z}\right) \right] + 6z(1-z) \right\}$$
$$= \frac{\alpha_s}{2\pi} \sum_q e_q^2 \int_x^1 \frac{dz}{z} g\left(\frac{x}{z}\right) \left\{ -P_{qg}^{(0)}(z) \left[\Delta_\epsilon - \ln\left(\frac{Q^2}{\mu^2}\right) \right] \right.$$
$$\left. + T_F \left[[z^2 + (1-z)^2] \ln\left(\frac{1-z}{z}\right) - 1 + 8z(1-z) \right] \right\}$$
$$F_1^{\gamma g} = \frac{F_2^{\gamma g}}{2x} - \frac{\alpha_s}{2\pi} T_F \sum_q e_q^2 \int_x^1 \frac{dz}{z} g\left(\frac{x}{z}\right) 4z(1-z) \,. \tag{3.274}$$

3.6.4.3 *The combined results for the $\mathcal{O}(\alpha_s)$ DIS structure functions* The above results, eqns (3.272) and (3.274), can be combined to give the NLO formula for $F_1^{(\gamma h)}$ and $F_2^{(\gamma h)}$. In the modified minimal subtraction, $\overline{\text{MS}}$, scheme we have

$$\frac{F_{1,2}^{(Vh)}}{\frac{1}{2}, x}(x, Q^2) =$$
$$\int_x^1 \frac{dz}{z} \sum_{f=q,\bar{q}} g_{Vf}^2 \left\{ f^{\overline{\text{MS}}}\left(\frac{x}{z}, \mu_F^2\right) \left[\delta(1-z) + \frac{\alpha_s}{2\pi} \left(P_{qq}^{(0)}(z) \ln \frac{Q^2}{\mu_F^2} + C_{1,2}^{(Vq)}(z) \right) \right] \right.$$
$$\left. + g^{\overline{\text{MS}}}\left(\frac{x}{z}, \mu_F^2\right) \frac{\alpha_s}{2\pi} \left(P_{qg}^{(0)}(z) \ln \frac{Q^2}{\mu_F^2} + C_{1,2}^{(Vg)}(z) \right) \right\}$$
$$F_3^{(Vh)}(x, Q^2) =$$
$$\int_x^1 \frac{dz}{z} \sum_{f=q,\bar{q}} g_{Vf}^2 \left\{ f^{\overline{\text{MS}}}\left(\frac{x}{z}, \mu_F^2\right) \left[\delta(1-z) + \frac{\alpha_s}{2\pi} \left(P_{qq}^{(0)}(z) \ln \frac{Q^2}{\mu_F^2} + C_3^{(Vq)}(z) \right) \right] \right\} \tag{3.275}$$

where we have also included the $\overline{\text{MS}}$ expression for $F_3^{(Vh)}$. In eqn (3.275) g_{Vf} gives the normalized strength of the exchanged gauge boson's coupling to the (anti)quark, for example $g_{\gamma q} = e_q$, whilst the coefficient functions are given by

$$C_1^{(Vq)} = \frac{1}{2} C_2^{(Vq)} - C_F z$$
$$C_2^{(Vq)} = C_F \frac{1}{2} \left[\frac{1+z^2}{1-z} \left(\ln\left(\frac{1-z}{z}\right) - \frac{3}{4} \right) + \frac{9+5z}{4} \right]_+$$
$$C_3^{(Vq)} = C_2^{(Vq)} - C_F(1+z) \tag{3.276}$$
$$C_1^{(Vg)} = \frac{1}{2} C_2^{(Vg)} - T_F 4z(1-z)$$

$$C_2^{(Vg)} = T_F z\left[[z^2+(1-z)^2]\ln\frac{1-z}{z} - 1 + 8z(1-z)\right]$$
$$C_3^{(Vg)} = 0\,.$$

Charge conjugation invariance implies $C_i^{(Vq)}(z) = C_i^{(\bar{V}q)}(z)$. We can also infer the form of the quark p.d.f.s from our results for F_2. In the $\overline{\rm MS}$ scheme the NLO (anti)quark, and for completeness the gluon, p.d.f.s are given by

$$\begin{aligned} q^{\overline{\rm MS}}(x,\mu_F^2) &= \int_x^1 \frac{{\rm d}z}{z}\left\{q\left(\frac{x}{z},\epsilon\right)\left(\delta(1-z) - \frac{\alpha_s}{2\pi}P_{qq}^{(0)}(z)\left[\Delta_\epsilon - \ln\frac{\mu_F^2}{\mu^2}\right]\right)\right. \\ &\qquad \left. - g\left(\frac{x}{z},\epsilon\right)\frac{\alpha_s}{2\pi}P_{gq}^{(0)}(z)\left[\Delta_\epsilon - \ln\frac{\mu_F^2}{\mu^2}\right]\right\} \\ &= \sum_{f=q,g}\int_x^1 \frac{{\rm d}z}{z} f\left(\frac{x}{z},\epsilon\right)\left[\delta(1-z)\delta_{qf} - \frac{\alpha_s}{2\pi}P_{qf}^{(0)}(z)\frac{1}{\epsilon}\left(\frac{4\pi\mu^2}{\mu_F^2 e^{\gamma_E}}\right)^\epsilon\right] \\ g^{\overline{\rm MS}}(x,\mu_F^2) &= \sum_{f=q,\bar{q},g}\int_x^1 \frac{{\rm d}z}{z} f\left(\frac{x}{z},\epsilon\right)\left[\delta(1-z)\delta_{gf} - \frac{\alpha_s}{2\pi}P_{gf}^{(0)}(z)\frac{1}{\epsilon}\left(\frac{4\pi\mu^2}{\mu_F^2 e^{\gamma_E}}\right)^\epsilon\right]. \end{aligned} \tag{3.277}$$

In the deep inelastic scattering, DIS, scheme F_2 is given by

$$F_2^{(Vh)}(x,Q^2) = \sum_{f=q,\bar{q}} g_{Vf}^2\left\{f^{\rm DIS}(x,\mu_F^2) + \frac{\alpha_s}{2\pi}\int_0^1\frac{{\rm d}z}{z}f^{\rm DIS}\left(\frac{x}{z},\mu_F^2\right)P_{qq}^{(0)}(z)\ln\left(\frac{Q^2}{\mu_F^2}\right)\right\}\,. \tag{3.278}$$

which is exact to all orders. At $\mathcal{O}(\alpha_s)$ F_1 and F_3 are given by eqn (3.275) with modified coefficient functions,

$$\begin{aligned} C_1^{(Vq)}(z) &= -C_F z \\ C_3^{(Vq)}(z) &= -C_F(1+z) \\ C_1^{(Vg)}(z) &= -T_F 4z(1-z)\,. \end{aligned} \tag{3.279}$$

All other coefficient functions vanish to $\mathcal{O}(\alpha_s)$ in the DIS scheme. In order to maintain the same expression for F_2, modified (anti)quark p.d.f.s are required. The relation between DIS and $\overline{\rm MS}$ scheme p.d.f.s is given by

$$\begin{aligned} q^{\rm DIS}(x,\mu_F^2) &= q^{\overline{\rm MS}}(x,\mu_F^2) + \frac{\alpha_s}{2\pi}\int_x^1\frac{{\rm d}z}{z}\sum_{f=q,g}f^{\overline{\rm MS}}\left(\frac{x}{z}\right)C_2^{(Vf)}(z) \\ g^{\rm DIS}(x,\mu_F^2) &= g^{\overline{\rm MS}}(x,\mu_F^2) - \frac{\alpha_s}{2\pi}\int_x^1\frac{{\rm d}z}{z}\sum_{f=q,\bar{q},g}f^{\overline{\rm MS}}\left(\frac{x}{z}\right)C_2^{(Vf)}(z)\,. \end{aligned} \tag{3.280}$$

Here the expression relating $g^{\rm DIS}$ to the $\overline{\rm MS}$ p.d.f.s is only the conventional one.

Comparing eqn (3.276) with (3.279) and eqn (3.277) with (3.280) we see the characteristic differences between the $\overline{\rm MS}$ and DIS factorization schemes. In the $\overline{\rm MS}$ scheme the coefficient functions are relatively complex whilst the p.d.f.s are very simple and contain no traces of any hard subprocess. By contrast, in the DIS scheme the coefficient functions describing DIS are very simple but the p.d.f.s are relatively complex and contain terms which are specific to the F_2 structure function of DIS. In the DIS scheme the simplicity of the coefficient functions only holds for DIS, whereas in the $\overline{\rm MS}$ scheme the simplicity of the p.d.f.s holds for all processes.

Before moving on to discuss the scale dependence of the p.d.f.s it is worthwhile to remind ourselves of how this calculation proceeded. We began by deriving the corrections to the partonic scatterings $Vq, Vg \to X$. The result was then put into the form suggested by the factorization theorem eqn (3.47). This required the coefficient function, $\hat{F}_i^{Vf}(x, \mu_F^2)$, and the parton-to-parton p.d.f., $f_{f'}(x, \mu_F^2)$, to be defined. Now, the short-distance coefficient function is universal and can be equally well used to describe $Vh \to X$ scatterings using eqn (3.47) but now with hadron-to-parton p.d.f.s. By exploiting the separation of long- and short-distance physics we are able to finesse the need to deal directly with a non-perturbative hadron. Finally, given an experimental measurement of $F_i^{Vh}(x, Q^2)$, it is possible to extract a combination of the p.d.f.s $f_h(x, \mu_F^2)$ describing the hadron's constituents, which can then be used in the description of other processes.

3.6.5 *The evolution of the parton density functions*

The p.d.f. which appears in eqn (3.254) is not a perturbatively calculable quantity but one which must presently be extracted from experimental data within a particular factorization scheme. We also know that the left-hand side of eqn (3.254) is independent of the arbitrary factorization scale, μ_F. Indeed, $q^F(x, \mu_F^2)$ was constructed in eqn (3.252) to ensure that the right-hand side is μ_F-independent to $\mathcal{O}(\alpha_s)$. If we differentiate eqn (3.254), or (3.252), with respect to μ_F we obtain an equation for the scale dependence, setting $\mu = \mu_F$, of the p.d.f.,

$$\mu^2 \frac{\partial q(x, \mu^2)}{\partial \mu^2} = \int_x^1 \frac{\mathrm{d}z}{z} \frac{\alpha_s}{2\pi} P_{\rm qq}(z) q\left(\frac{x}{z}, \mu^2\right) . \tag{3.281}$$

This is the basic form of the DGLAP equation; see eqn (3.49) and the discussion in Section 3.2.2.

The explicit calculations of the previous section show that the evolution of a quark p.d.f. includes contributions from $\mathrm{q} \to \mathrm{q(g)}$ and also from $\mathrm{g} \to \mathrm{q}(\bar{\mathrm{q}})$ splitting functions. Likewise, for an antiquark we should include contributions from $\bar{\mathrm{q}} \to \bar{\mathrm{q}}(\mathrm{g})$ and $\mathrm{g} \to \bar{\mathrm{q}}(\mathrm{q})$ splitting functions. At leading $\mathcal{O}(\alpha_s)$ the gluon p.d.f. evolves according to a similar equation with contributions from $\mathrm{g} \to \mathrm{g(g)}$, $\mathrm{q} \to \mathrm{g(q)}$ and $\bar{\mathrm{q}} \to \mathrm{g}(\bar{\mathrm{q}})$ splitting functions. More generally we have to consider $a \to b(cd)$ and higher order vertices. This opens up the possibility of $\mathrm{q} \to \mathrm{q}'(X)$ and $\mathrm{q} \to \bar{\mathrm{q}}'(X)$ splitting functions etc. and leads us to the evolution equations

$$\mu^2\frac{\partial q_i}{\partial\mu^2}(x,\mu^2) = \int_x^1 \frac{\mathrm{d}z}{z}\frac{\alpha_s}{2\pi}\left[P_{q_iq_j}(z,\alpha_s)q_j\left(\frac{x}{z},\mu^2\right) + P_{q_i\bar{q}_j}(z,\alpha_s)\bar{q}_j\left(\frac{x}{z},\mu^2\right) + P_{q_ig}(z,\alpha_s)g\left(\frac{x}{z},\mu^2\right)\right]$$

$$\mu^2\frac{\partial \bar{q}_i}{\partial\mu^2}(x,\mu^2) = \int_x^1 \frac{\mathrm{d}z}{z}\frac{\alpha_s}{2\pi}\left[P_{\bar{q}_i\bar{q}_j}(z,\alpha_s)\bar{q}_j\left(\frac{x}{z},\mu^2\right) + P_{\bar{q}_iq_j}(z,\alpha_s)q_j\left(\frac{x}{z},\mu^2\right) + P_{\bar{q}_ig}(z,\alpha_s)g\left(\frac{x}{z},\mu^2\right)\right]$$

$$\mu^2\frac{\partial g}{\partial\mu^2}(x,\mu^2) = \int_x^1 \frac{\mathrm{d}z}{z}\frac{\alpha_s}{2\pi}\left[P_{gg}(z,\alpha_s)g\left(\frac{x}{z},\mu^2\right) + \sum_{f=q,\bar{q}} P_{gf}(z,\alpha_s)f\left(\frac{x}{z},\mu^2\right)\right]. \tag{3.282}$$

The kernel functions $P_{ab}(z,\alpha_s(\mu^2))$ are associated with the branchings $b \to a(X)$ and can be calculated as power series in α_s,

$$P_{ab}(z,\alpha_s) = P_{ab}^{(0)}(z) + \frac{\alpha_s}{2\pi}P_{ab}^{(1)}(z) + \cdots . \tag{3.283}$$

In their general form, eqn (3.282), they look rather formidable but they actually simplify greatly since not all splitting functions are independent. The charge conjugation symmetry and the SU(n_f) flavour symmetry of QCD, for equal mass quarks, imply the relationships

$$\begin{aligned} P_{q_iq_j} &= P_{\bar{q}_i\bar{q}_j} \equiv \delta_{ij}P_{qq}^{NS} + P_{qq}^{S} \qquad & P_{q_ig} &= P_{\bar{q}_ig} \equiv P_{qg} \\ P_{\bar{q}_iq_j} &= P_{q_i\bar{q}_j} \equiv \delta_{ij}P_{\bar{q}q}^{NS} + P_{qq}^{S} \qquad & P_{gq_i} &= P_{g\bar{q}_i} \equiv P_{gq}\,. \end{aligned} \tag{3.284}$$

The $q \to q$ and $q \to \bar{q}$ splitting functions are usefully separated into flavour non-singlet (NS) and singlet (S) parts that are associated with the evolution of the valence and sea quarks, respectively. The splitting functions, P_{qq}^{S}, P_{qq}^{NS} and $P_{\bar{q}q}^{S}$ only start at $\mathcal{O}(\alpha_s^2)$, where $P_{qq}^{S(1)} = P_{\bar{q}q}^{S(1)}$. Thus, at leading order eqn (3.282) reduces to the simpler eqn (3.49). Since the virtualities involved in this initial state evolution are negative, these are the space-like splitting functions.

The treatment of radiative corrections for outgoing partons follows a similar pattern as that for incoming partons. It provides a similar factorization theorem for fragmentation functions and equations very much like eqn (3.282), which control the μ_F behaviour of the fragmentation functions (Owens, 1978; Uematsu, 1978). The leading order equations for the factorization scale dependence of the fragmentation functions are

$$\mu^2\frac{\partial D_q^h}{\partial\mu^2}(x,\mu^2) = \int_x^1 \frac{\mathrm{d}z}{z}\frac{\alpha_s}{2\pi}\left[P_{qq}(z,\alpha_s)D_q^h\left(\frac{x}{z},\mu^2\right) + P_{gq}(z,\alpha_s)D_g^h\left(\frac{x}{z},\mu^2\right)\right]$$

$$\mu^2\frac{\partial D_{\bar{q}}^h}{\partial\mu^2}(x,\mu^2) = \int_x^1 \frac{\mathrm{d}z}{z}\frac{\alpha_s}{2\pi}\left[P_{qq}(z,\alpha_s)D_{\bar{q}}^h\left(\frac{x}{z},\mu^2\right) + P_{gq}(z,\alpha_s)D_g^h\left(\frac{x}{z},\mu^2\right)\right]$$

$$\mu^2 \frac{\partial D_{\rm g}^{\rm h}}{\partial \mu^2}(x,\mu^2) = \int_x^1 \frac{{\rm d}z}{z} \frac{\alpha_{\rm s}}{2\pi} \left[P_{\rm gg}(z,\alpha_{\rm s}) D_{\rm g}^{\rm h}\left(\frac{x}{z},\mu^2\right) + \sum_{f=q,\bar{q}} P_{\rm qg}(z,\alpha_{\rm s}) D_{\rm f}^{\rm h}\left(\frac{x}{z},\mu^2\right) \right] . \tag{3.285}$$

Note the reversed order of the indices on the splitting functions compared to eqn (3.49). The structure and interpretation of these time-like equations are essentially the same as for the space-like equations and to $\mathcal{O}(\alpha_{\rm s})$ so are the splitting functions. However, beyond this leading order the space-like and time-like splitting functions differ. All the splitting functions are known to $\mathcal{O}(\alpha_{\rm s}^2)$ (Furmanski and Petronzio, 1982), see also (Hamberg and van Neerven, 1992), whilst partial results are becoming available at $\mathcal{O}(\alpha_{\rm s}^3)$. The $\mathcal{O}(\alpha_{\rm s}^2)$, time-like splitting functions can be found in Appendix E.

3.6.5.1 *Method of moments* Whilst the direct numerical solution of the space-like and time-like DGLAP equations is one option, semi-analytical approaches are also available. The convolution which occurs in the DGLAP equations can be separated using a Mellin transform into moment space:

$$\tilde{f}(n) = \int_0^1 {\rm d}x\, x^{n-1} f(x) \quad \Longleftrightarrow \quad f(x) = \frac{1}{2\pi\,{\rm i}} \int_{c-{\rm i}\infty}^{c+{\rm i}\infty} {\rm d}n\, x^{-n} \tilde{f}(n) . \tag{3.286}$$

The contour used in the inverse transformation must lie to the right of all singularities in the analytic continuation of $\tilde{f}(n)$. The moment space transformation of, for illustration only, a simplified DGLAP equation with $\mu_F^2 = Q^2$, is as follows:

$$\begin{aligned} Q^2 \frac{\partial f}{\partial Q^2}(x,Q^2) &= \frac{\alpha_{\rm s}}{2\pi} \int_x^1 \frac{{\rm d}z}{z} P(z,\alpha_{\rm s}) f\left(\frac{x}{z},Q^2\right) \\ \Longrightarrow \quad Q^2 \frac{\partial \tilde{f}}{\partial Q^2}(n,Q^2) &= \frac{\alpha_{\rm s}}{2\pi} \gamma(n,\alpha_{\rm s}) \tilde{f}(n,Q^2) . \end{aligned} \tag{3.287}$$

Here, the Mellin transform of the splitting function, $\gamma(n,\alpha_{\rm s}) \equiv \tilde{P}(n,\alpha_{\rm s})$, is known as the anomalous dimension. Equation (3.287) is now easily solved. Working to one-loop precision we find

$$\tilde{f}(n,Q^2) = \tilde{f}(n,Q_0^2) \left(\frac{Q^2}{Q_0^2}\right)^{\frac{\alpha_{\rm s}}{2\pi}\gamma^{(0)}(n)} = \tilde{f}(n,\mu^2) \left(\frac{\alpha_{\rm s}(Q_0^2)}{\alpha_{\rm s}(Q^2)}\right)^{\frac{\gamma^{(0)}(n)}{2\pi\beta_0}} . \tag{3.288}$$

The first solution assumes fixed $\alpha_{\rm s}$ whilst the second assumes the use of the running coupling, eqn (3.22). As the first form makes clear the anomalous dimension is so called because it modifies the naïve Q-dependence and acts as an additional scaling power. All information on the nature of the solutions are contained within the anomalous dimensions, which are fully equivalent to the Altarelli–Parisi kernels. Given the solution eqn (3.288), one then applies the inverse Mellin transform, eqn (3.286), to go back from the moment to the x-space:

see examples Ex. (3-33) and (3-34). In the more general case the Mellin transform of the DGLAP equations leads to matrix equations. These can be solved in essentially the same way after they are first diagonalized.

We shall now use this moment space equation to determine the coefficient C_{qq} in eqn (3.247) whilst avoiding the need to evaluate any virtual corrections. Consider the leading order evolution equation for the difference of two quark p.d.f.s, such as $(u-\bar{d})$ or $(u-\bar{u})$,

$$Q^2\frac{\partial q^{\rm NS}}{\partial Q^2}(x,Q^2)=\int_x^1\frac{{\rm d}z}{z}\frac{\alpha_s}{2\pi}P_{qq}(z)q^{\rm NS}\left(\frac{x}{z},Q^2\right)\,. \tag{3.289}$$

All dependence on the gluon p.d.f. has cancelled. This is the evolution equation for the non-singlet, in terms of its flavour SU(3) transformation properties, structure function. Exercise (3-8) investigates other useful combinations of p.d.f.s. Now, $\int_0^1{\rm d}x\,q^{\rm NS}(x)$ is a constant by virtue of the conservation of flavour quantum numbers within QCD. Referring to eqn (3.287) with $n=1$, this implies that $\gamma_{qq}(1,\alpha_s)=0$ for the $q\to qg$ splitting function. That is,

$$\begin{aligned}0&=\int_0^1{\rm d}z\,C_F\left\{\frac{1+z^2}{(1-z)_+}+C_{qq}\delta(1-z)\right\}\\&=C_F\left\{\int_0^1{\rm d}z\frac{(1+z^2)-2}{1-z}+C_{qq}\right\}\\&=C_F\left\{-\frac{3}{2}+C_{qq}\right\}\,,\end{aligned} \tag{3.290}$$

which supplies us with the value of C_{qq} and completes the expression for $P_{qq}^{(0)}(z)$. The same result viewed from an alternative perspective is discussed in Ex. (3-30) and a similar approach based on using momentum conservation can be applied to find C_{gg}, Ex. (3-29).

Of course these arguments rely on the physical interpretation of the p.d.f.s. In Section 3.6.4 we proceeded by direct calculation to fully evaluate the splitting functions. Given the full expressions for the splitting functions, eqn (3.50), we can evaluate the anomalous dimensions appearing in eqn (3.287). At the lowest order we find:

$$\gamma_{gg}^{(0)}(n)=2C_A\left[\frac{1}{(n-1)n}+\frac{1}{(n+1)(n+2)}+\frac{11}{12}-\sum_{m=1}^{n}\frac{1}{m}\right]-\frac{2}{3}n_fT_F \tag{3.291}$$

$$\gamma_{qq}^{(0)}(n)=C_F\left[\frac{1}{n(n+1)}+\frac{3}{2}-2\sum_{m=1}^{n}\frac{1}{m}\right] \tag{3.292}$$

$$\gamma_{qg}^{(0)}(n)=T_F\left[\frac{2+n+n^2}{n(n+1)(n+2)}\right] \tag{3.293}$$

$$\gamma_{gq}^{(0)}(n)=C_F\left[\frac{2+n+n^2}{n(n+1)(n+2)}\right] \tag{3.294}$$

These show that $\gamma_{qq}^{(0)}(1) = 0$, thereby proving conservation of flavour. A number of other conservation laws are also implied by eqns (3.291)–(3.294).

$$0 = \int_0^1 dz \left\{ P_{qq}^{NS}(z) - P_{qq}^{NS}(z) + n_f \left[P_{qq}^{S}(z) - P_{qq}^{S}(z) \right] \right\} \tag{3.295}$$

$$0 = \int_0^1 dz\, z \left\{ P_{gg}(z) + 2n_f P_{qg}(z) \right\} \tag{3.296}$$

$$0 = \int_0^1 dz\, z \left\{ P_{gq}(z) + P_{qq}^{NS}(z) + P_{qq}^{NS}(z) + n_f \left[P_{qq}^{S}(z) + P_{qq}^{S}(z) \right] \right\} \tag{3.297}$$

See Ex. (3-31) for further elaboration of how the momentum is shared within a hadron.

3.6.6 *Leading logarithms*

Our derivation of the DGLAP equation focused on treating a region of phase space which has a logarithmically enhanced cross section. Recall that introducing μ_F^2 to isolate the collinear singularity left behind a residual, large logarithm. There are two singular regions: the collinear region which gives logarithmic enhancements of the form $\alpha_s \ln(Q^2/Q_0^2)$ and the soft region which gives logarithmic enhancements of the form $\alpha_s \ln(1/x)$. These regions can overlap and give double logarithmic enhancements of the form $\alpha_s \ln(Q^2/Q_0^2) \ln(1/x)$. Processes which involve multiple parton final states can have up to one $\ln(Q^2/Q_0^2)$ and one $\ln(1/x)$ factor for each power of α_s. The phase space regions which contribute these leading logarithmic enhancements are associated with configurations in which 'successive' partons have strongly ordered transverse, k_T, and/or longitudinal, $k_L(\equiv x)$, momenta:

$$\text{LL}_Q\text{A:} \quad \begin{cases} \alpha_s L_Q \sim 1 \\ \alpha_s L_x \ll 1 \end{cases} \quad Q^2 \gg k_{nT}^2 \gg \cdots \gg k_{1T}^2 \gg Q_0^2 \tag{3.298}$$

$$\text{DLLA:} \begin{cases} \alpha_s L_Q L_x \sim 1 \\ \alpha_s L_Q \ll 1 \\ \alpha_s L_x \ll 1 \end{cases} \begin{cases} Q^2 \gg k_{nT}^2 \gg \cdots \gg k_{1T}^2 \gg Q_0^2 \\ x \ll x_n \ll \cdots \ll x_1 \ll x_0 \end{cases} \tag{3.299}$$

$$\text{LL}_x\text{A:} \quad \begin{cases} \alpha_s L_x \sim 1 \\ \alpha_s L_Q \ll 1 \end{cases} \quad x \ll x_n \ll \cdots \ll x_1 \ll x_0 \tag{3.300}$$

The solution of the DGLAP equation sums over all orders in α_s the contributions from the leading, single, collinear logarithms, $[\alpha_s \ln(Q^2/Q_0^2)]^n$ and the leading, double logarithms $[\alpha_s \ln(Q^2/Q_0^2) \ln(1/x)]^n$. This is the region of strongly ordered k_T and ordered x. It does not include the leading, single, soft singularities which are treated instead by the BFKL equation (Kuraev *et al.*, 1977; Balitsky and Lipatov, 1978) which describes the x-evolution of p.d.f.s at fixed Q^2. Figure 3.24 shows the $\ln(Q^2)$–$\ln(1/x)$ plane and the regions which are described by the various *leading logarithmic* (LL) summations. Relaxing one of the strong ordering

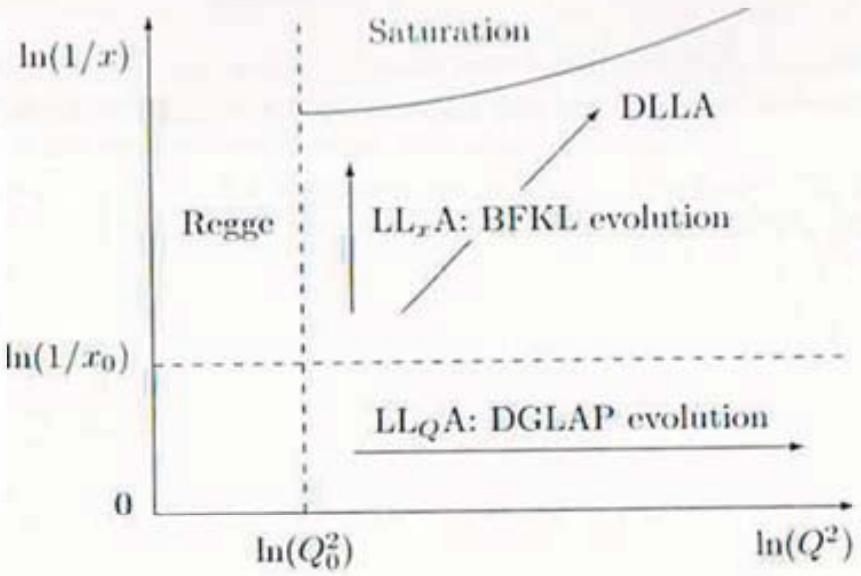

FIG. 3.24. The $\ln(Q^2)$–$\ln(1/x)$ plane showing the regions in which the LL_Q, LL_x, and DLL approximations hold. Also shown are the regions in which Regge phenomenology applies and where saturation/recombination effects have to be taken into account.

constraints in eqn (3.298) or eqn (3.300) gives rise to a *next-to-leading logarithmic* (NLL) enhancement to the cross section. These are suppressed by a factor α_s with respect to the LL-enhancement. Including summed NLL-terms modifies the DGLAP or BFKL equations whilst maintaining their general structure. We now discuss the *double leading logarithmic* (DLL) approximation, the BFKL equation, the combined evolution equations which incorporate both DGLAP and BFKL evolution and the generalizations to include parton recombination. We shall make more explicit the relationship between these equations and the leading logarithms in the following Section 3.6.7.

3.6.6.1 *The double leading logarithmic approximation* At small x and large Q^2 we must sum the leading $\alpha_s \ln(Q^2/Q_0^2)\ln(1/x)$ terms. This can be done directly from the DGLAP equations by keeping only the most singular $1/z$ terms in the splitting functions. At $\mathcal{O}(\alpha_s)$ only P_{gg} and P_{gq} have soft gluon singularities, but at $\mathcal{O}(\alpha_s^2)$ all splitting functions are singular as $z \to 0$. In this limit the lowest order parton distributions are given by (Rujula *et al.*, 1974)

$$F_2(x,Q^2) \sim xg(x,Q^2) \sim \tilde{g}(n_0,Q_0^2)\exp\sqrt{\frac{4C_A}{\pi\beta_0}\ln\left(\frac{\alpha_s(Q_0^2)}{\alpha_s(Q^2)}\right)\ln\left(\frac{1}{x}\right)} \qquad (3.301)$$

$$\text{with} \quad n_0 = \sqrt{\frac{C_A \ln(\alpha_s(Q_0^2)/\alpha_s(Q^2))}{\pi\beta_0 \ln(1/x)}}\,.$$

See Ex. (3-33), which also gives sub-leading terms. This solution shows a strong growth in the small-x partons and hence the structure functions, in particular $F_2(x,Q^2)$ (Glück *et al.*, 1995). The dependence on the initial distribution is only

via its n_0-th moment. If this initial distribution has too strong a small-x growth, then the above solution will not hold; for example, $xg(x,Q_0^2) \propto x^{-\lambda}$, $\lambda > 0$ leads to $xg(x,Q^2) \propto x^{-\lambda}$, independent of Q^2.

In what is known as 'double asymptotic scaling', in the limit $1/x$, $Q^2 \to \infty$ eqn (3.301) implies that for 'soft' $f(x,Q_0^2)$ then $\ln F_2(x,Q^2)$ depends linearly on $\sqrt{\ln(\alpha_s(Q_0^2)/\alpha_s(Q^2)) \times \ln(1/x)}$ and is independent of the complementary combination $\sqrt{\ln(\alpha_s(Q_0^2)/\alpha_s(Q^2)) \div \ln(1/x)}$ (Ball and Forte, 1994). Sub-leading terms only slightly complicate this statement.

3.6.6.2 *The BFKL equation* At small x and moderate $Q^2 > \Lambda^2_{\rm QCD}$, where gluons are dominant, we must sum the leading $\alpha_s \ln(1/x)$ terms whilst keeping the full Q^2-dependence. This means that we do not have strongly ordered k_T but instead integrate over the full range of k_T. This leads us to work with the unintegrated gluon p.d.f., $\mathcal{G}(x,k_T^2)$, which is related to the usual p.d.f. via

$$xg(x,Q^2) = \int^{Q^2} \frac{{\rm d}k_T^2}{k_T^2} \mathcal{G}(x,k_T^2) \,. \tag{3.302}$$

In phenomenological applications it is common to assume a narrow, Gaussian k_T distribution for the partons in a hadron, which is commensurate with confinement. Predictions for structure functions are then made using the so-called k_T factorization (Catani *et al.* 1990*a*; 1991*a*).

$$F_i(x,Q^2) = \int_0^x \frac{{\rm d}z}{z} \int \frac{{\rm d}k_T^2}{k_T^4} \hat{F}_i^{\rm box}(z,k_T^2,Q^2) \mathcal{G}\left(\frac{x}{z},k_T^2\right) \,. \tag{3.303}$$

Here $\hat{F}_i^{\rm box}$ is derived from the quark box diagrams that describe virtual-photon virtual-gluon scattering, $\gamma^* {\rm g}^* \to {\rm `q\bar{q}'} \to \gamma^* {\rm g}^*$. The unintegrated gluon p.d.f. satisfies the BFKL equation (Kuraev *et al.*, 1977; Balitsky and Lipatov, 1978); see also (Mueller, 1994) for an alternative derivation in terms of colour dipoles. At leading order the BFKL equation is given by

$$\frac{\partial \mathcal{G}(x,k_T^2)}{\partial \ln(1/x)} = \frac{C_A \alpha_s}{\pi} k_T^2 \int_{k_0^2}^{\infty} \frac{{\rm d}q_T^2}{q_T^2} \left\{ \frac{\mathcal{G}(x,q_T^2) - \mathcal{G}(x,k_T^2)}{|q_T^2 - k_T^2|} + \frac{\mathcal{G}(x,k_T^2)}{\sqrt{4q_T^4 + k_T^4}} \right\} . \tag{3.304}$$

Given the unintegrated gluon p.d.f. at one value of x_0, this equation allows you to calculate its value at smaller values of x, that is, larger values of $\ln(1/x)$. If α_s is fixed, then the equation can be solved analytically. In the small-x limit this basically gives a power law behaviour in x,

$$\mathcal{G}(x,k_T^2) \approx \tilde{\mathcal{G}}\left(x_0,\frac{1}{2}\right) \left(\frac{x}{x_0}\right)^{-\lambda} \frac{\sqrt{k_T^2}}{\sqrt{2\pi[\lambda'' \ln(x_0/x) + A]}} \exp\left(\frac{-\ln^2(k_T^2/\bar{k}_T^2)}{2[\lambda'' \ln(x_0/x) + A]}\right) . \tag{3.305}$$

The solution follows by first applying a Mellin transform and then using the saddle point method to evaluate the inverse. Here

$$\tilde{\mathcal{G}}(x_0,\omega) \equiv \int_0^\infty \frac{\mathrm{d}k_T^2}{k_T^2}\frac{\mathcal{G}(x_0,k_T^2)}{(k_T^2)^\omega}, \quad -\ln\bar{k}_T^2 = \frac{1}{\tilde{\mathcal{G}}}\frac{\mathrm{d}\tilde{\mathcal{G}}}{\mathrm{d}\omega}\left(x_0,\frac{1}{2}\right), \quad A = \frac{1}{\tilde{\mathcal{G}}}\frac{\mathrm{d}^2\tilde{\mathcal{G}}}{\mathrm{d}\omega^2}\left(x_0,\frac{1}{2}\right) \tag{3.306}$$

$$\lambda = 4\ln 2\frac{C_A\alpha_s}{\pi}\bigg|_{\alpha_s=0.2} \approx +0.5 \quad \text{and} \quad \lambda'' = 28\zeta(3)\frac{C_A\alpha_s}{\pi}\,. \tag{3.307}$$

The numerical value of the Riemann zeta-function is $\zeta(3) \approx 1.202\,056\,903\,2$. Due to eqn (3.303) the behaviour $\mathcal{G} \propto x^{-\lambda}$ feeds through to give $F_2 \propto x^{-\lambda}$. The k_T behaviour is typical of diffusion and reflects the lack of any k_T-ordering in BFKL dynamics; in essence there is a random walk in k_T as x decreases (Balitsky and Lipatov, 1978; Bartels and Lotter, 1993).

Actually, this observation highlights a problem. Given that the width of the Gaussian in $\ln(k_T^2/\bar{k}_T^2)$ is given by $\sqrt{[\lambda''\ln(x_0/x)+A]}$, then for sufficiently small x there will be support for $\mathcal{G}(x,k_T^2)$ from the non-perturbative region in k_T^2. Thus, if we use a running coupling, $\alpha_s(k_T^2)$, then it is necessary to introduce infrared cut-offs, for example $k_0^2 > 0$ in eqn (3.304), and other possible refinements such as including momentum conservation (Collins and Landshoff, 1992; Bartels *et al.*, 1996). Whilst numerical evaluations show that similar power law behaviour in x and diffusion in $\ln(k_T^2/\bar{k}_T^2)$ occurs (Askew *et al.*, 1993), these are essentially misguided due to the inherent instablity of the BFKL equation with running coupling. The situation is made worse by the NLL_x corrections to the BFKL kernel (Fadin and Lipatov, 1998), which gives

$$\lambda = 4\ln 2\frac{C_A\alpha_s}{\pi}\left(1-6.3\frac{C_A\alpha_s}{\pi}\right)\bigg|_{\alpha_s=0.2} \approx -0.1\,. \tag{3.308}$$

Such a large, negative correction basically invalidates perturbation theory and, if taken seriously, leads to negative cross sections. The source of these large corrections has been traced to large $\ln(Q^2/Q_0^2)$ terms coming from phase space restrictions (Salam, 1998). There are a number of putative solutions to this situation, which include resummation (Ciafaloni *et al.* 1999*a*; 1999*b*), imposing momentum conservation (Altarelli *et al.*, 2000) and imposing perturbative stability (Ball and Forte, 1999). A succinct review is provided by Ball and Landshoff (2000).

3.6.6.3 *Combined evolution equations* The DGLAP and BFKL equations describe evolution in two complementary regions. A number of attempts have been made to give a combined description of both regions in a single equation. Amongst these are an attempt to include $\ln(1/x)$ terms into the usual collinear factorization by adding summed corrections into the P_{gg} kernel appearing in the DGLAP equations (Ellis *et al.*, 1995; Ball and Forte, 1995). A second approach is given by the CCFM equation which uses angular ordering to describe both the x and the Q^2 evolution and has the DGLAP and the BFKL equations as limiting cases (Ciafaloni, 1988; Catani *et al.*, 1990*b*), see also (Andersson *et al.*, 1996*a*).

3.6.6.4 *Shadowing, gluon recombination and hot spots* If left unchecked, the rapid rise in the small-x gluon p.d.f. predicted by both the DGLAP and BFKL equations would violate unitarity. It also leads to a breakdown in the parton model picture of scattering off independent partons. At sufficiently high densities it becomes possible for a second parton to overlap in space with the first, so-called shadowing. The probability of this happening can be estimated as

$$\mathcal{P}_{\rm sat} \sim \frac{\alpha_{\rm s}(Q^2)/Q^2}{\pi R^2} N(x,Q)\,, \tag{3.309}$$

where the partons, predominently gluons, are taken to have an effective area, given by a typical QCD cross section, $\sigma \sim \alpha_{\rm s}(Q^2)/Q^2$ and number $N(x,Q)$. The denominator is taken to be of order the area of the hadron, with the radius $R \sim R_{\rm h} = 1/M_{\rm h}$. In general, $\mathcal{P}_{\rm sat}$ is small but especially for small x it may become large. When it becomes $\mathcal{O}(1)$ the hadron is said to saturate and the usual DGLAP equation may need to be modified to account for parton recombination,

$$\mu^2 \frac{\partial g}{\partial \mu^2} = P_{\rm gg} \otimes g + P_{\rm gq} \otimes q - \frac{81\alpha_{\rm s}^2}{16R^2\mu^2} \int_x^1 \frac{{\rm d}y}{y} (yg)^2\,. \tag{3.310}$$

A similar modification can be applied to the BFKL equation. In this GLR equation (Gribov *et al.*, 1983) the familiar first two terms lead to a growth in $g(x,\mu^2)$ due to emission whilst the third involves a suppression due to recombination, $gg \to g$. The competition between these two terms ensures that the gluon p.d.f. equilibrates below the unitarity bound.

The validity of eqn (3.310) is not assured, but it appears reasonable to use it to estimate the onset of shadowing (Askew *et al.*, 1993). It has been derived at DLL accuracy (Mueller and Qiu, 1986); however, this neglects $1/N_{\rm c}$ suppressed terms associated with pre-recombination interactions between the gluons (Bartels, 1993; Laenen and Levin, 1994). Its equivalent has also been derived for the BFKL equation in the colour dipole approach (Kovchegov, 1999). More significantly, it must be admitted that at saturation the high densities and field strengths occuring, $F^{\mu\nu} \sim 1/g_{\rm s}$, imply that the perturbation theory is no longer valid. This has led to the development of a treatment in terms of a semi-classical, effective field theory (McLerran and Venugopalan, 1999), which also leads to parton recombination (Iancu *et al.*, 2000).

The choice $R = R_{\rm h}$ in eqn (3.310) corresponds to a uniform distribution of the QCD fields across the hadron. However, it has been conjectured that this may not be the case and that partons inside the hadron may concentrate in dense hot spots centred on the valence quarks (Mueller, 1991). In this case one should use an $R < R_{\rm h}$. Such a behaviour is predicted by the BFKL equation but not the DGLAP equation. It predicts the number of gluon jets per unit rapidity localized to a transverse region of size $\Delta x_T^2 \sim 1/\bar{k}_T^2$ as

$$\frac{{\rm d}n}{{\rm d}\ln(1/x)} = \frac{C_A\alpha_{\rm s}}{\pi} \frac{x^{-\lambda}}{\sqrt{(\pi\lambda''/8)\ln(1/x)}}\,. \tag{3.311}$$

3.6.7 *The analysis of ladder diagrams*

In our discussion of DIS, Section 3.6.3, we encountered the Altarelli–Parisi splitting function $P_{qq}(z)$, eqn (3.246), when investigating the limit of near collinear emission. A point which may not yet have been appreciated is the universality of this result. That is, whenever we have a process which contains a $q \to qg$ vertex, then in the collinear limit its (azimuthally-averaged) contribution to the cross section will be described by the same factor

$$\frac{\alpha_s}{2\pi} P_{qq}(z) \mathrm{d}z \frac{\mathrm{d}k_T^2}{k_T^2} \,. \tag{3.312}$$

Similar expressions describe the collinear limits of $g \to q\bar{q}$ and $g \to gg$ vertices with P_{qq} replaced by P_{qg} and P_{gg}, respectively. This factorization of the matrix element squared then leads to much simpler expressions for a cross section in the collinear limit. Furthermore, the collinear emission regions of phase space are very important because they are responsible for one of the dominant, leading logarithmic, contributions to the cross section. In the other dominant region of phase space, the limit of soft gluon emission, we also have that the cross section simplifies significantly; see Section 3.7. In this way we can use simplified expressions to describe the bulk of a cross section. Of course, if our analysis focuses attention on a region of phase space which involves hard, non-collinear emission(s), then the approximate matrix elements may only be of limited use.

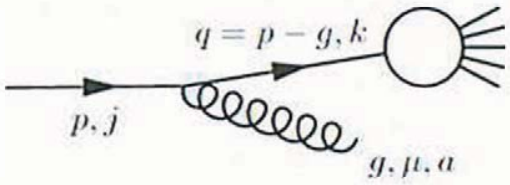

FIG. 3.25. The emission of a near collinear gluon off an incoming quark in an $n+1$ parton scattering

To see how this simplification occurs, consider the situation sketched in Fig. 3.25 where a quark entering an n-particle scattering emits a real gluon, which we shortly will take to be near collinear with the quark. The matrix element for this process is given by

$$\mathcal{M}_j^{(n+1)} = g_s T_{kj}^a \mathcal{M}_k^{(n)} \frac{(\not{p} - \not{g})}{(p-g)^2} \gamma_\mu \bar{u}(p) \epsilon^*(g)^\mu \,. \tag{3.313}$$

Introducing a gauge vector n^μ with, for convenience, $n^2 = 0$ (and $g \cdot n \neq 0$), we can use eqn (3.121) to sum over the gluon's physical, that is, transverse, polarizations in the matrix element squared to obtain

$$\sum \left| \mathcal{M}^{(n+1)} \right|^2 \Big/ \left[g_s^2 T_{kj}^a T_{jk'}^a = g_s^2 C_F \delta_{kk'} \right]$$

$$
\begin{aligned}
&= \mathrm{Tr}\left\{\cdots \frac{(\not p - \not g)}{(p-g)^2}\gamma_\mu \not p \gamma^\nu \frac{(\not p - \not g)}{(p-g)^2}\cdots\right\}\left(-\eta^{\mu\nu} + \frac{[g^\mu n^\nu + n^\mu g^\nu]}{n\cdot g}\right)\\
&= \mathrm{Tr}\left\{\cdots \frac{(\not p - \not g)}{(p-g)^2}\left(-\gamma_\mu \not p \gamma^\mu + \frac{1}{n\cdot g}[\not g \not p \not n + \not n \not p \not g]\right)\frac{(\not p - \not g)}{(p-g)^2}\cdots\right\}.\\
&= \mathrm{Tr}\left\{\cdots \frac{(\not p - \not g)}{(p-g)^2}\left(2\not p + \frac{2}{n\cdot g}[(g\cdot p)\not n - (n\cdot g)\not p + (n\cdot p)\not g]\right)\frac{(\not p - \not g)}{(p-g)^2}\cdots\right\}\\
&= \frac{1}{(2p\cdot g)^2}\frac{2}{(n\cdot g)}\mathrm{Tr}\left\{\cdots(\not p - \not g)[(g\cdot p)\not n + (n\cdot p)\not g](\not p - \not g)\cdots\right\}\\
&= \frac{1}{(2p\cdot g)}\frac{2}{(n\cdot g)}\mathrm{Tr}\left\{\cdots\left[(n\cdot(p-g))(\not p - \not g) + (p\cdot g)\not n + (n\cdot p)\not p\right]\cdots\right\}. \quad (3.314)
\end{aligned}
$$

The ellipsis in these expressions represent the contributions from $\mathcal{M}_k^{(n)}$ and $\mathcal{M}_k^{(n)*}$. In line two we used an identity based upon commuting γ-matrices to obtain line three and then again commuted γ-matrices in lines three and four, plus using $\not g \not g = g^2 = 0 = p^2 = \not p \not p$, to obtain an exact result. Now we wish to specialize to the near collinear limit. To do this we use a Sudakov decomposition of the quark and gluon momentum four-vectors (Sudakov, 1956),

$$
\begin{aligned}
& & q^\mu &= zp^\mu + \beta n^\mu + k_\perp^\mu \\
p^\mu = q^\mu + g^\mu \quad &\Longrightarrow \quad & g^\mu &= (1-z)p^\mu - \beta n^\mu - k_\perp^\mu . \qquad (3.315)
\end{aligned}
$$

Here n^μ could have been any four-vector, subject to $n\cdot p \neq 0$, but it proves most useful to make this the gauge vector whilst $k_\perp^\mu$ is transverse to both p^μ and n^μ, $p\cdot k_\perp = 0 = n\cdot k_\perp$, and $k_\perp^2 \equiv -k_T^2 < 0$. The gluon's on mass-shell constraint, $g^2 = 0$, determines $\beta = -k_T^2/(2(1-z)n\cdot p)$. The (negative) virtuality of the intermediate quark is given by

$$
q^2 = (p-g)^2 = -2p\cdot g = 2\beta n\cdot p = \frac{-k_T^2}{1-z} . \qquad (3.316)
$$

Adopting these variables eqn (3.314) becomes

$$
g_s^2 C_F \delta_{kk'}\frac{(1-z)}{k_T^2}\frac{2}{(1-z)}\mathrm{Tr}\left\{\cdots\left[(1+z^2)\not p + z\not k_T + \frac{k_T^2}{2(n\cdot p)}\not n\right]\cdots\right\}. \qquad (3.317)
$$

Now if we only wish to keep the leading term in the collinear limit, $k_T^2 \to 0$, then we can drop the second two terms in the square brackets to obtain

$$
\begin{aligned}
\sum\left|\mathcal{M}^{(n+1)}\right|^2 &= 2\frac{(1-z)}{k_T^2}g_s^2 C_F\frac{1+z^2}{(1-z)}\delta_{kk'}\mathrm{Tr}\left\{\cdots\not p\cdots\right\} + \mathcal{O}(1)\\
&\approx 2\frac{(1-z)}{k_T^2}g_s^2\hat{P}_{\mathrm{qq}}(z)\sum\left|\mathcal{M}^{(n)}\right|^2 . \qquad (3.318)
\end{aligned}
$$

Thus, in the collinear limit the matrix element factorizes into the product of the unregularized, lowest order Altarelli–Parisi splitting function, $\hat{P}_{\mathrm{qq}}(z)$, and the

matrix element squared for the process assuming no gluon emission took place. To obtain the cross section we must include the flux factor, an average over the initial spin and colour polarizations and the phase space, giving

$$\begin{aligned} \mathrm{d}^{n+1}\sigma &= \frac{1}{16\pi^2}\frac{\mathrm{d}k_T^2}{(1-z)}\mathrm{d}z \times 2\frac{(1-z)}{k_T^2} g_s^2 \hat{P}_{\mathrm{qq}}(z) \times \mathrm{d}^n\sigma \\ &= \frac{\mathrm{d}k_T^2}{k_T^2}\mathrm{d}z\frac{\alpha_s}{2\pi}\hat{P}_{\mathrm{qq}}(z) \times \mathrm{d}^n\sigma \,. \end{aligned} \tag{3.319}$$

Here we have made explicit the phase space element for the near collinear gluon; see Ex. (3-35).

The collinear factorization of the matrix element squared, eqn (3.318), does not depend on the nature of the sub-matrix element, $\mathcal{M}_n$, for the other n particles involved in the scattering. In this sense the Altarelli–Parisi kernel $\hat{P}_{\mathrm{qq}}$ is universal. A similar analysis can be applied to the collinear limits of $\bar{\mathrm{q}} \to \bar{\mathrm{q}}\mathrm{g}$, $\mathrm{g} \to \mathrm{q}\bar{\mathrm{q}}$, see Ex. (3-36), and $\mathrm{g} \to \mathrm{gg}$.

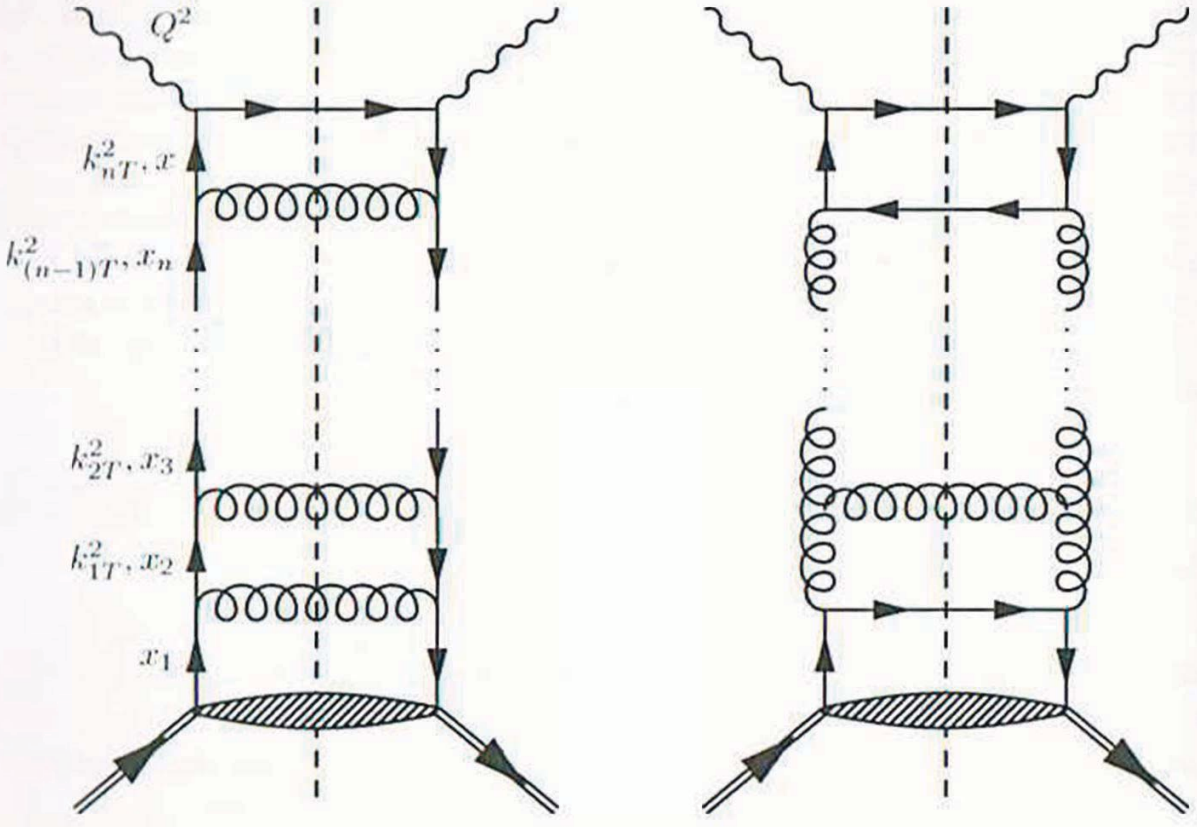

FIG. 3.26. On the left a ladder diagram dominated by $\mathrm{q} \to \mathrm{qg}$ branchings and on the right a ladder diagram dominated by $\mathrm{g} \to \mathrm{gg}$ branchings

Armed with collinear factorization we can give a less abstract and more physical interpretation of the relationship between the evolution equations and the leading logarithmic enhancements to cross sections. This traditional approach is based upon the analysis of Feynman diagrams (Dokshitzer, 1977). The aim is

to identify those diagrams and the associated regions of phase space which give rise to the leading logarithms and then sum them. The treatment of the single collinear and double logarithms is a situation where the use of a physical gauge proves invaluable (Frenkel and Taylor, 1976; Dokshitzer *et al.*, 1980). It can then be shown that the dominant contributions come from the so-called ladder graphs, such as Fig. 3.26, with strongly ordered branchings eqn (3.298) and (3.300). These ladders correspond to individual, tree-level Feynman diagrams squared. Diagrams involving the quartic gluon coupling give sub-leading contributions. Likewise, quantum interference between tree-level diagrams, which would give ladders with crossed rungs, only give sub-leading contributions. The strong ordering in k_T^2, which effectively implies ordering of the virtualities eqn (3.316), allows eqn (3.319) to be iteratively applied. In the case of an n-rung gluon ladder the cross section, $\sigma_n(x, Q^2)$, is given by:

$$\int_{Q_0^2}^{Q^2} \frac{\mathrm{d}k_{nT}^2}{k_{nT}^2} \frac{\alpha_s(k_{nT}^2)}{2\pi} \cdots \int_{Q_0^2}^{k_{3T}^2} \frac{\mathrm{d}k_{2T}^2}{k_{2T}^2} \frac{\alpha_s(k_{2T}^2)}{2\pi} \int_{Q_0^2}^{k_{2T}^2} \frac{\mathrm{d}k_{1T}^2}{k_{1T}^2} \frac{\alpha_s(k_{1T}^2)}{2\pi}$$
$$\times \int_x^1 \frac{\mathrm{d}x_n}{x_n} \hat{P}_{\mathrm{gg}}\left(\frac{x}{x_n}\right) \cdots \int_{x_3}^1 \frac{\mathrm{d}x_2}{x_2} \hat{P}_{\mathrm{gg}}\left(\frac{x_3}{x_2}\right) \int_{x_2}^1 \frac{\mathrm{d}x_1}{x_1} \hat{P}_{\mathrm{gg}}\left(\frac{x_2}{x_1}\right) g(x_1, Q_0^2) \,. \tag{3.320}$$

Associated with each rung are a k_T and an x integral, both of which may contribute a large logarithm in the collinear or soft limits, respectively. Equation (3.320) embodies an almost classical picture of a parton shower in terms of successive branchings. It is this which lies behind our interpretation of the Altarelli–Parisi equations and which will be further exploited in the development of all-orders Monte Carlo event generators.

The usual collinear leading logarithmic approximation is characterized by strongly ordered transverse momenta, $Q^2 \gg k_{nT}^2 \gg \cdots \gg k_{2T}^2 \gg k_{1T}^2 \gg Q_0^2$. Using the one-loop expression for $\alpha_s(k_T^2)$ the nested transverse momentum integrals become:

$$\begin{aligned}
\sigma_n(x, Q^2) &\propto \int_{Q_0^2}^{Q^2} \frac{\mathrm{d}k_{nT}^2}{k_{nT}^2} \frac{1}{2\pi} \frac{1}{\beta_0 \ln(k_{nT}^2/\Lambda^2)} \cdots \int_{Q_0^2}^{k_{2T}^2} \frac{\mathrm{d}k_{1T}^2}{k_{1T}^2} \frac{1}{2\pi} \frac{1}{\beta_0 \ln(k_{1T}^2/\Lambda^2)} \\
&= \frac{1}{(2\pi\beta_0)^n} \int_{Q_0^2}^{Q^2} \mathrm{d} \ln \left[\frac{\ln(k_{nT}^2/\Lambda^2)}{\ln(Q_0^2/\Lambda^2)}\right] \cdots \int_{Q_0^2}^{k_{2T}^2} \mathrm{d} \ln \left[\frac{\ln(k_{1T}^2/\Lambda^2)}{\ln(Q_0^2/\Lambda^2)}\right] \\
&= \frac{1}{n!} \left[\frac{1}{2\pi\beta_0} \ln\left(\frac{\ln(Q^2/\Lambda^2)}{\ln(Q_0^2/\Lambda^2)}\right)\right]^n \\
&= \frac{1}{n!} \left[\frac{1}{2\pi\beta_0} \ln\left(\frac{\alpha_s(Q_0^2)}{\alpha_s(Q^2)}\right)\right]^n \,.
\end{aligned} \tag{3.321}$$

In the second line, we have used a change of variables which makes the integrals simpler to evaluate. To do the momentum fraction integrals it is useful to work with the Mellin transform.

$$\tilde{\sigma}_n(m) \propto \int_0^1 \mathrm{d}x\, x^{m-1} \int_x^1 \frac{\mathrm{d}x_n}{x_n} \hat{P}_{\mathrm{gg}}\left(\frac{x}{x_n}\right) \cdots \int_{x_2}^1 \frac{\mathrm{d}x_1}{x_1} \hat{P}_{\mathrm{gg}}\left(\frac{x_2}{x_1}\right) g(x_1, Q_0^2)$$
$$= \left[\tilde{P}_{\mathrm{gg}}(m)\right]^n \tilde{g}(m, Q_0^2)\,. \tag{3.322}$$

The result follows by repeatedly applying the fact that the Mellin transform of a convolution is the product of the Mellin transforms of the components. Combining eqns (3.321) and (3.322) gives

$$\sum_n \tilde{\sigma}_n(m, Q^2) = \tilde{g}(m, Q_0^2) \sum_n \frac{1}{n!} \left[\frac{\tilde{P}_{\mathrm{gg}}^{(0)}(m)}{2\pi\beta_0} \ln\left(\frac{\alpha_{\mathrm{s}}(Q_0^2)}{\alpha_{\mathrm{s}}(Q^2)}\right)\right]^n$$
$$= \tilde{g}(m, Q_0^2) \left(\frac{\alpha_{\mathrm{s}}(\mu_0^2)}{\alpha_{\mathrm{s}}(Q^2)}\right)^{\frac{\tilde{P}_{\mathrm{gg}}^{(0)}(m)}{2\pi\beta_0}}\,. \tag{3.323}$$

which coincides with eqn (3.288). This demonstrates that the DGLAP equation sums the leading $\alpha_{\mathrm{s}} \ln(Q^2/Q_0^2)$ terms.

In the double leading logarithmic approximation we approximate $P_{\mathrm{gg}}(z)$ by $2C_A/z$ and impose strong ordering on the longitudinal integrals, $x \ll x_n \ll \cdots \ll x_2 \ll x_1 \ll 1$. This is in addition to the strongly ordered transverse momentum integrals which we evaluated in eqn (3.321). The longitudinal integral becomes

$$x\sigma_n(x) \propto x \int_x^1 \frac{\mathrm{d}x_n}{x_n} 2C_A \frac{x_n}{x} \cdots \int_{x_3}^1 \frac{\mathrm{d}x_2}{x_2} 2C_A \frac{x_2}{x_3} \int_{x_2}^1 \frac{\mathrm{d}x_1}{x_1} 2C_A \frac{x_1}{x_2} g(x_1, Q_0^2)$$
$$= (2C_A)^n \int_x^1 \frac{\mathrm{d}x_n}{x_n} \cdots \int_{x_3}^1 \frac{\mathrm{d}x_2}{x_2} \int_{x_2}^1 \frac{\mathrm{d}x_1}{x_1} G_0(Q_0^2)$$
$$= \frac{1}{n!} \left[2C_A \log\left(\frac{1}{x}\right)\right]^n G_0(Q_0^2)\,. \tag{3.324}$$

In the second line we have taken $xg(x, Q_0^2) = G_0(Q_0^2)$. Again the nested integrals are straightforward to evaluate and lead to a second $1/n!$ factor. Combining eqns (3.324) and (3.321) gives

$$\sum_n \sigma_n(x, Q^2) = G_0(Q_0^2) \sum_n \frac{1}{(n!)^2} \left[\frac{C_A}{\pi\beta_0} \ln\left(\frac{\alpha_{\mathrm{s}}(Q_0^2)}{\alpha_{\mathrm{s}}(Q^2)}\right) \ln\left(\frac{1}{x}\right)\right]^n$$
$$\sim G_0(Q_0^2) \exp\sqrt{\frac{4C_A}{\pi\beta_0} \ln\left(\frac{\alpha_{\mathrm{s}}(Q_0^2)}{\alpha_{\mathrm{s}}(Q^2)}\right) \ln\left(\frac{1}{x}\right)}\,. \tag{3.325}$$

Here, we have recognised the sum $\sum_n (y/2n!)^{2n}$ as the power series for the modified Bessel function $I_0(y)$ which has the asymptotic form $\mathrm{e}^y/\sqrt{2\pi y}$ (Arfken and Weber, 1995). This result coincides with eqn (3.301).

Strictly speaking, the ladder diagrams, such as Fig. 3.26, are only schematic. For example, at one-loop they should be understood to also represent diagrams

that include vertex and propagator corrections. This leads to a running coupling in eqn (3.320) which softens the Q^2 dependence in our results,

$$\int_{Q_0^2}^{Q^2} \frac{\mathrm{d}k_T^2}{k_T^2}\alpha_s = \begin{cases} \alpha_s \ln(Q^2/Q_0^2) & \alpha_s \text{ fixed} \\ \beta_0^{-1} \ln(\alpha_s(Q_0^2)/\alpha_s(Q^2)) & \alpha_s \text{ running} . \end{cases} \tag{3.326}$$

Here, we have used the transverse momentum in the branching as the argument of α_s. An n-rung ladder diagram can also be used to represent the nth-order term, $[\alpha_s \ln(1/x)]^n$, in the solution of the BFKL equation (Gribov *et al.*, 1983). Here, each rung does not have a simple meaning but represents the sum of contributions from a set of real emission diagrams and interference with virtual diagrams. We also mention that the recombination term in eqn (3.310) can be represented by the merging of two ladders into a single ladder in what has been christened a 'fan diagram'.

3.6.8 *The Drell–Yan process*

The Drell–Yan process (Drell and Yan, 1971) is the production of high-mass lepton pairs from the decay of an electroweak boson produced in a hadron–hadron collision. Originally these were e^+e^- or $\mu^+\mu^-$ pairs coming from the decay of a virtual photon but, as collision energies have increased, it now includes the contribution from Z exchange and also $e\nu_e$ and $\mu\nu_\mu$ pairs coming from $W^\pm$ decays. Historically, the Drell–Yan process has proved very important; see the book by Cahn and Goldhaber (1989) for several original papers. It was pivotal in the discovery of heavy quarks, which manifested themselves as quarkonium resonances: charm and the $J(\psi)$ in 1974 and bottom and the Υ in 1978. It was also the process which in 1983 led to the discovery of the massive electroweak gauge bosons, the $W^\pm$ and the Z.

Theoretically, the Drell–Yan process is favoured because the final state particles are individually colourless and therefore are unaffected by the strong force. The high mass of the time-like photon, $Q^2 > 0$, ensures that small distance physics is probed and that pQCD is applicable. Within QCD the significance of the Drell–Yan process is due to its rôle as the prototype process within hadron–hadron collisions to be described using the same factorization approach that we used to treat DIS. Neglecting Z exchange, the underlying lowest order (tree-level) subprocess is quark–antiquark annihilation to a virtual photon, $h_1h_2 : q\bar{q} \to \gamma^*(Q^\mu) \to \ell^+\ell^-$. Therefore, the process offers a direct probe of a hadron's antiquark content; see Ex. (3-37). In the framework of eqn (3.72) the cross section is given by

$$\frac{\mathrm{d}\sigma^{(0)}}{\mathrm{d}Q^2}(h_1h_2 \to \gamma^*(Q) \to \ell^+\ell^-) = \tag{3.327}$$
$$\int_0^1 \mathrm{d}x_1 \int_0^1 \mathrm{d}x_2 \sum_q \left[q_{h_1}(x_1)\bar{q}_{h_2}(x_2) + \bar{q}_{h_1}(x_1)q_{h_2}(x_2)\right] \frac{\mathrm{d}\hat{\sigma}^{(0)}}{\mathrm{d}Q^2}(q\bar{q} \to \ell^+\ell^-)(Q, \hat{\tau}) .$$

Here, we introduce the following scaling variables

$$\hat{\tau} = \frac{Q^2}{\hat{s}} = \frac{\tau}{x_1 x_2} \quad \text{and} \quad \tau = \frac{Q^2}{s}\,, \tag{3.328}$$

with $\hat{s} = (x_1 p_1 + x_2 p_2)^2 = x_1 x_2 s$. Note that in eqn (3.327) we are careful to include both contributions coming from the quark (antiquark) being in hadron 1 (2) and *vice versa*. We have also temporarily suppressed the p.d.f.s' dependence on the scale Q^2. The differential cross section for the hard subprocess is given by:

$$\frac{\mathrm{d}\hat{\sigma}}{\mathrm{d}Q^2}(\mathrm{q\bar{q}} \to \ell^+\ell^-) = \frac{4\pi\alpha_{\mathrm{em}}^2}{3N_c Q^4} e_{\mathrm{q}}^2 \delta(1-\hat{\tau}) \equiv \frac{\sigma_{\mathrm{DY}}^{(0)}}{Q^2} e_{\mathrm{q}}^2 \delta(1-\hat{\tau})\,. \tag{3.329}$$

This has been obtained from eqn (3.93) using crossing, allowing for the changed average over initial state colours and multiplying by unity in the form $1 = \int \mathrm{d}Q^2 \delta(Q^2 - \hat{s})$. The factor $\sigma_{\mathrm{DY}}^{(0)}$ sets the scale for the cross section and contains its dimensions. Combining eqns (3.327) and (3.329) gives

$$\frac{\mathrm{d}\sigma}{\mathrm{d}Q^2} = \frac{\sigma_{\mathrm{DY}}^{(0)}}{Q^2}\tau \int_\tau^1 \frac{\mathrm{d}x}{x}\left[q_{\mathrm{h}_1}(x)\bar{q}_{\mathrm{h}_2}\left(\frac{\tau}{x}\right) + \bar{q}_{\mathrm{h}_1}(x) q_{\mathrm{h}_2}\left(\frac{\tau}{x}\right)\right] e_{\mathrm{q}}^2 \quad \approx \frac{\tau F(\tau)}{Q^4}\,. \tag{3.330}$$

If the p.d.f.s are scale independent, that is, they do not depend on Q^2, as in the naïve parton model, then the differential cross section $\mathrm{d}\sigma/\mathrm{d}Q^2 \propto Q^{-4} \times$ a function of τ. This result follows on dimensional grounds and is the same scaling as we saw in DIS.

3.6.8.1 *The $\mathcal{O}(\alpha_s)$ corrections to the Drell–Yan process* The calculation of the $\mathcal{O}(\alpha_s)$ corrections to the Drell–Yan process follows very much the same procedures as those used for DIS (Altarelli *et al.*, 1979*a*: Kubar-André and Paige, 1979). Here we only outline the results using $\gamma^* \to \ell^+\ell^-$ production for illustration: W and Z production follow the same lines whilst including the decay orientation of the lepton pair adds no new insights. A useful guide to the calculations is given by Willenbrock (1989).

There are basically two new contributions at $\mathcal{O}(\alpha_s)$; charge conjugation symmetry relates quark and antiquark initiated processes. There is the gluon bremsstrahlung correction to the lowest order process, $\mathrm{q\bar{q}} \to \gamma^*$. We expect this to show collinear singularities when the gluon becomes parallel to either the incoming quark or antiquark, but to be free of final state singularities after we include the one-loop, virtual corrections to $\mathrm{q\bar{q}} \to \gamma^*$. It is also free of ultraviolet singularities. There is also the gluon initiated process $\mathrm{gq} \to \gamma^* \mathrm{q}'$. We expect this to contain a collinear singularity when the scattered quark lies antiparallel to the incoming quark in the C.o.M. frame. This is equivalent to the gluon undergoing a near collinear $\mathrm{g} \to \mathrm{q\bar{q}}$ branching in a fast moving frame. The appropriate generalization of eqn (3.327) is given by

$$\frac{\mathrm{d}\sigma}{\mathrm{d}Q^2}(\mathrm{h_1 h_2} \to \gamma^*(Q) \to \ell^+\ell^-) = \int_0^1 \mathrm{d}x_1 \int_0^1 \mathrm{d}x_2$$

$$\times\left\{\sum_{q}\left[q_{h_1}(x_1)\bar{q}_{h_2}(x_2)+\bar{q}_{h_1}(x_1)q_{h_2}(x_2)\right]\left(\frac{d\hat{\sigma}^{(0)}}{dQ^2}(q\bar{q}\to\gamma^*)+\frac{d\hat{\sigma}^{(1)}}{dQ^2}(q\bar{q}\to\gamma^*g)\right)\right.$$
$$\left.+\sum_{f=q,\bar{q}}\left[g_{h_1}(x_1)f_{h_2}(x_2)+f_{h_1}(x_1)g_{h_2}(x_2)\right]\frac{d\hat{\sigma}^{(1)}}{dQ^2}(gq\to\gamma^*q')\right\}. \qquad (3.331)$$

The Feynman diagrams for the two new, hard subprocesses have been given in Figs. 3.23 and 3.22, but now are read from right to left. Crossing also allows us to obtain the matrix elements with minimal effort. However, we cannot directly take over the phase space integrals as they involve different regions. The result of these calculations are

$$\frac{d\hat{\sigma}^{(1)}}{dQ^2}(q\bar{q}\to\gamma^*g)=\frac{\sigma^{(0)}_{DY}}{Q^2}e_q^2\frac{\alpha_s}{2\pi}\left\{-2P^{(0)}_{qq}(\hat{\tau})\left[\Delta_\epsilon-\ln\left(\frac{Q^2}{\mu^2}\right)\right]+H_{q\bar{q}}(\hat{\tau})\right\}$$
$$\frac{d\hat{\sigma}^{(1)}}{dQ^2}(gq\to\gamma^*q')=\frac{\sigma^{(0)}_{DY}}{Q^2}e_q^2\frac{\alpha_s}{2\pi}\left\{-P^{(0)}_{qg}(\hat{\tau})\left[\Delta_\epsilon-\ln\left(\frac{Q^2}{\mu^2}\right)\right]+H_{gq}(\hat{\tau})\right\}. \qquad (3.332)$$

where for convenience we have introduced the coefficient functions

$$H_{q\bar{q}}(z)=C_F\left[4(1+z^2)\left(\frac{\ln(1-z)}{1-z}\right)_+-2\frac{1+z^2}{1-z}\ln z+\left(\frac{2\pi^2}{3}-8\right)\delta(1-z)\right]$$
$$H_{gq}(z)=T_F\left[2\left[z^2+(1-z)^2\right]\ln\left(\frac{(1-z)^2}{z}\right)+3+2z-3z^2\right]. \qquad (3.333)$$

The structure of eqns (3.331) and (3.332) is very similar to the corresponding expressions which arose in the NLO description of DIS, eqns (3.272) and (3.274). It is the power of factorization that essentially the same separation of the cross section into factorization scale dependent long-distance p.d.f.s and short-distance coefficient functions will treat the collinear singularities in the NLO description of the Drell–Yan process. Indeed, introducing the $\overline{\text{MS}}$ p.d.f.s, eqn (3.277), into eqn (3.331) gives

$$\frac{d\sigma}{dQ^2}(h_1h_2\to\gamma^*(Q)\to\ell^+\ell^-)=\frac{\sigma^{(0)}_{DY}}{Q^2}\int_0^1dx_1\int_0^1dx_2$$
$$\times\left\{\sum_q\left[q^{\overline{\text{MS}}}_{h_1}(x_1,\mu_F^2)\bar{q}^{\overline{\text{MS}}}_{h_2}(x_2,\mu_F^2)+\bar{q}^{\overline{\text{MS}}}_{h_1}(x_1,\mu_F^2)q^{\overline{\text{MS}}}_{h_2}(x_2,\mu_F^2)\right]e_q^2\right.$$
$$\left.\times\left(\delta(1-\hat{\tau})+\frac{\alpha_s}{2\pi}\left[2P^{(0)}_{qq}(\hat{\tau})\ln\left(\frac{Q^2}{\mu_F^2}\right)+H_{q\bar{q}}(\hat{\tau})\right]\right)\right.$$
$$\left.+\sum_{f=q,\bar{q}}\left[g^{\overline{\text{MS}}}_{h_1}(x_1,\mu_F^2)f^{\overline{\text{MS}}}_{h_2}(x_2,\mu_F^2)+f^{\overline{\text{MS}}}_{h_1}(x_1,\mu_F^2)g^{\overline{\text{MS}}}_{h_2}(x_2,\mu_F^2)\right]e_q^2\right.$$

$$\times \frac{\alpha_s}{2\pi}\left[2P_{qg}^{(0)}(\hat{\tau})\ln\left(\frac{Q^2}{\mu_F^2}\right)+H_{qg}(\hat{\tau})\right]\Bigg\}, \tag{3.334}$$

which is independent of the factorization scale to $\mathcal{O}(\alpha_s)$. The $\overline{\text{MS}}$ coefficient functions in this expression depend on the factorization scheme, that is, which finite terms are absorbed into the p.d.f.s and are therefore different in the DIS scheme; see Ex. (3-38). The $\mathcal{O}(\alpha_s^2)$ corrections to Drell–Yan have also been calculated (Zijlstra and van Neerven, 1992).

3.6.8.2 *Transverse momentum in Drell–Yan processes* The measurement of the W boson mass to high accuracy is very desirable as it facilitates tests of the Standard Model of electroweak interactions at the quantum (loop) level; see, for example, the report by Altarelli *et al.* (1989). Since the W decays to a charged lepton and a neutrino its mass reconstruction at hadron–hadron colliders must necessarily be indirect. The preferred method is based upon measuring the boost-invariant transverse momentum distribution of the charged lepton. Assuming that the W is produced with no transverse momentum and neglecting its width, one expects

$$\frac{1}{\sigma}\frac{d\sigma}{dp_{T\ell}^2}=\frac{3}{M_W^2}\left(1-2\frac{p_{T\ell}^2}{M_W^2}\right)\sqrt{1-4\frac{p_{T\ell}^2}{M_W^2}}\,. \tag{3.335}$$

This strongly peaked distribution is very sensitive to M_W, but to be useful we must be confident that we understand the underlying transverse momentum distribution of the W boson.

At $\mathcal{O}(\alpha_s^0)$ the massive vector bosons produced in the Drell–Yan process have zero transverse momentum. At $\mathcal{O}(\alpha_s^1)$ the $q\bar{q}\to Vg$ and $gq\to Vq'$ ($g\bar{q}\to V\bar{q}'$) processes provide a good description of high-p_T vector boson production. Now, at order $\mathcal{O}(\alpha_s^n)$ the cross section behaves as

$$\frac{1}{\sigma}\frac{d\sigma}{dp_T^2}=\frac{1}{p_T^2}\left[\alpha_s^n A_{n,2n-1}\ln^{2n-1}\left(\frac{M_V^2}{p_T^2}\right)+\cdots\right], \tag{3.336}$$

so that care must be exercised in the low-p_T region, $M_V \gg p_T \gg \Lambda_{QCD}$. The need to sum these large logarithms was first recognized by Dokshitzer *et al.* (1980) and an impact parameter space formalism for summing them developed (Collins and Soper 1981; 1982; Collins *et al.* 1985). Impact parameters are the Fourier conjugate variables to p_T. In computing the effect of multiple gluon radiation it is important to impose momentum conservation, $\sum_n \boldsymbol{k}_{nT} = \boldsymbol{p}_T$, on the (soft) gluon bremstrahlung (Parisi and Petronzio, 1979); this greatly reduces the possibility of obtaining $p_T = 0$. A numerical implementation of this formalism (Ladinsky and Yuan, 1994) proved the necessity to include a Gaussian smearing of the initial partons' impact parameter distribution in order to counter convergence and infrared problems. Analytic expressions for the coefficients in eqn (3.336) are available up to N^{3}LL accuracy (Kulesza and Stirling, 1999). In an alternative form of eqn (3.336) the right-hand side can be resummed by 'exponentiating' the leading logarithmic terms $\alpha_s^n \ln^{n+1}(M_V^2/p_T^2)$, which have been

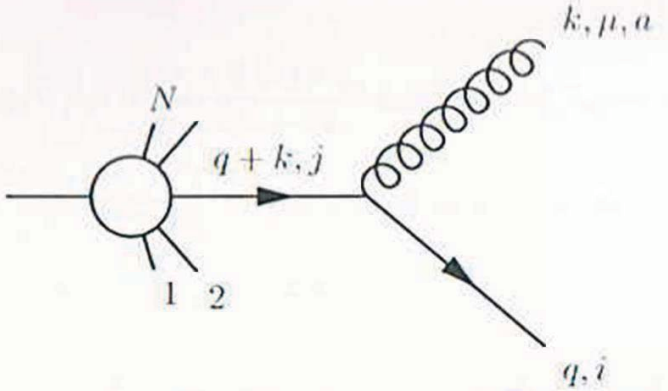

FIG. 3.27. The emission of a soft gluon from one of N hard, final state partons

calculated to NLLA accuracy (Frixione *et al.*, 1999). From the impact parameter space results it is then possible to derive expressions for the p_T-space. In order to describe the full p_T range, it is important to match these low-p_T summed calculations to the high-p_T fixed order calculations. This has been carried out (Ellis *et al.*, 1997; Ellis and Veseli, 1998), though there remain problems in ensuring a smooth cross-over at $p_T = M_V$. To compare with actual measurements, experimental data are available for the p_T-distribution of Z bosons (D0 Collab. 2000*a*, 2000*b*; CDF Collab. 2000) and W bosons (D0 Collab., 2001).

3.7 The treatment of soft gluons

We learnt in Section 3.5 that matrix elements become singular when soft gluons are emitted and that these singularities cancel in sufficiently inclusive observables such as a total cross section. When less inclusive measurements are made, for example, by observing any soft particles above an energy threshold, the cancellation is incomplete and there remain logarithmic enhancements to the emission probability. That said, the effects of these soft gluons are mitigated due to their lack of energy. In this section, first we show how matrix elements simplify in the limit of soft gluon emission and then we investigate their physical effects (Bassetto *et al.*, 1983).

As gluons become softer their wavelengths grow and they become sensitive only to an event's global structure. Specifically, the distribution of soft gluon radiation depends only on the momenta and colour connections of the hard, final state partons and not on any internal dynamics. This is known as Low's theorem for the case of soft photon emission. To see how this arises consider a hard process involving N final state partons with momenta $\{p_i^\mu\}$, all of whose relative transverse momenta are large compared to $\Lambda_{\rm QCD}$. This condition ensures that all internal particles are well off mass-shell, such that their large virtualities shield the collinear and soft singular regions. Thus, adding a soft gluon with momentum $k^\mu = \omega(1, \hat{\boldsymbol{n}})$, $\omega \ll E_i$, can give rise to soft singularities only if it is emitted from an external parton. A typical such Feynman diagram is illustrated in Fig. 3.27.

Suppose that the gluon is emitted by a final state quark, then the corresponding matrix element is given by

$$\begin{aligned}\mathcal{M}_i^{(N+1)}(q,k) &= g_s T^a_{ij}\epsilon^*(k)_\mu \bar{u}(q)\gamma^\mu \frac{(\not{q}+\not{k}+m)}{(q+k)^2-m^2}\mathcal{M}_j^{(N)}(q+k)\\ &= g_s T^a_{ij}\epsilon^*(k)_\mu \bar{u}(q)\frac{\left[-(\not{q}-m)\gamma^\mu + 2q^\mu + \gamma^\mu \not{k}\right]}{2q\cdot k}\mathcal{M}_j^{(N)}(q+k)\\ &= g_s T^a_{ij}\epsilon^*(k)_\mu \frac{q^\mu}{q\cdot k}\bar{u}(q)\mathcal{M}_j^{(N)}(q) + \mathcal{O}(\omega)\,. \end{aligned} \tag{3.337}$$

Here we have exploited, after a suitable re-arrangement, the Dirac equation satisfied by the basis spinor and neglected terms proportional to k compared to those proportional to q. This neglect of recoil effects is known as the eikonal approximation. The structure obtained is universal, that is, the same form would hold for emission off an antiquark, another gluon or even a coloured scalar; see Ex. (3.39). The reason is that the soft gluon has a correspondingly long wavelength and is unable to resolve the spin structure of the emitting particle. Adding up the contributions from all the hard partons we obtain

$$\mathcal{M}^{(N+1)} = g_s\epsilon^*(k)_\mu\left(\sum_{i=1}^{N}\hat{T}_i^a\frac{p_i^\mu}{p_i\cdot k}\right)\times\mathcal{M}^{(N)}\,. \tag{3.338}$$

Here the colour charge operators, $\hat{T}_i^a$, generate the appropriate colour factors for a gluon, colour a, emitted by parton i. They act as follows:

$$\begin{aligned}\hat{T}^a_{\rm q}|\cdots;q,i;\cdots\rangle &= +T^a_{ij}|\cdots;q,j;\cdots\rangle\\ \hat{T}^a_{\bar{\rm q}}|\cdots;\bar{q},i;\cdots\rangle &= -T^a_{ji}|\cdots;\bar{q},j;\cdots\rangle\\ \hat{T}^a_{\rm g}|\cdots;g,b;\cdots\rangle &= -{\rm i}\,f_{abc}|\cdots;g,c;\cdots\rangle\,.\end{aligned} \tag{3.339}$$

To obtain the matrix element squared we need to use an expression for the gluon polarization sum, eqn (3.121), which allows us to write

$$\left|\mathcal{M}^{(N+1)}\right|^2 = -g_s^2 J\cdot J^\dagger\left|\mathcal{M}^{(N)}\right|^2 \quad\text{with}\quad J^{a\mu}(k;p_i) = \sum_i \hat{T}_i^a\left(\frac{p_i^\mu}{p_i\cdot k}-\frac{n^\mu}{n\cdot k}\right)\,. \tag{3.340}$$

Here J^μ is known as the insertion current. For a colour neutral system, such as in an e^+e^- event, we have $\sum_i \hat{T}_i = 0$, so that the second term, proportional to the gauge vector n^μ, can be safely dropped. It is also absent in the Feynman gauge. Henceforth we drop it. Including the phase space then gives the following form for the soft gluon emission cross section (Marchesini and Webber, 1990),

$$\begin{aligned} & d\sigma^{(N+1)}\\ &= -\frac{\alpha_{\rm s}}{2\pi}J(k)\cdot J^\dagger(k)\frac{{\rm d}^3\boldsymbol{k}}{2\pi\omega}{\rm d}^{(N)}\sigma\\ &= -\frac{\alpha_{\rm s}}{2\pi}\sum_{i\neq j}\hat{T}_i\cdot\hat{T}_j\,\omega^2\left[\frac{p_i\cdot p_j}{(p_i\cdot k)(p_j\cdot k)}-\frac{1}{2}\frac{p_i^2}{(p_i\cdot k)^2}-\frac{1}{2}\frac{p_j^2}{(p_j\cdot k)^2}\right]\frac{{\rm d}\omega}{\omega}\frac{{\rm d}\Omega_k}{2\pi}{\rm d}^{(N)}\sigma\end{aligned}$$

ordering of any colour matrices.

For completeness we also include some relevant Feynman rules from the standard electroweak theory. Here the propagators for the vector bosons, $V = \gamma$, $\mathrm{W}^{\pm}$ or Z, are given by

$$\frac{\mathrm{i}}{p^2 - M_V^2 + \mathrm{i}\,\epsilon}\left(-\eta^{\mu\nu} + (1-\xi)\frac{p^\mu p^\nu}{p^2 - \xi M_V^2 + \mathrm{i}\,\epsilon}\right) , \tag{B.2}$$

whilst their couplings to fermions take the form

$$-\,\mathrm{i}\,e\kappa\gamma_\mu(v_f + a_f\gamma_5) . \tag{B.3}$$

The individual coefficients appearing in this expression are collected in the following table:

Boson	κ	v_f	a_f
γ	e_f	1	0
Z	$1/(2\sin\theta_{\mathrm{w}}\cos\theta_{\mathrm{w}})$	$I_3^f - 2e_f\sin^2\theta_{\mathrm{w}}$	$-I_3^f$
$\mathrm{W}^{\pm}$	$V_{ff'}/(2\sqrt{2}\sin\theta_{\mathrm{w}})$	1	-1

Here for the fermion f, e_f is its electric charge measured in units of the positron charge $e > 0$; I_3^f is its third component of weak isospin, $I_3 = +\frac{1}{2}$ for up-type quarks or neutrinos, and $I_3 = -\frac{1}{2}$ for down-type quarks or charged leptons. For the corresponding antiparticles the signs are reversed. For charged current interactions involving quarks, the coefficients $V_{ff'}$ are the respective elements of the Cabbibo–Kobayashi–Maskawa matrix, the dominant elements of which are $V_{\mathrm{ud}} \approx 0.975 \approx V_{\mathrm{cs}}$, $V_{\mathrm{us}} \approx 0.222 \approx -V_{\mathrm{cd}}$ and $V_{\mathrm{tb}} \approx 1$. For leptons one effectively has $V_{\nu_\ell\ell'} = \delta_{\ell\ell'}$. The parameter θ_{w} is the weak mixing angle with $\sin^2\theta_{\mathrm{w}} \approx 0.223$.

B.2 Phase space and cross section formulae

Once the amplitude squared for a process has been evaluated, it is necessary to include the flux factor and the (differential) phase space in order to obtain the (differential) cross section. We consider the general process $p_a + p_b \to p_1 + \cdots + p_n$ for which the cross section is given schematically by

$$\mathrm{d}\sigma = \frac{1}{\text{flux}} \times |\mathcal{M}|^2 \times \mathrm{d}\Phi_n . \tag{B.4}$$

Here it should be understood that the cross section and phase space are typically multi-differential quantities. For head-on collisions the flux factor is given by

$$\begin{aligned} \text{flux} &= 4\sqrt{(p_a\cdot p_b)^2 - (m_a m_b)^2} \\ &= 4|\boldsymbol{p}_a^\star|\sqrt{s} = 4|\boldsymbol{p}_a^{\mathrm{lab}}|m_b \qquad\qquad s = (p_a+p_b)^2 \\ &\approx 2s . \end{aligned} \tag{B.5}$$

In the second line the flux is given in terms of the C.o.M. momenta, $\boldsymbol{p}_a^\star = -\boldsymbol{p}_b^\star$, and the laboratory variables $\boldsymbol{p}_a^{\mathrm{lab}}$ and $p_b^{\mathrm{lab}} = (m_b, \boldsymbol{0})$. The third line is appropriate

in the limit of negligible particle masses. In the case of a particle decay the flux factor is given by twice the decaying particle's mass, flux $= 2M$.

A differential element of the Lorentz invariant n-body phase space for the outgoing particles is given by

$$\begin{aligned} &\mathrm{d}\Phi_n(p_a + p_b : p_1, \ldots, p_n) \\ &\quad = (2\pi)^4 \delta^{(4)} \left(p_a + p_b - \sum_{i=1}^{n} p_i \right) \prod_{i=1}^{n} \begin{cases} \dfrac{\mathrm{d}^4 p_i}{(2\pi)^3} \delta^{(+)}(p_i^2 - m_i^2) \\ \dfrac{\mathrm{d}^3 \boldsymbol{p}_i}{(2\pi)^3 2E_i} \end{cases} . \end{aligned} \tag{B.6}$$

In the second version the on mass-shell δ-function has been explicitly integrated out and the positive energy solution $E_i = +\sqrt{\boldsymbol{p}_i^2 + m_i^2}$ selected. Using eqn (B.6) and eqn (B.4) it is easy to verify that the dimensionality of the phase space is given by $3n$, whilst the mass dimension of $|\mathcal{M}|^2$ must be $4 - 2n$.

In many practical situations the incoming particles are unpolarized and the spins of the final state particles are not measured. The same applies for their colours. To take this into account one has to sum the amplitude squared over the spins and colours of the outgoing particles and average over the spins and colours of the incoming particles. Thus, in eqn (B.4) we use

$$|\mathcal{M}|^2 \longrightarrow \overline{\sum} |\mathcal{M}|^2 \equiv \prod_{R=a,b} \frac{1}{2N_R} \times \sum_{\text{spin,colour}} |\mathcal{M}|^2 , \tag{B.7}$$

where the colour degeneracy is $N_R = N_c$ for a quark or an antiquark and $N_c^2 - 1$ for a gluon and where we allow two spin polarizations for the external fermions and massless external gluons or photons.

APPENDIX C

DIMENSIONAL REGULARIZATION

C.1 Integration in non-integer dimensions

Dimensional regularization is the preferred method in QCD for rendering ultraviolet divergent loop integrals finite. The basic idea is to work in $D = 4 - 2\epsilon$ space–time dimensions. Then, given suitable definitions, we evaluate the loop momentum integrals with any divergences appearing as poles in $1/\epsilon$. This renders the theory finite, for $D < 4$, so that we can carry out the renormalization procedure and afterwards take the limit $\epsilon \to 0$.

In D dimensions the structure of the QCD Lagrangian is unaltered: it contains the same kinetic and interaction terms and, therefore, has the same Feynman rules. There is only one change, the replacement $g_s \to g_s\mu^\epsilon$, where μ is an arbitrary unit mass ('tHooft, 1973). This is needed to ensure that each term in the Lagrangian density has the correct mass dimension; see Ex. (3-17).

Before explaining the method, it is useful to introduce a few standard manipulations which makes the final integrals easier to carry out. We illustrate this approach using the following typical integral which arises in the calculation of the fermion self-energy,

$$I = g_s^2\mu^{4-D}\int \frac{\mathrm{d}^D k}{(2\pi)^D}\,\frac{\gamma^\mu(\not{k}+\not{p}+m)\gamma_\mu}{[(k+p)^2-m^2+\mathrm{i}\epsilon][k^2+\mathrm{i}\epsilon]}\,. \tag{C.1}$$

For the moment, we have not set $D = 4$ but left it free. We have also introduced an arbitrary mass μ which serves to preserve the canonical dimension of the integral for $D \neq 4$. This integral has a superficial degree of divergence $D - 3$, obtained by counting the number of powers of the loop momentum in the integrand, suggesting a potential linear divergence in $D = 4$ dimensions. At the expense of introducing extra integrals, eqn (C.1) is simplified by combining the two terms in the denominator using the identity

$$\begin{aligned}&\frac{1}{A_1^{n_1}A_2^{n_2}\cdots A_k^{n_k}}\\ &\quad=\frac{\Gamma(n_1+n_2+\cdots+n_k)}{\Gamma(n_1)\Gamma(n_2)\cdots\Gamma(n_k)}\int_0^1 \mathrm{d}\alpha_1\cdots\mathrm{d}\alpha_k\,\frac{\alpha_1^{n_1-1}\alpha_2^{n_2-1}\cdots\alpha_k^{n_k-1}\delta(1-\sum_i\alpha_i)}{(\alpha_1A_1+\cdots+\alpha_kA_k)^{n_1+n_2\cdots+n_k}}\,.\end{aligned} \tag{C.2}$$

Here the exponents $\{n_i\}$ need not be integer. The $\{\alpha_i\}$ are known as Feynman parameters. Applying this result to eqn (C.1), and at the same time integrating out the δ-function, gives

$$I = g_s^2 \mu^{4-D} \int \frac{\mathrm{d}^D k}{(2\pi)^D} \int_0^1 \mathrm{d}\alpha \frac{\gamma^\mu (\not{k} + \not{p} + m)\gamma_\mu}{(\alpha[(k+p)^2 - m^2 + \mathrm{i}\epsilon] + (1-\alpha)[k^2 + \mathrm{i}\epsilon])^2}$$
$$= g_s^2 \mu^{4-D} \int \frac{\mathrm{d}^D k}{(2\pi)^D} \int_0^1 \mathrm{d}\alpha \frac{\gamma^\mu (\not{k} + \not{p} + m)\gamma_\mu}{((k+\alpha p)^2 - \alpha m^2 + \alpha(1-\alpha)p^2 + \mathrm{i}\epsilon)^2} \,. \quad \text{(C.3)}$$

In the second line we have 'completed the square', which after shifting the momentum variable, $k^\mu \to k^\mu - \alpha p^\mu$, yields

$$I = g_s^2 \mu^{4-D} \int \frac{\mathrm{d}^D k}{(2\pi)^D} \int_0^1 \mathrm{d}\alpha \frac{\gamma^\mu \left[\not{k} + (1-\alpha)\not{p} + m\right]\gamma_\mu}{(k^2 - A + \mathrm{i}\epsilon)^2}$$
$$= g_s^2 \mu^{4-D} \int_0^1 \mathrm{d}\alpha \, \gamma^\mu \left[(1-\alpha)\not{p} + m\right]\gamma_\mu \int \frac{\mathrm{d}^D k}{(2\pi)^D} \frac{1}{(k^2 - A + \mathrm{i}\epsilon)^2} \,. \quad \text{(C.4)}$$

Here, we introduced $A = \alpha m^2 - \alpha(1-\alpha)p^2$. This change of variable and the re-ordering of the integrals is legitimate because we will choose D to make the integral convergent. The k^μ term vanished because the integrand is isotropic and no longer has a preferred direction. The p^μ dependence is now via p^2 in A. This means that the apparent linear divergence of eqn (C.1) is in reality only a logarithmic divergence.

At this point you are reminded that in Minkowski space $k^2 = E^2 - \boldsymbol{k}^2$, so that the temporal and spatial components are not on an equal footing. To remedy this situation we transform to Euclidean space, $E \mapsto \mathrm{i}k_0$, so that $k^2 \to -k_E^2 = k_0^2 + \boldsymbol{k}^2$. For the case at hand this gives

$$\int_{-\infty}^{+\infty} \frac{\mathrm{d}E}{2\pi} \int \frac{\mathrm{d}^{D-1} k}{(2\pi)^{D-1}} \frac{1}{(E^2 - \boldsymbol{k}^2 - A + \mathrm{i}\epsilon)^2}$$
$$= \mathrm{i} \int_{-\infty}^{+\infty} \frac{\mathrm{d}k_0}{2\pi} \int \frac{\mathrm{d}^{D-1} k}{(2\pi)^{D-1}} \frac{1}{(-k_0^2 - \boldsymbol{k}^2 - A + \mathrm{i}\epsilon)^2}$$
$$= \mathrm{i}(-1)^2 \int \frac{\mathrm{d}^D k_E}{(2\pi)^D} \frac{1}{(k_E^2 + A - \mathrm{i}\epsilon)^2} \,. \quad \text{(C.5)}$$

A subtlety in this manipulation is the rôle played by the infinitesimal $\mathrm{i}\epsilon$ in the denominator. Essentially, we have used a closed contour in the complex E-plane that goes along the real axis, down the complex axis and closes in the first and third quadrants. Now the integrand has poles at $k^0 = \pm(\sqrt{\boldsymbol{k}^2 - A} - \mathrm{i}\epsilon)$ which, thanks to the $\mathrm{i}\epsilon$ term ($\epsilon > 0$), lie just outside the contour and thereby ensure the equality of the two integrals in eqn (C.5). Following these manipulations the example integral eqn (C.1) becomes

$$I = \mathrm{i}\, g_s^2 \mu^{4-D} \int_0^1 \mathrm{d}\alpha \, \gamma^\mu \left[(1-\alpha)\not{p} + m\right]\gamma_\mu \int \frac{\mathrm{d}^D k_E}{(2\pi)^D} \frac{1}{(k_E^2 + A - \mathrm{i}\epsilon)^2} \,. \quad \text{(C.6)}$$

We now explain the method of dimensional regularization as applied to eqn (C.6). First, we introduce polar coordinates whilst still keeping D free, which yields

$$I = \mathrm{i}g_s^2\mu^{4-D}\int_0^1 \mathrm{d}\alpha\ \gamma^\mu\left[(1-\alpha)\not{p}+m\right]\gamma_\mu \int\frac{\mathrm{d}^{D-1}\Omega}{(2\pi)^D}\int \mathrm{d}k_E \frac{k_E^{D-1}}{(k_E^2+A-\mathrm{i}\epsilon)^2}\ . \tag{C.7}$$

Since by design the required integral eqn (C.6) is isotropic, the angular integrals can be treated separately. The D-dimensional expression for the angular integrals is given in terms of the Euler Γ-function, eqn (C.24),

$$\int \mathrm{d}^{D-1}\Omega = \frac{2\pi^{D/2}}{\Gamma(D/2)}\ . \tag{C.8}$$

This result coincides with the standard expressions, $2\pi, 4\pi, 2\pi^2, \ldots$ for positive integers $n = 2, 3, 4, \ldots$ However, thanks to the use of the Γ-function, the result is analytic in D so that we can use analytic continuation to define the result for non-integer and even complex values of D. The derivation of this result can be found in Ex. (3-18). Finally, there is the k integral which we treat as a regular integral. It is of the standard Euler β-function form:

$$\int \mathrm{d}k_E \frac{k_E^{D-1}}{(k_E^2+A)^n} = \frac{\Gamma(D/2)\Gamma(n-D/2)}{2\Gamma(n)}A^{D/2-n}\ . \tag{C.9}$$

Combining eqns (C.8) and (C.9), with $n = 2$, allows eqn (C.6) to be written as

$$\begin{aligned} I &= \mathrm{i}g_s^2\mu^{4-D}\frac{\Gamma(2-D/2)}{(4\pi)^{D/2}\Gamma(2)}\int_0^1 \mathrm{d}\alpha\ \gamma^\mu\left[(1-\alpha)\not{p}+m\right]\gamma_\mu A(\alpha)^{D/2-2} \\ &= \mathrm{i}\frac{g_s^2}{(4\pi)^2}\Gamma(2-D/2)\int_0^1 \mathrm{d}\alpha\ \gamma^\mu\left[(1-\alpha)\not{p}+m\right]\gamma_\mu\left(\frac{A(\alpha)}{4\pi\mu^2}\right)^{D/2-2}\ . \end{aligned} \tag{C.10}$$

For future reference the basic D-dimensional integral is given by (Bollini *et al.*, 1973)

$$\int \frac{\mathrm{d}^D k}{(2\pi)^D}\frac{(k^2)^n}{(k^2-A)^m} = \mathrm{i}\,(-1)^{n-m}\frac{A^{n-m+D/2}}{(4\pi)^{D/2}}\frac{\Gamma(n+D/2)\Gamma(m-n-D/2)}{\Gamma(D/2)\Gamma(m)}\ . \tag{C.11}$$

The procedure leading to this result was illustrated for the case of a scalar integrand. If the integrand depends on one of the components of k_E, say k_1, then we write the integral as

$$\int d^D k f(k_1, k^2) = \int \mathrm{d}^{D-1}k\mathrm{d}\,k_1 f(k_1, k^2) = \int \mathrm{d}^{D-2}\Omega\,\mathrm{d}s\,s^{D-2}\mathrm{d}k_1 f(k_1, k_1^2+s^2)\ . \tag{C.12}$$

In this way, the integral over k_1 is treated as a normal integral and the D-dimensional treatment is reserved for the remaining 'isotropic' components of k.

Before investigating the $D \to 4$ limit of eqn (C.10) we must first deal with the γ-matrices. This is discussed in Section C.2. Using the D-dimensional algebra of γ-matrices it is easy to show that

$$\gamma^\mu \left[(1-\alpha)\not{p} + m\right] \gamma_\mu = -(D-2)(1-\alpha)\not{p} + Dm \,. \tag{C.13}$$

Substituting this result in eqn (C.10) and at the same time writing $D = 4 - 2\epsilon$ gives

$$\begin{aligned} I &= \mathrm{i}\,\frac{g_s^2}{(4\pi)^2}\Gamma(\epsilon)\int_0^1 \mathrm{d}\alpha\,\left[-(2-2\epsilon)(1-\alpha)\not{p} + (4-2\epsilon)m\right]\left(\frac{A(\alpha)}{4\pi\mu^2}\right)^{-\epsilon} \\ &= \mathrm{i}\,\frac{\alpha_s}{4\pi}\,\frac{\Gamma(1+\epsilon)}{\epsilon}\int_0^1 \mathrm{d}\alpha\,\left[-2(1-\alpha)\not{p} + 4m + \epsilon(2(1-\alpha)\not{p} - 2m)\right]\left(\frac{A(\alpha)}{4\pi\mu^2}\right)^{-\epsilon} \,. \end{aligned} \tag{C.14}$$

In the second line we used eqn (C.25) to make explicit the pole associated with the $D \to 4$, $\epsilon \to 0$ limit. Using eqn (C.26) together with $x^\epsilon = \mathrm{e}^{\epsilon \ln x}$, we can now investigate the $\epsilon \to 0$ limit of eqn (C.14), which becomes

$$\begin{aligned} I &= \mathrm{i}\,\frac{\alpha_s}{4\pi}\int_0^1 d\alpha\Bigg\{\left[-2(1-\alpha)\not{p} + 4m\right]\left[\frac{1}{\epsilon} - \gamma_\mathrm{E} + \ln(4\pi) - \ln\left(\frac{A(\alpha)}{\mu^2}\right)\right] \\ &\qquad + 2(1-\alpha)\not{p} - 2m\Bigg\} + \mathcal{O}(\epsilon) \\ &= \mathrm{i}\,\frac{\alpha_s}{4\pi}\left\{(-\not{p} + 4m)\left(\frac{1}{\epsilon} - \gamma_\mathrm{E} + \ln(4\pi)\right) + \not{p}\left[1 + 2\int_0^1 d\alpha(1-\alpha)\ln\left(\frac{A(\alpha)}{\mu^2}\right)\right]\right. \\ &\qquad \left. -m\left[2 + 4\int_0^1 \mathrm{d}\alpha\,\ln\left(\frac{A(\alpha)}{\mu^2}\right)\right]\right\} \,. \end{aligned} \tag{C.15}$$

In this expression it may be noted that the inclusion of the mass μ takes care of the dimensions in the logarithm. What we find is that the ultraviolet divergence in eqn (C.1) is now isolated as a simple $1/\epsilon$ pole. Experience will confirm that $1/\epsilon$ always occurs in the combination

$$\Delta_\epsilon \equiv \frac{1}{\epsilon} + \ln(4\pi) - \gamma_\mathrm{E} \,. \tag{C.16}$$

There remains a finite part given in terms of tedious but calculable α-integrals.

It must be admitted that our approach to dimensional regularization has been a little cavalier. That our results hold is thanks to the work of others ('tHooft and Veltman, 1972). In essence, what we have done is to first identify those dimensions, $D < 4$ in the example above, for which the desired integral is finite; this means free of both ultraviolet, $k \to \infty$, and, if massless particles appear in the loop, infrared, k, $k \cdot p \to 0$, divergences. The integral is computed and then expressed as an analytic function of D which can be used to continue the integral into the vicinity of $D = 4$.

C.2 D-dimensional γ-matrix algebra

In accord with the discussion of Section 3.3.1, also in the general case of D dimensions we require $\gamma_0^\dagger = +\gamma_0$ and $\gamma_i^\dagger = -\gamma_i$ for $i = 1, 2, 3, \ldots$; the same Clifford algebra $\{\gamma^\mu, \gamma^\nu\} = 2\eta^{\mu\nu}\mathbf{1}$; and the linearity and cyclicity of traces. As these rules essentially coincide with those assumed earlier, we can use the same manipulations on the traces of γ-matrices in D as in 4 dimensions. One word of warning is to remember that $\eta^\mu{}_\mu = D$, which leads to extra terms proportional to $D-4$ appearing in some results; compare eqn (3.83) and Ex. (3-19). Finally, remembering that each trace is proportional to the trace of the D-dimensional unit matrix, we define $\mathrm{Tr}\{\mathbf{1}\} = f(D)$ where f is any well behaved function of D subject to the boundary condition $f(4) = 4$. The simplest choice is $f(D) = 4$. Since in practical applications we will always take the limit $\epsilon \to 0$, any difference $f(D) - 4 = \mathcal{O}(\epsilon)$ can only contribute to divergent graphs, $\propto 1/\epsilon^n$, and, as we shall learn, the additional terms are equivalent to a change in the finite part of the counterterms and so unobservable by renormalization group invariance.

Whilst it does not arise in pure unpolarized QCD calculations, for the sake of radiative corrections to chiral weak processes, we mention the treatment of γ_5. The usual properties of γ_5 are: $\gamma_5^\dagger = \gamma_5$, $(\gamma_5)^2 = \mathbf{1}$ and $\{\gamma_5, \gamma_\mu\} = 0$. Unfortunately, if we require results that are analytic functions of D then the anti-commutativity property obliges $\mathrm{Tr}\{\gamma_5\gamma_{\mu_1}\cdots\gamma_{\mu_n}\} = 0$ for any n. However, in $D = 4$ dimensions we can realize γ_5 as $\gamma_5 = \mathrm{i}\gamma_0\gamma_1\gamma_2\gamma_3$ and obtain the result $\mathrm{Tr}\{\gamma_5\gamma_\mu\gamma_\nu\gamma_\sigma\gamma_\tau\} = \mathrm{i}\epsilon_{\mu\nu\sigma\tau}$. This conflict highlights the fact that γ_5 is intrinsic to four dimensions. One resolution is to use the $D = 4$ definition of γ_5 and modify the anticommutators ('tHooft and Veltman, 1972) to obey

$$\gamma_5 = \mathrm{i}\gamma_0\gamma_1\gamma_2\gamma_3 \quad\Longrightarrow\quad \begin{cases} \gamma_5\gamma_\mu = -\gamma_\mu\gamma_5 & \mu = 0, 1, 2, 3, \\ \gamma_5\gamma_\mu = +\gamma_\mu\gamma_5 & \text{otherwise.} \end{cases} \tag{C.17}$$

The price of this solution is the loss of Lorentz invariance. Thus, when γ_5 is present we must treat separately the sets of components $\mu < 4$ and $\mu \geq 4$.

C.3 D-dimensional phase space

The generalization of the n-body phase space to D dimensions is straightforward,

$$\mathrm{d}\Phi_n = (2\pi)^D \delta^{(D)}\left(p_a + p_b - \sum_{i=1}^n p_i\right) \prod_{i=1}^n \left\{ \frac{\mathrm{d}^D p_i}{(2\pi)^{(D-1)}} \delta^{(+)}(p_i^2 - m_i^2) \right. \\ \left. \frac{\mathrm{d}^{D-1}\boldsymbol{p}_i}{(2\pi)^{(D-1)} 2E_i} \right. . \tag{C.18}$$

Again the $\delta^{(+)}(x) = \Theta(x^0)\delta(x)$ ensures that we only include contributions from positive-energy particles. The case of $n = 1$ is particularly simple,

$$\mathrm{d}\Phi_1 = 2\pi\delta^{(+)}(p_1^2 - m_i^2)\Big|_{p_1 = p_a + p_b} . \tag{C.19}$$

We will illustrate the use of eqn (C.18) for the case $n = 2$, such as might occur in a two-to-two scattering, which gives

$$\begin{aligned} \mathrm{d}\Phi_2(Q \to p_1 + p_2) &= \int \frac{\mathrm{d}^{D-1}p_1}{(2\pi)^{D-1}2E_1} \int \frac{\mathrm{d}^{D-1}p_2}{(2\pi)^{D-1}2E_2} (2\pi)^D \delta^{(D)}(Q - p_1 - p_2) \\ &= \frac{1}{4(2\pi)^{D-2}} \int \frac{\mathrm{d}^{D-1}p_1}{E_1 E_2} \delta(Q^0 - E_1 - E_2) \,. \end{aligned} \tag{C.20}$$

Here, we have $E_i = \sqrt{\boldsymbol{p}_i^2 + m_i^2}$ and, after integrating out the spatial momentum components of the second final state particle, $\boldsymbol{p}_2 = \boldsymbol{Q} - \boldsymbol{p}_1$. We shall now specialize to the C.o.M. frame, $Q^\mu = (\sqrt{\hat{s}}, \boldsymbol{0})$, which is generally the most convenient, and assume that there is an explicit dependence on the longitudinal component, $p_L = p\cos\theta^*$, of the outgoing momentum in the integrand. The phase-space integral becomes

$$\begin{aligned} \int \mathrm{d}\Phi_2 &= \frac{1}{4(2\pi)^{D-2}} \int \frac{\mathrm{d}p_L \, d^{D-2}p_T}{E_1 E_2} \delta(\sqrt{\hat{s}} - E_1 - E_2) \\ &= \frac{1}{4(2\pi)^{D-2}} \int \frac{\mathrm{d}p_L \, \mathrm{d}^{D-3}\Omega \, \mathrm{d}p_T \, p_T^{D-3}}{E_1 E_2} \delta\left(p_T - \sqrt{\hat{p}^2 - p_L^2}\right) \frac{E_1 E_2}{p_T \sqrt{\hat{s}}} \\ &= \frac{1}{4(2\pi)^{D-2}} \frac{2\pi^{(D_2)/2}}{\Gamma\big((D-2)/2\big)} \int_{-\hat{p}}^{+\hat{p}} \frac{\mathrm{d}p_L}{\sqrt{\hat{s}}} (\hat{p}^2 - p_L^2)^{(D-4)/2} \\ &= \frac{1}{8\pi} \frac{\hat{p}}{\sqrt{\hat{s}}} \left(\frac{4\pi}{\hat{p}^2}\right)^\epsilon \frac{1}{\Gamma(1-\epsilon)} \int_{-1}^{+1} \mathrm{d}\cos\theta \sin^{-2\epsilon}\theta \\ &= \frac{1}{4\pi} \frac{\hat{p}}{\sqrt{\hat{s}}} \left(\frac{\pi}{\hat{p}^2}\right)^\epsilon \frac{1}{\Gamma(1-\epsilon)} \int_0^1 \mathrm{d}v \big[v(1-v)\big]^{-\epsilon} \,. \end{aligned} \tag{C.21}$$

In the final line we have changed variables to $v = (1 + \cos\theta)/2$, which proves useful for some applications. If the integrand is a scalar, that is, does not depend explicitly on p_L, then we can reduce eqn (C.21) to

$$\int \mathrm{d}\Phi_2 = \frac{1}{4\pi} \frac{\hat{p}}{\sqrt{\hat{s}}} \left(\frac{\pi}{\hat{p}^2}\right)^\epsilon \frac{\Gamma(1-\epsilon)}{\Gamma(2-2\epsilon)} \,. \tag{C.22}$$

We will also need eqn (C.18) for the case $n = 3$, which can be written as

$$\int \mathrm{d}\Phi_3 = \frac{Q^2}{2(4\pi)^3} \left(\frac{4\pi}{Q^2}\right)^{2\epsilon} \frac{1}{\Gamma(2-2\epsilon)} \int_0^1 \mathrm{d}x_1 \int_{1-x_1}^1 \mathrm{d}x_2 \frac{1}{\big[(1-x_3)(1-x_2)(1-x_3)\big]^\epsilon} \,. \tag{C.23}$$

At this point we also mention the number of spin-polarization states which should be used when averaging the matrix element squared in D dimensions. Given the standard choice $\mathrm{Tr}\{1\} = 4$, the (anti)quarks as usual should be taken to have two spin-polarization states. On the other hand, it is conventional to give massless gluons $D - 2 = 2(1 - \epsilon)$ spin-polarization states.

C.4 Useful mathematical formulae

Here we collect some useful mathematical results. Further discussion can be found in the standard mathematical physics texts, such as the book by Arfken and Weber (1995).

We make frequent use of the Euler Γ-function, which can be defined by the convergent integral

$$\Gamma(z) = \int_0^\infty \mathrm{d}t\, t^{z-1}\mathrm{e}^{-t} \quad \mathcal{R}e\{z\} > 0\,. \tag{C.24}$$

Integration by parts will confirm the important identity

$$\Gamma(1+z) = z\Gamma(z)\,. \tag{C.25}$$

Thus, for positive, integer values of z, $\Gamma(z) = (z-1)!$, which explains the alternative name 'factorial function'. Equation (C.25) can also be used to shift the argument and define the Γ-function when $\mathcal{R}e\{z\} < 0$. This also shows that there are simple poles at $z = 0, -1, -2, \ldots$. We also need the expansion

$$\Gamma(1+\epsilon) = 1 - \gamma_{\mathrm{E}}\epsilon + \left(\frac{\pi^2}{12} + \frac{1}{2}\gamma_{\mathrm{E}}^2\right)\epsilon^2 + \mathcal{O}(\epsilon^3)\,, \tag{C.26}$$

where $\gamma_{\mathrm{E}} = 0.577\,215\,664\,901\cdots$ is the Euler–Mascheroni constant. We will also often use the related Euler β-function integral,

$$\int_0^1 \mathrm{d}x\, x^m(1-x)^n = \frac{\Gamma(1+m)\Gamma(1+n)}{\Gamma(2+m+n)} \quad \mathcal{R}e\{m,n\} > -1\,. \tag{C.27}$$

APPENDIX D

R_γ, R_l AND R_τ FOR ARBITRARY COLOUR FACTORS

This chapter contains a compilation of the ingredients that go into the theoretical prediction for R_l and R_τ. All expressions are given for arbitrary colour factors, which allows to evaluate not only the QCD-SU(3) predictions, but also the predictions for alternative theories with an unbroken gauge symmetry based on a simple Lie group. This is needed, for example, by any analysis which aims at a measurement of the colour factors from R_l and R_τ. Keeping the colour factors, it is convenient to redefine the coupling constant such that the amplitude for gluon emission from a quark is independent of the gauge group of the theory. Absorbing a factor 2π as well yields the redefined coupling

$$a_s = \frac{\alpha_s C_F}{2\pi} \,. \tag{D.1}$$

The predictions of the theory for n_f quark degrees of freedom then can be expressed as function of the free parameter a_s and the variables

$$f_A = \frac{C_A}{C_F} \,, \quad f_T = \frac{T_F}{C_F} \quad \text{and} \quad f_n = n_f \frac{T_F}{C_F} \,. \tag{D.2}$$

All expressions apply for the $\overline{\text{MS}}$ renormalization scheme and cover at least the dominant contributions. In some cases, the higher order expressions are known but are not quoted here, since the main objective of this section is to provide simple expressions that allow a fast evaluation of the respective effects.

D.1 The running coupling constant and masses

The variation of the strong coupling constant a_s and renormalized masses $\overline{m}$ with the renormalization scale of the theory is described by a coupled system of differential equations,

$$\frac{\mathrm{d}a_s}{\mathrm{d}\ln\mu^2} = -b_0 a_s^2 - b_1 a_s^3 - b_2 a_s^4 \cdots \tag{D.3}$$

$$\frac{\mathrm{d}\ln\overline{m}}{\mathrm{d}\ln\mu} = -g_0 a_s - g_1 a_s^2 \cdots \,. \tag{D.4}$$

The parameters b_i and g_i depend on the specific theory. The leading coefficients (Jones, 1974; Caswell, 1974; Tarasov *et al.*, 1980; Tarrach, 1981; Nachtmann and Wetzel, 1981) are, c.f. Section 3.4.5,

$$b_0 = \frac{11}{6} f_A - \frac{2}{3} f_n \tag{D.5}$$

$$b_1 = \frac{17}{6} f_A^2 - \frac{5}{3} f_A f_n - f_n \tag{D.6}$$

$$b_2 = \frac{2857}{432} f_A^3 - \frac{1415}{216} f_A^2 f_n + \frac{79}{108} f_A f_n^2 - \frac{205}{72} f_A f_n + \frac{11}{18} f_n^2 + \frac{1}{4} f_n \tag{D.7}$$

and

$$g_0 = 3 \tag{D.8}$$

$$g_1 = \frac{3}{4} + \frac{97}{12} f_A - \frac{5}{3} f_n \,. \tag{D.9}$$

Equation (D.3) determines how the strong coupling constant evolves for a fixed number of active flavours, whereas in practical applications one often has to relate a value of α_s from a scale μ_4 with $n_f = 4$ active quark flavours to the measurement at a scale μ_5 with $n_f = 5$ flavours. The treatment of flavour thresholds is described in Bernreuther and Wetzel (1982), Bernreuther (1983), Marciano (1984), and Rodrigo and Santamaria (1993), c.f. Section 3.4.5. With $a_s = a_s(n_f, \mu)$, the coupling constant $a_s(\pm) = a_s(n_f \pm 1, \mu)$ for a different number of flavours, but at the same energy scale μ, can be expressed as a power series in the original coupling. To $\mathcal{O}(a_s^3)$ the expansion is given by

$$a_s(\pm) = a_s \mp a_s^2 \frac{4}{3} f_T \bar{L} + a_s^3 \left[\left(\frac{4}{3} f_T \bar{L} \right)^2 \mp \left(\frac{10}{3} f_A f_T + 2 f_T \right) \bar{L} \mp \left(\frac{8}{9} f_A f_T - \frac{17}{12} f_T \right) \right] \,, \tag{D.10}$$

where $\bar{L} = \ln(\overline{m}(\overline{m})/\mu)$ is the logarithm of the ratio between the fixed point of the $\overline{\text{MS}}$ running mass of the extra quark flavour $\overline{m}(\overline{m})$ and the matching scale μ. Note that the matching condition eqn (D.10) implies that two measurements at the same energy scale with different numbers of active flavours, in general, will see a different coupling strength. Only for a point μ close to $\overline{m}(\overline{m})$ is the coupling continuous, as one would naively expect. The numerical value of the point of continuity depends on the order of the perturbative expansion. Up to NLO, it coincides with $\overline{m}(\overline{m})$.

In the context of arbitrary colour factors it would be preferable to express eqn (D.10) as a function of the pole masses M of the quarks rather than the $\overline{\text{MS}}$ running masses $\overline{m}$, since the latter already absorb part of the radiative corrections of the specific theory. To leading order the pole mass M is related to the running mass according to

$$\overline{m}(M) = \frac{M}{1 + 2a_s(M)} \,. \tag{D.11}$$

From the leading order term, eqn (D.4), one obtains

$$\overline{m}(\mu) = \overline{m}(M) \left(\frac{\mu}{M} \right)^{-a_s g_0} \,, \tag{D.12}$$